THREE-DIMENSIONAL ANALYSIS OF TUNNELLING EFFECTS ON STRUCTURES TO DEVELOP DESIGN METHODS

by

Alan Graham Bloodworth

Brasenose College

Michaelmas Term 2002

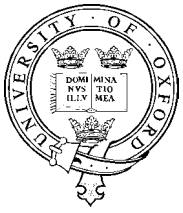

A thesis submitted for the degree of Doctor of Philosophy at the University of Oxford

THREE-DIMENSIONAL ANALYSIS OF TUNNELLING EFFECTS ON STRUCTURES TO DEVELOP DESIGN METHODS

by

Alan Graham Bloodworth

Brasenose College

Michaelmas Term 2002

A thesis submitted for the degree of Doctor of Philosophy at the University of Oxford

ABSTRACT

The subject of this thesis is the verification of a three-dimensional numerical modelling approach for the prediction of settlement damage to masonry buildings due to tunnelling in soft ground. The modelling approach was developed by previous researchers at Oxford, and was applied to three sites, representative of a range of practical configurations. The first involved the excavation of a shaft close to the corner of an eighteenth century church in London. The second involved tunnelling with very low cover beneath the foundations of a terrace of cottages at Ramsgate, Kent. The third was the relatively well-known case of tunnelling beneath the Mansion House, London, for construction of the extension to the Docklands Light Railway in the late 1980's.

The overall conclusion of the project is that the modelling procedures are suitable for application to the detailed assessment of the response of buildings to tunnelling. Particular features of the procedures are that the building is modelled together with the ground and a representation of the tunnel excavation, and in three dimensions. It has been confirmed that all these features are necessary to model the building response, which may include a combination of shear deformation, arching and bending behaviour. Further lessons have been learned concerning the importance of the self-weight of the building in determining overall settlements, how to model openings such as doors and windows in façades, and whether it is necessary to model the building foundation. It has not proved possible, through lack of time, to model the advance of tunnels beneath buildings within this thesis. This, however, is observed to be an important effect in the field, particularly in causing damage to internal walls. It is recommended that further research be carried out in this area.

This project made use of large-scale non-linear finite element analysis. The demand on computing resources was high, stimulating many enhancements to the software, the most important of which was parallelisation of the analysis program for use on the Oxford Supercomputer. To obtain optimum results, larger model sizes are required. The computing resources to enable this should become more commonly available within the next few years, enabling the modelling techniques to be used routinely.

ACKNOWLEDGEMENTS

I would like to especially thank my supervisor, Professor Guy Houlsby, for his encouragement and very helpful advice to me throughout my research. I have been very fortunate that he is my supervisor, and have learned many lessons in working under his guidance and leadership that I will remember for an extremely long time.

I also acknowledge with gratitude the support of the Royal Commission for the Exhibition of 1851, and feel honoured to have been awarded one of their Industrial Fellowships, without which this project would not have been possible.

I also owe many thanks to my fellow researcher, Claus Wisser, for the comradeship we experienced and for the countless useful conversations we had, often as we solved computing related problems. I am also grateful to Dr Charles Augarde who shared a particular interest in this research area. Thanks are also due to the staff of the Oxford Supercomputing Centre, with whom we enjoyed a convivial relationship both inside and outside the laboratory.

I owe a debt of gratitude also to many of my former colleagues at Brown and Root, in particular to Mr Martin Knights, my Industrial Supervisor, for his support throughout the project. My thanks also go to Dr Y C Lu and Steve Macklin for the real interest they showed in my work throughout and for the many in depth discussions we had, and to Matthew Crow and Paul Nowak for their assistance in obtaining field data from Ramsgate and Maddox Street respectively.

My time on the Ramsgate site was challenging, often cold and sometimes frustrating but overall it was fun, assisted by all the members of the site team who made me very welcome. Thanks go especially to Simon Morgan, Tim Newman and Stuart Threadingham.

Finally I would like to thank all my friends and family for their support and kindness to me throughout my research and in writing this thesis. There is one person to whom I am eternally grateful. She stayed with me throughout and her love and encouragement for me never stopped. We started as firm friends and she became my wife. To her I dedicate this thesis. Thank you Kathy.

CONTENTS

1 INTRODUCTION

1.1 Tunnelling in soft ground in urban areas

Tunnelling is increasingly being seen as an environmentally preferable means of providing infrastructure such as transportation and utilities to densely populated urban areas. It is often cost-effective as an alternative to over-ground solutions, when the risk and cost of disruption during construction is taken into account. The number of tunnelling schemes in cities under construction or being planned worldwide is increasing. The September 1999 issue of the journal Tunnels and Tunnelling International reported on major metro projects in Bogota, Cairo, Copenhagen, Hong Kong, Kuala Lumpur, London, Madrid, Nanjing City, Rio de Janeiro, Rome, Singapore, Tel Aviv, Tehran and Washington D.C.

It is common for major cities, especially in coastal or estuarial locations, to be founded on alluvial deposits of clays, silts and sands, usually classified as soft ground. Ground movements in response to the excavation of the tunnel will be transmitted to the surface. If there are surface structures founded on either shallow or deep foundations, these may be affected.

Tunnels of 2m diameter and upwards are usually constructed by tunnel boring machine (TBM), depending on the precise ground conditions. A typical example would be running tunnels for a metro. The TBM comprises a rotating cutter head powered by a motor contained within a cylindrical advancing shield. Behind the shield, a lining, either of precast concrete or cast iron, is erected. For shorter lengths and awkward shapes, for example junctions and underground stations (Figure 1-1), tunnels are typically excavated by hand with or without a shield and a sprayed concrete primary lining is often cost effective.

The amount of surface settlement that results depends partly on what methods, if any, are being applied to control the ground movements ahead of or around the excavation. In a closed-face machine, the pressure on the face is maintained as close as possible to the overburden pressure thus reducing ground movements into the face. In an open-faced machine, the face is effectively unsupported. Grouting the annulus behind the completed lining serves to reduce radial movements of the surrounding soil. Other methods may also be applied for limiting the spread of ground movements to the surface, for example ground improvement by soil nailing or permeation grouting. Compensation grouting may be used to compensate directly for the effects of the ground movements upon specific surface structures.

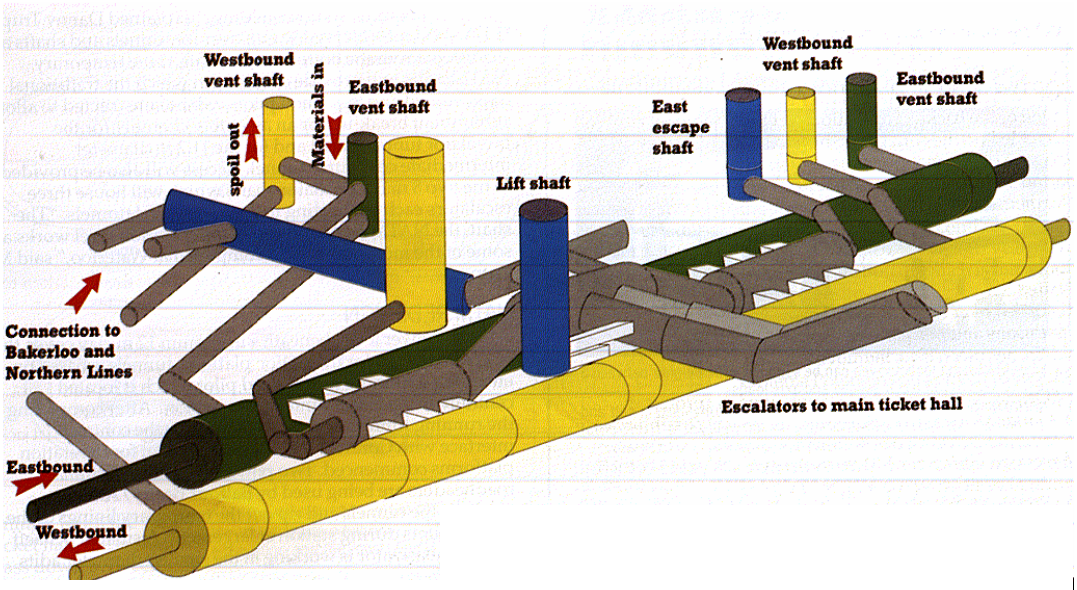

Figure 1-1: Tunnelling works under Waterloo Station, London, for the Jubilee Line Extension (World Tunnelling, Feb. 1996)

1.2 Risk of damage to surface structures due to soft ground tunnelling

A typical TBM tunnelling operation may remove a volume of original ground material that is 1% - 2% greater than the volume of the completed tunnel including its lining. For a 5m-diameter tunnel in stiff clay with a cover of 10m under a 'greenfield' site, the effect on the surface would be to generate a settlement trough with a maximum depth of between

12mm and 24mm and a maximum ground slope of 1 in 900 to 1 in 450. At the lower bound of this range the movements would probably not be significant, but at the upper bound damage could result. It is important to have methods for predicting not only the characteristics of the ground movement, but also its effects on structures.

Different forms of structure will be affected in different ways by the settlement trough. Structures that are not continuous at foundation level, for example bridges, or that have deep piled foundations toeing to a level below the influence of the tunnel, might well be able to accommodate the resulting differential settlements or span across the whole trough.

Continuous structures on shallower foundations will be more adversely affected. These will often be low-rise, older structures of load-bearing masonry. Although load-bearing masonry is actually quite good at accommodating differential ground movements, it does so by cracking and hence by accepting damage. This damage may in extreme cases lead to a loss of strength or stability of the building leading to structural failure. It is more likely, however, to have a less catastrophic effect and to be repairable, but at a cost. It is this cost, and the accompanying disruption to the function of the building, which may be an important impact of the tunnelling scheme, and therefore needs to be estimated by the civil engineers. The cost will be greater for high value buildings of historical and national importance.

More modern steel or concrete frames may be able to resist the imposed ground movements by a combination of their strength and stiffness, particularly by making use of the non-structural elements such as infill walls and floors. Provided structural failure is not induced, damage would probably not be noticeable.

The effect of tunnelling-induced ground movements on surface settlements in the ‘greenfield’ case has been explored by gathering field information from many sites. Data on the response of buildings to tunnels, and their interaction with settlement troughs, is more difficult to obtain. There are so many different possible configurations of structural material, form (including foundation type), geometry and location relative to the tunnel that a large number of case histories would be required for an effective empirical study. In practical terms, obtaining data from buildings is a complex exercise. Building owners and

tunnel engineers would prefer that there was no movement due to tunnelling, so the tunnel alignment is often chosen to avoid sensitive structures as much as possible. Sometimes protection measures are specified, and case histories where there has been no such intervention are relatively rare. There may also be restrictions on the publication of data involving sensitive structures.

1.3 Design approaches for acceptable risk

The distribution of damage in a building, particularly one of masonry construction, exhibits characteristics of a stochastic rather than deterministic phenomenon. Therefore design philosophies have employed techniques of classifying buildings according to the probability of a certain threshold of damage being experienced. This leads to a staged assessment process in which buildings under consideration are eliminated when they are shown, by progressively more complex analyses, to lie within acceptable risk levels (Lake *et al*., 1996, Mair *et al*., 1996).

This staged approach was used for the design of the Jubilee Line Extension in London (Linney, 1999). Three stages of assessment were performed. The first two assumed that the ground displacements experienced by the building were the same as those expected in the 'greenfield' situation, *i.e.* without the building present. In the first stage, buildings that are expected to experience a maximum settlement less than 10mm or a maximum ground slope less than 1 in 500 were eliminated. In the second stage, the maximum tensile strain in the building was calculated, based on the imposed ground movements and certain simplifying assumptions about structural behaviour. If it fell within a certain threshold, the building could then be eliminated at that stage. The fact that the damage level calculated is probably a conservative estimate, as the ground and structure will in reality interact, is borne in mind at this stage but the actual interaction effects are not quantified.

The third stage is to carry out a detailed evaluation of risk of damage to the structure. According to Mair *et al*. (1996), the assessment should take account of such factors as tunnel construction sequence and method, the three-dimensional geometry of the problem, structural details of the building and its foundation and soil/structure interaction effects

between the building and the ground. There is no doubt that all of these effects are realistic and important for a detailed analysis. However, at present there are no broadly accepted validated approaches in the literature or tools available for designers to apply at this stage. There is thus need for more research in this area.

1.4 Objectives of this research project

This project planned to use numerical modelling to investigate the response of buildings to tunnelling. It aimed to explore similar effects to those considered in a stage three assessment as described in Section 1.3. A numerical model with this capability would be verified against case history information. In doing so, further understanding of the important parameters for a detailed evaluation would be sought. The aim at the start was not necessarily to produce a tool to carry out a stage three assessment, such as a software package or a set of design charts, although these could be a by-product of the work, or the product of work to follow. Rather, the intention was to investigate the feasibility of the option of using numerical modelling for detailed evaluation and identify the resources that were likely to be required, both in human and computing terms.

It is recognised that there are other approaches distinct from numerical modelling that could be taken to explore this area, for example gathering case history data for an empirical study, small-scale laboratory testing or centrifuge modelling. However, the aim of this project was to exploit specific advantages of three-dimensional non-linear numerical analysis for this purpose. These were the ability to model any geometry without having to simplify to two dimensions, representation of the advance of a tunnel heading, and the ability to vary the parameters of the constitutive models of soil and masonry to suit those of case history examples, and to carry out parametric studies.

The basic elements of the numerical modelling procedure to be used in this project were implemented in the first phase of a research programme at the University of Oxford, commencing in 1993. The approach uses a non-linear finite element method in three dimensions, modelling a building coupled to the ground and the incremental excavation of a tunnel heading. A key aspect of the work at Oxford is to model the building together with

the ground and tunnel, in a combined or "fully coupled" analysis. The first phase is described in detail in the theses of Chow (1994), Augarde (1997) and Liu (1997), and summarised in the paper by Burd *et al*. (2000). This project forms part of a second phase of research and development, which looks more towards the industrial application of the methods developed in the first phase.

The planned activities for this project were as follows: Firstly, case history data of building responses to tunnel excavation would be obtained. Approximately three to four well-documented sites, involving tunnelling in soft ground under or near masonry buildings but without any intervention measures such as compensation grouting, were sought. At the outset, the Mansion House case history, the subject of three published papers in 1994, was considered a good example. Three-dimensional finite element models of the sites would then be assembled and analysed. The results would be compared with the field data and reasons for any differences would be explored. Experience gained from each analysis would be applied to the next, any useful enhancements to the analysis software made, and the performance of the existing software and hardware examined. A base of experience of carrying out three-dimensional analyses, and overcoming practical difficulties in the process, would be obtained.

The incorporation of protective measures that may be used on site into the analyses, such as compensation grouting, was deemed to be beyond the scope of this project. A parallel research project at Oxford was given the brief of exploring this area. Although case history data from any site could be considered, there was a preference for sites on over-consolidated clays similar to London clay, and for masonry structures (for the reasons indicated in Section 1.2).

The time allowed for the research was three years commencing in October 1996. The project sponsors were the candidate's employer, Howard Humphreys and Partners Ltd., and the Royal Commission for the Exhibition of 1851. Howard Humphreys, as well as allowing for the candidate to be engaged full time on the project for its duration, were also to have an important role in assisting in the obtaining of case history data, from its own projects both past and present and from outside sources.

1.5 Structure of the thesis

Chapter 2 explores in more detail previous research that is the basis of currently accepted design approaches in this subject. It discusses the basic simplifications that are typically made, reviews the literature, and highlights the important issues that a stage three assessment would need to address. It also looks critically at existing methods used at stage two.

Chapter 3 describes how previous researchers have applied numerical modelling to the structure, ground and tunnel problem. It reviews the 2-D and 3-D numerical analysis carried out under the first phase of the research project at Oxford, and presents new parametric studies carried out in 2-D as part of this project.

Chapter 4 discusses the implementation of the numerical modelling procedures for this project. It describes the pre-processing, analysis and post-processing stages, and the developments made to them during the project. Performance of the hardware and software is discussed, and the changes required to the software to be able to transfer it to the Oxford Supercomputer are described.

Chapters 5 to 7 describe the analysis of three case histories. Broadly, each chapter contains an overview of the site under consideration, a description of the observations made in the field, the aims and assumptions of the numerical model for that specific site, the results obtained and a comparison with the observations, and a discussion of the lessons learnt relevant to the verification of the numerical modelling procedures.

Chapter 8 contains concluding remarks, summarising the main findings of the project. It draws together the experience gained in Chapters 5 to 7, and assesses how effective the numerical modelling has been, in the context of the needs of a stage three assessment. It considers how the actual project activities carried out varied from those originally planned and why, and contains recommendations for future research.

2 PREVIOUS RESEARCH AND CURRENT DESIGN APPROACHES

2.1 Introduction

Previous researchers have explored how ground movements close to the tunnel are translated into a distribution of settlements on the surface of the ground. The initial studies were confined to field observations; later work has applied analytical solutions, laboratory and centrifuge modelling and numerical modelling techniques. These are described in Section 2.3, after a description of the fundamental reasons why movements occur around tunnels in soft ground, in Section 2.2.

It is shown that when the presence of a building on the surface is included, the value of numerical modelling becomes apparent by comparison with the above techniques. The effect of tunnelling-induced settlements on buildings is a major criterion in choice of tunnel alignment by designers. The currently available design methods, based on treating the combined problem as an extension of the 'greenfield' situation, are described and their shortcomings noted in Section 2.4.

2.2 Causes of ground movements around tunnels in soft ground

2.2.1 Characterisation of soft ground

Soft ground may consist of cohesive or cohesionless material. Sites used as case histories are frequently classified as one of these two types, although in reality no site ever fits either definition exactly. Previous researchers have recognised a difference in ground movements due to tunnelling in the two types of material, with movements in cohesionless

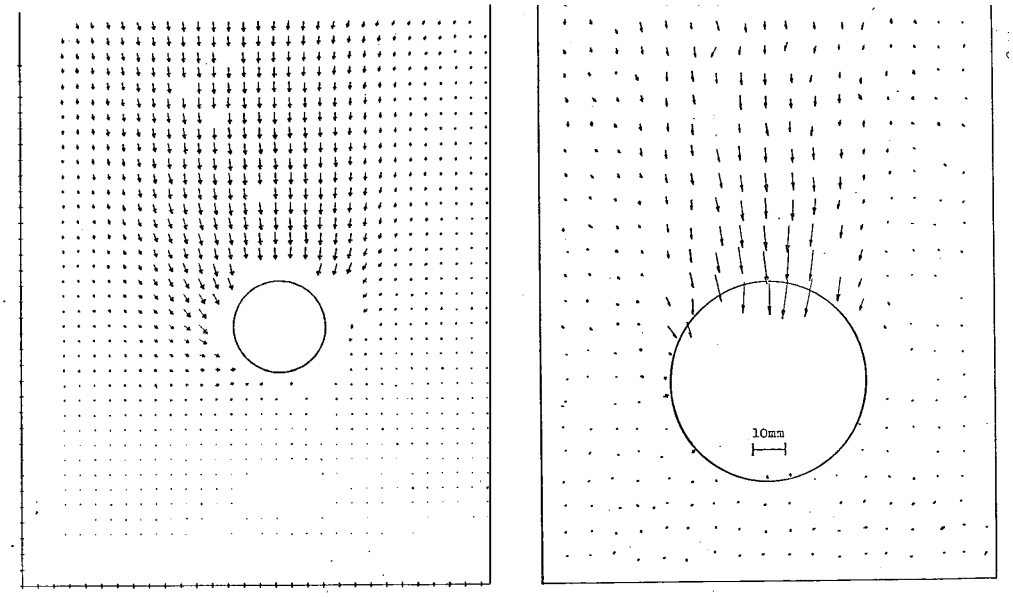

Kaolin clay (Mair, 1979) Dense sand (Potts, 1976)

Figure 2-1: Comparison of vectors of ground movement around tunnels in sand and clay, recorded in centrifuge experiments

ground appearing to be restricted to a narrower region above the tunnel than in cohesive soils (Fig. 2-1).

This study has been limited to the numerical modelling of stiff overconsolidated clays, common in parts of the U.K. and northern Europe historically that were overlain by ice sheets. The emphasis is on the most prominent of these in the U.K. from the point of view of construction activity, which is London clay. However, there is no reason why the modelling procedures may not be applied to softer clays and cohesionless materials, subject to the verification of suitable constitutive models.

2.2.2 Ground movements and volume loss due to an advancing tunnel heading

Ground movements are an inevitable consequence of constructing a tunnel in soft ground. It is not possible to create a void instantaneously and provide an infinitely stiff lining to fill it exactly. In the time taken to excavate, the ground around the tunnel is able to displace inwards as the stress relief is taking place. Thus it will always be necessary to

remove a larger volume of ground than the volume of the finished void. This extra volume excavated is termed the 'volume loss'.

Figure 2-2 shows a schematic section of the advance the tunnelling process for soft ground tunnelling. The shield contains a motor that powers rotating cutters that remove material from the face. During this continuous process, the ground displaces into the face from a zone of influence ahead and to the sides of the face. This gives rise to 'face' loss.

In order to advance the shield it is necessary to excavate an oversized hole. This is achieved by means of a bead with a cutting edge on the front of the shield. After the bead has passed, the ground has the opportunity to move inwards radially. Depending on the rate of deformation of the soil relative to the rate of advance, it may close completely onto the shield.

The lining, which is of slightly smaller diameter than the shield, is erected immediately behind it. The annulus between the lining and ground is normally filled with grout one or two rings back. Thus there is a further opportunity for the ground to displace radially onto the lining, until the grout has hardened sufficiently to resist the earth pressures. The sum of the two radial displacements is termed 'radial' ground loss. The face loss and radial loss total to give the overall volume loss, V_L, for the construction of the tunnel, measured in m^3

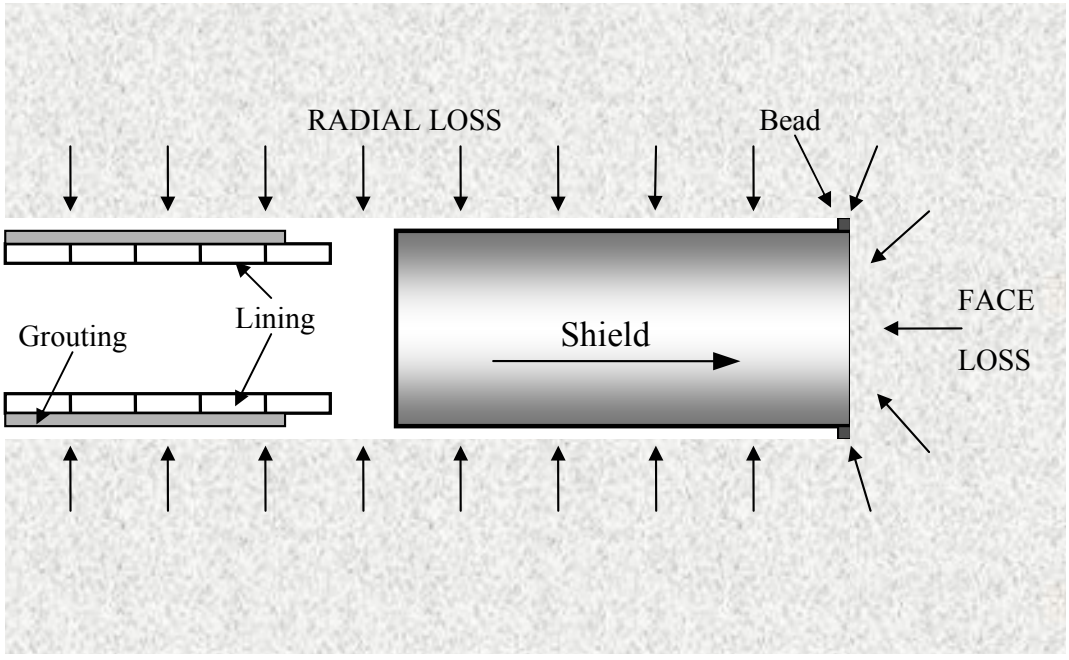

Figure 2-2: Sources of ground losses during the shield tunnelling process

per metre advance of the tunnel drive.

It is hard to make general assertions about the relative magnitudes of the face and radial components of the volume loss, as there is limited case history data of sufficient detail. Macklin and Field (1999) reported an investigation of movements around an advancing 2.8m diameter tunnel in London clay. They were able to relate changes in lateral earth pressure and surface settlement to the position of the advancing tunnel heading. In that case, about 70% of the surface settlement at a particular section took place after the tail of the shield had passed, during lining installation and grouting.

This project is concerned primarily with the impact at the surface of excavating a tunnel, especially the interaction of ground movements with a surface structure. The net volume of the surface settlement trough will be approximately equal to the volume loss at the tunnel in most ground conditions. If the ground response is at constant volume (*i.e.* undrained), the relationship will be exact. This assumption, usually made for stiff clays, enables a measure of the volume loss to be made, which would otherwise be difficult to obtain directly at the tunnel.

V_L is normally expressed as a percentage $V_L\%$ of the gross area of the finished tunnel. Assuming a circular tunnel of outside diameter d,

$$V_L\% = \frac{V_L \quad \text{x } 100\%}{(\pi d^2/4)} \qquad (2\text{-}1)$$

The choice of tunnelling machine type usually depends on its ability to excavate the heading and remove the spoil in a safe and controlled manner. Some tunnelling machines may also control volume loss to within tight limits. In particular, face loss may be reduced or even eliminated by applying pressure to the face equal to the mean *in situ* horizontal stress. In earth pressure balance machines (EPBM), the compartment at the face is maintained at a pressure above atmospheric by controlling the rate at which spoil is removed by a screw conveyor. This machine is used in softer soils or permeable soils where water inflow into the face may be a problem, and relies upon the spoil behaving as a plastic continuum under pressure. The addition of bentonite slurry (a slurry machine) may assist this process in sands and gravels. However, in harder impermeable materials, such as

overconsolidated clays, the spoil may not break down enough at the heading for either method to be practicable. In these circumstances, an open-faced machine is used, relying on the strength, stand-up time and low permeability of the clay for face stability.

It is much harder to control the radial loss. One option is to inject slurry into the annulus around the shield. However because the shield is moving forward, and because the erection of the lining must necessarily be carried out at atmospheric pressure, prevention or even control of radial movements is not really practicable. It can be the most significant cause of settlement, especially if grouting of the annulus is not carried out immediately (*e.g*. Quqing, 1990). The best approach is to keep a steady fast rate of advance, and rely on dealing with the problem by treating its effects (surface settlements) rather than at source. The use of compressed air to maintain pressure in the tunnel during the entire excavation and lining cycle has safety implications and is usually too expensive.

Prediction of the total amount of volume loss would be useful for tunnel designers, but is difficult because volume loss apparently depends on a number of factors that are not known at the design stage. These include the tunnelling machine type, the construction sequence and the effectiveness of the grouting behind the lining, the latter being a 'workmanship' factor. The designer ideally knows the soil properties and *in situ* stress state. It is also known from observation (*e.g.* McCaul *et al*., 1986) that volume loss does not necessarily increase with stress (or depth).

Macklin (1999), after earlier work by Mair *et al*. (1981) and O'Reilly (1988), combined case history and centrifuge modelling results to propose a prediction method for volume loss in overconsolidated clays. His method used the concept of stability number, explained in Section 2.3.3. The data fell between fairly well defined upper and lower bounds. The spread either side of the median design line is likely to be due to a combination of variability in soil behaviour and of workmanship factors, as conceptualised by Lee and Rowe (1991) with the inclusion of a workmanship term in the calculation of their 'gap' parameter. These factors cause variability, because their effect depends on the rate at which soil responds, relative to the time taken for the event to occur that triggers the same

soil response. Investigation of these rate effects is beyond the immediate scope of this study, but would make an interesting topic for further consideration.

The above discussion is relevant in tunnelling where the void is excavated and then a stiff segmental lining is erected. Tunnels may also be constructed by a process of excavation followed by application of a sprayed concrete primary lining. Conceptually there will still be both face loss, as before, and radial loss (due to deflection of the primary lining during and after curing). Bowers *et al*. (1996) report on ground movements due to the Heathrow Express Trial Tunnel. The focus of this project has not been on tunnels with sprayed concrete linings, although there is no reason in principle why they could not be modelled.

2.2.3 Short, medium and long term ground movements

Time dependency in the mechanical behaviour of soil influences ground movements resulting from tunnelling, leading to the classification of short, medium and long-term movements. Each of these regimes of behaviour is itself a steady-state response of the ground to changes in internal or external conditions. The true transient behaviour – the part of the response in each regime that is dependent on the initial conditions – is beyond the scope of this and other studies of tunnelling-induced ground behaviour, although it might be an interesting subject for further study.

Short-term ground movements are identified to occur during at most the first four days after excavation in London clay. This is a timescale that is shorter than, or comparable with, the time taken by the advance of the tunnel heading that is the cause of ground movements. Macklin and Field (1999) reported short-term settlements taking place at a section over a period of 24 hours before and after the passage of the shield. There is evidence that the movements start and stop almost instantaneously with advance of the tunnel heading. The response of the ground is at constant volume to the suddenly imposed new stress regime, which is essentially one of unloading at the tunnel boundary. Rowe and Lee (1989) proposed that it was the extension modulus in clays that was particularly relevant to tunnelling problems. The response may be entirely elastic or include

irrecoverable strains. Apart from very locally to the tunnel, strains are small (say less than 0.1%) and not enough to cause failure or alter the structure of the soil significantly. Thus the constitutive model for the soil can be assumed unchanged during this phase.

Medium and long-term settlements are thought to be the result of creep, ageing and consolidation (Mitchell *et al*., 1997), *i.e.* alterations in the properties of the soil at constant load. The timescale over which they occur depends on the ground conditions, ranging from weeks or months for sands and soft clays to years for stiff clays.

The relative magnitude of short and long-term movements depends on many factors and it is hard to generalise. Case histories suggest that for a typical site on stiff clay, around 60% of the total settlement occurs in the short term (Simons and Som, 1970; Morton and Au, 1975). Attewell and Selby (1989) observed long-term settlements up to 2.5 times the short term, but also that the long-term trough widths tended to be wider. This meant that the curvature of the trough, the factor most likely to cause damage to structures, was similar to that in the short term. In addition, surface structures are more able to accommodate long-term settlements by creep and stress redistribution. Thus it is the short-term movements that remain the chief issue of concern for engineers, and are the subject of this study.

2.3 The prediction of ground movements due to tunnelling

2.3.1 Introduction

A more detailed understanding of the mechanisms by which ground movements occur at tunnel excavations could be beneficial in predicting the volume loss, deducing the mechanisms of interaction with surface structures, and designing countermeasures against settlement. Empirical methods based on case history data, analytical methods (upper and lower bound and closed-form), laboratory 1*g* model testing, centrifuge modelling and numerical analysis have all been employed. For the potential value of numerical analysis to be realised, a sufficiently accurate constitutive model for the soil in the appropriate

stress/strain range is required. Any modelling technique, either laboratory or numerical, must represent the tunnelling process to an acceptable degree of accuracy.

2.3.2 Empirical 'greenfield' settlement troughs

In 1969, Ralph Peck described settlement data from over twenty case histories available to him at that time, and was able to deduce that the short-term transverse settlement trough in the 'greenfield' could be approximated by a normal distribution or Gaussian curve (Peck; Schmidt, 1969). Further data published since has supported this general assertion. The equation for the assumed trough shape is thus:

$$S = S_{max} \exp(-y^2/2i^2) \qquad (2\text{-}2)$$

Where S = surface settlement

S_{max} = maximum surface settlement (over tunnel axis)

y = transverse distance from tunnel centreline

i = trough width parameter, analogous to the standard deviation of the normal distribution

The important features of the trough shape are shown in Figure 2-3. The value of the trough width parameter i, the distance from the axis to the point of inflexion of the trough (assumed symmetric) determines the maximum settlement for a given volume loss. Peck noticed that soils of different classes, for example cohesionless or cohesive, gave distinct ratios of trough width parameter to tunnel depth (Section 2.2.1). Following from this, O'Reilly and New (1982) expressed the trough width parameter in the form:

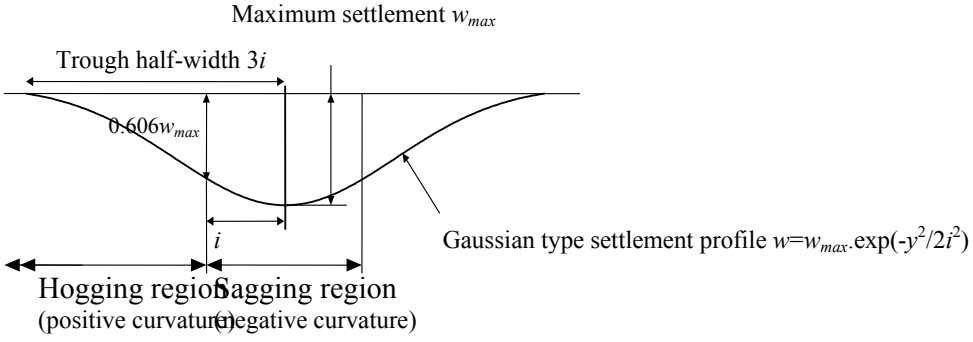

Figure 2-3: The Gaussian model of transverse tunnelling-induced settlements

$$i = Kz_0 \quad (2\text{-}3)$$

Where K is a dimensionless constant, depending on soil type and z_0 is the depth of the tunnel axis below ground level.

Based on data from 19 locations at 11 sites on cohesive ground and 16 locations at 5 sites on cohesionless soils, all in the United Kingdom, O'Reilly and New proposed the empirical relationships:

$$i = 0.43z_0 + 1.1 \text{ for cohesive soil} \quad (2\text{-}4)$$

$$i = 0.28z_0 - 0.1 \text{ for non-cohesive soil} \quad (2\text{-}5)$$

The fit to the available data was found to be better for cohesive soils. The data used covered a wide range of tunnel axis depths, from 3.4m to over 34m. It thus appeared justified to take K as a constant value, independent of both tunnel depth and diameter. Later work by other researchers has confirmed that for cohesive soils K is usually in the range 0.4 to 0.5, and for cohesionless soils in the range 0.25 to 0.35.

The volume of the trough at the surface, commonly equated to the volume loss at the tunnel (Section 2.2.2), is evaluated as the integral of the Gaussian distribution curve:

$$V_s = \int S_{max} \exp(-y^2/2i^2)\, dy \quad (2\text{-}6)$$

$$= (2\pi)^{1/2}\, i\, S_{max} = V_L \quad (2\text{-}7)$$

The expression for S may be rewritten, substituting for S_{max}, as:

$$S = V_L/(2\pi)^{1/2}.i \exp(-y^2/2i^2) \quad (2\text{-}8)$$

This Gaussian model is frequently used to carry out predictions of effects on surface structures, although no researcher has yet compiled a case history study of the combined case, including structures, that is as comprehensive as those of Peck or O'Reilly and New.

Attewell and Woodman (1982) extended this model to derive a settlement trough in the longitudinal direction (Fig. 2-4), using a cumulative Gaussian distribution. It is assumed that exactly half the total settlement has occurred at the position of the heading and that the longitudinal trough parameter is equal to the trough width parameter. The latter assumption is somewhat conservative, as observed longitudinal troughs show a flatter distribution.

Mair *et al*. (1993) extended the tools available to the engineer for empirical assessment based on the Gaussian model by using case history data to derive formulae for subsurface settlements due to tunnelling in clays.

A method for prediction of horizontal ground surface movements (and hence strains) was proposed by O'Reilly and New (1982). There was acknowledged to be relatively little field data for corroboration, but centrifuge testing (*e.g.* Mair, 1979) suggested that the vectors of ground movements above a tunnel in stiff clay generally converged on a point somewhere between the tunnel axis and the tunnel invert. O'Reilly and New approximated the 'sink' thus formed to be at the tunnel axis. Thus:

$$S_H/S = y/z_0 \qquad (2\text{-}9)$$

$$\text{Hence } S_H = S.y/z_0 \qquad (2\text{-}10)$$

Where S_H = horizontal ground movement, and the other terms are as defined previously.

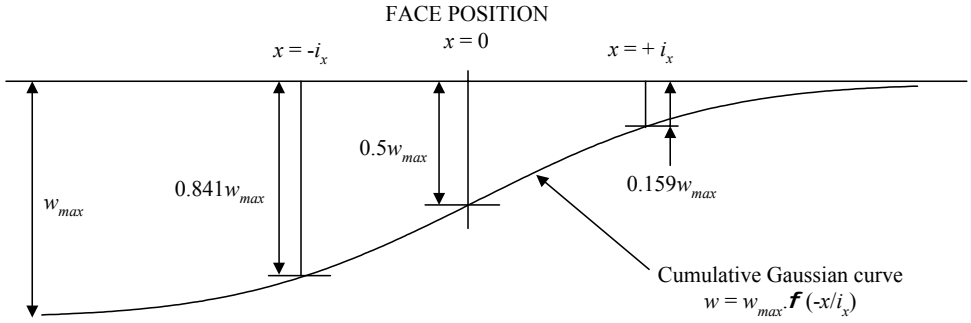

Figure 2-4: Empirical longitudinal settlement trough based on Gaussian model

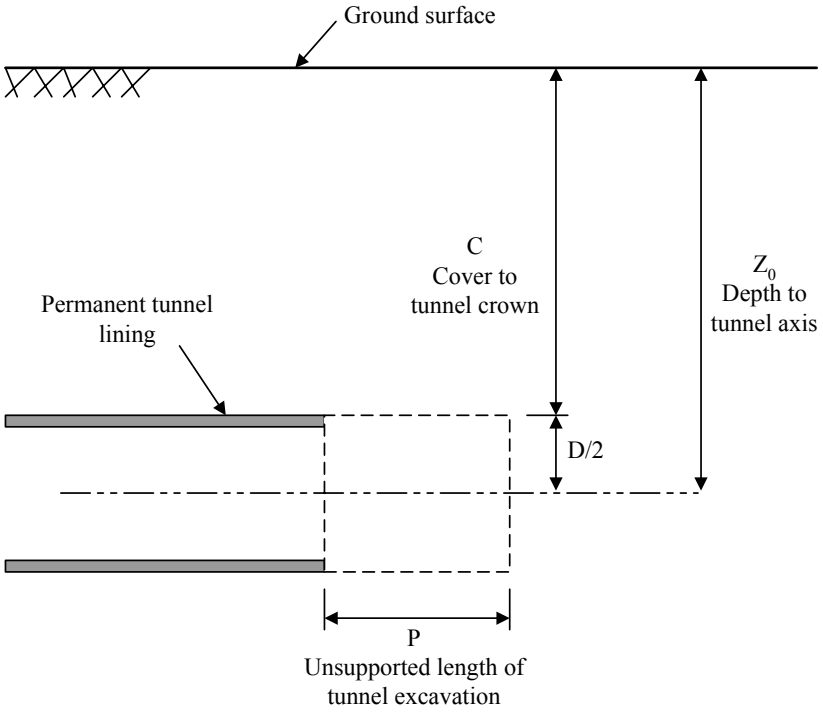

Figure 2-5: Geometric parameters of a tunnel heading for calculation of stability number at collapse

2.3.3 Mechanisms of short-term settlement response

Analytical approaches often require the identification of non-dimensional groups of the important parameters influencing a problem. One such group is the stability number (or overload factor) N defined by Broms and Bennermark (1967) as:

$$N = (\sigma_Z - \sigma_T)/s_u \qquad (2\text{-}11)$$

Where σ_Z = overburden pressure at tunnel axis

σ_T = tunnel support pressure (if any)

s_u = undrained shear strength of clay

Centrifuge model tests (Mair, 1979; Kimura and Mair, 1981) on tunnel headings in kaolin clay showed how the stability number at collapse (N_{TC}) could be correlated with

parameters describing the tunnel heading geometry (Fig. 2-5). Mair *et al*. (1981) defined the 'load factor' (LF) as the ratio N/N_{TC}. They correlated the volume loss obtained in centrifuge experiments and in 2-D finite element analysis of unlined tunnels with LF, and showed how the LF concept could be used to compare results from geometrically different tunnels.

Davis *et al*. (1980) presented lower and upper bound analytical solutions for the collapse load of a shallow tunnel with support pressure in a cohesive soil. They considered the cases of a plane strain unlined circular tunnel (radial ground movements), a plane strain heading (face movements) and a circular tunnel heading (the full three-dimensional case). The difference between the lower and upper bound collapse loads was greatest (with almost a factor of two between them) for the three-dimensional case, indicating the difficulty in applying analytical solutions in three dimensions. They plotted their analytical solutions in terms of N_{TC} against the cover to diameter ratio (C/D). Data from centrifuge modelling (Mair, 1979) confirmed the solutions for a plane strain unlined circular heading, with best agreement for C/D less than 3.

This value of C/D has since become established as a practical transition between shallow tunnels, where the failure mechanism involves the ground surface, and deep tunnels, where the failure mechanism is symmetric about the tunnel axis and the surface has little influence.

Observations from centrifuge tests have been used directly to give more information on the soil behaviour above tunnels (Mair, 1979; Potts, 1976). Mackin and Field (1998) compared vectors of subsurface movement above tunnels with such data.

Verruijt and Booker (1996) presented approximate analytical solutions for the surface settlements resulting from uniform shrinkage and from ovalisation of a tunnel in elastic half-space. Uniform shrinkage gave a wider settlement trough than observed in practice, but the ovalisation gave a much narrower trough with some heave either side of the tunnel. It thus appeared that practical trough shapes could be explained in terms of a combination of radial shrinkage (representing ground loss due to over-excavation) and ovalisation of the

tunnel lining. It was also appreciated that the material model used was linear elastic and that the small strain soil stiffness was not modelled.

Mair and Taylor (1993) developed solutions for the growth of plasticity and excess pore pressure around deep tunnel openings.

2.3.4 Laboratory and centrifuge testing

Laboratory 1*g* testing can perform a useful role to identify the main influences in a problem such as tunnelling. Kim *et al*. (1996) report tests on the interaction between closely spaced tunnels, finding that significant bending moments could be induced in a tunnel lining due to excavation of another tunnel within two diameters. De Moor and Taylor (1989) carried out model tests using a 250mm diameter triaxial test apparatus with the tunnel represented as a hollow open-ended brass cylinder aligned in the axial direction. Nakai *et al*. (2000) report tests on tunnelling in sand, where the finished tunnel is modelled by a solid cylinder and the volume loss due to the advance of the tunnel by removal of 4mm thick rods arranged around the annulus of the cylinder.

Centrifuge modelling is used to reproduce the *in situ* stress state, and hence soil properties, more accurately. Mair (1979) used the centrifuge to model the collapse of a shallow unlined tunnel in clay. Recent work has used the centrifuge to investigate the influence of soil nailing on settlements above tunnels (Kuwano *et al*., 2000), spile reinforcement of the face (Calvello and Taylor, 2000) and settlements in two-layer soil sites (Grant and Taylor, 1996). Grant and Taylor (2000) used centrifuge modelling in an attempt to verify the analytical solutions of Mair and Taylor (1993), with reasonable agreement. Areas of disagreement were related to the finite depth of the tunnel in the centrifuge, compared to the assumption of an axisymmetric stress state in the analysis.

Researchers conducting model tests in the laboratory or centrifuge are inevitably limited by cost and time as to the number of experiments that may be carried out, and thus the amount and quality of data obtained. Some centrifuge experiments require a long time for sample preparation, and it is difficult to model realistically the tunnelling process and the advance of a tunnel heading in a centrifuge. An attempt to introduce a surface structure

into any scale model, not yet tried, would encounter major problems of scaling of the structural elements that are made of concrete or masonry, and adequately representing the connection between structure and soil via the foundation. In all of these areas numerical modelling has advantages. Laboratory testing still has a role, however, in verification and comparison of ground behaviour with numerical modelling.

2.3.5 Numerical modelling of the short-term settlement trough

Previous researchers have attempted to reproduce in numerical modelling the main characteristics of the transverse trough shape described in Section 2.3.2.

Rowe *et al*. (1983) modelled a two-dimensional plane strain heading using an elastic, perfectly plastic soil model. The desired volume loss was modelled by starting the analysis with a 'gap' between the outside of the rigid lining and the excavated surface of the soil. This gap was intended to model not only the physical annulus between lining and soil in the optimum case, but also an allowance for workmanship factors such as the advancing shield (Section 2.2.2) wandering off its theoretical line. They noted that heave of the invert of the tunnel in the model due to the stress relief by the excavation had a dramatic effect in reducing the resulting surface settlements. This however was not usually observed in the field. By increasing the stiffness of the soil beneath the tunnel, the heave was greatly reduced. They concluded that in this case it was the extension modulus of the soil in the invert that was important, rather than the compression modulus.

El Nahhas *et al*. (1992) were interested in the response of the lining, and modelled it in two dimensions by excavating soil elements in the tunnel and allowing the soil to deform, switching on a rigid lining when the appropriate volume loss was reached.

Finno and Clough (1985) conducted 2-D analyses in plane strain in the transverse and longitudinal directions, and compared the results with site data in soft clay. A modified Cam-clay soil model was used. Pore pressure changes were limited to a region within two diameters of the tunnel face. The model predicted the heave occurring ahead of the face with an earth pressure balance machine.

2.3.6 Constitutive models for short term tunnelling settlements

Previous researchers (*e.g.* Chow, 1994; Jardine *et al*., 1986) have shown that the choice of constitutive model for the soil is very important to the calculated response of the ground, especially the ground movements. The trough shape at the surface is a result of soil response at small strains, less than 0.1%, over a wide area above the tunnel. Although anisotropy and horizontal stress ratio may have some influence, the most important issue is the relatively high initial stiffness of the soil at very small strains. Numerical models with linear elastic soil properties give significantly wider settlement troughs than observed in the field.

Jardine *et al*. (1986) presented a non-linear elastic constitutive model for low plasticity (over-consolidated) clays. This model allowed for a high initial stiffness, gradually reducing with strain. This was shown to give rise to an apparent increase of stiffness with depth, which is often observed in the field and sometimes applied to linear elastic models. The model was not demonstrated for a tunnelling problem, which has the particular feature that the ground is undergoing unloading.

An alternative family of constitutive models has been developed, based on an assumption of work-hardening plasticity. These are capable of capturing the effects of stress history on soil behaviour, and can therefore in theory model unloading and cyclic loading. Stallebrass and Taylor (1997) demonstrated a model with three nested yield surfaces – an initial yield surface, history surface and critical state failure surface. They applied this model to the case of a 2-D plane strain foundation, showing how the displacements close to the footing, and the redistribution of stress beneath the footing, compared favourably to centrifuge modelling data.

Houlsby (1999) has also developed a kinematic hardening model, from plasticity theory based upon fundamental thermodynamics (Collins and Houlsby, 1997). Nested yield surfaces are surrounded by an outer failure envelope. Figure 2-6 shows the response of the yield surfaces on translation in stress space from the origin ‘O’ to ‘A’ and back to ‘O’. The model is not complicated to apply, requiring only a set of non-dimensional hardening and shear strength parameters that describe the reduction in shear stiffness as each yield surface

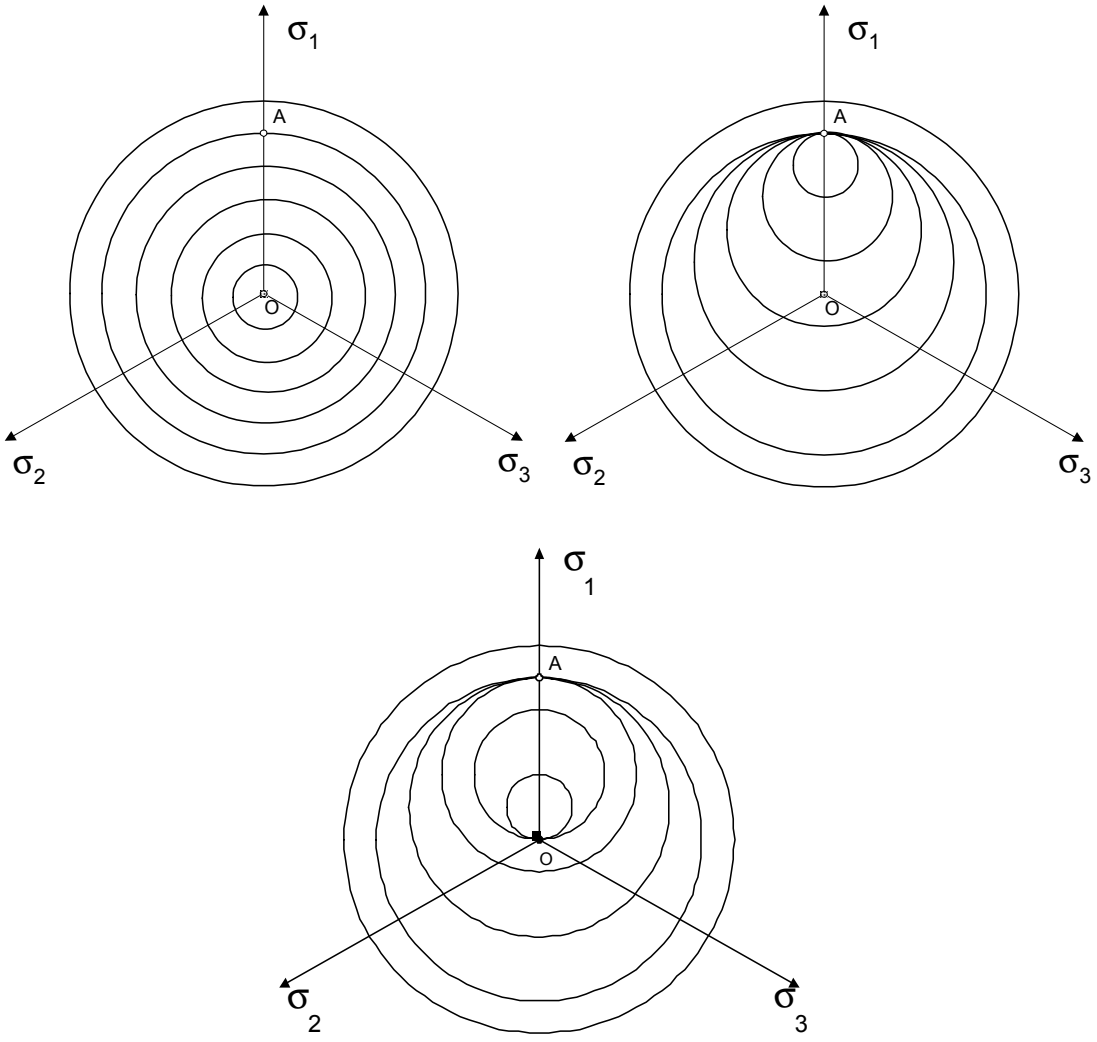

Figure 2-6: Translation of nested yield surfaces in kinematic hardening model under action of stress path from origin to A and back

is reached. Figure 2-7 shows the shear stiffness/shear strain relationship implemented to model London clay for this project, using nine yield surfaces. This follows the 'S'-shaped curve that is typical of many soils (Houlsby, 1999).

In the current implementation of the kinematic hardening model, the outer surface is a perfectly plastic von Mises surface. Once this surface is reached, the material loses all stiffness and load is shed elsewhere, meaning that consolidation and contractile yielding, as encountered in critical state models, cannot be reproduced. An enhancement to cater for this is under development. In the meantime, the model is still suitable for representing

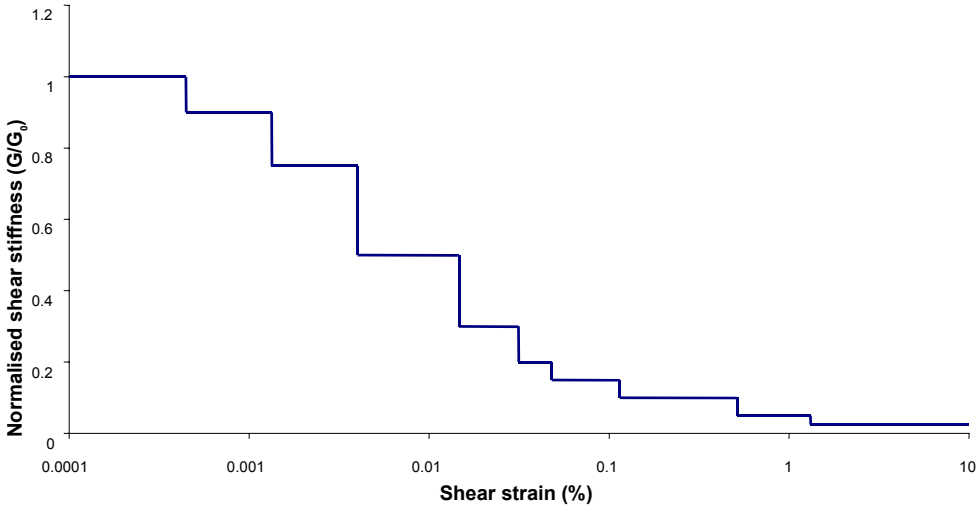

Figure 2-7: Variation of tangent shear stiffness with shear strain for nine-surface kinematic hardening model

general small strain (pre-failure) deformation of stiff clays. It was applied in this project to model the short-term undrained response of London clay.

The relationships between strength and stiffness and depth z below the surface usually used to model London clay during this project were as follows:

For shear strength, $s_u = 60 + 6z$ kPa (2-12)

For initial stiffness, $G_0 = 30000 + 3000z$ kPa (2-13)

Thus the rigidity index G_0/s_u is fixed at 500. This profile is the same as that used by Liu (1997).

2.4 The combined structure, ground and tunnel problem

2.4.1 Introduction

Attention has focussed so far on the ground movements originating due to tunnelling in soft ground. The presence of a surface structure or structures within the zone of influence of the tunnel will now be included. The surface structure would be expected to have its own zone of influence within the ground that is affected by its self-weight and stiffness characteristics. At the intersection of the two zones of influence there will in principle be an interaction effect, potentially causing behaviour quite distinct from that if only either the

building or the tunnel were present. The behaviour of the building, and the resulting damage to it, will depend on the size of the intersection of the zones of influence, geometry, soil and structure properties and volume loss mechanisms.

This interaction between building and ground is particularly difficult to predict, and laboratory or centrifuge models become impracticable. Observations from the field are essential for understanding the problem, but are limited for the reasons discussed in Chapter 1. Numerical modelling in three dimensions is the alternative that is the subject of this study.

However, previous researchers have made simplifying assumptions about the nature of the combined problem to be able to continue applying methods such as empirical observation, centrifuge modelling and numerical modelling in similar ways as for assessment of the 'greenfield' case. The main such simplifying assumption has been to consider the problem of a tunnel passing under a building as two-dimensional. Secondary assumptions made by various researchers are that:

1. The surface structure does not interact with the tunnelling-induced ground movements but rather deforms according to the movements that would be expected in the 'greenfield' case.
2. The possibility of the structure becoming damaged, altering its stiffness and response to the ground is not allowed for.
3. As an alternative to assumption 1, interaction between the structure and tunnelling-induced ground movements is allowed for, but the resulting deformation is limited to being expressed as a modification of the movements that would be expected in the 'greenfield' case. This does not allow for the presence of the structure causing a fundamentally different mechanism of behaviour.

The remainder of Section 2.4 will discuss the current design approaches resulting from having made the above simplifying assumptions.

2.4.2 Assessment assuming structure deformation follows 'greenfield' profile

This approach has the advantage of being relatively straightforward, given that the 'greenfield' trough is well understood from site observations. If simplified assumptions are also made for the building behaviour, analytical solutions for the resulting strains and damage in the building may be derived. Since it might be expected that the stiffness of a building would normally reduce the maximum settlement and curvature of the settlement trough, this approach is generally felt to overestimate the stresses in the real situation, giving a conservative basis for design and assessment.

2.4.2.1 TENSILE STRAIN AND DAMAGE CATEGORISATION

Burland and Wroth (1975) proposed that building damage could be related to the tensile strain occurring in a building due to the influence of a general settlement trough (not necessarily due to tunnelling). The concept was developed for masonry buildings. Their work followed earlier studies by Skempton and MacDonald (1956) and Polshin and Tokar (1957) that both correlated building damage to the angular distortion of the building. Burland and Wroth idealised the building as a two-dimensional elastic plain façade, acting as a beam in pure bending or combined bending and shear (Fig. 2-8). They introduced the quantity 'relative deflection', deriving from it the maximum tensile strain in the building. This required assumptions to be made about the position of the neutral axis. They showed,

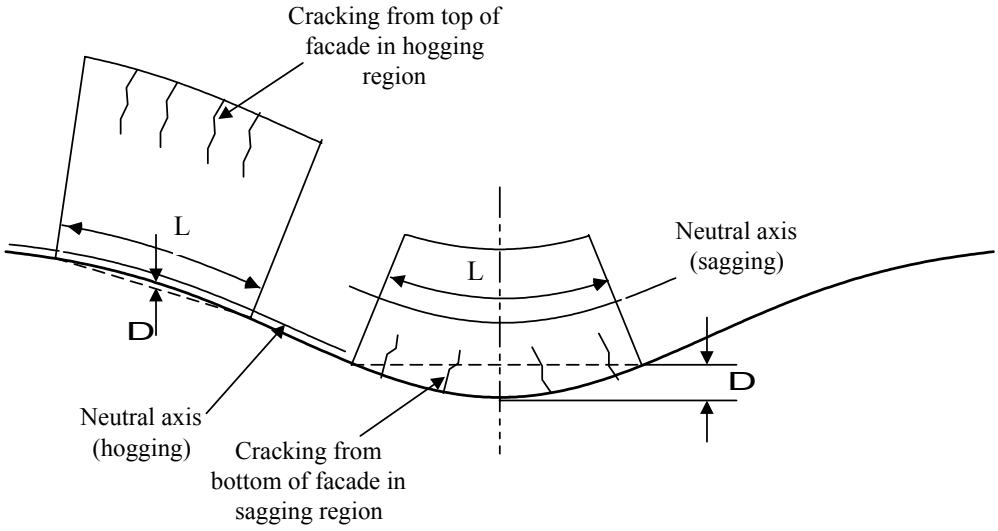

Figure 2-8: Idealisation of building as an elastic beam and definition of relative deflection Δ (Burland and Wroth, 1975)

with reference to case histories of building performance, that when the building as a beam was in sagging, the neutral axis could reasonably be taken to be at mid-depth of the section. When the building was in hogging, the foundation could normally provide sufficient restraint against tension, but that in the case of a masonry building the remainder of the façade could not. Thus the neutral axis would move down to the foundation at the lower extreme fibre. This was consistent with observations of cracking opening up from the tops of walls in the hogging regions of settlement troughs. Thus for a given deflection ratio, the maximum tensile strain due to bending would be twice as great in the hogging region and would occur at the top of the building.

Expressions were derived for the maximum tensile strains due to bending (ε_b) and shear (ε_d, diagonal strain) as functions of the 'deflection ratio', Δ/L. These were later generalised by Burland *et al*. (1977) to:

$$\Delta/L = (L/12t + 3IE/2tLHG).\varepsilon_b \qquad (2\text{-}14)$$

$$\Delta/L = (1 + HL^2G/18IE).\varepsilon_d \qquad (2\text{-}15)$$

Where Δ/L = deflection ratio

L = length of building in hogging or sagging region of settlement trough

H = height of building

t = distance to extreme fibre in hogging or sagging region

E = Young's modulus of building, assumed elastic

G = shear modulus of building

I = moment of inertia of building acting as a beam

In a separate but related piece of research, Burland *et al*. (1977) proposed a classification system for the damage to a masonry structure due to ground movement. The philosophy adopted was to classify the damage by ease of repair. This was expressed in terms of the typical sizes and numbers of cracks, for example a crack width of 5 – 15mm or a number of cracks greater than 3mm was classified as "Moderate" damage (Table 2-1).

Degree of Damage	Description of typical damage (ease of repair)	Approximate crack width (mm) (Burland *et al*., 1977)	Limiting tensile strain (%) (Boscardin and Cording, 1989)
0 Negligible	Hairline cracks of less than about 0.1mm are classed as negligible	< 0.1	0.0 – 0.05
1 Very slight	Fine cracks which can easily be treated during normal decoration	1	0.05 – 0.075
2 Slight	Cracks easily filled. Re-decoration probably required. Some repointing may be required externally	5	0.075 – 0.15
3 Moderate	The cracks require some opening up and can be patched by a mason. Recurrent cracks can be masked by suitable linings. Repointing of external brickwork and possibly a small amount of brickwork to be replaced.	5 – 15 or a number of cracks > 3	0.15 – 0.3
4 Severe	Extensive repair work involving breaking-out and replacing sections of walls, especially over doors and windows.	15 – 25 but depends on number of cracks	>0.3
5 Very severe	This requires a major repair job involving partial or complete rebuilding.	> 25 but depends on number of cracks	

Table 2-1: Classification system for damage to masonry buildings

2.4.2.2 EFFECT OF HORIZONTAL STRAINS

Burland and Wroth (1975) considered that normally the stiffness and tensile strength of the foundation was enough to prevent horizontal tensile strains in the ground from being transmitted to the superstructure. However, Boscardin and Cording (1989) highlighted case histories where this was apparently not the case, although the phenomenon was more dependent on precise structural form than the effect of vertical settlements. They proposed a method for allowing for horizontal tensile strain that is transmitted to the building by simply adding the tensile strain to the strains due to bending and shear calculated using the approach of Burland and Wroth. They also proposed the addition of tensile strain thresholds to the damage categorisation of Burland *et al*. (1977) (Table 2-1), based on the research available to them.

2.4.3 Assessment allowing interaction between the structure and tunnelling-induced ground movements

This problem has been found to be too complex for the application of analytical closed-form solutions, even when limited to two dimensions. Practical difficulties are also encountered with laboratory and centrifuge modelling (Section 2.3.4). Researchers have therefore turned to observations from case histories, and to numerical modelling. The key feature of this project is to combine these by obtaining case history data and using it to verify a numerical model.

Potts and Addenbrooke (1997) (Section 2.4.3.2) used numerical modelling of the combined structure and ground problem in two dimensions but expressed the outcome as a modification to the 'greenfield' scenario. Verification of their model against site data was not offered.

2.4.3.1 CASE HISTORY OBSERVATIONS

Good quality case histories of tunnelling settlements interacting with buildings have an important role to play in developing models and solutions to the problem. One of the aims of this project was to obtain data, which could be used for analysis, from fairly well defined case histories of masonry buildings on stiff clay soil. The literature was reviewed for possible examples. Although in principle information contained in a published paper or article could be used for a back-analysis, it is preferable to obtain the raw site data. This would typically consist of drawings of the building and tunnel, site investigation data, monitoring layout, recordings of monitoring data and a record of the progress of the tunnel with time. It was found that the number of published case histories that were even remotely relevant to the criteria were few, broadly for the reasons mentioned in the Introduction (Chapter 1). Other researchers have also encountered this problem.

The most important case history known at the outset of this project was that of the Mansion House in London (Fig. 2-9). It includes a tunnel, London clay soil and a masonry building. Extensive monitoring was carried out during construction, and good data was obtained, including that of cracking to the building. The background to the project is

described in three papers published in the ICE Proceedings in 1994: Frischmann *et al*. (1994), Forbes *et al*. (1994) and Price *et al*. (1994). Tunnels were constructed in the vicinity of the Mansion House for the extension of the Docklands Light Railway to Bank, in two phases in 1988 and 1990/91. The raw data was obtained in April 1998 for this project from the archives of Mott Macdonald Consulting Engineers (who advised the Docklands Light Railway (DLR) during the projects), after gaining approval from the Committee for the Long-Term Monitoring of the Mansion House. The modelling of the Mansion House is the subject of Chapter 7.

Good quality data has been recorded and published from a variety of tunnels in London clay (*e.g.* Barrett and Tyler, 1976; McCaul *et al*., 1986) but the cases have not included buildings. There was hope at the start of this project that data might become available from the tunnelling works during 1993 – 1997 of the Jubilee Line Extension (JLE). An extensive research project led by CIRIA (Burland *et al*., 1996) received funding under the Government's LINK programme for Construction, Maintenance and Refurbishment and from the Engineering and Physical Sciences Research Council totalling £380k, plus contributions from London Underground Ltd. (LUL) and a number of industrial companies. Unfortunately, neither Howard Humphreys nor Oxford University were parties to the original agreement, and although approaches were made to the project managers that some data be released for analysis at Oxford, it was not forthcoming. The remainder of the data of settlements recorded by the JLE team and the project's contractors is thought to be

Figure 2-9: The Mansion House (Frischmann *et al*., 1994)

contractually sensitive material until any claims relating to property damage are resolved.

Sugiyama *et al*. (2000) report on ground movements and compensation grouting used during the construction of 5.85m diameter tunnels in sands and gravels in East London by slurry machine. The settlement trough at a row of terraced houses was reported to have widened compared to the greenfield case, although settlements were small (3mm maximum) mainly due to the control of face pressure and immediate grouting behind the shield.

Shirlaw and Doran (1988) describe ground movements and settlements due to tunnelling for the Singapore metro, mainly in soft clay. Monitoring of buildings (two or three storey) and even damage is mentioned, but no details are given in the paper. The authors were representing the client, who may have further data. They also consider tunnel-to-tunnel interaction.

Forth and Thorley (1995) describe monitoring of the ground and buildings during the construction of the Island Line of the Hong Kong metro, which actually took place in the early 1980's. They report behaviour of buildings as being that of following the ground settlement trough, although many were actually piled. The data was complicated by the use of dewatering and compressed air in some places, and the ground conditions were variable.

De Schrijver and Hemerijckx (1991) report on the monitoring of ground and structures during the construction of a metro line in Antwerp in medium sand. However the greatest settlement at any building was only 2 – 3mm and there was no damage.

Major tunnelling schemes under construction or projected to start soon that were reported in 1997 included those in Athens (Anagnostou *et al*., 1997; also Mihalis and Kavvados, 2000), Lisbon (Simic and Craig, 1997) and Toronto (Garrod and Finch, 1997).

A new class of case histories – of tunnelling in close proximity to other tunnels and underground structures – are being reported, *e.g.* Cooper and Chapman (2000) and Samuel *et al*. (2000), both in London. These may prove to be useful examples for future research using three-dimensional modelling, as the increasingly crowded underground space leads to more such situations being encountered.

The second major source of data for this project was envisaged to be past or present tunnelling projects directly involving Howard Humphreys. The company has a track record of providing design and consultancy services to London Electricity for the construction of tunnels for the routing of high voltage electricity supplies into London. The first such project, in 1991, included the construction of a shaft adjacent to a church in Maddox Street, west London and provided the data for the first case history to be modelled (Chapter 5).

The St. John's Wood to Back Hill tunnel was driven under the masonry arch tunnel of the District and Circle Line near Euston in early 1997. Extensive monitoring was carried out because of the presence of the operational railway. Movements occurred, but they were less than predicted and there was no sign of damage (Samuel *et al.*, 2000; Lu *et al.*, 1999).

Under the same tunnelling contract, a hand drive approximately 60m in length was constructed during July – August 1997 at Longford Street near Euston as a spur tunnel to the main cable tunnel. This hand drive passed at an inclined angle under the foundations of a two-storey reinforced concrete structure that functioned as a basement car park (Fig. 2-10). At its shallowest point, the crown of the tunnel was 3m below one of the foundation pads of the structure. The structure extended a relatively long distance in each direction compared to the expected settlement trough width for the tunnel.

Although the structure was not a masonry building, movements were likely to be small and no damage was expected, it was an opportunity to obtain field data for this project.

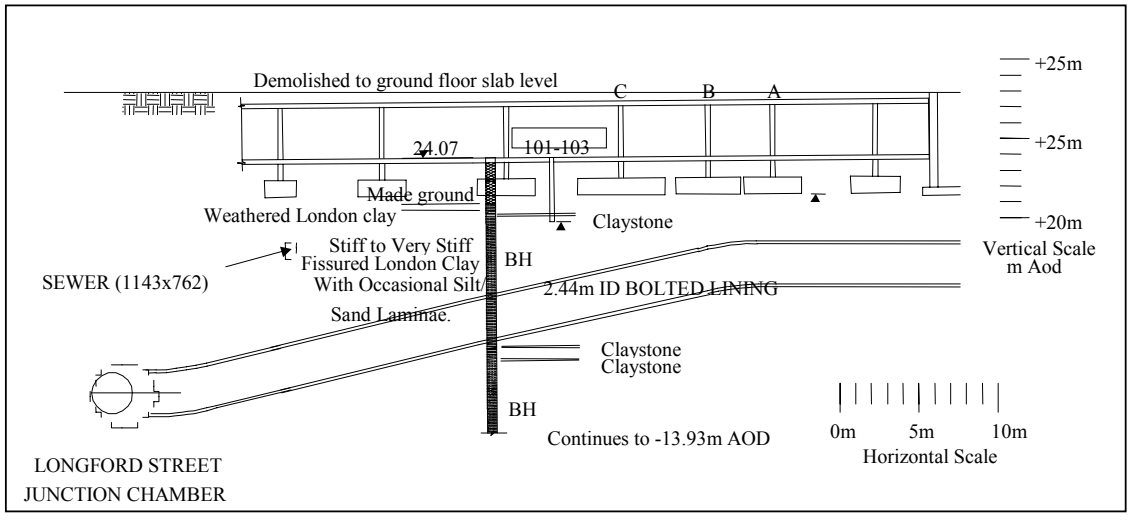

Figure 2-10: Section through spur tunnel and basement structure at Longford Street

Monitoring instrumentation was specified and its installation supervised, in collaboration with Howard Humphreys and the contractor. Three subsurface levelling points were designed and installed with the aim of measuring the volume loss (Mair *et al*., 1993). Monitoring of precise levelling points was carried out daily while the tunnel was advancing underneath. The effect of the structure was to increase the width of the settlement trough at both surface and subsurface levels (Bloodworth and Macklin, 2000). A lower than expected volume loss of 0.8% was observed, stimulating the work of Macklin (1999) on correlating volume loss with load factor (Section 2.2.2).

The West Ham to North Greenwich cable tunnel was constructed in early 1998 to provide power to the Millennium Exhibition site. During the design phase, the route of the tunnel was examined for suitable sites to monitor settlement effects on buildings for this project. Predicted 'greenfield' settlements were 6 – 8mm and the tunnel alignment mostly followed the line of public roads and the River Lee, avoiding buildings. At one location where the tunnel crossed derelict land, detailed monitoring of ground movements around the tunnel heading was carried out (Macklin and Field, 1999).

Monitoring was also carried out where the tunnel passed about 8m beneath two sheet-pile river retaining walls, at Crown Wharf and Orchard Wharf. The data was processed during construction to obtain the overall tilt and settlement of the walls as the tunnel heading passed. The final wall settlements at the two locations are shown in Figures 2-11 and 2-12, together with predictions of 'greenfield' settlements at the ground surface behind the wall and subsurface at the toe of the wall (Mair *et al*., 1993).

The results were consistent in both cases with the settlement of the walls following the 'greenfield' ground movements at the toes of the sheet piles. Thus the walls appeared to respond flexibly to the imposed ground movements in the vertical direction, presumably with the sheet piles sliding relative to each other at the clasps. There is some evidence in both cases of flattening of the settlement trough away from the tunnel centreline, perhaps because the displacement field there was insufficient to overcome friction between the clasps, enabling the structure to respond more stiffly. At the north end of the Orchard

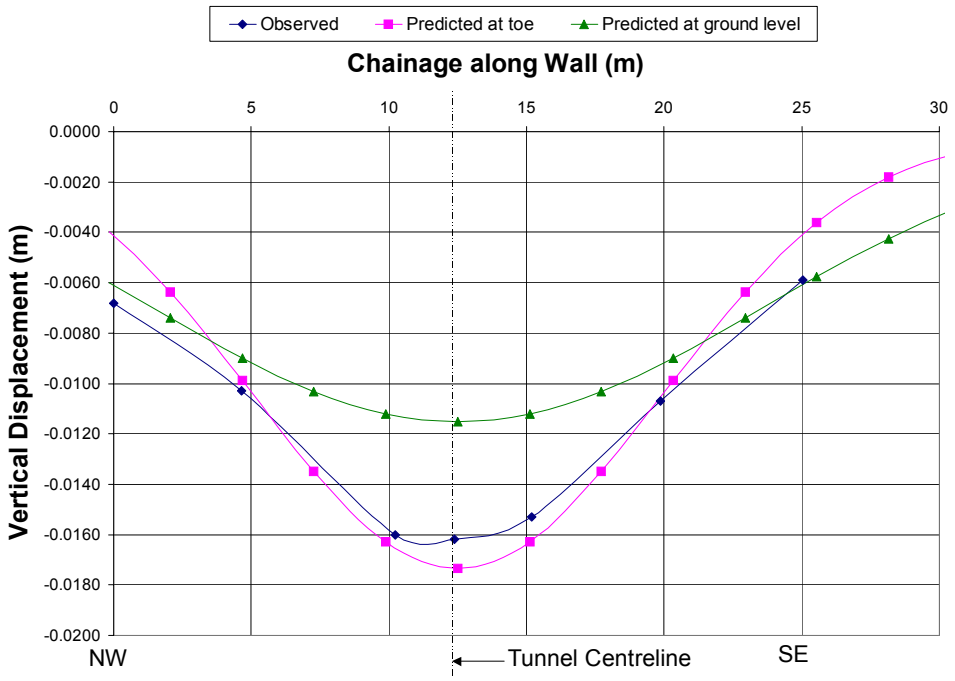

Figure 2-11: Crown Wharf River Wall: Final observed settlements and predictions assuming 4% ground loss

Wharf wall line, the structure type changes from sheet pile to concrete gravity wall, and the effect of the structural stiffness in flattening the settlement trough is evident (Fig. 2-12).

Outward movement of the top of the walls of up to 20mm was also noted. It would have been feasible in principle, and interesting, to analyse the combined tunnel, ground and

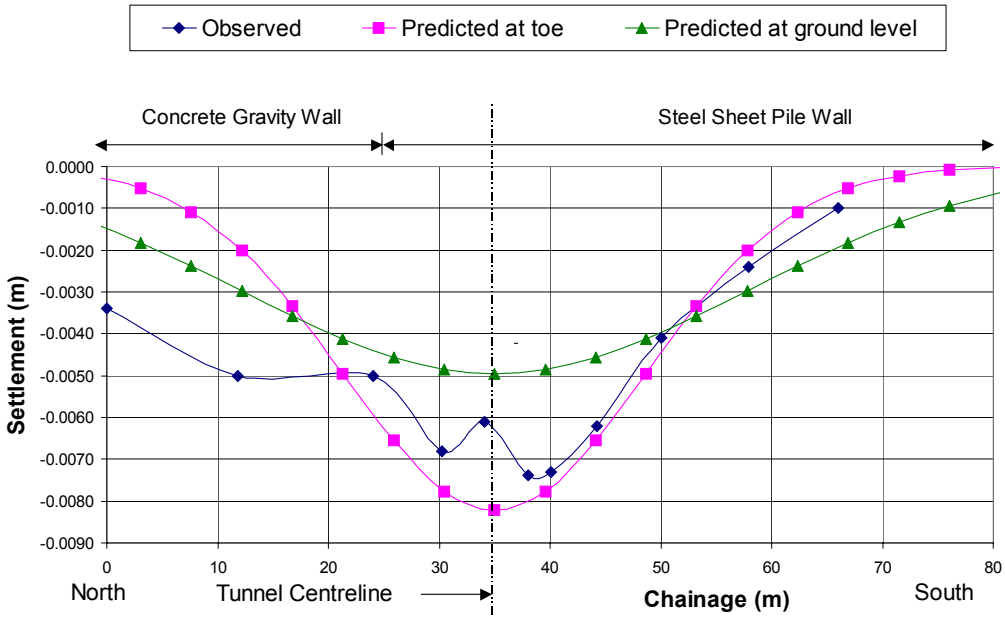

Figure 2-12: Orchard Wharf River Wall: Final observed settlements and predictions assuming 2% volume loss

wall for this project with the aim of reproducing the tilt and settlement observed. However, it was felt that, given the limitations on time, effort would be concentrated on examples of buildings rather than retaining walls and other structures. This also applied to the case of the cable tunnel crossing beneath the masonry arch tunnel at Euston, mentioned above.

A comprehensively reported case history of tunnelling under buildings that led to significant damage dates from the 1970's (Breth and Chambosse, 1975). A 6.7m diameter tunnel was constructed with sprayed concrete lining at a low cover of only 10 – 12m in stiff Frankfurt clay beneath buildings. The C/D ratio was thus only 1.5 – 1.8 and interaction with the surface could be expected. The behaviour of three buildings, two of reinforced concrete framed construction with masonry infill panels and one of load-bearing masonry, was described.

There is no explicit information given on soil properties. If a typical London clay strength profile of $s_u = 60 + 6z$ is assumed, then the stability number N is 2.8. The stability number at collapse, N_{TC}, based on $P/D = 0$, is 7.2. Hence the load factor is estimated as 0.35, implying that significant plasticity in the ground would be expected.

The concrete framed buildings responded to the settlement trough with relatively high stiffness, tilting with hardly any angular distortion. Damage occurred, however, where there was an abrupt change in stiffness, for example between a building and its annex, and was concentrated in one or two large cracks.

The masonry building interacted with the ground movements in a more complex way (Fig. 2-13). Settlements were very large, up to 150mm maximum. One wing of the building was built on a very heavy vaulted basement, which appeared to contribute towards the wing behaving fairly stiffly. However, large cracks were still caused running vertically through the full depth of the building in the hogging regions of the settlement troughs. At one point a crack runs through the vaulted basement itself, possibly aided by the tensile horizontal ground strains that should in theory occur on the hogging side of the point of inflexion. Again some cracking occurred at abrupt changes in stiffness, causing fewer but larger cracks. Because the cover to diameter ratio was small and the settlements large, it is

plausible that a failure mechanism through the soil was developing. This may be compared with the work of Liu (1997) (see Chapter 3, Section 3.2).

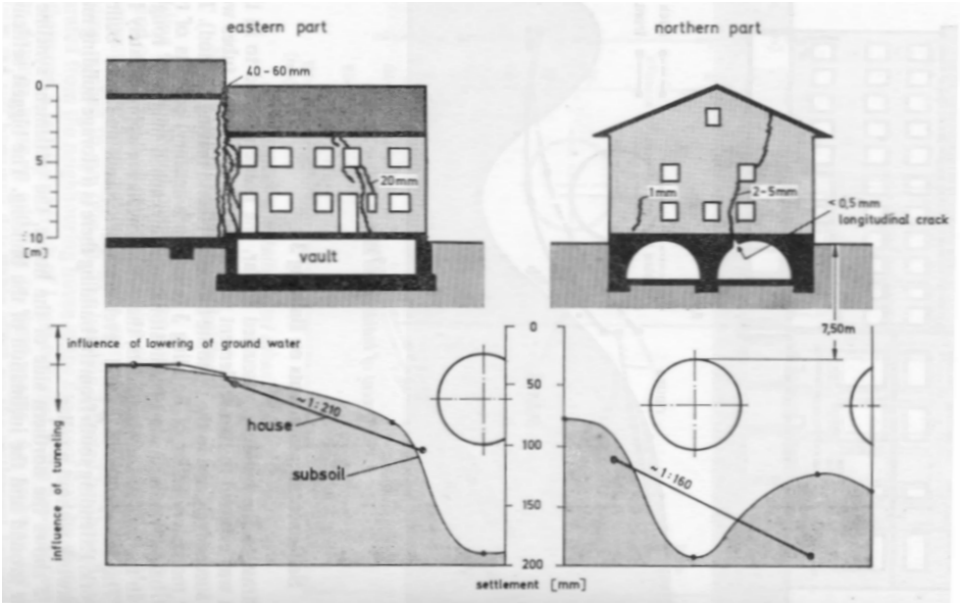

Figure 2-13: Interaction of a masonry building with vaulted basement to tunnel-induced settlements (Breth and Chambosse, 1975)

2.4.3.2 EFFECT OF THE STRUCTURE IN TERMS OF MODIFICATION OF 'GREENFIELD' SETTLEMENT TROUGH

A recent study by Potts and Addenbrooke (1997) has attempted to express the interaction between structures and tunnel-induced ground movements in terms of the modification of the 'greenfield' settlements that would have occurred, due to the presence of a building.

They carried out two-dimensional finite element analysis of a circular tunnel in plane strain with a weightless elastic building of varying stiffness, dimensions and eccentricity relative to the tunnel. A parametric study was carried out and modification factors for the 'greenfield' deflection ratios (Section 2.4.2.1) in hogging and sagging, and horizontal tensile strains due to the presence of the building were calculated. Design curves for these modification factors were proposed. The modified parameters would then be used to evaluate the maximum tensile strains in the building and hence the damage using the classification of Table 2-1.

The possibility of damage occurring and affecting the structure properties was not considered. Data from the field was not offered in support of the numerical analyses. There is also a major problem of selection of an appropriate stiffness for the building in a two-dimensional analysis.

The building was only modelled as weightless, contrasting with the work of Liu (1997) (Section 3.2) who allowed for buildings of various weights. A weightless building has the advantage of not increasing the stability number in the ground in a two-dimensional analysis, and therefore allowing reasonable representation of the ground, particularly closer to the tunnel. However, the stress field in the building and in the soil just under the building will not be realistic, and therefore effects such as stress arching, noted by Liu as being important to the structural behaviour, will be missed.

London clay soil was modelled as undrained, using a non-linear elastic-plastic constitutive model. The building was defined by its width B, eccentricity to the tunnel e, axial stiffness EA and bending stiffness EI, elastic and was in rough contact with the ground.

The tunnel modelled was intended to be a typical underground railway tunnel with a diameter (D) of 4.146m at two depths z_0 to the tunnel axis from the building foundations of 20m and 34m. The tunnel is 'deep' in both cases ($C/D > 3$; Section 2.3.3). N_{TC} calculates to be about 4.0 in both cases by the method of O'Reilly (1988).

The value of undrained strength s_u of the soil required to evaluate N was not given explicitly in the paper. Using the expression for increase of strength with depth for London clay commonly used in this project, an estimate may be obtained:

$\sigma_v = 20z_0 = 400$kPa and 680kPa

$s_u = 60 + 6z_0$ kPa = 180kPa and 264kPa

N is approximately 2.5 in both cases, giving a load factor of about 0.6. Hence it is likely that although there will be some development of plasticity in the ground, it will not be extensive, and elasticity and small strain plasticity will govern the behaviour (expected for N/N_{TC} less than 0.75).

A range of building stiffness was used in two series of analyses:

1. A wide stiffness range was covered: EI from 4320kNm^2 – 4.32x10^{10}kNm^2 and EA from 150kN – 1.5x10^{9}kN.
2. A more practicable stiffness range, representing a single slab and one-, three- and five-storey buildings assuming axial straining over the full height (an upper bound on the real stiffness). EI from 6443kNm^2 to 1.11x10^{9}kNm^2 and EA from 3.423x10^{6}kN to 20.76x10^{6}kN. Eccentricity e varied from zero to 28m, for a maximum 44m long building.

The volume loss was 1.5% in the analyses. The modification factors due to the presence of the structure were shown to be independent of volume loss.

The results from the first series showed that as the shear stiffness of the building decreases, the trough shape approaches the 'greenfield', with a trough width parameter approximately $0.5z_0$ (in agreement with the empirically predicted value). As the relative bending stiffness increases, the trough width is increased, up to maximum of $1.5z_0$ depending on the axial stiffness. Horizontal ground movements decrease with increasing axial stiffness but are insensitive to bending stiffness.

The modification factors for deflection ratios and maximum tensile horizontal strains show similar trends. It was found from the results of the second series that with zero eccentricity an upper bound envelope on the modification factor against bending stiffness could be drawn. Similar envelopes could be drawn for different values of e/B, and are presented as a design chart in the paper.

Potts and Addenbrooke aimed to offer a more advanced method to designers for prediction of settlement effects on buildings, as a development of the previous work of Burland and Wroth, Boscardin and Cording and others. However, the limitations of the assumption that the combined structure/ground problem may be treated as a modification of the 'greenfield' situation are not clarified. The numerical work is presented in isolation without reference to case history data that might confirm the physical mechanisms predicted by the analyses. In particular, the choice of the ratio e/B as a basis for quantifying

the effect of building eccentricity is not explained physically and hence is not proved to be a sound basis for a design chart. Although two tunnel depths were chosen for analysis, both would be anticipated to behave fundamentally as deep tunnels, whereas a shallow tunnel was not modelled.

2.5 Summary

It is well known that ground movements and settlements occur when tunnels are excavated in soft ground. The fundamental cause of most of the movement is 'volume loss', which takes place as the soil moves into the advancing face and radially onto the lining as the tunnel advances. The mechanism of volume loss is inherently linked to the type of tunnelling process taking place. Knowledge of the amount of volume loss expected is key to predicting the effects of tunnelling on surface structures.

Often the volume loss can be predicted based on experience of previous sites in similar ground conditions with similar tunnelling processes. Researchers have also demonstrated more rational techniques for prediction, based on a correlation of volume loss with load factor (a measure of the factor of safety of the tunnel heading against collapse) together with an allowance for workmanship effects. These in turn can often only be assessed with reference to previous experience.

The short-term settlement response of the ground is regarded as the most important for its effects on surface structures. During this phase, the soil properties may be assumed unchanged and it responds with small strain behaviour. Medium and long-term settlements due to consolidation and other effects tend to be more widely distributed, and many structures can accommodate them by creep.

A prediction technique for short term 'greenfield' settlements that is universally applied in practice is based on a survey of case history information, in which it was found that the transverse surface settlement trough due to tunnelling typically followed a Gaussian or normal distribution profile. Researchers have found that the ratio between a measure of the trough width and the tunnel depth depended chiefly on the soil type, and much effort has been expended in assessing this parameter K. The techniques have also been extended

longitudinal, horizontal and subsurface ground movements, all based on the original Gaussian model. These techniques are very convenient to use for estimating 'greenfield' surface settlements but it is hard to see how the philosophy of carrying out a survey of case history information and proposing a design curve could be extended to cases including surface structures, as the number of possible configurations and structural forms is vast, and case history data is very limited.

Closed form solutions, laboratory 1*g* and centrifuge testing have also all played an important part in gaining an understanding of the 'greenfield' response of the ground. However, these techniques are also difficult to extend to include buildings. Therefore, researchers recently have been focussing more on the use of numerical analysis, and this is also the direction taken by this project.

Any numerical analysis technique must include a credible representation of the tunnelling process, in particular the volume loss occurring. It must also use an appropriate constitutive model for the soil. It is recognised that linear elastic soil models give trough widths that are too wide, and that it is necessary to model the small strain behaviour of the soil. Models based on work hardening plasticity involving kinematic hardening have been found to be appropriate, as they can model small strain behaviour, the effect of stress history and cyclic loading.

Adding a representation of a structure to a numerical model of the ground and tunnel is still a challenging problem. Previous researchers have made simplifying assumptions, such as modelling in two dimensions, neglecting interaction between the structure and ground, and assuming the building remains undamaged. A recent researcher proposed design charts for the modification of the 'greenfield' trough to take account of the presence of the structure. These were based on numerical analysis of the building, ground and tunnel together, but the building was simplified to an elastic weightless simple beam, and the tunnel was deep.

Case history data remains an important source of information on the interaction of surface structures with tunnelling. Because the problem is complex, the quality of data required to improve the state of knowledge is necessarily high, and few projects meet the

required standard. Two of the most promising are the Mansion House and Jubilee Line Extension projects. One of the objectives of this project is to seek out data that can be used to verify a numerical model. It is particularly difficult to obtain records of sites where damage occurred to the structures, as naturally designers and contractors avoid this wherever possible. Often settlements are controlled either at the face using EPBM techniques, or above the tunnel using compensation grouting, which further increases the complexity of the situation.

This project has involved collaboration between an industrial partner, Howard Humphreys, and the University of Oxford. This industrial contact has provided opportunities for access to field data throughout the project from a number of sites. These sites were investigated and assessed against the broad criteria discussed in Chapter 1. Two of the sites, Maddox Street and Ramsgate Harbour, became the subject of detailed analysis, presented in Chapters 5 and 6. Other sites, including the Longford Street spur tunnel and the West Ham to North Greenwich cable tunnel, were not applicable to detailed analysis but nevertheless provided some interesting observations, reported on in brief in this chapter.

3 NUMERICAL MODELLING OF THE COMBINED BUILDING, GROUND AND TUNNEL PROBLEM IN TWO AND THREE DIMENSIONS

3.1 Introduction

In order to progress the understanding of building interaction with tunnelling-induced settlements, and address many of the shortcomings of current design methods for this problem, a programme of research has been undertaken in the Civil Engineering Research Group at Oxford University since 1993. The first phase, up to the commencement of this project, concentrated on developing the required tools in three-dimensional finite element analysis of buildings and tunnels. As well as working in 3-D, the main aims were to achieve realistic representations of a building, ground and tunnel excavation in one combined model, including appropriate constitutive models for stiff clay and masonry, and numerical procedures for modelling excavation, tunnel lining installation and volume loss.

In the first phase, a number of 2-D analyses of a building and ground were undertaken and reported on by Liu (1997), as a precursor to a small number of full 3-D demonstration analyses (Burd *et al*., 2000). These initial 2-D analyses are discussed in Section 3.2. Work carried out in this project to expand and enhance the phase one 2-D analyses is described in Section 3.3. In Section 3.4, three-dimensional analysis of tunnelling problems is introduced with a survey of work by other researchers. In Section 3.5, phase one 3-D demonstration analyses of the combined building, ground and tunnel are introduced and their main findings discussed.

3.2 Phase one two-dimensional analyses

The approaches outlined in Section 2.4.2 apply a known settlement trough to a building in two dimensions and calculate the maximum tensile strain resulting, assuming that the building remains elastic throughout.

Liu (1997) carried out finite element analyses applying the Gaussian settlement trough (Section 2.3.2) to a model of a building, represented in 2-D as either a plain wall or a typical façade with openings. The constitutive models used for the building were either linear elastic or elastic, no-tension, the latter having been implemented by Liu into the finite element program OXFEM (Chapter 4).

The elastic, no-tension model is macroscopic (*i.e*. the material is modelled as a continuum rather than as discrete masonry units), and uses the smeared cracking approach. Cracking is represented by altering the stiffness properties locally by reducing the tangent stiffness to near zero in a principal direction once the principal stress becomes tensile, without modelling individual cracks (Fig. 3-1).

Cracking may occur in either one or both principal directions. The cracks may also re-close, restoring full elastic properties, when one or both of the cracking strains becomes zero, in which case the strain parallel to the crack direction is retained as a non-recoverable residual strain. The average strain at integration points in a region of the mesh after cracking is a measure of the size and spacing of cracking in the structure, which may be correlated to the damage category using the approach of Burland *et al*. (1977) (Section

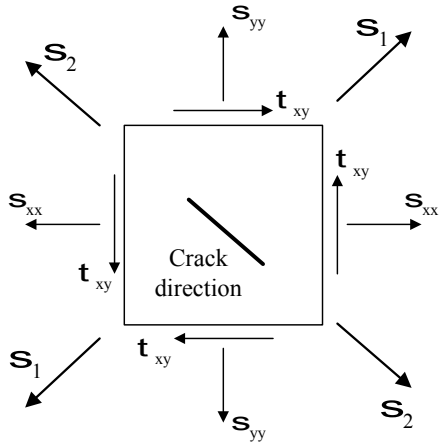

Figure 3-1: Principal stress and crack directions in masonry constitutive model

2.4.2.1).

This model for masonry has the advantage of being relatively simple to implement, with only six parameters in the input:

1. Young's modulus in compression times wall thickness (*Et*)
2. Poisson's ratio (ν)
3. Residual tensile strength (*c*)
4. Stiffness reduction ratio (ε_0^{cr}) (rate of reduction of tensile stiffness with strain)
5. Ratio between residual tensile and original Young's modulus (f_1)
6. Ratio between residual tensile and original shear modulus (f_2).

Figure 3-2 shows the stress-strain relationship. Parameters 3 – 6 are included to improve numerical stability, mitigating abrupt changes in stiffness and strength as loading is increased. They do not aim to represent physical phenomena, for example the tensile strength of real masonry. The final solution is typically found to be insensitive to the particular values of these parameters, provided stability is achieved.

Typical values of the parameters for the analysis of a 225mm thick masonry wall with Young's modulus of 2.0GPa are given in Table 3-1.

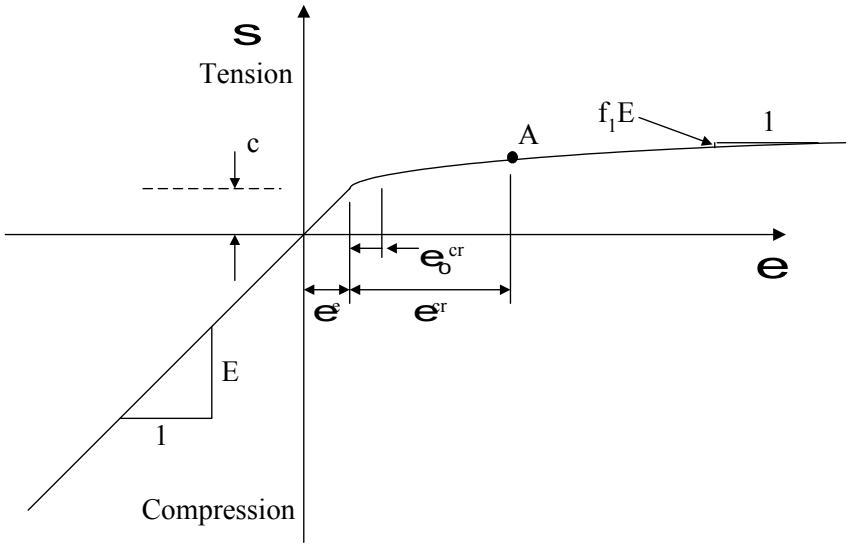

Figure 3-2: Stress-strain relationship for masonry constitutive model

Et	ν	c	ε_0^{cr}	f_1	f_2
$450.0x10^3$	0.2	10.0	$4.0x10^{-6}$	0.01	0.01

Table 3-1: Typical parameters for elastic, no-tension masonry constitutive model (units kN, m)

Because the constitutive model is highly non-linear in tension, even with the gradual reduction in stiffness, over-integration of the shape function over the element is required. This means more Gauss points are required: 16 in a linear strain 6-noded triangle rather than the usual 3. The finite element mesh itself should also be reasonably fine, leading to greater resource requirements. The masonry model was only implemented in 2-D by Liu, so cannot at present model out-of-plane effects in a façade, or solid elements of masonry (for example a mass foundation).

Liu (1997) initially carried out 2-D analyses applying a 'greenfield' settlement trough profile to a 20m x 8m *elastic* façade. The tunnel represented was 5m in diameter, with a shallow axis depth of 10m and a volume loss of 1.6% (S_{max} = 25mm, i = 5m). The resulting prediction of damage of category "Slight" was comparable to that predicted by the analytical method of Burland and Wroth (1975) (Section 2.4.2.1), with maximum tensile strain at the bottom edge of the façade in the sagging region over the tunnel centreline.

A masonry façade of the same geometry subjected to the same settlement trough showed quite different behaviour (Fig. 3-3). The response in the central part of the façade over the tunnel centreline was dominated more by shear than bending, with fairly well distributed cracking damage up to category "Severe". Above this region, the stress

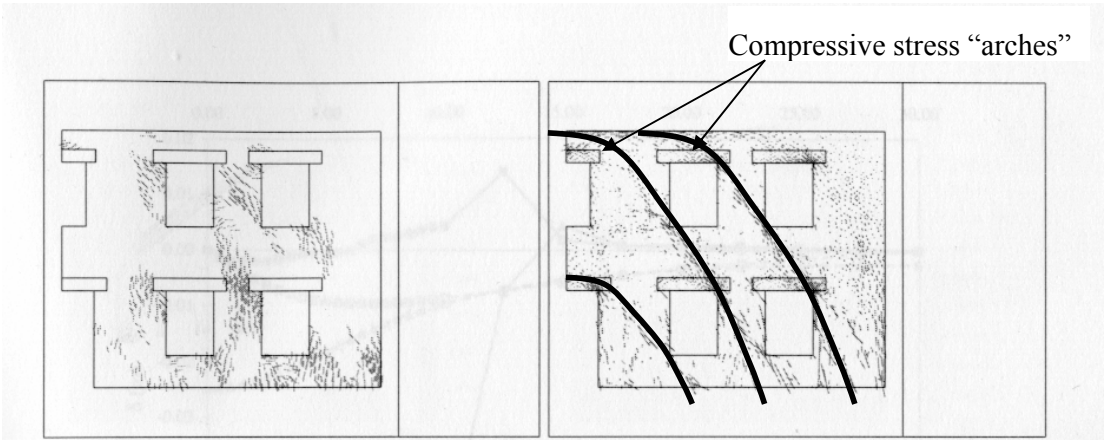

Figure 3-3: Cracking and arching behaviour of a masonry façade with openings (Liu, 1997)

distribution and direction indicated that an arch had been formed with its crown near the top and springing at the end of the façade. This arch protected the region in the top quadrant from damage. The damage distribution may have been affected by the necessity to fix the façade in the horizontal direction along the bottom edge as a restraint against it spreading horizontally, causing widespread tensile failure, a function normally performed by the underlying soil. This additional restraint may have contributed towards the shear damage over the tunnel. However, the observation of arching action was to become key in Liu's work. The openings acted as concentrators of higher stresses and cracking damage.

Liu moved on to carry out combined two-dimensional parametric studies of building interaction with tunnel settlements. The same planar 20m x 8m façade with openings was used as previously, with either elastic or masonry properties, and the tunnel was 5m in diameter with z_0 = 10m. Hence C/D was 1.5, again a 'shallow' tunnel in the terms of O'Reilly (1988). The tunnel was unlined – the ground was allowed to displace inwards during the analysis and the resulting volume loss calculated. The soil was modelled as London clay with the kinematic hardening model developed at Oxford (Section 2.3.6). A 'greenfield' settlement trough width parameter i of 7m was obtained, wider than the 5m predicted by the Gaussian model.

Davis *et al*. (1980) had shown that N_{TC} for plane strain behaviour, based on mechanisms of failure that involve the surface, lies between 2.9 and 3.4 (Section 2.3.3). Liu's analyses including building weight, the effect of which is to increase vertical stresses and hence the stability number in the soil in 2-D analyses. N varied from 1.6 ('greenfield') to 3.6 for a building of weight 30kN/m^3, calculated in accordance with O'Reilly (1988) for $C/D < 2.8$. Hence the load factor was in the range 0.5 to 1.0, higher than for a typical tunnelling situation in London clay where it is usually less than 0.5 (Macklin, 1999). For higher load factors, the amount of plasticity in the soil will tend to increase, as failure is approached.

Initially the building was placed symmetrically over the tunnel centreline. The damage was generally less than for the 'greenfield' trough imposed on the building, as expected. Again arching effects were noted, causing diagonal tensile cracking in the façade. This

time the arch compressive forces had to react against the ground instead of rigid supports, causing the ground surface to deflect downwards and outwards locally. This was enough in the sagging region to lead to net outward movement.

As the building weight increased, *N* increased and the proportion of yielded soil in the ground increased. This caused larger settlements on excavation of the tunnel. The arching forces and the magnitude and extent of damage in the façade increased.

Although it could be argued that variation of soil self-weight has little significance in practice, increasing it increased *N*, the magnitude of settlements and the resulting building damage.

An interesting conclusion of Liu's 2-D work was that the settlement trough could be described in terms of changes in settlement over short length scales under the building ("local" settlement effects) superimposed on an overall "global" settlement trough. The "global" trough shape and size was more affected by variation in building weight than by building stiffness within the practical ranges of these parameters considered.

Varying the stiffness did, however, affect the local arching behaviour in the building, which in turn determined the local settlement effects. As the stiffness was reduced, the arching action became less distinct, causing the pressure on the soil to be more uniform. The settlement trough under the building became smoother, increasing differential settlements across the footprint and therefore increasing damage. Horizontal movements also increased, and this was another contributory factor to damage. With zero stiffness, the building acts as a surcharge, and the settlement trough follows the 'greenfield' shape, increasing in amplitude as the building weight increases.

The fundamental difference in behaviour between elastic and masonry façades was also seen. In an elastic façade, stress 'cables' as well as arches can develop. The façade can therefore span fairly effectively across the settlement trough, with the bottom edge less likely to sag over the tunnel, causing damage. Hence in the elastic case, settlement troughs are flatter than in the 'greenfield', as observed by Potts and Addenbrooke (1997).

Liu also carried out a 2-D parametric study varying the eccentricity of the façade. It was found that the settlements increased to a maximum when the edge of the building

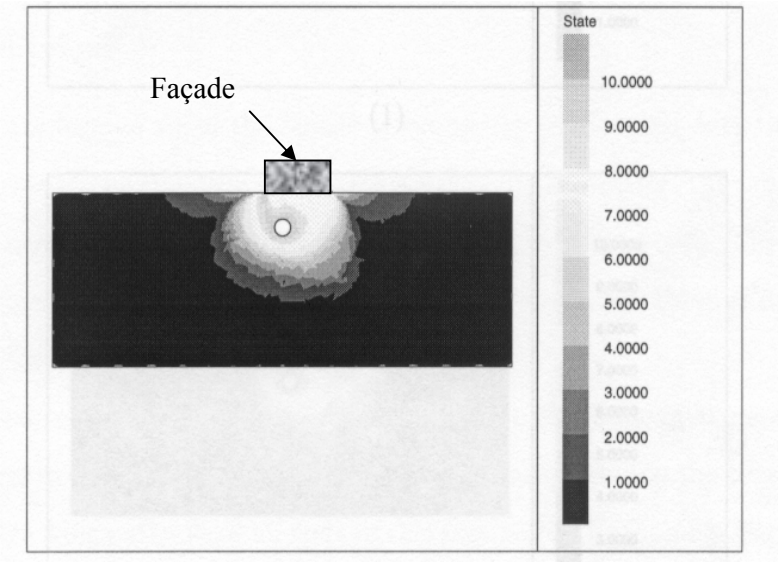

Figure 3-4: State of the soil under eccentric heavy façade

coincided with a line of potential failure through the soil from the tunnel to the approximate position of the point of inflexion of the greenfield trough at y = 5m (Fig. 3-4). This was thus an example of the building interacting with the soil to accentuate a potential failure mechanism that had a lower stability number at collapse (N_{TC}) and hence a higher load factor (LF) than the symmetric case. The effect was more accentuated for the heavier building. This kind of interaction could not be detected by an analysis that imposes a 'greenfield' trough on a building, or by the work of Potts and Addenbrooke (1997), that did not cover a wide enough range of stability number, or consider the weight of the building.

If the façade was positioned in the hogging region, the effect of the sign of horizontal strain was highlighted. When it is tensile (in the global hogging region), compressive stress arches from the building cannot form. The building is pulled apart along the bottom edge, causing vertical cracks. Where the building sags due to its own weight but is in the hogging part of the global settlement trough, the situation may be approximated as a beam with the neutral axis at the top.

The main findings of Liu's work were that the global settlement trough magnitude was most sensitive to building weight and to stability number, and that the local interaction

behaviour under the building was more sensitive to building stiffness. The latter was linked with the development of stress arches as the mechanism by which the building finds support. These findings were not discovered by Potts and Addenbrooke (1997), who did not consider building self-weight, did not model the stability number realistically and who simplified the building into a beam with no depth.

3.3 Extension to the phase one two-dimensional modelling

3.3.1 Introduction

The work of Liu (1997) discussed in Section 3.2 was important in understanding the behaviour of a masonry building interacting with the ground, and highlighted some deficiencies in the earlier work of Potts and Addenbrooke (1997) (Section 2.4.3.2). There were however some areas where it seemed that improvements might be possible. The depth of tunnel chosen, with a C/D ratio of 1.5, was shallow, and the effect of including building weight as well brought the tunnel close to failure, a problem exacerbated by the tunnel having been unlined. In addition, the 'greenfield' trough widths obtained in the analyses were consistently wider than expected from the empirical Gaussian model. Therefore, some further analyses in 2-D were performed as part of this project. In the first instance, attempts were made to improve the prediction of 'greenfield' trough width. Following this, parametric studies were carried out with a deeper tunnel, at depth ratio C/D =3, and a refined mesh.

3.3.2 'Greenfield' settlement trough width

An initial series of analyses were carried out using the same mesh as Liu (1997), with 447 nodes and 202 elements (Fig. 3-5). A lining of Hermitian beam elements (Augarde, 1997) was added to the tunnel. This enabled the volume loss to be controlled by applying a uniform shrinkage strain to the lining. The soil was modelled as London clay with the kinematic hardening model. The aim was to reproduce the value of the trough width

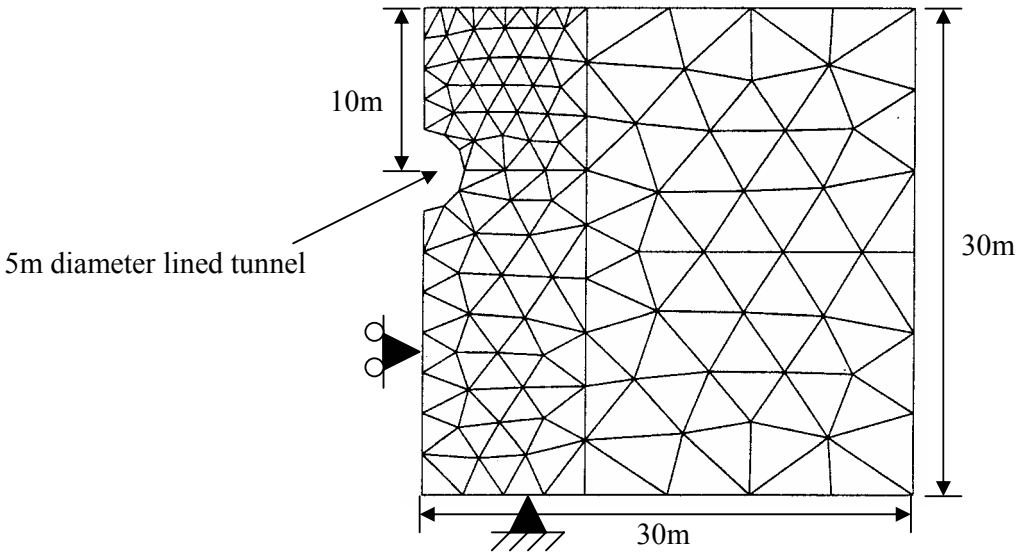

Figure 3-5: Small 2-D half-mesh (after Liu, 1997)

parameter i = 5m predicted by the Gaussian model. The plots in Figure 3-6 show the surface settlements obtained whilst varying a number of parameters in the model.

The volume loss was varied in the range 1% - 4% (Fig. 3-6(a)). The model correctly predicted the maximum settlement increasing linearly with volume loss, but the trough width parameter i was constant at 8.3m. 2% volume loss was used for the remainder of the tests.

The next parameter considered was the *in situ* total stress ratio, σ_h/σ_v. Many previous researchers, including at Oxford, have taken $\sigma_h/\sigma_v = 1$, although field data has suggested that higher values may occur in practice in London clay. It was conceivable that increasing σ_h/σ_v would have the effect of restraining the soil above the tunnel, reducing the width of the zone affected by the tunnel-induced settlements.

Figure 3-6(b) shows the results from the model for σ_h/σ_v varying in the range 1.0 – 3.0. The model is seen to be rather sensitive to increase in this parameter above 1.5, with distortion of the trough shape occurring. There is a tendency for the trough width to increase with σ_h/σ_v. An increasing proportion of the soil is yielding and losing stiffness in the material model, resulting in the instability observed.

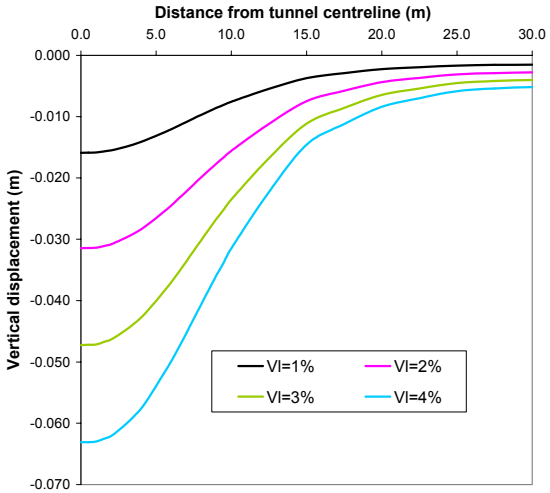

(a) Variation of volume loss

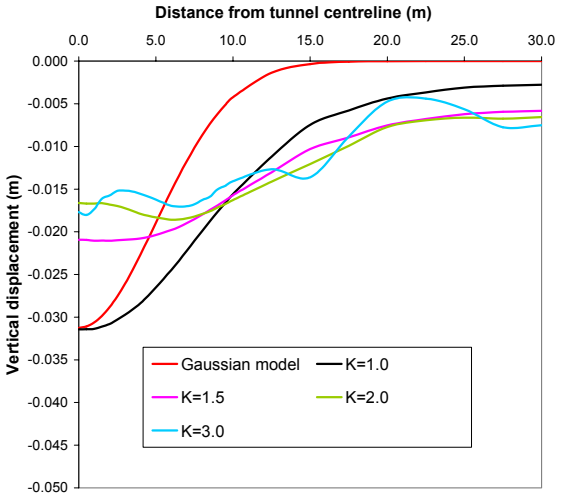

(b) Variation of *in situ* stress ratio $K=\sigma_h/\sigma_v$

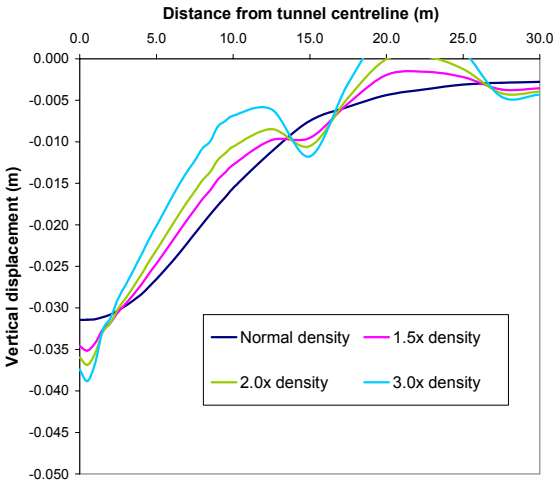

(c) Variation of soil self-weight

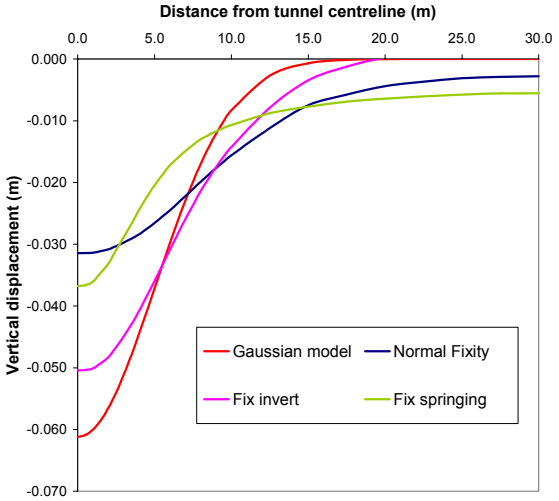

(d) Application of external fixity to lining

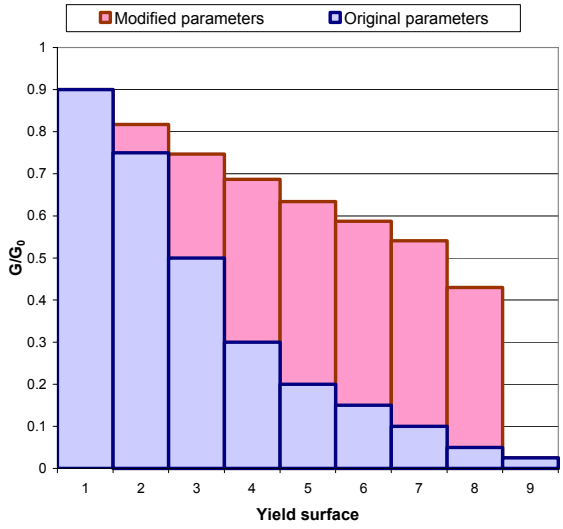

(e) Modified parameters for nested yield surface model

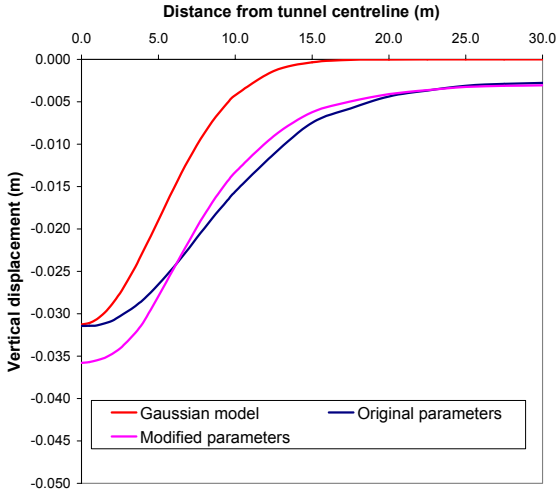

(f) Effect of modified parameters in kinematic hardening model

Figure 3-6: Sensitivity analyses of variation of parameters for small 2-D half-mesh

Somewhat similar behaviour may be seen if the density of the soil is increased, while keeping the soil strength and stiffness constant (Fig. 3-6(c)). This directly increases the stability number at the tunnel and the result is increasing instability in displacements. A value of γ_{soil} of 20kN/m^3 was used for the remainder of the analyses.

The effect of altering parameters in the kinematic hardening soil model was then explored. As discussed in Section 2.3.6, the reduction of shear stiffness with shear strain as progressive yield surfaces are reached in the model follows an 'S'-shaped relationship characteristic of most soils. In the case of the tunnelling problem, it was conceivable that the surface trough width could be narrowed by flattening the 'S' curve, increasing the range of shear strain at which high stiffness is maintained, followed by a more abrupt reduction in stiffness at high shear strain. This might have the effect of reducing the extent of yielding above the tunnel, limiting the strain to a small part of the model that had yielded fully.

The modification to the relationship is compared to the original in Figure 3-6(e). The resulting settlement trough shapes are shown in Figure 3-6(f). The trough width is reduced, but not dramatically (i = 6.8m). The effect on the distribution of yielded soil is shown in Figure 3-7, in which State 0 is elastic, States 1 – 9 are progressive yield and State 10 is full yield. Although the modified soil has generally reached a higher state over a wider region,

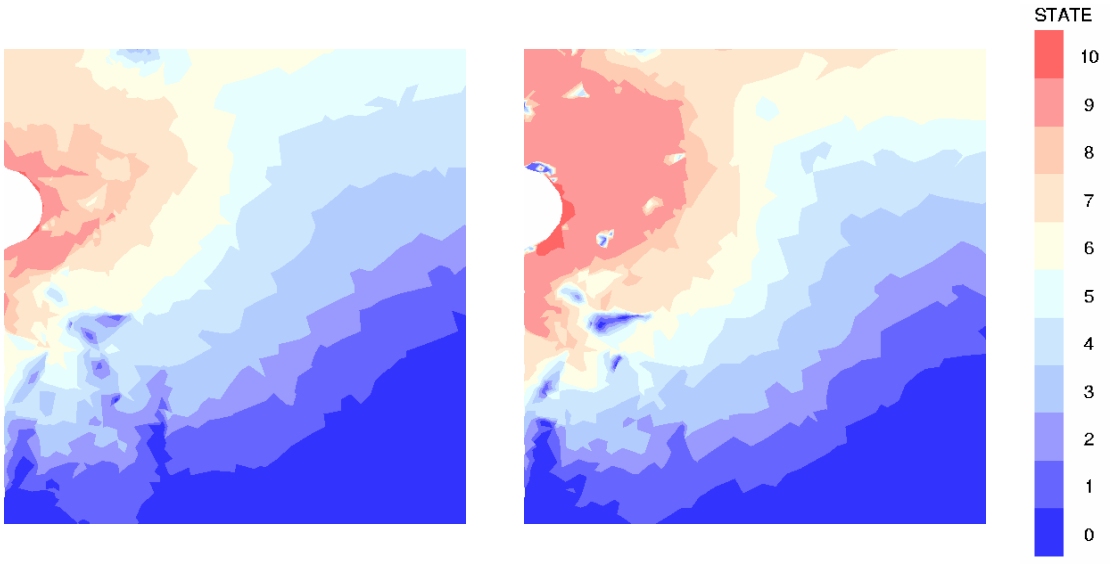

Original model parameters **Modified model parameters**

Figure 3-7: State of soil in kinematic hardening model

the higher stiffness even in state 9 has caused a narrower trough. Although this work demonstrated the sensitivity of the model to the stiffness relationship, there were no other clear reasons for proceeding to change the relationship from that already established.

It became apparent from this series of 2-D 'greenfield' analyses that modelling volume loss by uniform shrinkage of the tunnel lining was resulting in yielding and displacement of a significant region of soil beneath the tunnel (*e.g.* Fig. 3-7). This contrasted with centrifuge experiments that showed very little movement into the invert (Section 2.2.1, Fig. 2-1). Therefore, two options of introducing additional external restraint to the tunnel lining were explored (Fig. 3-8). The aim was to improve the agreement between the numerical model and the centrifuge observations, overcoming the apparent shortcoming in the numerical modelling technique of uniform lining shrinkage.

The results are shown in Figure 3-6(d), compared with the original model (with no fixity to the lining) and to the Gaussian trough shape. The effect of both options has been to reduce the trough width compared to the original model. Fixing the springing gives an i value very close to the Gaussian model, and reasonable agreement with the Gaussian trough shape in the near field, up to about y = 7m. Beyond this, however, the trough is distorted, with settlements too great in the far field, presumably because the effect of pulling up soil in the invert has passed around the fixed springing and reached the surface.

The trough resulting from fixing the invert is a better approximation to the Gaussian model throughout. The value of i is calculated at 6.3m, about 25% wider than the Gaussian

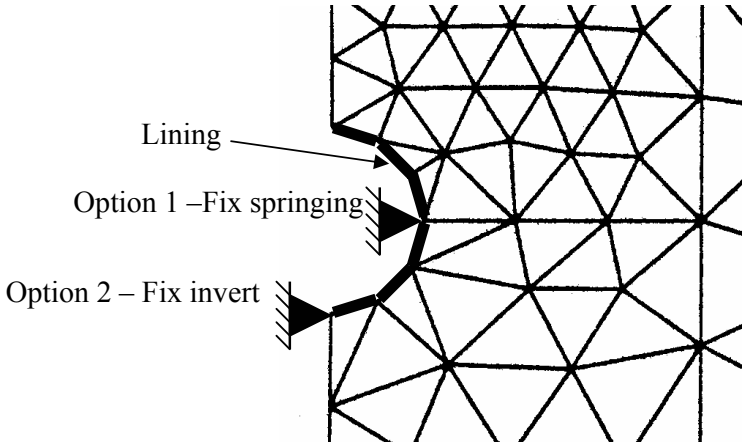

Figure 3-8: Options for external restraint to tunnel lining to improve trough width predictions

value, but still representing an improvement in the prediction of surface settlements. The approach has the apparent disadvantage of being an intervention in the modelling of the tunnel excavation process that is hard to justify, apart from its apparent beneficial effect on predictions at the surface. However, the technique of shrinking the tunnel lining uniformly to represent volume loss is itself only a modelling approximation, one which has the aim of reproducing settlement profiles away from the tunnel that are as realistic as possible. It is accepted that strains and displacements in the ground close to the tunnel will not be truly representative of the field situation.

3.3.3 Refined two-dimensional 'greenfield' model

Because of the major advance in computing power that became available during this project (see Chapter 4), more ambitious analyses could be attempted than were possible in Liu's research. In two-dimensional modelling, the boundaries of the mesh could be pushed further away and the mesh refined over a considerable proportion of its area. A larger number of analyses could be carried out more quickly, enabling parametric studies.

A new mesh was generated, with approximately 6000 nodes (12,000 degrees of freedom) and 3000 six-noded linear strain triangular elements (Fig. 3-9). The tunnel depth was increased so that the ratio C/D equalled 3, with the aim of obtaining the behaviour more typical of a 'deep' tunnel. The kinematic hardening soil model was used, with the typical London clay profile (Section 2.3.6) and the tunnel was lined to control the volume

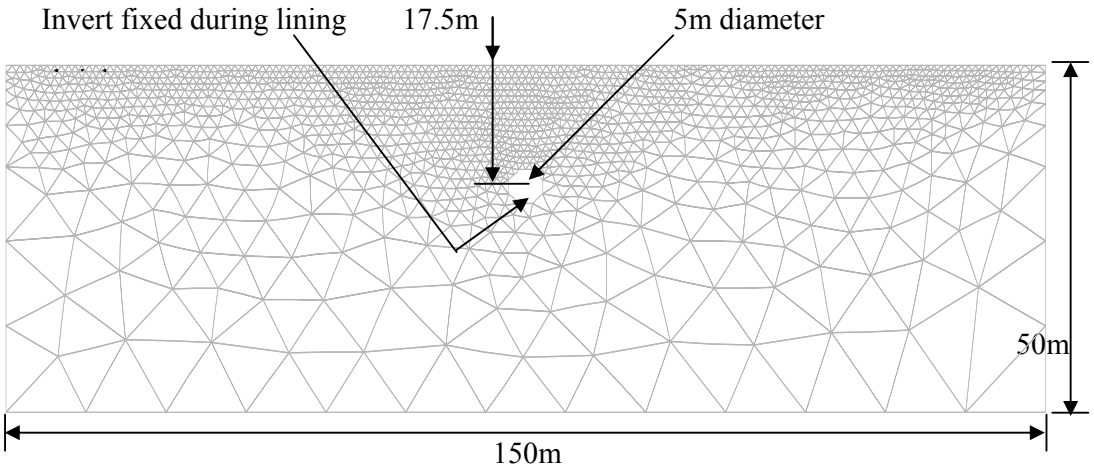

Figure 3-9: Mesh for ground for refined two-dimensional study

loss. The invert of the tunnel was fixed prior to applying the shrinkage to model volume loss, as described in the previous Section. Standard parameters of 2% volume loss, $\sigma_h = \sigma_v$ and $\gamma_{soil} = 20kN/m^3$ were used.

The 'greenfield' settlement trough obtained in the analysis is compared with the Gaussian shape in Figure 3-10(a). It shows an apparent improvement on the previous model results, with a trough width parameter i = 9.6m compared to 8.75m expected from the Gaussian model (a 10% difference).

This better performance could either be attributed to the much refined mesh, particularly in the region above the tunnel, or to the deeper tunnel, with C/D = 3 rather than 1.5, giving a better representation of the typical tunnelling problems used originally to derive the Gaussian model. To test which of these effects was dominant; a third model was analysed, with the shallow tunnel (5m diameter at 10m depth) but a refined mesh (and a fixed invert as before). The resulting trough shape (Fig. 3-10(b)) is significantly wider than the Gaussian model, with i = 8.6m, and even wider than from the original unrefined mesh of Liu (1997). Thus the conclusion is that numerical modelling of shallow tunnels will not give agreement with the Gaussian model for settlement trough widths, even with mesh refinement.

Figures 3-10(c) and (d) show the horizontal surface displacements obtained from the two refined meshes. Here, the Gaussian model prediction is based on the assumption that the vectors of ground movement are orientated towards the tunnel axis (O'Reilly and New, 1982) (Section 2.3.2). For the shallow tunnel model, both the form (allowing for the trough being too wide) and the magnitude of maximum movement are similar to the Gaussian model. For the deeper tunnel model, the form is similar but the maximum movement is about 30% larger than expected, implying that the effective focus of ground movements is a point about 6m above the tunnel axis, 11.5m below the surface.

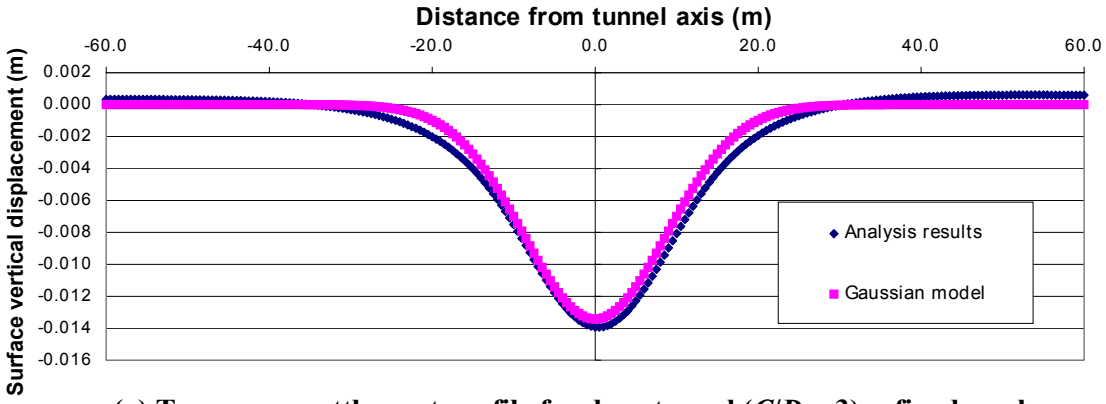

(a) Transverse settlement profile for deep tunnel (C/D = 3) refined mesh

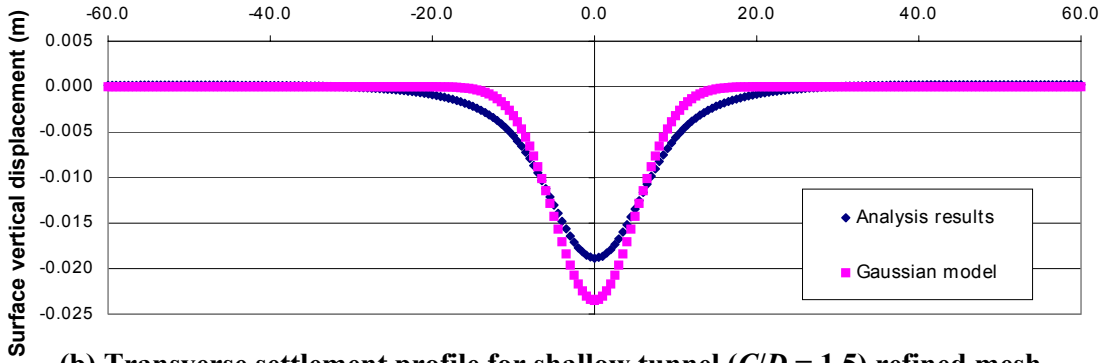

(b) Transverse settlement profile for shallow tunnel (C/D = 1.5) refined mesh

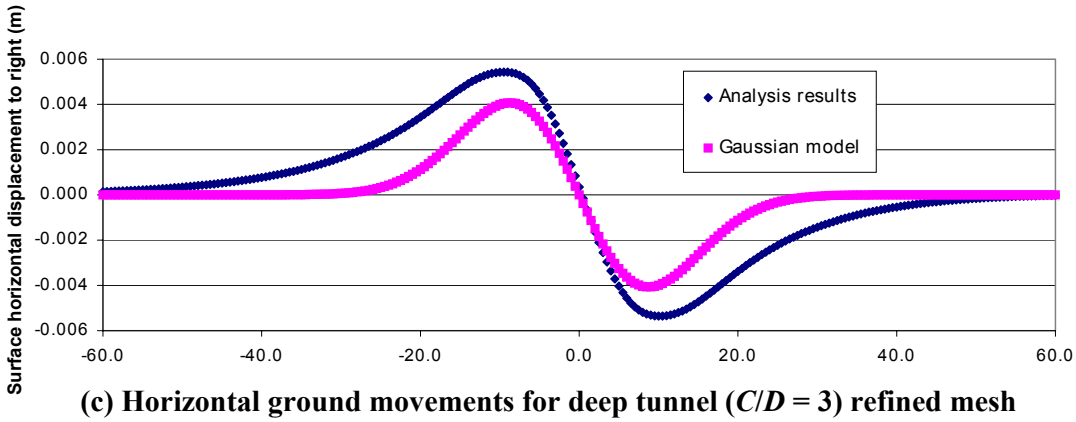

(c) Horizontal ground movements for deep tunnel (C/D = 3) refined mesh

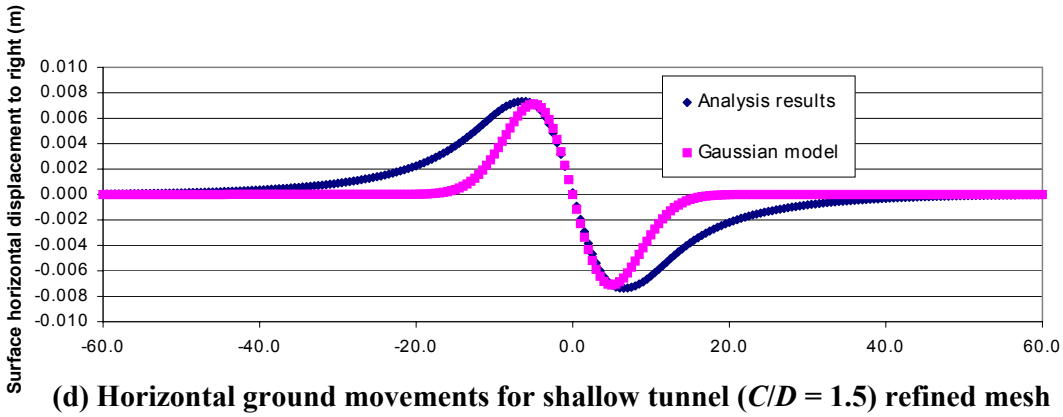

(d) Horizontal ground movements for shallow tunnel (C/D = 1.5) refined mesh

Figure 3-10: Ground movement profiles for refined mesh 2-D analyses and comparison with Gaussian model

3.4 3-D modelling of tunnelling problems by other researchers

3.4.1 Linear modelling

Hanafy and Emery (1981) moved beyond 2-D plane strain modelling by conducting axisymmetric analyses of the excavation of a tunnel and the switching on of lining elements. Their main interest was in the lining loads calculated when the lining was erected at increasing distances behind the tunnel face.

Lee and Rowe (1990a,b) carried out three-dimensional finite element analyses of the advance of a shallow tunnel heading through linear elastic soil. The model had 15,000 degrees of freedom, which required considerable computing power for the time, thus limiting the number of analyses that could be undertaken. Cases of unlined and of rigidly lined tunnels were compared. They demonstrated a heave occurring ahead of the advancing face, something not readily reproduced in a 2-D plane strain analysis. Shear stresses ahead of the face were found to be less significant than behind. The state of stress ahead of the face was reasonably close to triaxial compression, and behind the face to triaxial tension. The field data of Lee and Rowe (1991) was back analysed, and reasonable agreement for surface settlements was obtained, although the settlement troughs predicted were too wide, as is commonly the case for elastic analysis (also Dias *et al*., 2000).

Eisenstein *et al*. (1994) carried out 3-D finite element analysis of an advancing tunnel in linear elastic soil. A lining was erected at a distance equal to the tunnel radius behind the face. They recorded relief of vertical stress above and below the tunnel, and arching of the soil over the tunnel.

Swoboda and Hafez (1995) were interested in the behaviour of tunnels with sprayed concrete linings, relevant after the collapse of station tunnels during construction at Heathrow in 1994. Three-dimensional analysis was used for junctions between tunnels. A detailed constitutive model for the concrete lining was used, with the lining modelled by three layers of shell elements, each representing a stage in the application and curing of the sprayed concrete. The analysis was successfully completed, although site data for comparison was lacking.

Elastic modelling has been popular in rock mechanics applications. Particular areas of interest have been stresses in the lining at junctions between tunnels and stress concentrations in the lining at interfaces between soil strata. Clark (1993) analysed the excavation of a shaft, modelled by removing solid elements from the tunnel and switching on thin shell elements to represent the lining, tied to the surrounding soil by multi-point constraints.

3.4.2 Non-linear modelling

Mair (1993) and Gunn (1993) first pointed out the need for 3-D non-linear analyses to solve tunnelling problems. A few researchers have attempted this more recently, finding in the process a much greater requirement for computing resources than for linear analysis, due to the need to apply the load over a number of increments.

Netzel and Kaalberg (1999) performed three-dimensional analyses of masonry buildings for assessment of settlement damage risk due to the planned construction of the North-South Line in Amsterdam. The buildings under consideration were terraces of masonry houses on piled foundations, which were modelled as planar façades. However the buildings were not modelled combined with the ground. Instead, the empirical predicted settlement trough was applied to the toes of the piles. The material model for the façades was an elastic tension-softening model, elastic up to a tensile stress of 0.3MPa, followed by linear softening with strain to zero stiffness after 0.10% to 0.15% strain. The representation of the buildings was fairly detailed, including typical openings and internal walls. A parametric study was carried out, varying tunnel position and depth relative to the building, although the tunnel orientation was kept parallel to the building frontages. The results were compared with empirical predictions (Burland *et al*., 1977) (Section 2.4.2.1). The main conclusions were that openings acted as stress concentrations to increase damage significantly, and that the longitudinal settlement trough caused an important mode of cracking damage in the front façade of the building. These conclusions justify a three-dimensional non-linear analysis.

Soga *et al*. (2000) report on a different three-dimensional non-linear modelling technique. The advance of a tunnel heading through soft ground is modelled not by excavating elements from a large block of soil but rather by advancing the surrounding soil past a stationary tunnel heading. This is achieved by attaching the mesh to the tunnel heading and progressively advancing through the mesh data representing the soil properties, stress and strain states and external loads. There is no proposal in their paper to model buildings explicitly, which apparently would require re-meshing of the model at each excavation increment in order to advance the building geometry past the tunnel heading.

3.5 Phase one three-dimensional analyses

Augarde (1997), Liu (1997) and Houlsby *et al.* (1999) describe in detail the modelling procedures developed at Oxford up to the start of this project. Special features associated with these procedures have been incorporated in the finite element analysis program OXFEM developed at Oxford (Section 4.3). The main features of the three-dimensional modelling technique (as shown in Figures 3-11, 3-12 and 3-13) are as follows:

1. Ten-noded isoparametric tetrahedral elements were used for the ground. These elements have been found to have good performance against locking in analyses conducted at constant volume, *i.e.* undrained.
2. An unstructured mesh (sometimes known as a ‘free’ mesh) was found to be desirable for the ground to enable an increase in mesh density in regions close to the tunnel and building footprint where more detail is required. This required the use of commercial mesh-generation software.
3. A representation of a load-bearing masonry building in three dimensions was sought. It was conceivable that 3-D continuum elements could be used. However, because the primary action of a load-bearing wall is in its plane, it was felt to be possible to simplify the model, significantly reducing the number of degrees of freedom, by using 2-D plane stress elements.

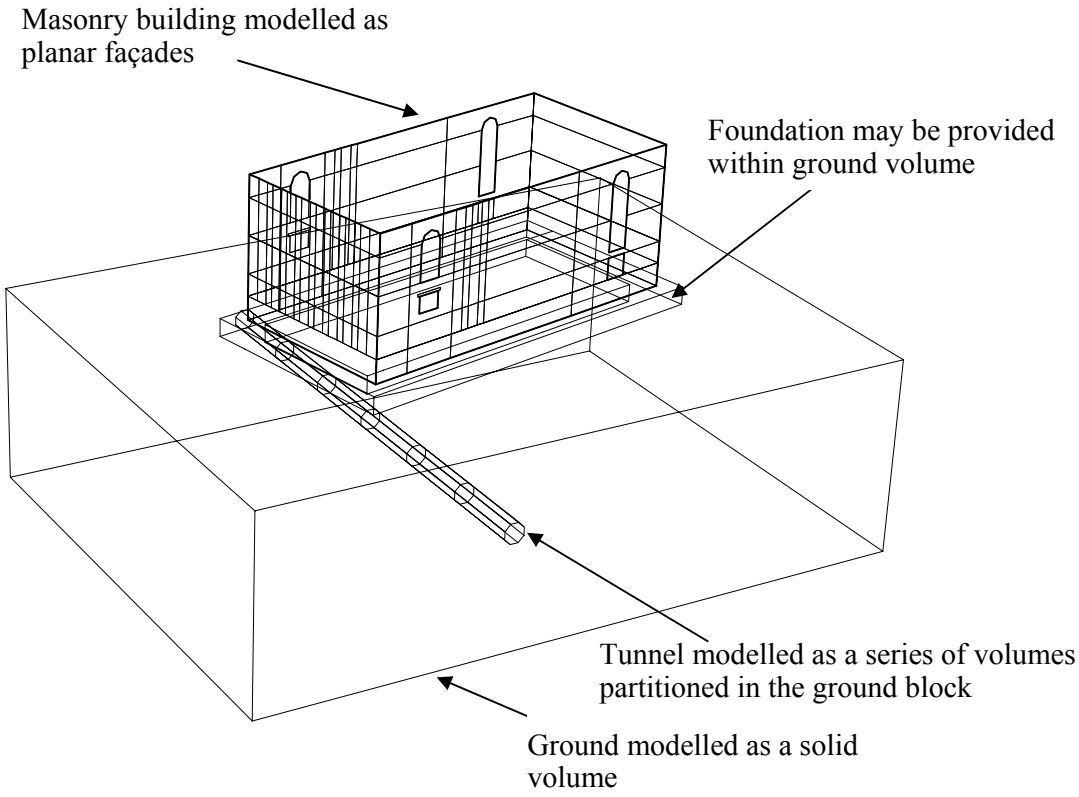

Figure 3-11: Geometry of typical combined three-dimensional model of ground, tunnel and building

4. To connect 2-D façades, and to facilitate the use of 2-D and 3-D finite elements in the same mesh, a tying scheme was developed to give the displacement constraints required (Liu, 1997; Houlsby *et al*., 2000).
5. The advance of the tunnel heading was modelled by excavation of soil elements and addition of elements representing a lining. The excavation is implemented by applying, on the boundary of the excavation, nodal loads calculated as the resultant of the body forces on the model after excavation has taken place, minus the nodal loads due to the stresses that existed prior to excavation (Augarde *et al*., 1995). The soil elements that have been excavated are removed from the list of elements active in the mesh for the next loading stage. Elements to model the lining are added to the list, so that their stiffness and body force terms are included for the remainder of the analysis.
6. The tunnel lining must provide sufficient axial and bending stiffness to stabilise the surrounding soil in the model. Although continuum elements could be used, shell

elements should in theory achieve the same results but with a simpler mesh. Augarde (1997) implemented a faceted shell element, in which the plate components overlap (Augarde *et al*., 1998). This overcame the problem encountered with most shell elements, that they possess both translational and rotational degrees of freedom, which cause numerical problems when attached to elements containing only translational freedoms.

7. The effect of volume loss during the tunnel construction is modelled by shrinking the lining in the tangential direction, reducing the radius of the tunnel (Figure 3-13). Although this method may produce unrealistic stresses and strains both in the lining and the ground close to the tunnel, at greater distances from the tunnel the results should be similar to those calculated by techniques that model the tunnel construction in more detail, *e.g.* Lee and Rowe (1990a,b).

Both Liu and Augarde also carried out a small number of three-dimensional analyses. These used a shallow 5m-diameter tunnel at 10m depth, combined with a building consisting of a box of four façades that was 20m x 10m in plan and 8m high. Cases of the tunnel running symmetrically under the building, and at a skew of 45^{o} under one corner were examined. The main observations of Augarde (1997) were that:

1. There may be additional restraint against damage if both points of inflexion of the settlement trough are spanned. More studies varying both the skew angle and location of the building were needed to confirm this.
2. When the tunnel heading was advanced incrementally, damage to the rear façade is caused before the tunnel reaches it by movements transmitted from the front via the side walls. The result is greater final damage to the rear façade.

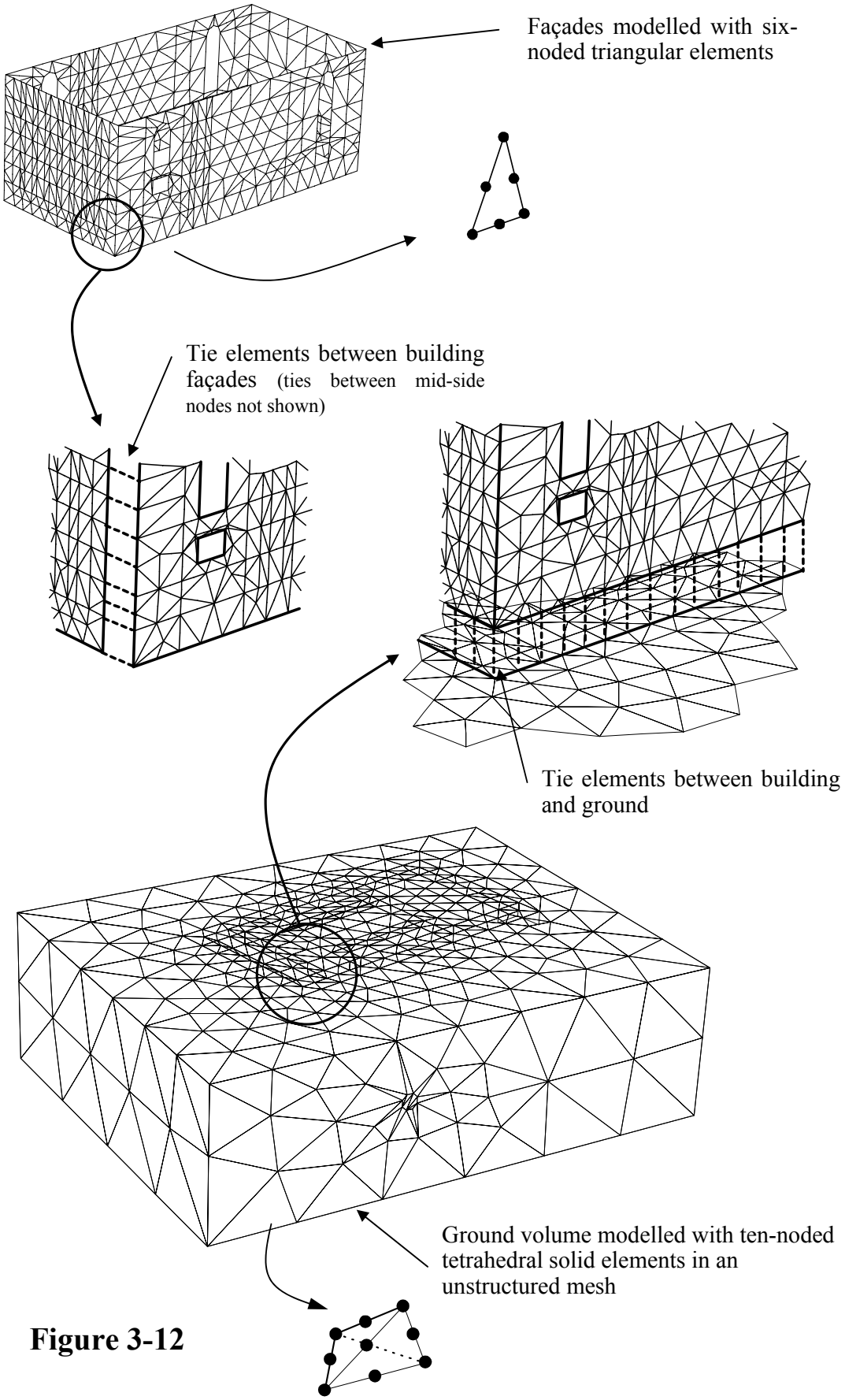
Façades modelled with six-noded triangular elements
Tie elements between building façades (ties between mid-side nodes not shown)
Tie elements between building and ground
Ground volume modelled with ten-noded tetrahedral solid elements in an unstructured mesh

Figure 3-12

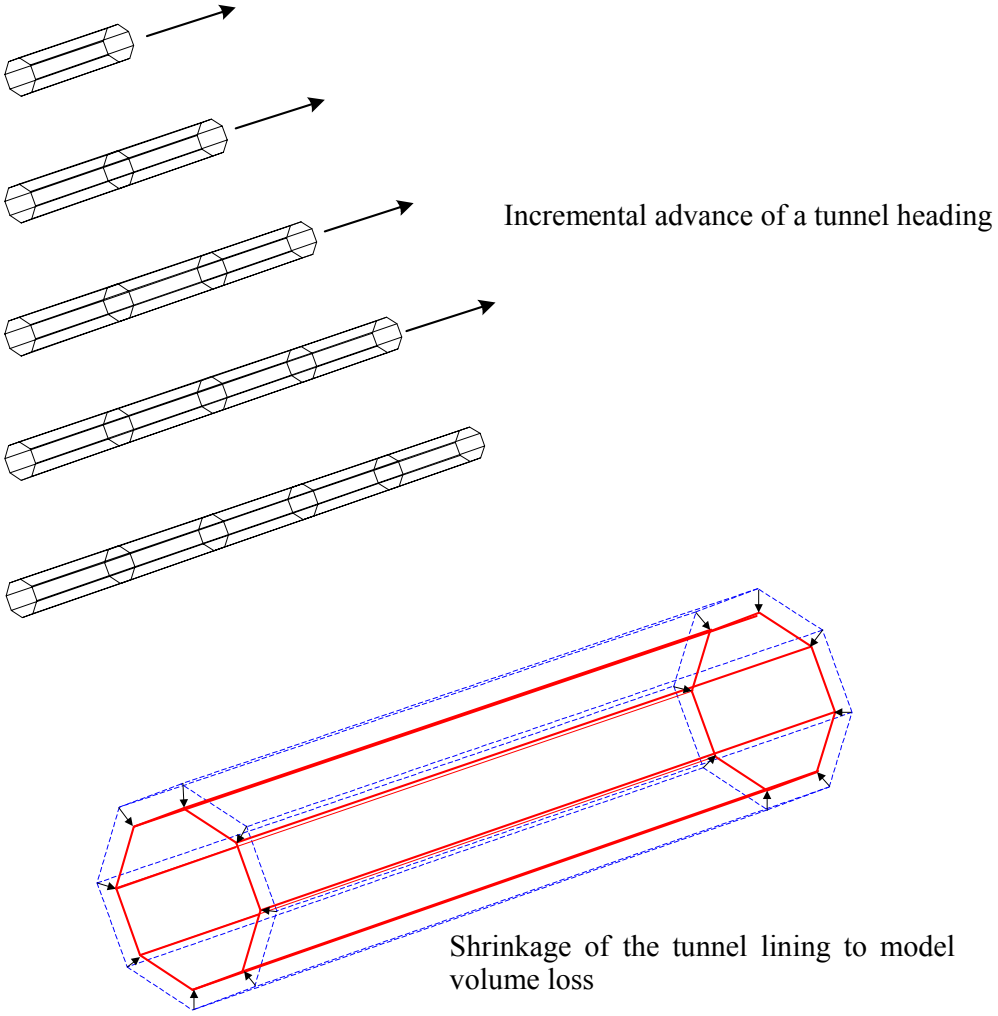

Figure 3-13: Modelling of the tunnel lining

3.6 Summary

The previous chapter showed how numerical modelling is the method of research most able to extend predictions of tunnelling effects from the 'greenfield' to cases involving surface structures. Any analysis that does not consider the surface structure combined with the ground can be regarded as simplifying the problem to such an extent that important physical mechanisms may not be picked up.

The emphasis of phase one of the research programme at Oxford has been to model the building and ground together from the start, with realistic and credible representations of the building, ground and tunnelling process, and selecting appropriate constitutive models for each component of the model. Initially in phase one, two-dimensional plane strain analyses were carried out, and further 2-D analyses were also performed as part of this project.

The phase one 2-D analyses demonstrated the use of a masonry material model for the building, which allows cracking and degradation of stiffness in tension and hence can represent the effect of damage to the building. Interaction between the building and ground was obtained, and the effects of variation of both building weight and stiffness were examined. Increased building weight increased the magnitude of settlements and damage, and if the building was positioned in a location such that it interacted with the mechanism of shear planes in the ground above the tunnel, even larger settlements and rotations of the building took place. It is likely however that the effects of building weight were exaggerated, because in a 2-D analysis the vertical stress due to the weight of the building is transferred down to the tunnel, increasing the load factor at the excavation and therefore the amount of plasticity generated in the soil. This is an inherent disadvantage of any 2-D analysis. Similar arguments apply to the building stiffness, which is hard to estimate for a 2-D analysis.

The phase one 2-D analyses exhibited the perceived disadvantage that the ‘greenfield’ settlement trough was too wide compared to the Gaussian model. In this project, this issue has been reassessed. Vastly increasing the mesh refinement did not improve the situation. However the phase one tunnel was relatively shallow, with a ratio of cover to diameter (C/D) of 1.5. By increasing C/D to 3, a much better agreement with the Gaussian model was obtained. This raises the possibility that tunnels with low cover give wider settlement troughs than conventional Gaussian predictions would suggest (and, in fact, that the Gaussian model is conservative in these situations in its predictions of maximum curvature at the ground surface). This issue has not been researched in any further detail in this project, as most documented case histories and most practical situations in tunnelling for

infrastructure involve deeper tunnels. One of the three cases analysed in 3-D for this project, the Ramsgate Harbour Tunnel, involved a very shallow tunnel, and special measures were required in order to reproduce the observed ‘greenfield’ settlement trough. It is strongly recommended that researchers attempting to validate numerical models of tunnelling situations against ‘greenfield’ data draw a clear distinction between shallow and deep tunnels. It also recommended that the Gaussian model be treated with caution when applied to shallow tunnels, for which it may be conservative.

Tunnelling beneath a surface structure is inherently a three-dimensional problem, and in order to obtain a realistic representation of the stresses in the building (and their effects on building behaviour, including arching), the stresses in the soil, the stability number at the tunnel and hence the response of the soil mass and the effect of building stiffness, a 3-D combined analysis is required. This has been the emphasis of the research programme at Oxford. In phase one, modelling procedures were developed for tunnel excavation, lining and volume loss, a building consisting of two-dimensional façades tied to the ground (to represent a traditional load-bearing masonry structure) and a constitutive model for masonry. Demonstration analyses showed the feasibility of the techniques. One of the key objectives of this project is to investigate how applicable these techniques are to real sites and how practicable they are to apply.

4 IMPLEMENTATION OF NON-LINEAR THREE-DIMENSIONAL ANALYSIS FOR THIS STUDY

4.1 Introduction

This chapter is concerned primarily with the practicalities of carrying out three-dimensional non-linear finite element analysis, the difficulties encountered and the lessons learnt. The process is described as consisting of pre-processing, analysis and post-processing phases. The performance of the hardware used on the project is discussed, in particular the benefit of parallel processing on the Oxford Supercomputer. At the end the principal lessons learnt are summarised.

Finite element analysis consists of the discretisation of a continuous system into a mesh of nodes and elements of finite size and the assembly and solution of the set of equations:

$$[K] . \{u\} = \{P\} \qquad (4\text{-}1)$$

Where:

$[K]$ is the stiffness matrix for the system evaluated at the nodes

$\{u\}$ is the vector of displacements at the nodes

$\{P\}$ is the vector of applied loads

The number of degrees of freedom of the system is the multiple of the number of nodes and the number of displacement freedoms at each node, which may be translational or rotational and which may vary between different regions of a mesh. The number of degrees of freedom defines the rank of the matrix $[K]$ and determines the computing resources required in solving the matrix equation given above. The move from two-dimensional to three-dimensional analysis does not change the basic nature of the calculation, only its size.

In practical problems of any size, the global stiffness matrix $[K]$ is assembled from the contributions of the individual element stiffness matrices. A stiffness matrix $[K_e]$ for an element is derived from the equation

$$[K_e] = \int [B^T][D][B]dV \qquad (4\text{-}2)$$

Where:

[B] is the strain-displacement relationship relating the strains $\{\varepsilon\}$ within the element to the displacements $\{u\}$ of the nodes, *i.e.* $\{\varepsilon\} = [B] \cdot \{u\}$

[D] is the material constitutive matrix, by which the stresses $\{\sigma\}$ are calculated from the strains at the integration points: $\{\sigma\} = [D] \cdot \{\varepsilon\}$

For constant strain elements, triangles in two-dimensions or tetrahedra in three dimensions, the terms in $[B^T][D][B]$ are all constants, so $[K_e]$ may be calculated directly. However, for higher order elements, numerical integration is required to obtain $[K_e]$. Gaussian Quadrature is often used, in which sampling points (Gauss points) are located in the element and each given a weighting. A polynomial of degree $(2n\text{-}1)$ is integrated exactly by n-point Quadrature.

In general, finite element meshes are stiffer than the theoretical continuum mechanics solution. As the finite element mesh is refined, the solution should approach that of the theory.

In linear finite element modelling, the terms in [B] and [D], and therefore $[K_e]$ are constant throughout the analysis. This means that $[K_e]$, once calculated, may be stored and reused through the whole analysis with no loss of accuracy.

In many practical problems the material constitutive behaviour is such that the [D] matrix is not independent of strain, giving rise to a nonlinear problem. Most civil engineering materials, such as soil, rock, masonry and concrete exhibit this phenomenon. Materials range from ‘weakly’ non-linear, in which the variation of stiffness with strain is continuous, to ‘strongly’ non-linear, in which abrupt changes in stiffness may occur; for example in the cracking behaviour of concrete or masonry.

This variation of the [D] matrix makes it necessary to re-evaluate the stiffness matrix at intervals during the analysis, and also to apply the load in increments that are small enough to reflect the stress-strain behaviour of the material, otherwise inaccurate results will be obtained.

4.2 Pre-processing techniques

In the pre-processing stage in finite element analysis, the physical problem is idealised and described to the computer in terms of its geometry, element topology, material properties, external loads and excavation sequence. The resulting data is the input to the analysis phase (Section 4.3).

The first stage in pre-processing is to examine the site under consideration and determine the geometry, ground and structure material properties and excavation sequence for the tunnel. It was found helpful to draw up a set of hand sketches of the geometry of the tunnel and building to form the input to the computer model. Important decisions are required concerning the level of detail at which to model the site, in particular the building, and an advance in understanding of this issue was sought during this project. The design of the model should also cater for the information required from it. For example on this project, output from the models was sought at the known locations of the site instruments, for comparison. The choice of tunnel increment size might be determined by how often in time monitoring data is available, compared to the rate of advance. When using the technique for predictions, output from the model is required with sufficient accuracy from the correct locations and at sufficient frequency to assist in applying the observational method during construction.

4.2.1 Software requirements

The assembly of a finite element model of the complexity being explored in this study requires a number of relatively sophisticated software tools. Most of this sophistication is related to the need to model in three dimensions, rather than two as in most previous

studies. Experience gained on this project has highlighted the following as necessary elements for any pre-processing software:

1. Creation of problem geometry in three dimensions. The typical level of complexity achieved in this project was to produce a block of ground with a single straight tunnel aligned along a principal axis of the block. The tunnel itself was usually sub-divided into a number of (say 5 – 10) excavation stages. Each of the façades of a typical building, which usually included openings and other features, was modelled in this study as a separate entity, although the building could conceivably be modelled as one.
2. Mesh generation. Meshes are created on the required surfaces and volumes. For efficient use of computing resources during the analysis stage, unstructured meshes are desirable (Section 3.5), which cannot be meshed by hand and which require a more sophisticated mesh generator than for regular meshes. It is highly desirable to have control over the local element size at any location in the model, to overcome problems in fitting the mesh to the geometry and obtaining solution convergence, and to keep the overall mesh size within limits. The additional facility to prescribe nodes at certain locations on the boundary of individual entities (ground, building façades) was required in this study in order to obtain coincident nodes when the entities were combined into one finite element model.
3. Checking the mesh. Even with the most advanced 3-D mesh generator, experience has shown that it is vital to run checks on the mesh produced. These include checking for voids or overlapping elements by calculating the overall mesh volume, and optimising solution convergence and accuracy by checking for elements that violate set criteria for shape, aspect ratio or distortion.
4. Application of boundary conditions. Boundary conditions may be applied to single nodes, lines of nodes along an edge or to a whole surface. In this study, only restraints of translational degrees of freedom were required.
5. Partitioning of the mesh and the facility to specify different element types or material properties in different parts of the mesh.

6. Obtaining information about the mesh, for example node and element numbers or node co-ordinates, in order to specify output from the analysis at certain nodes, elements or degrees of freedom.
7. Output of the mesh information (nodes, elements, restraints etc.) in a form that may be used or manipulated by the analysis software, and preferably also easily understandable by the user.
8. Processing of the mesh information in order to produce an input file for the analysis software, if not already formed in (7). In this study, a number of separate utility programs written in FORTRAN 90 were used for this purpose.

4.2.2 Use of the SDRC I-DEAS Master Series suite of programs

This software package was used for preparing the mesh for analysis, carrying out steps (1) – (7) in Section 4.2.1 above. It is a sophisticated Computer Aided Engineering package, produced by the Structural Dynamics Research Corporation of the U.S.A. The 'Master Series' title refers to the series of related Applications in the suite- Design, Drafting, Simulation, Test, Manufacturing, Management and Circuit Board Design. Most of these Applications offer facilities in solid modelling.

The Simulation Application provided all the tools needed for this project. This Application offers a number of Tasks: Master Modeller, Master Assembly, Boundary Conditions, Meshing, Model Solution, Post Processing, Optimisation and others. The Tasks encompass thermal, vibrational and dynamic analyses as well as static analysis. In this project, the Master Modeller Task was used to create the 3-D solid geometry (step (1) above). Figure 4-1 shows an example of a 'wireframe' of the solid geometry obtained during this Task. The Boundary Conditions Task dealt with step (4). The Meshing Task completed steps (2), (3) and (5) – (7). In step (7), the mesh was output in the format used by the commercial finite element package ABAQUS, which satisfied the requirements of being a readable and concise text format for further manipulation.

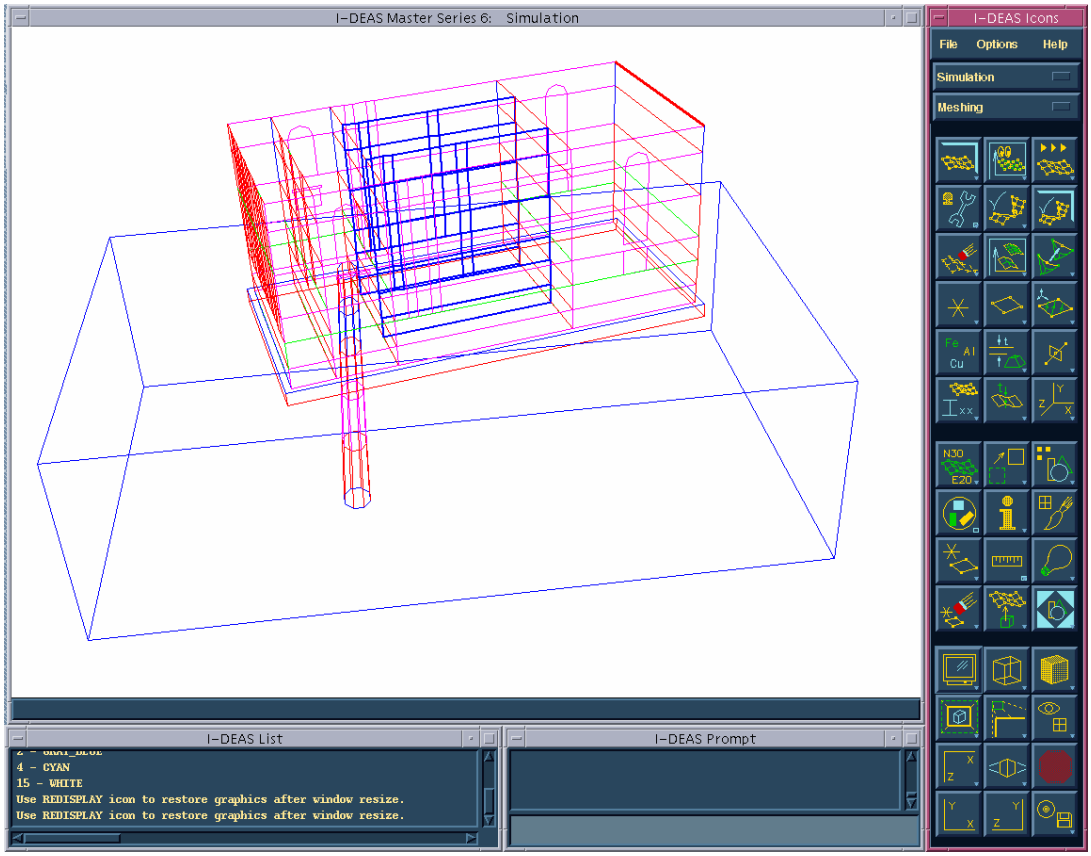

Figure 4-1: Three-dimensional geometry of Mansion House model, generated in SDRC I-DEAS Master Modeller

The Model Solution Task may be used to conduct a finite element analysis of the assembled mesh, as an alternative to exporting the mesh for use by other software. In the early stages of this project, simple analyses were carried out to explore its capability. Although user-specified material models are possible, in practice only variations of elastic-plastic models are feasible, and not the kinematic hardening model or the masonry model used for this project. In addition, more unusual element types such as the faceted shells are also not available. Thus I-DEAS itself could not be used for the analysis stage, but only for pre-processing.

The I-DEAS Master Series package is a very powerful one, and as such requires a significant investment in time for familiarisation. The lesson learnt on this project was that the best approach for learning how to use the package is to work through the on-line tutorials that provide comprehensive guidance on all the features of the Master Modeller,

Boundary Conditions and Meshing Tasks. Adopting this strategy, it should be possible to become familiar with I-DEAS for this application in a period of two weeks.

Developing and storing a three-dimensional solid geometry and mesh is a complex task. The software is often unable to 'undo' sophisticated operations. In addition the software may fail to undertake some operations correctly, leading to the corruption of the model file. An example of this is drawing the footprint of the building on the ground after partitioning the tunnel within the ground, when the program was liable to 'forget' the separate volumes that make up the tunnel. Therefore careful planning and a methodical approach to the execution of the modelling process were required.

Other lessons applicable to any 3-D mesh generator were also learned:

1. The smallest features of the model, in this project typically the tunnel, should always be meshed first.
2. Complex geometry or very small features, of size say 1% of the whole model, should be avoided as they can cause meshing errors.
3. Because meshing errors, which may lead to voids, overlapping elements or misplaced midside nodes on elements, are not always reported automatically by the program, it is imperative manually to apply the program's in-built checking functions. Even after that, it is advisable to check the mesh visually in critical areas and to carry out further independent checks, for example on the total number of tie elements required to connect the building and ground.

Once familiarity and experience was gained with I-DEAS as described above, it was found that drawing up and meshing a full model of ground, tunnel and building could be achieved in a day. Including the initial hand preparation and the processing of the output from I-DEAS to form the input file to OXFEM gives a total time for the pre-processing stage of about a week, depending on the complexity of the site. In the case of the Mansion House model, described in Chapter 7, two weeks were required.

The I-DEAS model files are quite economical on storage space, requiring 10 – 20 MB. The main program requires about 1GB of storage and a platform with a high graphics specification. A Silicon Graphics O2 workstation was used.

4.2.3 Utilities for pre-processing to generate the OXFEM input file

As mentioned in Section 4.2.1 (step (8)), further processing of the mesh information output by I-DEAS is required to obtain the input data in the correct format for the OXFEM program, and to add further information. A family of utility programs has been written in FORTRAN 90 for this purpose. In this project, these utilities were collected together and their documentation completed, using the Intranet, to make them more accessible to other users, updating and amending them when necessary. The collection was also expanded to minimise the requirement for hand intervention during pre-processing. The most significant utilities are:

1. CONVERT5, after Augarde (1997), converts the ABAQUS format text file produced by I-DEAS, containing the node co-ordinates, element topology and boundary conditions into the correct format to be read by the OXFEM program. It has been updated several times as part of this research as the OXFEM input format has developed, most significantly with the introduction of sets (see Section 4.2.4).
2. LINING_GEN (Augarde, 1997) generates the element topology for the overlapping faceted shell elements for the tunnel lining, based on the OXFEM input format file and the lists of elements that are excavated at each stage of tunnel advance.
3. OFFSET, written during this research, enables constants to be added to all nodal and element numbers in an OXFEM format input file. This enables parts of a model, such as façades of a building, to be added or removed from an input file without having to generate it from scratch from an I-DEAS output file using CONVERT5.
4. OXOPT is run as the final step of pre-processing prior to analysis. This program, written by Prof. Guy Houlsby, carries out automatic element reordering to minimise the front width in the frontal solver in OXFEM (Section 4.3.1), using Sloan's algorithm (Sloan and Randolph, 1983).

An aim of this research has been to simplify the pre-processing by reducing the number of steps and separate programs required. Considerable benefit has been gained by enhancing the subroutine in OXFEM that reads the input file (Section 4.2.4), making it more tolerant of the exact formatting, reducing the workload of the user and making certain smaller utilities for formatting purposes redundant. It should be possible in the future to integrate further the utilities with OXFEM by sharing the same input subroutine, thus ending the need to update each utility individually each time the OXFEM input format is changed, for example when a new feature is added.

4.2.4 Developments in the OXFEM input format

A typical OXFEM format input file is shown in Figure 4-2. The file is of a modular format, with the type of data contained in each model identified by a header beginning with a '*'. The data is read in free format.

The main enhancements to the input format carried out during this project were:

1. Introduction of variable length lists. Previously, a list of numbers, for example elements to be excavated at a particular stage, had to begin with the number of members of the list. Frequently this meant extra work for the user. The need for this was removed by counting the number of members in the list first (by reading it in as character strings and examining the contents) then allocating an array of exactly the correct size. This was part of a general move to use of allocatable array structures that reduced the need for the user to declare maximum array dimensions in a module prior to compilation.
2. Rationalisation of result files. Three different result file types are commonly used – nodal output (displacements and forces), stress output and material state output. Originally only one output file of each type could be obtained. In this project, the storage of information on all the result file types was brought into a single data structure – a linked list of derived type arrays. This enabled any number of each type of file to be requested, enabling results from different parts of the model to be directed to

different files, improving post-processing capability. The data structure is flexible, allowing more types of result file, containing a selection of the exact output required by the user, to be incorporated in future.

3. Introduction of set format. This was achieved via the '*NSET' and '*ELSET' modules (Fig. 4-2). Previously, lists of nodes or elements had to be presented each time they were required in a module. Some modules, for example prescribed displacements and result files, could only read in information on one node or element on a line at a time, leading to long data files. Set format eliminated these problems, by enabling the modules to handle sets of nodes or elements at a time, the set only having to be declared once. The data structure is again linked lists of derived type arrays, containing allocatable pointers so that space is allocated for each set to suit exactly the required number of members. The main advantages of a linked list are that it is not necessary to know how many sets of each type there are, and all relevant subroutines can handle sets of either type, by passing to them just the pointer to the start of the required list.

```
**Two five element cubes with surcharge, two load stages
*SMALL
*DIMENSION
300
*NODES
     1   0.0000000E+00   0.1000000E+02   0.0000000E+00
     2   0.0000000E+00   0.0000000E+00   0.0000000E+00
     3   0.1000000E+02   0.0000000E+00   0.0000000E+00
     4   0.1000000E+02   0.1000000E+02   0.0000000E+00
     5   0.0000000E+00   0.1000000E+02   0.1000000E+02
     6   0.1000000E+02   0.1000000E+02   0.1000000E+02
     7   0.1000000E+02   0.0000000E+00   0.1000000E+02
     8   0.0000000E+00   0.0000000E+00   0.1000000E+02
     9   0.1000000E+02   0.1000000E+02   0.2000000E+02
    10   0.0000000E+00   0.1000000E+02   0.2000000E+02
      ...
    43   0.1000000E+02   0.1000000E+02   0.1500000E+02
    44   0.5000000E+01   0.1000000E+02   0.2000000E+02
    45   0.0000000E+00   0.1000000E+02   0.1500000E+02
    46   0.0000000E+00   0.5000000E+01   0.2000000E+02
    47   0.0000000E+00   0.0000000E+00   0.1500000E+02
*TYPE   1  10   1
6010    6004
     1     4     7     2     3    17    18    19    20    21    22
     2     4     2     7     5    19    18    17    23    24    25
     3     8     2     5     7    26    24    27    28    18    25
     4     2     5     4     1    24    23    19    29    30    31
     5     6     7     5     4    32    25    33    34    17    23
     6    12     7     9    11    35    36    37    38    39    40
     7    12     9     7     5    37    36    35    41    42    25
     8     6     9     5     7    43    42    33    32    36    25
     9     9     5    12    10    42    41    37    44    45    46
    10     7     5     8    12    25    27    28    35    41    47
*DISPLACEMENTS
bottom_surface   1    0.000000000E+00  1  2
bottom_surface   2    0.000000000E+00  1  2
bottom_surface   3    0.000000000E+00  1  2
sides_1_3   2  0.000000000E+00  1  2
sides_2_4   1  0.000000000E+00  1  2
*SURCHARGE, STAGE=1, Q=20.0, NSET=surface_nodes, ELSET=surface_elements
*CALCULATION
test4.out
  20   0.001
  10   0.001
*MATERIALS
1   5   30000.00  1.5E+06   60.0   3000.0    150000   6.0  10.0  9
0.90  0.02     0.75  0.04     0.50  0.06     0.30  0.10     0.20  0.15
0.15  0.20     0.10  0.30     0.05  0.50     0.025 0.70
*ONODES
test4.nod
-10  2   10   10   1
*OGAUSS
test4.str
-10   2   10   10  1
*OSTATE
test4.sta
-10   2   10   10   1
*ELSET, ELSET=bottom_surface
1  4  19  20  22  29  31
*ELSET, ELSET=sides_1_3
7  8  11  12  18  21  22  26  28  35  38  39  47  5  6  9  10
23 30  31  34  33  42  43  44  45
*ELSET, ELSET=sides_2_4
5  8  10  12  24  26  27  29  30  41  45  46  47
6  7   9  11  17  20  21  32  34  36  39  40  43
*NSET, NSET=surface_nodes
9  10  11  12  37  38  40  44  46
*ELSET, ELSET=surface_elements
6  9
*END
```

Figure 4-2: Sample OXFEM input data file

4.3 Finite element analysis using the OXFEM program

4.3.1 Introduction to the OXFEM program

OXFEM (OXford Finite Element Method) has been in continuous development as an in-house program in the Civil Engineering Research Group, since it was first conceived for the large displacement analysis of unpaved roads (Burd, 1986). It has been applied to a range of geotechnical and structural problems.

At the heart of the program is the routine that solves the stiffness equation given in the introduction to this chapter, to obtain the nodal displacements. In OXFEM, an optimised frontal solver carries this out. The solver loops over the elements in the order specified in the input file as generated using the OXOPT reordering utility (Section 4.2.3). Stiffness terms for degrees of freedom active on the mesh are added to a frontal matrix. When the element containing the last occurrence of a particular degree of freedom is encountered, the stiffness terms for that degree of freedom are eliminated and stored in a buffer. When all the degrees of freedom have been thus eliminated, back-substitution takes place. The advantage of this method is that the stiffness matrix for the whole model is not assembled at one time.

At the start of each loading stage the external and internal loads and body forces are evaluated. The total load for the stage is then sub-divided and applied in a number of equal steps. After each step, the stresses and nodal forces are updated. The difference between the updated nodal forces and those applied at the start of the step is an out of balance force, which is subtracted from the load applied in the next step.

The OXFEM program was originally written in FORTRAN 77. One of the main activities carried out co-operatively by the members of the research group during the period of this project has been to update the whole program to FORTRAN 90. This was stimulated by the availability of new compilers for the SUN workstations on which the program is run within the group. One of the main benefits of using FORTRAN 90 has been the feature of run-time allocation of arrays. This has enabled the program to be compiled to suit the size of the analysis to be undertaken and the platform available, with far fewer

hardwired parameters to define initial array sizes. It has also led to tidier, more efficient code, with a greater number of intrinsic routines available to the programmer, for example routines to carry out matrix operations.

As the FORTRAN language has evolved and system architectures have become more complex, new compilers have come into use. The increasing complexity of the programming implementation has led to less tolerance of laxness in programming style. For example, while FORTRAN 77 would always initialise all elements of a newly declared array to zero, FORTRAN 90 compilers cannot be relied upon to do this. In addition, both debugging utilities and the compilers' own self-checking have become less effective, so that often an error bound violation is not flagged as an error.

The result of these developments has been that on some occasions, historical OXFEM code that functioned perfectly under FORTRAN 77 has failed under FORTRAN 90. If the failure is due to non-zeroing or an array bound violation, the analysis may not terminate but instead give an incorrect solution. It was realised that in order to manage the transition to FORTRAN 90 effectively, and to ensure security of the program in all future developments and enhancements, certain structures and operating procedures were required. These were agreed by the OXFEM Development Group and implemented by Dr Augarde, Claus Wisser and myself in co-operation. The main items were:

1. The FORTRAN source code was to be automatically copied to archive monthly, so previous versions of the program could be recovered at any time if needed for verification purposes.
2. A portfolio of test problems was established. These could be used for benchmarking the performance of new code or new platforms, but their main purpose was for verification of the program when new code or compilers were introduced. The 'correct' solutions to the problems were stored. Some of the problems could be independently verified by known analytical solutions. They aimed to cover a wide range of 2-D and 3-D problems under various loading including excavation, and with linear and non-linear material models.

3. A booking-out system was established so that each of the program developers was aware of which subroutines were currently being developed by someone else. This prevented problems occurring when developers made their own copies of the source code and developed it independently, leading to alternative versions of the program that were extremely difficult to reconcile at a later date. The booking-out was recorded manually in a log file – it was considered that there were not enough people involved in programming to justify setting up a Revision Control System (RCS) under UNIX.
4. The documentation of the program would be completed, and henceforth maintained up to date. Great advantage was gained by implementing this using the Intranet, analogous to the on-line help of most commercial software, as opposed to the traditional way of producing a paper manual. The information is freely available to all members of the Group simultaneously and is always current. The result was a comprehensive user guide, including information on how to compile and run the program on different platforms, and how to use the benchmarking test problems. Much of this documenting work was carried out as part of this project.

Considerable effort was expended during 1998 and 1999 in updating the code to FORTRAN 90 and in verifying the resulting program.

4.3.2 Capabilities of the OXFEM program

These may be summarised as follows:

- Element types available: Continua, interfaces (including ties), membranes, bars, beams and shells.
- Shape functions: Constant, linear, quadratic and cubic strain.
- Integration rules (Gauss type): For 2-D triangular elements- 3 point (exact to order 2), 6 point (exact to order 4) and 16 point (exact to order 8). For 3-D tetrahedral elements- 4 point (exact to order 2), 5 point (exact to order 3) and 16 point (exact to order 4).
- Material models available: Elastic perfectly-plastic von Mises, variable elasticity, nested yield loci kinematic hardening model, elastic, no-tension masonry model,

Matsuoka sand model, elastic perfectly plastic interface material, elastic beam and elastic shell material.

- Loading types: Discrete nodal loads, surface tractions, normal surcharge or pressure (implemented for this project) and body forces.
- Restarting and rescuing: Important when the run times are long (say one day), as a program termination due to, for example, the disk quota being exceeded, would lead to a significant waste of resources and user time. Two systems have been implemented: both function by writing the important arrays describing the model and its current state to a scratch file on disk at the end of a load stage. 'Rescue' enables an analysis to be restarted from the last complete step and proceed as before. The 'restart' facility enables an analysis to be restarted from the end of a load stage specified by the user but with new input parameters. This enables a parametric study (*e.g.* different volume losses applied at a tunnel) or an investigation of the sensitivity of a solution to step size at a particular stage to be carried out.

4.3.3 Analysis features added to OXFEM

A few features were required to be added to the analysis part of the program specifically for this project, in addition to the major improvements to the input file handling described in Section 4.2.4.

Under the guidance of Dr Augarde, patch loading on surfaces of three-dimensional meshes was implemented. This was required to model surcharge acting vertically downward on a model of a soil block to represent ground above the model that was not included because it was above foundation level.

Shrinkage of the tunnel lining in three dimensions to model volume loss was achieved by previous researchers by extracting the shell elements into a separate model, prescribing inwards radial nodal displacements and obtaining the resulting set of nodal forces. These became external loads on the lining in the main model. This was a laborious process, and a more efficient means of applying the shrinkage within OXFEM was sought. Dr Augarde had written a routine to apply shrinkage to facetted shell elements in certain orientations,

and this was modified early in this project for the Maddox Street model and later generalised to be able to handle tunnels at any orientation.

The facility to add (or remove) a building mesh from a model part way through an analysis was implemented as an extension to the existing excavation routines. It was thought that, by giving the ground the opportunity to reach equilibrium before adding the building, convergence to the correct solution when the building was relatively heavy would be improved. In the event, the facility was not used in earnest. The main challenge was catering for the removal of the associated tie elements and disabling the degrees of freedom at the reaction nodes that were no longer connected.

The move towards run-time allocated data structures under FORTRAN 90 was mentioned in Section 4.3.1. The aim initially was to make more efficient use of limited computing resources, by only declaring array sizes to fit the problem exactly. Other useful benefits were in saving user time in calculating the required array sizes to be declared in a module and in re-compiling the code, and in reducing errors and failed runs when the choice of array bounds was inadvertently set too small. One of the most important such arrays was the frontal matrix used to store the coefficients in the frontal solver. This two-dimensional array, of typical rank 1000 – 2000 for a large combined problem, was a significant requirement on memory. As part of this project, a pre-front was added to the frontal solver routine, to evaluate the maximum front width required without assembling the stiffness equations. The frontal array was then allocated.

A number of other enhancements to the code were made as a result of moving to parallel execution of the OXFEM program (Section 4.5). One major enhancement was in more efficient storage of the frontal matrix. Data had been entered in and extracted from the matrix on a row-by-row basis. However, by exploiting column-by-column array storage in FORTRAN 90, a speed increase could be obtained. In order to access any particular member of an array, the microprocessor loads a whole block of the array containing that member into its cache memory – a relatively time-consuming operation. Manipulating the array column-by-column enables the processor to make full use of the

contents of the cache before reloading it. Transposing the frontal matrix to facilitate column-by-column access gave a speed increase of 2.5 times on a standard workstation.

4.3.4 Advantages and limitations of the in-house program

The implementation of software to carry out finite element analysis in-house has certain advantages, although caution should also be exercised over some issues. The main advantages are that new modelling procedures may be implemented from scratch by researchers in the group without having to seek approval or further information from any outside source. The whole of the source code is available to the individual researcher for them to view and amend. There is therefore no limit to what procedures may be coded and tested, thus making the in-house program an important tool for original research in numerical analysis.

Examples of features key to this project that would not normally be available in commercial packages are the kinematic hardening constitutive model, overlapping faceted shell elements and tie elements. In addition very few commercial packages are optimised for parallelisation, which has been key to this project (Section 4.5). Commercial packages usually allow for user-defined material constitutive models, but may not allocate sufficient state variables per integration point.

Commercial software suppliers frequently co-operate with users of their software, both academic institutions and industrial companies, to produce new element formulations and constitutive models. In these cases, the benefit to both parties tends to be more tangible and dependable.

The in-house program is the result of development in which progress occurs in a series of steps, as funding is obtained for particular projects and new research ideas are explored. The result is a program with very advanced capabilities in some areas but perhaps no capability in other areas that commercial packages would have, because the features have not been needed in the past. Examples of such features missing in OXFEM are temperature effects, useful for applying strain to parts of the model, time-dependent effects such as creep and consolidation, and dynamics. The latter two areas are likely to be the subjects of

the next phase of the development of the program. Other features in OXFEM, such as surface traction and surcharge loading, are only implemented for certain element types. The structural capability of OXFEM is limited to thin elastic beam and plane stress elements, plus the facetted shells.

Commercial packages usually incorporate pre- and post- processing capabilities, as discussed in Sections 4.2 and 4.4. OXFEM itself does not have the facility for these operations, but can be used with commercial packages such as I-DEAS. There is still a role for in-house utilities developed in parallel with the main OXFEM program, for example for special element generation or contouring. The number of these should be kept to a minimum, as they require maintenance.

The development of the OXFEM program in a series of stages has caused some difficulties in its use. Until the start of this project, less attention had been paid to some of the basic infrastructure of the program – the user interface at input and output, data structures within the program and documentation, than to implementing new features for research. As the intention of this project was to use the program rather than specifically add new features, these other aspects became more pertinent, and this project has acted to stimulate developments in these areas to bring them into line with the general technical capability of the program.

The structure of the program, with most data stored in fixed-length integer and real arrays, has become complex, increasing the maintenance overhead and the need for internal documentation. The move towards FORTRAN 90, including more flexible derived data types, should help to improve the program structure and make it easier to expand and develop in the future. FORTRAN itself is evolving towards an object-orientated format, which will enable the code to be more efficiently written.

4.4 Post processing and visualisation of results

4.4.1 2-D techniques

Results on planes, for example stresses and strains in the façades of a building, or settlements on the surface of the ground, may be displayed using contour plots, either with lines or fill. Many of the figures of this type in this thesis were produced using the program 2CAN, written in-house by Prof. Guy Houlsby. 2CAN can produce plots in either colour or greyscale, and is particularly useful for generating the plots of cracking damage patterns shown in Chapters 6 and 7. In these plots, for example Figure 6-26 on page 6-29, the density of lines per unit area is a measure of the number of cracks, and the width of the individual lines the strain across the crack. The direction of cracking is indicated by the direction of the lines.

4.4.2 3-D techniques

The development of 3-D modelling has led to the generation of significantly more data to handle at the post-processing stage. This requires more advanced tools for analysis and display than 2-D contouring, and the use of colour is even more useful. The development of such tools could be carried out in-house but would be time-consuming. In this area, as in pre-processing, commercial packages may be exploited. I-DEAS can import scalar or tensor data, provided it is presented in its own particular Simulation Universal Format. It can then display the deformed mesh or integration point output interpolated on slices through the mesh. The scientific language MATLAB has similar capability (Mathworks Inc., 1997), achieved by interpolating the data onto a 3-D grid. It has the advantage of being a more universally available package than I-DEAS, is designed specifically for data analysis and requires input data in only a simple column format.

4.5 Hardware requirements and performance

OXFEM has been run under UNIX on Sun Microsystems workstations within the Civil Engineering Research Group. A Sun UltraSparc 2 workstation with 2x300Mhz processors

and 256MB RAM was acquired just prior to this project in 1996. It became apparent during the course of this project that the performance decayed rapidly for large problems of the order of 20,000 degrees of freedom (d.o.f.), due to the real RAM having being exceeded and virtual RAM on disk being used, for which access times were much slower. Parallel processing using both processors was not available at that time. Therefore the configuration of the machine was changed to 1x400MHz and 512MB in 1997. A second 400MHz processor was added in 1998.

Figure 4-3 shows the improvement in the execution times on the UltraSparc 2 workstation for the Maddox Street model (Chapter 5), a typical full non-linear model including a building, with 13,500 d.o.f. It can be seen that the overall run time for this model was reduced from about 8 days to 2 days over the project. In October 1998, a factor of 2.5 times improvement was obtained by optimising the storage of the frontal matrix, as discussed in Section 4.3.3. The remainder of the improvement is broadly due to the enhancements to the hardware. It was found that increasing available RAM had a greater effect in reducing run times than processor speed. The early analysis with the Maddox Street model showed that run times began to increase rapidly once the memory requirement exceeded the physical RAM, causing the program to write to virtual RAM on disk, for which access times are much higher.

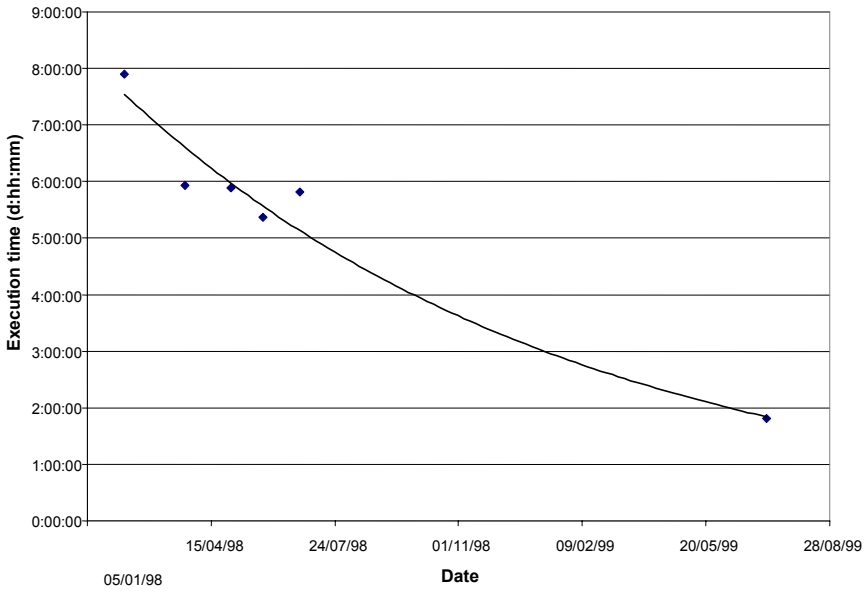

Figure 4-3: Execution times over project duration for Maddox Street models (13,500 d.o.f. and 110 load steps) on UltraSparc 2 workstation

In April 1998, eighteen months after the start of this project, the Oxford Supercomputer "OSCAR" was commissioned. The full user service was available from June 1998. OSCAR was a Silicon Graphics Origin 2000 Supercomputer with 86x195MHz processors and 21GB of RAM in total. Users scheduled jobs to run on 4, 8, 16, 32 or 64 processors in parallel – the use of the machine for purely sequential running was not encouraged. The architecture was configured as shared memory, so that from the programmer's standpoint it was not necessary to declare storage of variables and sharing of computational load explicitly between processors. A number of programming models were available for programming in parallel to exploit the resource, of which Open MP was the simplest to implement on existing code without requiring extensive modifications; it was used to 'parallelise' the OXFEM source code. Pre- and post-processing were still performed on the local workstations.

A fuller explanation of the details of transferring the OXFEM program and configuring it to run in a parallel environment is given in the paper Bloodworth *et al*. (1999). It was found that the move to OSCAR, with its more advanced compilers, stimulated a range of improvements to the existing sequential code, such as to the frontal solver. A considerable speed-up in execution time was obtained, such that the time for execution of the Maddox Street model reduced to only 5 hours with 8 processors. In addition, significantly larger models could be analysed without exceeding the available RAM, allowing over 30,000 degrees of freedom (Chapters 6 and 7).

Figure 4-4 shows the relationship observed between time taken per step in the frontal solver and the maximum frontwidth in the model, for a range of models both with and without buildings analysed on OSCAR. It can be seen that the trend may be approximated by a power law of order slightly greater than 3. This is not unreasonable given that the number of floating point operations required to multiply an n x n matrix by a vector of length n is $n^2(n\text{-}1)$ (there will also be a slight overhead).

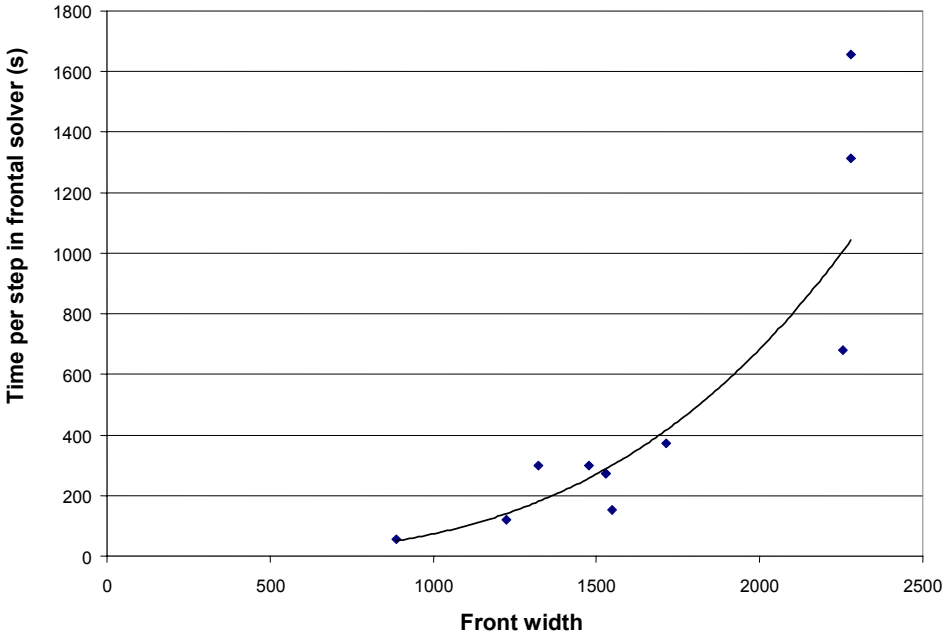

Figure 4-4: Time per step in frontal solver against maximum frontwidth for various 3-D models executed on "OSCAR"

There is a reasonable amount of scatter in Figure 4-4. The points above the trendline at high frontwidth are from the full model of Mansion House (Chapter 7), which included a particularly detailed building mesh. This is likely to have caused the frontwidth to remain close to its maximum value for longer in the frontal solver than would be the case for a typical model of the ground alone. Maximum frontwidth itself depends on the number of degrees of freedom in the model; the relationship (Fig. 4-5) is approximately linear, with points above the line tending to relate to more complex buildings.

4.6 Discussion on effectiveness and limitations of implementation

The implementation has been shown to be in general successful, with completion of numerous large-scale (30,000 degrees of freedom or more) non-linear analyses of three-dimensional and realistic problem geometries. This success has been the result of important enhancements to both software and hardware, some continuing the approach of previous researchers at Oxford, and some having been new initiatives.

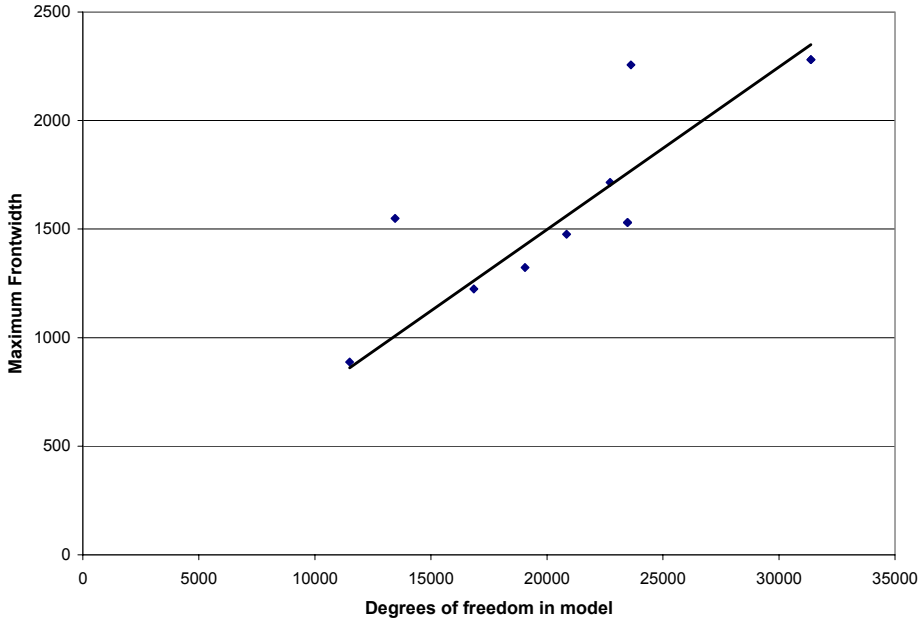

Figure 4-5: Increase of maximum frontwidth with model size

Many of the enhancements to the software were in the pre-processing stage, stimulated by the need to build and amend models more quickly in order to experiment and conduct parametric studies related to the site data available. These considerably reduced the amount of hand manipulation of data required at the input stage. In parallel with the developments to the software directly, the importance of having adequate documentation and maintenance of the software infrastructure was highlighted as contributing greatly towards faster and more reliable model development. Test problems, example input files and a user guide for the main software and associated utilities were placed on the local Intranet, from which they could be accessed quickly at any time. Some difficulties with compilers, debugging and updating the code to FORTRAN 90 were experienced, but future researchers should be able to benefit from the effort expended. A philosophy of programming with maintenance and future expansion of the program in mind has been promoted on this project.

Three-dimensional mesh generation was carried out using a commercial package, and is always likely to remain so. The inter-relationship between solid modelling and mesh generation was interesting to note. This may have implications for how design and drafting must be integrated further in future.

At present the OXFEM program is only available locally at Oxford, where there is access to considerable computing power at the Oxford Supercomputing Centre. Access to machines of this type on a commercial basis is feasible. It is, however, a specialised platform with its own particular way of operating – one of the main problems is the lack of guarantee of turnaround of work on a particular day, due to the shared nature of the resource and the many other users.

The Supercomputer enables very large analyses to be carried out in just one or two days. In the future, it should be possible to network clusters of PCs together to perform the same function as a bespoke supercomputer, bringing the cost down considerably.

4.6.1 Recommendations for future work

The increasing move towards object-orientated programming and more flexible data structures is to be encouraged, as it improves program structure and the efficiency of coding and maintenance. It is even more important to maintain standards of coding when a program is under a continuous and long-term development by many different researchers.

Investment in providing some of the features of standard commercial packages within OXFEM, for example temperature loading, would make the possible transition to a commercial program in the future, should the need and opportunity arise, more viable. On balance an in-house program is probably essential to a research institution seriously engaged in numerical analysis, but needs careful management.

During this project, major effort was expended in developing the pre-processing and analysis stages of the implementation, to improve the throughput of large analyses. However relatively little improvement was made in the post-processing stage, where it could be possible to integrate it more closely with the earlier stages. It is recommended that a complete review of the tools used for this stage be undertaken.

One of the main difficulties encountered on this project was diagnosing the causes of failure to converge to a stable solution for the large non-linear analyses, with mixed non-linearity, being undertaken. There is an immediate need for development of fundamental tools for this purpose.

Computing resources available to a project of this type will continue to increase due to advances in computing technology. Figure 4-6 shows the trend of run times for the Maddox Street model over the lifetime of this project. It suggests that, provided developments in both hardware and software (particularly for parallel processing) continue as they did during the period 1996 – 1999, run times as low as 10 minutes for analyses of such complexity should be achievable in the not too distant future.

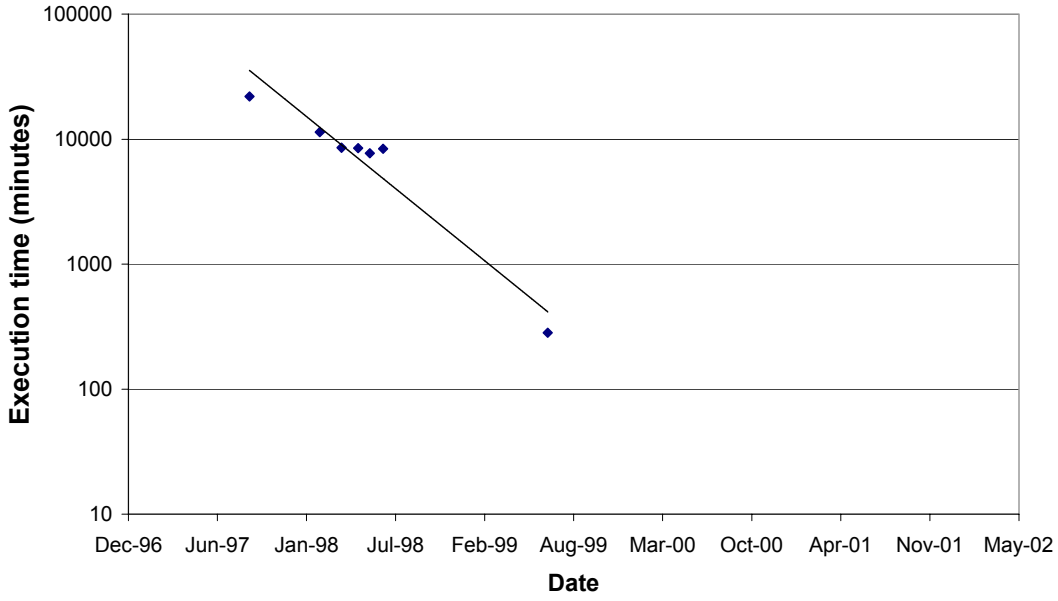

Figure 4-6: Past and projected execution time for Maddox Street model

5 ANALYSIS OF THE EFFECTS ON ST. GEORGE'S CHURCH, HANOVER SQUARE, OF THE MADDOX STREET SHAFT CONSTRUCTION

5.1 Introduction

This site was the first to be modelled for this project, with the data having been obtained, soon after its commencement, from the archives of Howard Humphreys. The case history is relatively straightforward, and served to aid the process of familiarisation with the software tools, and as a stimulus for many of the developments to the implementation that were discussed in Chapter 4. Modelling this site has also demonstrated the validity of certain techniques for modelling a masonry building, in particular its openings and foundations, that could then be applied to the more complex models described in Chapters 6 and 7. The actual results from the Maddox Street model show reasonable agreement with the site observations, although the quantity and quality of the site data are not sufficient to enable many very specific conclusions to be drawn.

5.2 Background to the case history

5.2.1 Overview of the construction project

Howard Humphreys and Partners Consulting Engineers designed and supervised the construction in 1991/92 of a 2.5m diameter tunnel, 12m to 25m below ground, for a new electricity supply into the West End of London. The preferred option for the route was to follow public roads, for legal reasons and also to minimise the impact on surface structures. Shafts were required at intervals for access during construction, in particular at sharp changes in tunnel direction where it was only possible to excavate the tunnel by hand. One such shaft was in Maddox Street, which is bounded on the north side by a

terrace of four storey brick Georgian houses, and on the south side along its entire length by an 18th century stone-clad brick church. The 4m diameter 15m deep shaft was constructed 5m from the northeast corner of the church (Fig. 5-1). No protective measures such as compensation grouting were used, but monitoring of ground and structure movements was carried out and observations of damage to buildings were made.

Good data was made available to this project on the site investigation, the tunnel and shaft geometry and construction sequence and the settlement monitoring along the façades of the buildings facing Maddox Street. There is the disadvantage that other buildings around the shaft were not monitored, and hence a complete picture of ground settlements in the area cannot be developed. The determination of the damage to the buildings monitored, due to shaft construction, was made difficult by the large amount of pre-existing cracking, particularly at lower levels in the buildings.

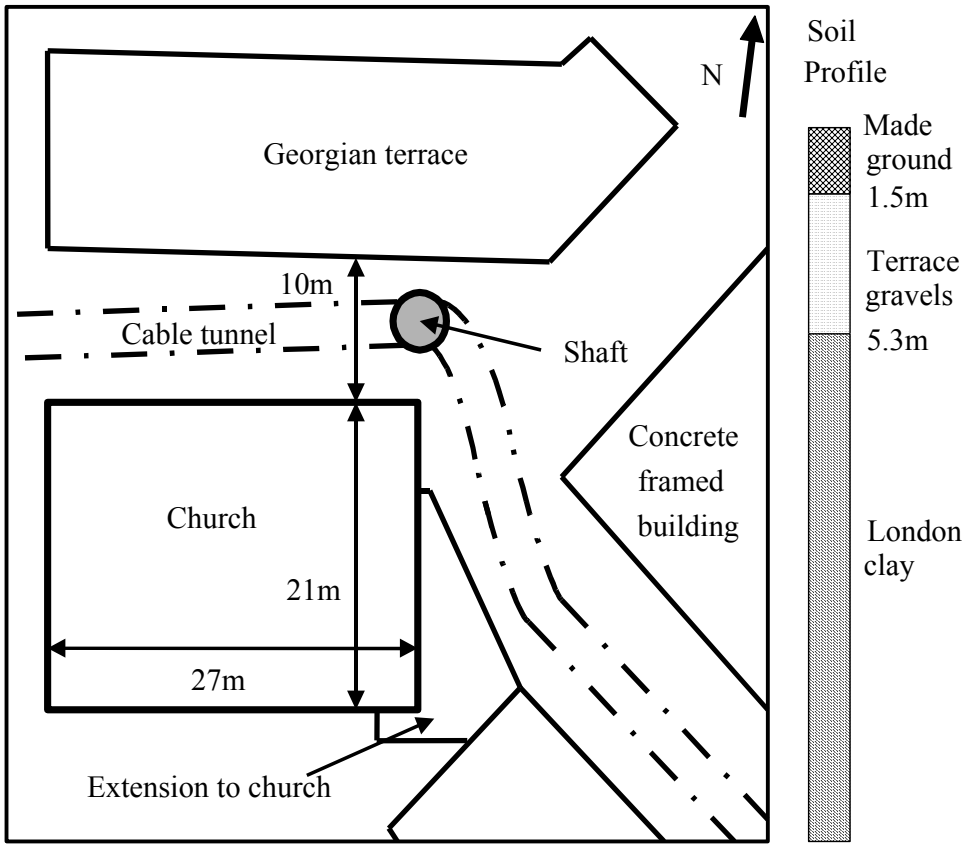

Figure 5-1: Plan on Maddox Street site showing shaft, tunnel and surrounding buildings

5.2.2 Ground conditions

The tunnel at this location passed entirely through the London clay strata. Investigation for the shaft consisted of a borehole sunk in the roadway to the same location and depth, six months prior to construction. It showed 1.5m of pavement and made ground, 3.8m of terrace gravels, then London clay to depth, a typical profile for that area of London. Samples of the London clay were taken for laboratory testing, including unconsolidated undrained triaxial (UUT) tests. The results of the UUT tests are shown in Figure 5-2. Tests were performed on 100mm and 38mm diameter samples, and show a clear trend for the smaller samples to give higher strengths, as would be expected. Also shown in Figure 5-2 is the relationship between strength and depth used by previous researchers at Oxford to model London clay (Section 2.3.6), and it can be seen that there is generally good agreement with the U100 results, especially from 9m depth.

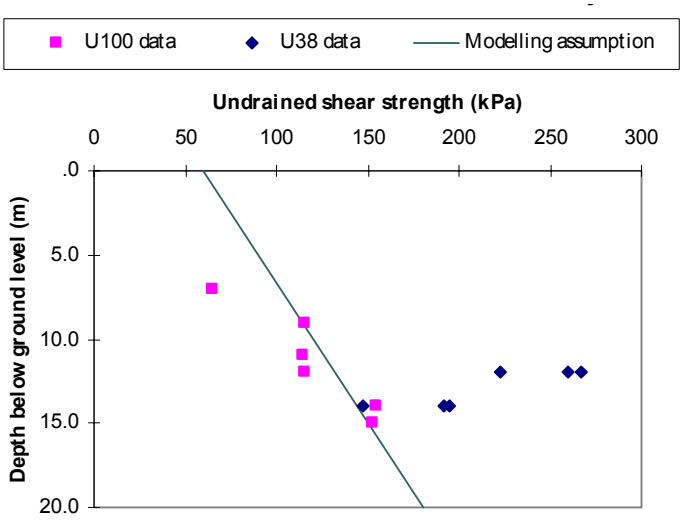

Figure 5-2: Maddox Street shaft borehole investigation- results from UUT tests on London clay

5.2.3 Shaft and tunnel construction

Howard Humphreys produced predictions for settlement prior to construction. For the tunnel, the methods of New and O'Reilly (1982, 1988) were used. For the shaft, the assumption of a circular retaining wall in stiff clay was made and the forward movements and settlements calculated by hand (Burland *et al.*, 1979). The predictions were of 2.5mm

settlement due to the tunnel, above its axis away from the shaft. These increased to 13.5mm at the northeast corner of the church due to the effect of the shaft, with differential movements along one façade of the order to 1/1275, which would not typically be expected to cause damage. Hence it was not believed necessary to provide protection measures for the buildings, but a monitoring programme was instigated to provide a mechanism for warning of excessive settlements. Condition surveys of buildings in the vicinity were carried out before and after construction.

The as-built construction programme showed that the shaft was constructed first, during the period 21st March to 22nd April 1991. The excavation of short lengths of tunnel by hand on either side of the shaft immediately followed this. The main drives by open-faced shield commenced to the southeast down Mill Street on 26th April, and to the west along Maddox Street on 2nd July.

The shaft was sunk by the caisson method, to limit ground disturbance and construction noise, and was lined with 150mm thick precast concrete segments. At tunnel level a 400mm thick ring wall was cast to stiffen the shaft at the openings. At the base of the shaft, 14.8m below ground level, a 1000mm thick slab was cast.

Settlement monitoring by precise levelling was carried out covering the whole construction period, from March 1991 to February 1992. Monitoring points were attached to the façades each side of Maddox Street - eight on the church and eight on the Georgian terrace. The frequency of reading was every two days when construction was occurring in the vicinity, reducing to weekly at other times.

5.2.4 Buildings

St George's Church, Hanover Square was constructed between 1721 and 1725 and remains largely as originally built. A site visit was carried out in May 1997 to examine the structure of the church and confirm key dimensions. The structural form is of load-bearing masonry, with stone-clad brick masonry walls up to 1m thick. Foundations are believed to be shallow pad or strip footings about 3m below current ground level. A half-basement extends under most of the plan area of the church, the roof of which is constructed of brick

masonry vaults, supporting the floor of the main meeting chamber above. The main chamber occupies the majority of the 27m by 21m plan area of the building and extends the full height to roof level; it is essentially open-plan with columns at intervals supporting wooden balcony structures around the perimeter. The roof is of timber construction spanning the full width of the building.

At the western end of the building a portico extends out into the street and a 30m tall bell tower rises from within the church (Fig. 5-3). The site survey revealed that the tower is effectively self-supporting on its own load-bearing masonry walls, and does not rely on the outer perimeter walls for support.

Windows are evenly distributed around three façades of the church in three rows. Figure 5-3 shows one of the larger arched windows in the top row. The 5m by 3.5m east window dominates the centre of the fourth façade.

Floor plans of the Georgian terrace were obtained from the surveyors who inspected the buildings, and photographs of the exterior were taken during the site visit. It was apparent that the terraced houses had been altered somewhat in structural form in their conversion to offices, with creation of larger openings and removal of internal walls. However, it could still be seen that they were of load-bearing masonry type, with half-basements.

Figure 5-3: View to front of St George's Church and detail at arched window openings

5.3 Observed settlements and effects on structures

5.3.1 Settlement Monitoring

A plot of the development of the settlements along the north façade of the church is shown in Figure 5-4, compared with the designers' predictions. At completion of the shaft sinking, the maximum settlement was about 4mm at the corner of the church. This increased to 8mm after completion of the tunnel drives. The distribution of settlements along the façade also changed from being localised at the northeast corner due to the shaft, to being more uniformly distributed after construction was completed. This may also be seen in Figure 5-5 for the east façade. Although the settlements recorded are relatively small, consistent trends were observed during construction, indicating good repeatability and accuracy.

Because of the presence of buildings all around the shaft, it was not possible to record a 'greenfield' settlement profile due to the shaft. Because measurements were only taken on buildings on one side of the shaft, it is also not possible to calculate a volume loss figure for the shaft. Both of these are limitations of this case history.

The Georgian terrace experienced a gradient of settlement along its length, from 5mm maximum down to zero. The remainder of the buildings in Maddox Street to the north east

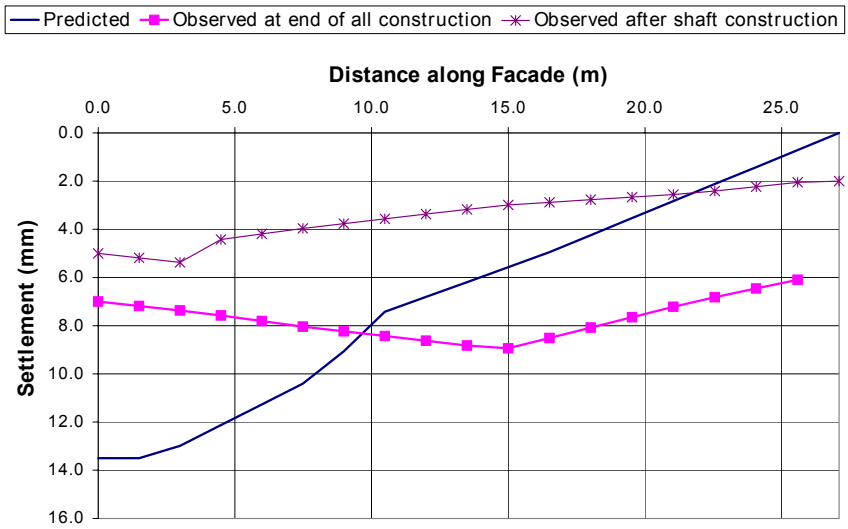

Figure 5-4: Predicted and observed settlements along north façade of St. George's Church

of the shaft, together with the newer buildings on the corner of Maddox Street and Mill Street opposite the church, were considered to be unaffected by the tunnelling.

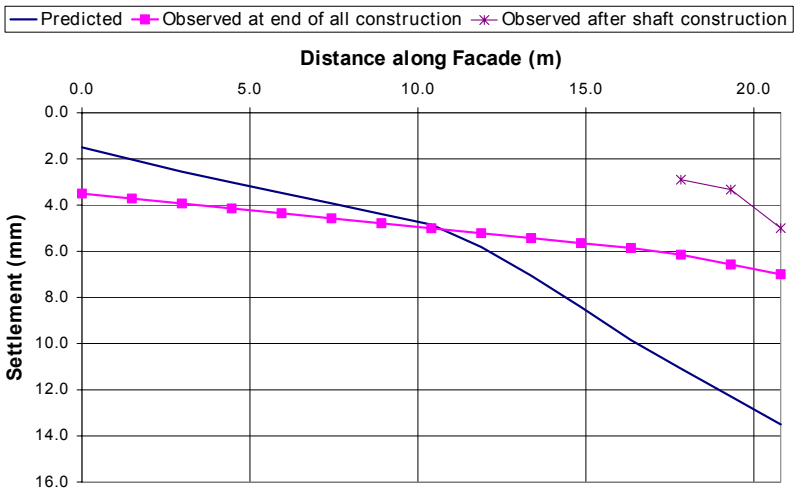

Figure 5-5: Predicted and observed settlements along east façade

5.3.2 Effects on structures

Pre-construction condition surveys were carried out on buildings with predicted angular distortions of greater than 1/2000, which comprised Nos. 38, 42 and 44 Maddox Street in the Georgian terrace, plus the church. Extracts of the surveys, together with pre-construction photographs of the interior and exterior of the church were obtained from the surveyors. The surveys recorded such extensive pre-existent cracking in the basements of the terrace and in the crypt of the church that it was very difficult to identify with any certainty new cracking when the buildings were re-surveyed after all construction. It was agreed with the building owners that no discernible additional damage had occurred.

5.4 Modelling aims and assumptions

5.4.1 Ground

The top surface of the model was chosen to be the foundation level of the church, 3m below ground level. The meshes for the building façades could then be attached to the model directly, using tie elements (Section 3.5). It was not possible to include the ground

above that level, because the 2-D plane stress façades cannot accept out-of-plane loading and hence 'retain' soil. The effect of the weight of the ground not included was represented by setting up initial stresses through the depth of the model that matched the profile in the field. The self-weight of the soil was taken as 20kN/m^3. Because of the choice of model surface level, the shaft would appear as 12m deep in the model.

Referring to the borehole (Section 5.2.2), the foundations were believed to rest on approximately 2m of terrace gravels underlain by London clay to depth. Thus the majority of the volume of the soil responding to the shaft that would govern the building response was London clay. A suitable constitutive model for the gravels had not been implemented in OXFEM at this stage. Therefore the soil was modelled as entirely London clay, with undrained shear strength of 78kPa at the top of the model (3m below ground level), increasing with depth at 6kPa/m, and a rigidity index (ratio of shear modulus to shear strength) of 500 throughout. These properties had been used by previous researchers at Oxford and are in broad agreement with site investigation data (Fig. 5-2).

The choice of boundaries of the model soil block was governed by keeping a balance between placing them far enough away from the region of interest so as to not affect the results adversely, whilst also maintaining economy on the overall model size. The soil below the base level of the shaft was expected not to displace significantly, so a shallow model depth of 20m was used. In order to give enough space for the building and the extent of its zone of influence to shaft base level, a plan dimension of 70m x 70m was taken. Figure 5-6 shows the overall dimensions taken for the model, including the shaft and building.

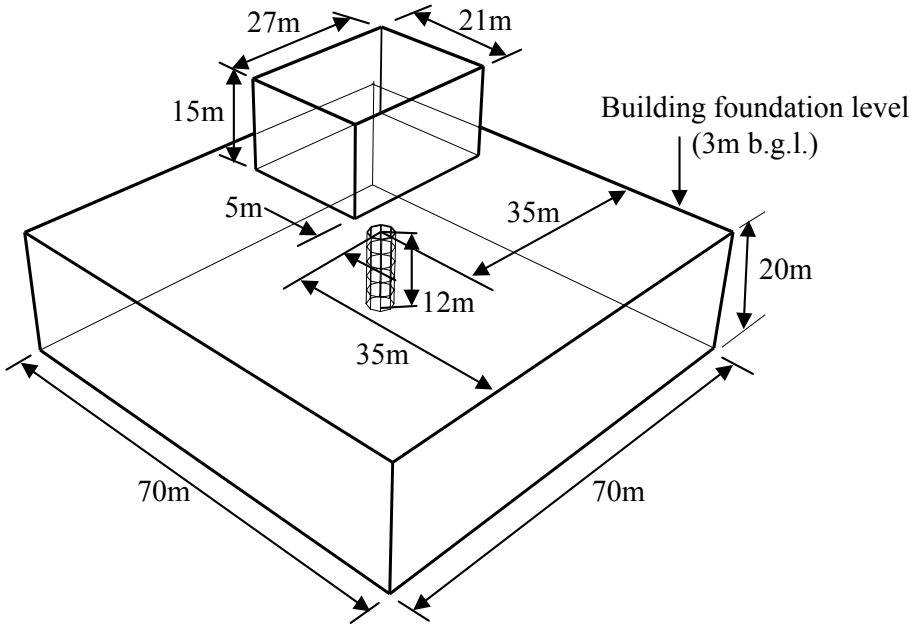

Figure 5-6: Maddox Street combined 3-D model dimensions

5.4.2 Excavations (shaft and tunnels)

The most interesting response of the building was observed to be due to the construction of the shaft, and therefore for simplicity the tunnels were not included in the model. The shaft was modelled as an octagonal section with the same cross-sectional area as the real shaft.

The lining was modelled as an elastic material. The stiffness was initially calculated based on a code value for Young's modulus of 28.4GPa for Grade 40 concrete and a lining thickness of 150mm as shown on the drawings. However, convergence problems were experienced, due to insufficient out-of-plane (bending) stiffness in the shells. Therefore it was necessary to increase the modulus to a high value, and 100,000GPa was chosen. The effect of this was to make the calculated stress in the lining too high, and to make the shaft effectively rigid, but this was not a significant factor in modelling the effects on the building.

The shaft was sunk by the caisson method, which is generally believed to cause less ground movement than the underpinning method. The actual volume loss due to construction of the shaft is not known, because the full displacement field around the shaft

was not recorded, and thus can only be estimated. The cutting edge on the caisson would have resulted in an annular void 20mm wide all around the shaft. If the surrounding ground had moved in to fill this completely, a volume loss of 2% would have resulted. Bentonite slurry was used in the annulus to mitigate this. Some heave of the clay into the base of the shaft was inevitable. Therefore, a volume loss of 2% was chosen as a compromise figure for the initial analyses.

5.4.3 Buildings

Since the church was the most important building, for which the best information was available, it was chosen for modelling. As the terrace on the north side and the church are on opposite sides of the settlement bowl due to the shaft, it seemed reasonable to assume that there is little interaction between the two.

The church was modelled as a 'box' of four planar façades, rectangular in plan to match the overall outline of the actual building. The site data showed that observed settlements decreased almost to zero at the western end of the building, and therefore less detail was provided there. In particular the tower (for which there was no settlement information) was neglected completely, in the belief that it would respond to any ground movements independently of the outer walls of the church. The portico and other openings at the west end were also neglected. The roof and internal balconies were not modelled on the grounds that they were of wooden construction and therefore of low weight and stiffness compared to the load-bearing walls, and therefore not influential on the building response. In the early models, no allowance for the possible mass masonry foundations was made, although in a later model the vaulted basement structure and its foundations were represented as an elastic raft on the surface of the model within the building footprint.

The effect of the openings arranged at regular intervals around the whole of the building could not be ignored. Openings are believed to have two main effects in the structural behaviour of masonry:

1. Causes of stress concentration, initiating discrete cracking from the corners and edges when stresses are sufficiently high.

2. Causes of a reduction in the stiffness of the façade as a whole, affecting its global flexural and shear response to ground movements.

Photographs taken during the visit to the church showed cracks from the top of windows in the north façade, which could have been caused or accentuated by the shaft construction. It was conceivable to model every opening in the church discretely, but as each would require the mesh to be refined locally, the overall effect would have been to increase the number of d.o.f. in the model significantly. Thus only openings closest to the shaft, where the distortions were greatest, together with the large east window were modelled in this way. Many of the windows in the church are almost rectangular, and for these elastic lintels were provided to prevent failure of the elastic, no-tension masonry material over the opening, as done by Liu (1997). The larger top row windows are actually arched (Fig. 5-3), and it was found to be possible to reproduce this shape approximately, and obtain a stable solution without needing a lintel.

An alternative solution was sought for the remainder of the model, where it was hoped to reproduce the effect of the openings on the global building behaviour. Two approaches to modelling stiffness reduction were used:

1. The “fully smeared” approach, in which an average stiffness for the whole façade is used, calculated as a reduction on the full masonry stiffness equal to the proportion of the total façade area occupied by the windows. This was used on the south and west façades, farthest from the source of settlement.
2. A “semi-smeared” approach recognises that openings aligned vertically may act as discrete vertical columns of reduced stiffness. This is similar to the approach used by Simpson (1994) except that his “strata” of reduced stiffness represented horizontal rows of openings. Vertical columns should model better the important phenomenon of formation of cracking from the top of the façade, propagating downwards in a hogging region. This approach was used for the openings on the north and east façades that were farthest from the shaft. On the north façade, the stiffness of the vertical regions

was taken as 40% of the intact façade stiffness, representing approximately the proportion of cross-section remaining on a vertical section through the openings.

The masonry was modelled using elastic, no-tension material (Section 3.2) with a Young's modulus of 20GPa, a value estimated from literature as the stiffness of the stone masonry units that clad the building, the mortar joints being relatively narrow. The Poisson's ratio was taken as 0.2, and typical values taken for the remaining parameters were as shown in Table 3-1. The exact properties of the bulk masonry are not known, and even if they could be obtained by testing, significant pre-existent cracking in all the buildings would undoubtedly have an effect, especially on the stiffness. The work of Liu (1997) showed that within the practical range of stiffness values to be expected for real buildings, building response is not very sensitive to elastic stiffness, but instead is rather more sensitive to the distribution of the self-weight of the building into the ground. This would be confirmed by sensitivity analyses.

5.4.4 Analysis sequence

A sequence for carrying out a combined non-linear three-dimensional analysis was originally developed and used by Augarde (1997), and the experience gained then was applied on this project. Some modifications were made to suit developments in the OXFEM program and requirements of specific models, but the general stage-by-stage approach was as follows:

1. Apply initial stresses to the soil and self-weight to the building over 20 or 40 steps.
2. Allow 10 steps without any loading applied, in order that out-of-balance forces remaining from the first stage are minimised. At the end of this stage, zero all strains and displacements in the model and "heal" all cracking in elastic, no-tension masonry material.
3. Remove elements from the tunnel to represent the first increment of excavation, and at the same time switch on the corresponding lining elements. This normally required at least 40 steps for stability.

4. In many of the more complex models, allow a stage of 10 steps with no loading applied, for the same reason as stage 2.
5. Apply radial shrinkage to the lining, to model volume loss. As in stage 3, 40 steps were normally required.
6. Allow another stage of 10 steps, as above. At the end of this stage, output results of nodal displacements and forces and Gauss point stresses and state variables for the excavation increment.
7. Repeat stages 3 to 6 for the remainder of the increments of excavation (if any).

In the case of the Maddox Street shaft analysis, detailed modelling of the incremental excavation sequence was not required, because the shaft was excavated relatively quickly and the resulting short-term settlements were only evident once it was completed. Therefore an attempt was made to excavate the entire shaft in one analysis stage. However, this failed to converge to a stable solution. Hence an analysis with five excavation stages, each of 2.4m depth of shaft, was tried. It was found that run times were excessive with the resources available at the time, of the order of three weeks, and a stable solution was not always reached when the building was included.

Therefore most of the analyses were commenced with the shaft already excavated and lined, including a base "slab" of shell elements to restrict heave whilst the ground was reaching equilibrium under the weight of the building. This required only 70 calculation steps, taking six days. There will be a small loss of accuracy setting up the stresses in the ground due to the building by this method. The volume loss was then modelled in the normal way by shrinking the lining. In the first main series of analyses carried out (Section 5.5), the base cap was removed before the volume loss was applied. It was thought from the results of these series that the resulting overall volume loss was too great, due to heave of the soil into the base of the shaft in the model. For the sensitivity analyses, the OXFEM program was adapted so that the shrinking of the lining could take place with the base cap still in position. The difference in the final settlements by making this change was, however, relatively small, as can be seen from the results reported in Section 5.6.

5.4.5 Summary of analyses carried out

With the modelling approach for the church, ground and shaft decided and with 2% volume loss chosen as a reasonable value, a main group of analyses were carried out with and without the building to explore the general validity of the chosen approaches (Section 5.5).

Sensitivity analyses were then undertaken on certain parameters (Section 5.6). The number of these was limited due to the long run times at this stage in the project (Section 4.5).

Finally, different modelling approaches, for example for the openings in the façades and for the foundation, were tried (Section 5.7).

5.5 Main analyses

5.5.1 Description of analyses

The following analyses were carried out:

1. A 'greenfield' model, of the shaft and soil alone.
2. A combined 3-D analysis including shaft, soil and church. A view of part of the finite element mesh for this analysis is given in Figure 5-7.
3. Analysis of the church alone, prescribing the displacements calculated from the 'greenfield' analysis, Analysis 1.

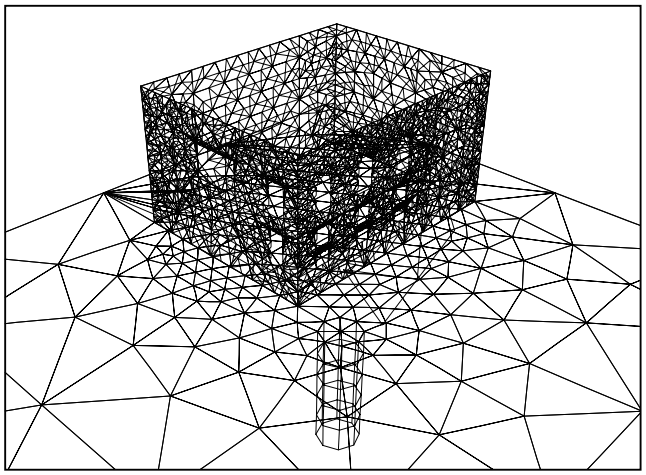

Figure 5-7: Detail from finite element mesh for combined 3-D analysis

The important output from Analysis 1 is the 'greenfield' surface settlement bowl profile due to the construction of the shaft, from which the 'greenfield' settlements around the perimeter of the building footprint may be obtained, for comparison with Analysis 2.

Analysis 2 is the most important. The soil settlements over the whole surface and around the building footprint would be expected to be different from Analysis 1. In addition damage to the building may well have occurred, which will be compared with the site observations.

The aim of Analysis 3 was to gauge whether it is beneficial in practice to undertake the combined Analysis 2, or whether applying the 'greenfield' displacements to the building is sufficient. There was found to be no overall benefit in computing time by using this approach, but it could enable a problem that exceeds the capacity of the computing resources to be run, effectively as two parts. However, the interaction effects between ground and structure would not be reproduced.

5.5.2 Results and discussion

The settlements over the soil surface for the 'greenfield' Analysis 1 are shown in Figure 5-8 and for the combined model (Analysis 2) in Figure 5-9. It can be seen that the presence of the building modifies the settlement trough shape, as expected, with the weight of the building appearing to drive settlements further. For example, the settlement at the

Figure 5-8: Surface settlements for 'greenfield' model (Analysis 1)

(building footprint shown but building not present)

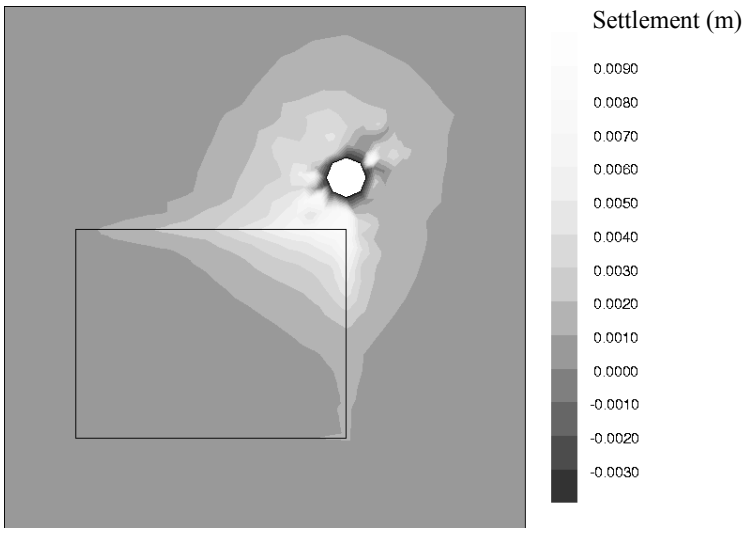

Figure 5-9: Surface settlements for combined model (Analysis 2)

corner of the building nearest the shaft increases from 3mm to 9mm with the building present. The initial settlements of the building due to its own self-weight prior to shaft construction are effectively excluded from the Figure because all displacements in the model are zeroed prior to excavation (Section 5.4.4). Therefore the settlements shown in Figure 5-9 are entirely due to the interaction between the building and the excavation.

More detail on the settlement profile affecting the building may be obtained by plotting settlement with distance along the façades, and this is presented for the east and north façades in Figures 5-10 and 5-11. The other façades did not settle significantly or

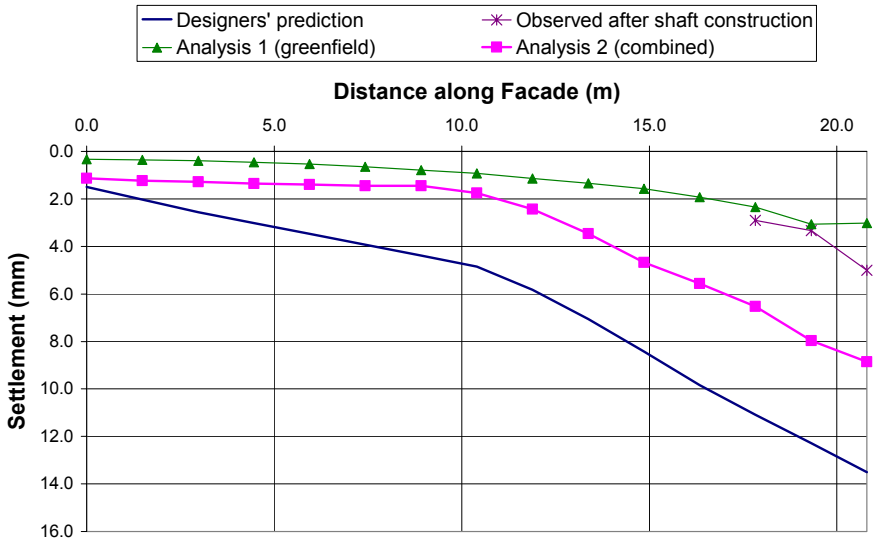

Figure 5-10: Settlement profiles along base of east façade

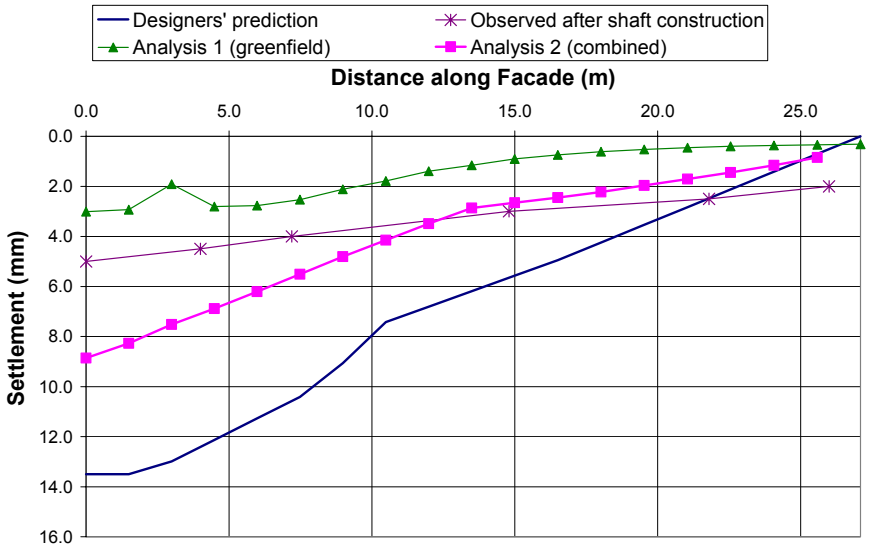

Figure 5-11: Settlement profiles along base of north façade

experience any damage in any of the main analyses.

The results from the combined analysis of soil and building show the bases of both façades responding with Gaussian type half-troughs, but with a somewhat pronounced point of maximum hogging. The maximum settlement of 9mm calculated at the northeast corner is approximately twice what was observed. The calculated 'greenfield' settlements without the building also follow Gaussian type half-troughs, a bit smoother in general but with a reduced maximum settlement of only 3mm at the corner and with signs of localised irregular "spiky" behaviour near the corner.

A preliminary conclusion can thus be made that the volume loss used in the analyses was probably too high, with the true figure being around 1.25% ± 0.5%.

Plots of damage category for the north and east façades of the building for Analyses 2 and 3 are presented in Figures 5-12 to 5-15. The façade has been divided into regions and the damage category based on the average cracking strain over all the Gauss points within the region. This may lose information on some localised cracking behaviour but makes it easier to compare quantitatively the results of different runs (Liu, 1997). Some judgement is required on the division of the façades into regions. These were chosen to highlight regions adjacent to openings and areas of different stiffness. Reduced region sizes were used where more detail was required, *e.g.* in the northeast corner of the church.

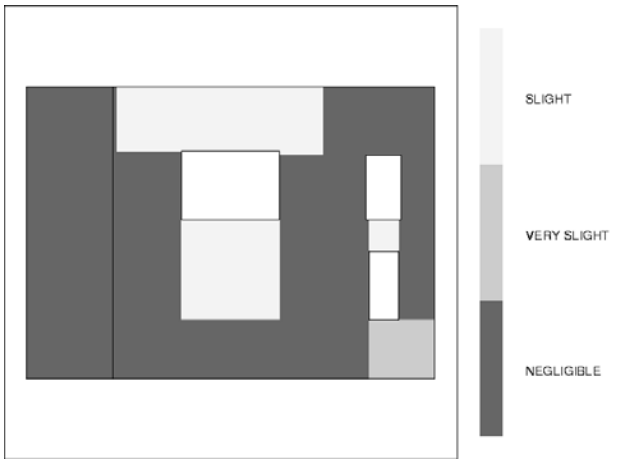

Figure 5-12: Damage to east façade predicted by combined analysis (Analysis 2)

The greatest damage category observed is "Slight", observed for all façades in all three analyses. The distribution of the damage, in particular the position of the "Slight" damage, is distinct for each run. "Slight" damage implies cracks of 1 to 5mm (Section 2.4.2.1). No specific new cracking of this magnitude was observed on site because there was pre-existent cracking to this magnitude, particularly affecting the east façade and the basement level. Thus the predictions may be regarded as not definitely proved accurate, but are quite plausible in suggesting "Slight" damage, and certainly not under-predictions of the real damage.

Figures 5-12 and 5-13 show the results for the combined analysis, Analysis 2. This predicts the largest amount of damage on the east façade, with "Slight" damage all around the larger opening, with further damage associated with the northeast corner. The north

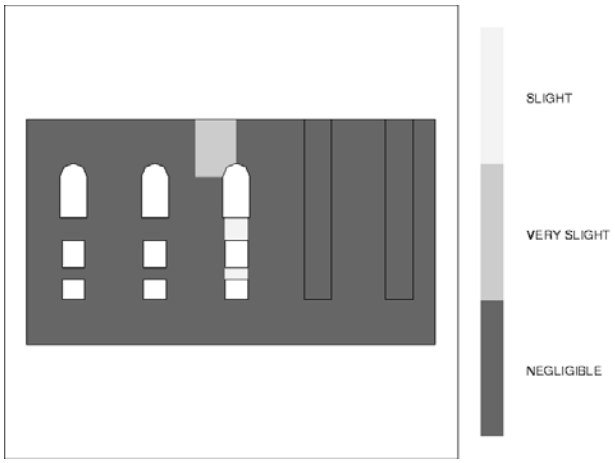

Figure 5-13: Damage to north façade predicted by combined analysis (Analysis 2)

façade experienced damage that appears to follow a particular column of openings (Fig. 5-13). It can be seen, by comparison with Figures 5-10 and 5-11, that for both façades these areas of damage associated with openings are also associated with the hogging part of the settlement profile, which was quite pronounced for both. This suggests that an interaction effect is occurring, when the hogging region of the settlement trough coincides with an opening or openings. The openings accentuate local damage in that area, reducing its stiffness and in turn magnifying the hogging profile, producing in effect a "hinge" that saves the remainder of the façade from major damage. It would have been difficult to predict where these hinges were going to form without conducting a 3-D analysis in this case.

The results for Analysis 3 (Figures 5-14 and 5-15) show damage of "Very slight" and "Slight" categories concentrated at the corners of both façades nearest the shaft. This is consistent with the 'greenfield' settlements applied, which were fairly small, and slightly irregular near the corner. Although the magnitudes of damage are similar for Analyses 2 and 3, the locations are quite different.

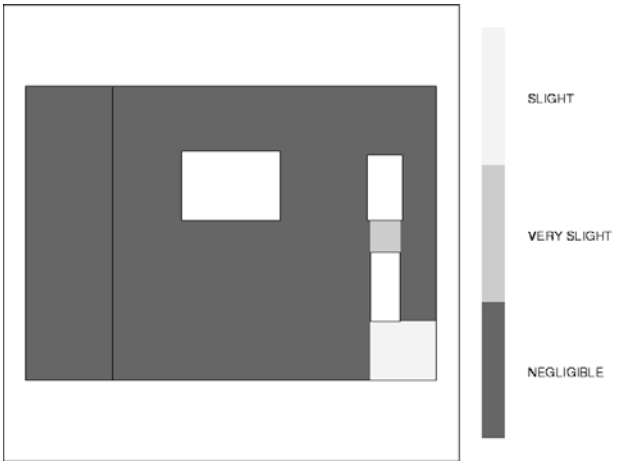

Figure 5-14: Damage to east façade predicted by Analysis 3

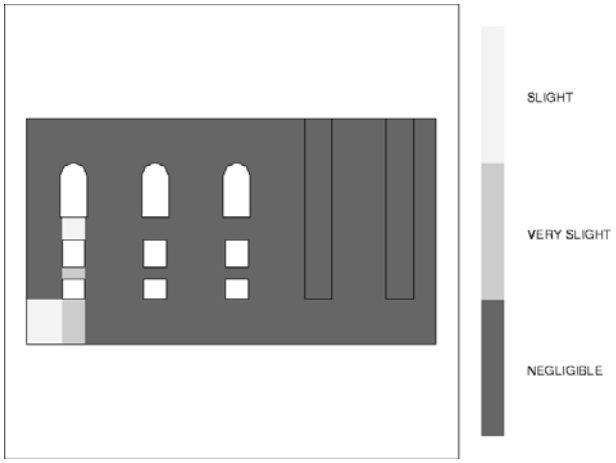

Figure 5-15: Damage to north façade predicted by Analysis 3

5.6 Sensitivity analyses

Sets of sensitivity analyses were carried out, varying certain properties of the soil and building that might be expected to influence the outcome of the analysis. The first two sets were concerned with varying the applied volume loss either side of the base value of 2%. The third and fourth sets varied the building self-weight and stiffness respectively. Finally, an analysis was carried out with the building façades modelled using elastic material rather than elastic, no-tension masonry material.

For these sensitivity analyses and the further analyses described in Section 5.7, the model was re-meshed from that described in Section 5.5. The aim was to introduce provision for a raft foundation beneath the building by partitioning a volume 2m deep in the soil beneath the plan area of the building (Section 5.7.3). For the analyses described in this Section, the properties of this volume were always set to the same as the surrounding soil.

The shaft lining was also modelled in a slightly different way from previously, with the base cap left in place throughout the analysis rather than removed prior to applying the volume loss, as discussed in Section 5.4.4.

The results for the base 'greenfield' model with 2% loss were hardly affected by these changes, with the maximum settlement on the building footprint reducing from 3.0mm to 2.9mm and with very similar settlement profiles. However in the combined model, the

response of the building north façade was altered, with the concentration of damage moving from midway along the façade to near the end farthest from the shaft. The only rational explanation for this shift is the refinement of the soil mesh under the full plan area of the building in providing for the raft, leading to the soil responding relatively more flexibly compared to the building. This then allowed the constraint on the north façade at the far end at the connection with the west façade to have an increased significance in the response of the north façade. More details will be given in the following Sections.

5.6.1 Variation of volume loss for 'greenfield' model

Analysis reference	Volume loss	Maximum settlement on building footprint
Maddox5	2%	2.9mm
Maddox51	1%	1.0mm
Maddox54	4%	6.9mm

The volume loss was varied over the practical range, from 1% to 4%. The increase in settlements with volume loss would have been expected to be linear, but is actually slightly nonlinear, with larger than expected maximum settlement at high volume loss. Examination of the settlement profiles along, for example, the north façade (Fig. 5-16), shows that this deviation from linearity may be attributed to shallow "ripples" in the soil surface, which are unlikely to affect the overall performance of the model, especially at low volume losses.

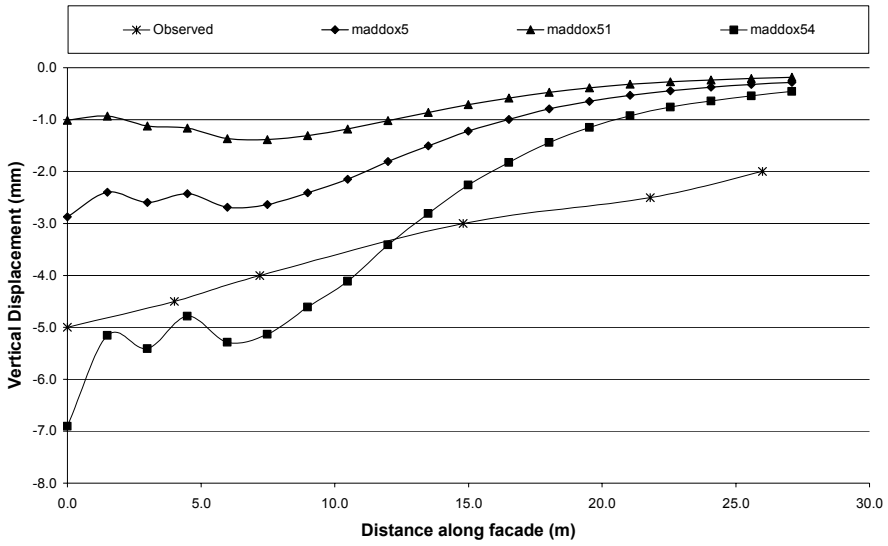

Figure 5-16: Settlement profiles along footprint of north façade for 'greenfield' models

5.6.2 Variation of volume loss for combined model

Analysis reference	Volume loss	Maximum settlement on building footprint	Max. damage category: N façade	Max. damage category: E façade
Maddox5b	2%	8.9mm	Slight	Very slight
Maddox5b1	1%	5.2mm	Slight	Negligible
Maddox5b3	3%	12.5mm	Moderate	Slight
Maddox5b4	4%	16.0mm	Moderate	Slight

With the building introduced into the model, the maximum settlement for a given volume loss is much greater than for the 'greenfield'. This must be due to the increased yielding of the soil that is under stress due to the building self-weight. This effect was observed and commented on with respect to 2-D analyses in Chapter 3, but also appears to have some significance in 3-D analyses. The effect has probably been overestimated in these models due to the façades acting as concentrated line loads on the soil beneath; in a real building, the weight of the building would be distributed over the soil by means of a foundation. An attempt to model a foundation for the Mansion House is reported in Chapter 7.

Figures 5-17 and 5-18 show the damage distribution, averaged over zones, for the east and north façades for the base combined model (2% ground loss). These may be compared with Figures 5-12 and 5-13 for the earlier model of the same case with the less refined mesh. The east façade is less damaged, with the pronounced point of hogging shown in

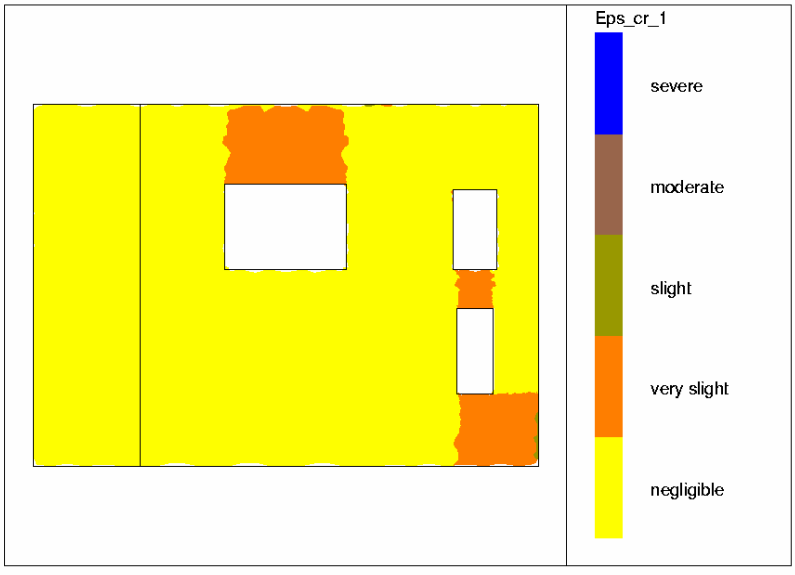

Figure 5-17: Damage category for east façade, combined model with 2% volume loss (maddox5b)

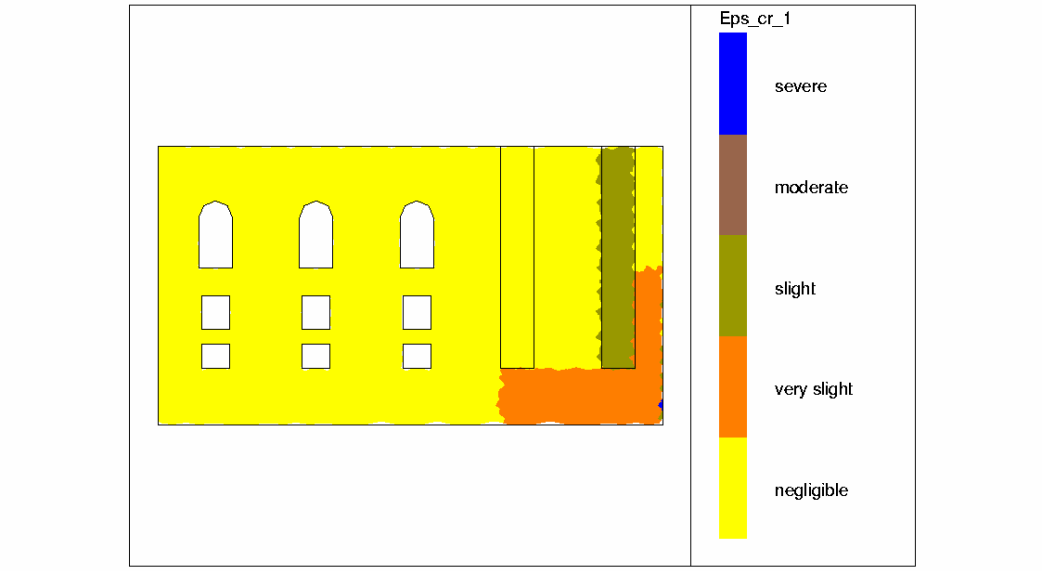

Figure 5-18: Damage category for north façade, combined model with 2% volume loss (maddox5b)

Figure 5-10 halfway along the façade under the window no longer so evident.

The maximum damage in the north façade is unchanged, but its location has moved from around the openings halfway along the façade to the region of reduced stiffness at the far end. This raises the possibility that the constraint on vertical movement of the façade where it is connected to the next façade by means of the tie elements is contributing to the damage pattern. The settlement profile along the north façade (Fig. 5-19) shows a sudden change concentrated over the last 4m or so that may be correlated with the damage.

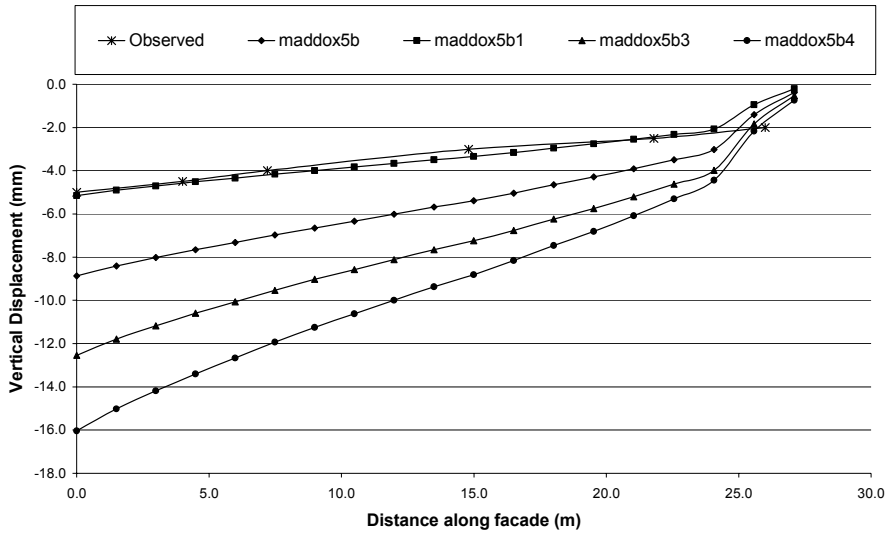

Figure 5-19: Settlement profiles along north façade; combined models with variation of volume loss

The remarkably good agreement of the observed settlements with the combined model with 1% volume loss is also to be noted.

5.6.3 Variation of building self weight

Analysis reference	Masonry self-weight (kN/m^3)	Maximum settlement on building footprint (mm)	Maximum building damage category
Maddox5b	20.0	8.9	Slight
Maddox5w01	2.0	3.3	Negligible
Maddox5w13	26.0	10.9	Moderate
Maddox5w2	40.0	19.2	Severe

It is normally possible to estimate the weight of a real building to within 10%. Within these bounds, the results above indicate that the outcome of the analysis would be similar. Thus it is reasonable to assume that for a given building, the results are unaffected by building weight within the practical range.

The above series of analyses were carried out to explore the importance of modelling building weight at all in the 3-D analysis. A trend is found in which increasing weight gives increasing settlements and building damage, as also observed by Liu (1997). For the light building (analysis Maddox5w01), the maximum settlement is similar to the 'greenfield' case (analysis Maddox5, Section 5.6.1).

5.6.4 Variation of building stiffness

Analysis reference	Masonry Young's modulus (GPa)	Maximum settlement on building footprint (mm)	Maximum building damage category
Maddox5b	20.0	8.9	Slight (N façade)
Maddox5s01	2.0	10.2	Moderate (E façade)
Maddox5s10	200.0	8.7	Negligible

The stiffness of a building is much more difficult to assess than the weight. This is particularly true in a framed building, in which non-structural elements such as cladding and internal partitions may contribute significantly to the global bending and shear stiffness. In a load-bearing masonry structure, it is easier to make an assessment because most of the stiffness is concentrated in the load-bearing walls, but it is probably still

possible to be a factor of three out, due to the variability of masonry including the effect of pre-existent cracking.

This set of analyses varied the stiffness of the masonry by a factor of ten either side of the base value. It can be seen that maximum settlement, which is largely governed by building weight, was relatively unaffected but the damage to the building changed by a category or more. Figure 5-20 shows the settlements along the east façade, in which the low stiffness building follows a profile similar to the 'greenfield' (Maddox5) but scaled up, whereas the other models show increasing amounts of smoothing to the trough shape. The interaction with the building is illustrated by the damage to the low stiffness façade shown in Figure 5-21, which may be compared to Figure 5-17 for the base building stiffness.

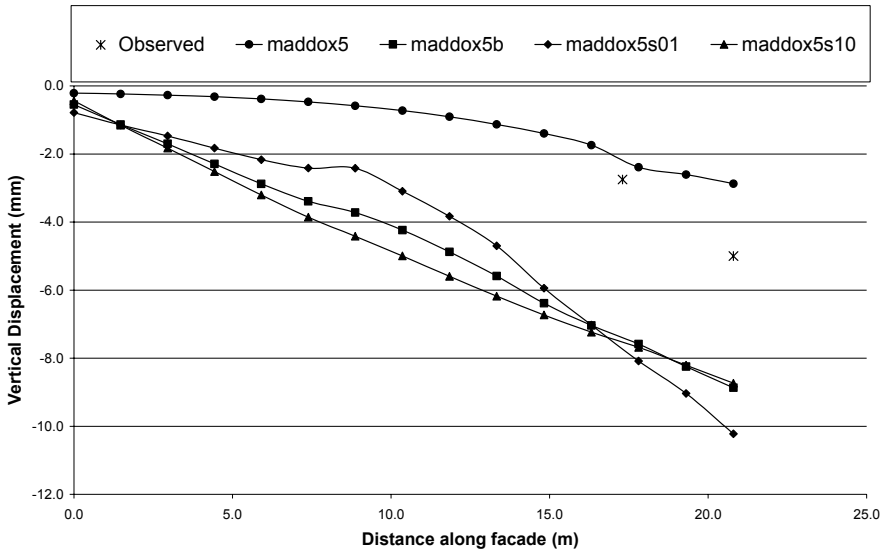

Figure 5-20: Settlement profiles along east façade for variation of building stiffness

5.6.5 Elastic building

Analysis reference	Building material type	Volume loss	Masonry Young's modulus (GPa)	Masonry self-weight (kN/m^3)
Maddox5b	Elastic, no-tension masonry	2%	20.0	20
Maddox5bel	Elastic	2%	20.0	20

Previous researchers at Oxford (Liu, 1997 and Augarde, 1997) compared the response of elastic façades to façades of elastic, no-tension material and found that the elastic

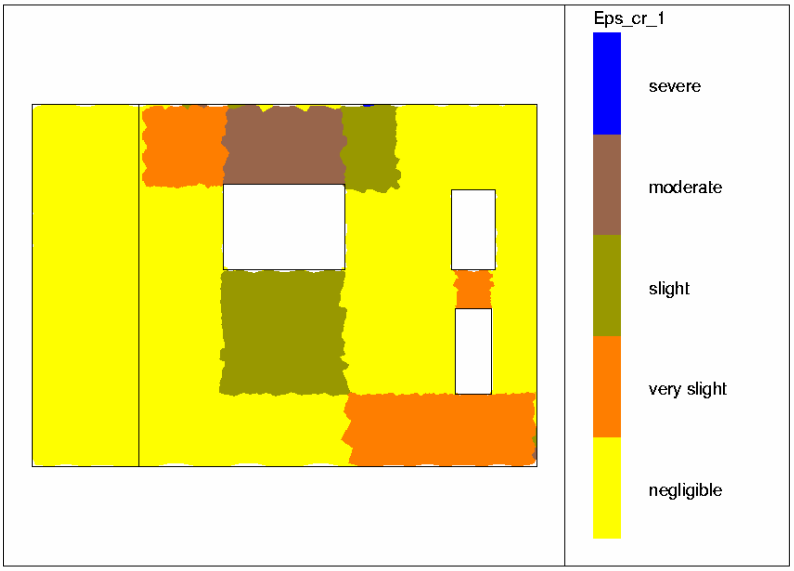

Figure 5-21: Damage category for east façade, low stiffness building (maddox5s01)

façades gave considerably greater smoothing of the settlement trough due to the ability of the elastic material to tolerate tension 'cables' within the façade as well as compressive 'arches', and hence span much more effectively across the tunnel when it passed beneath the building.

In this case, the excavation is occurring to one side of the building. The elastic building is seen to tilt as a rigid body towards the shaft, with very little distortion within the façades (Fig. 5-22). The strain within the façade is very small, only 26με maximum (Fig. 5-23),

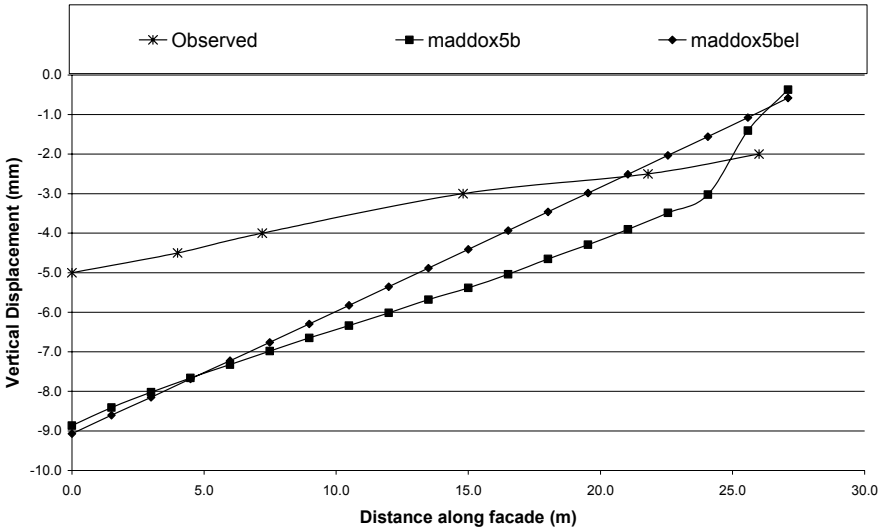

Figure 5-22: Settlement profiles along north façade; elastic building compared with elastic, no-tension masonry building

compared to a value of 500με that would correlate with "Very slight" damage.

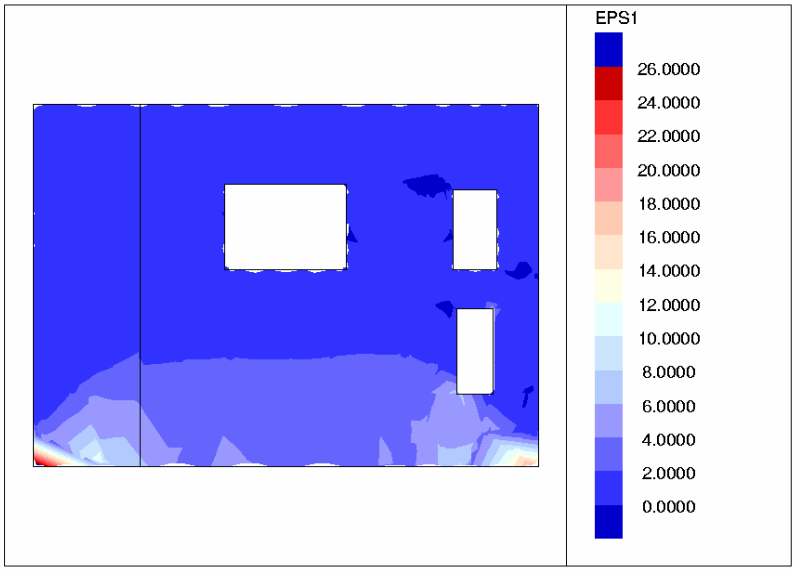

Figure 5-23: Contours of maximum principal strain in north façade for elastic building model (maddox5bel)

5.6.6 Variation of soil strength

Analysis reference	Profile of soil undrained strength (kPa) with depth *z* (m) below ground level	Maximum settlement on building footprint (mm)	Maximum building damage category: N façade	Maximum building damage category: E façade
Maddox5b	60 + 6*z*	8.9	Slight	Very slight
Maddox5y12	114 + 6*z*	7.3	Negligible	Slight
Maddox5y9	96 + 6*z*	7.5	Negligible	Very slight
Maddox5y6	78 + 6*z*	8.1	Very slight	Very slight
Maddox5y0	42 + 6*z*	10.2	Slight	Very slight
Maddox5ym3	24 + 6*z*	13.0	Moderate	Slight
Maddox5ym6	6 + 6*z*	UNSTABLE	-	-

One of the key variables at any real site is the soil strength and stiffness. For this project, London clay with a rigidity index (ratio of stiffness to undrained strength s_u) of 500 was assumed. This is in the middle of the range that is normally assumed by designers, which is from 200 to 1000 or so.

The profile of stiffness with depth may be measured with reasonable confidence by means of pressuremeter tests. s_u may also be obtained from pressuremeter tests and from

undrained triaxial tests on good quality samples. It normally increases linearly with depth although there may be more variability near the surface.

In this set of analyses, s_u was assumed to increase at a constant 6kPa per metre depth for all analyses. The reference level at which s_u was taken as 60kPa was varied in steps of 3m. Thus, for the surface 10m or so of soil, the stiffness varied by a factor of two across all the analyses, with the base analysis Maddox5b in the mid-range. This is not much more than the range of uncertainty from a typical site investigation. The results show the influence of soil properties on the damage category predicted for the building, and the study implies that a high quality investigation would be needed to complement the use of the analysis techniques in practice.

5.7 Alternative modelling approaches

5.7.1 Exchange of discrete openings for vertical regions of reduced stiffness

Analysis reference	Description of N façade	Maximum damage category in N façade
Maddox4b (Analysis 2 in Section 5.5)	3 columns of windows nearest shaft, 2 columns of reduced stiffness (40% stiffness)	Slight
Maddox4b7	5 columns of reduced stiffness (40% stiffness)	Slight

With the earlier model of Maddox Street that was discussed in Section 5.5, the north façade was amended to replace all the discrete openings with vertical regions of reduced stiffness. This was then run to compare with Analysis 2. The results are shown in Figures 5-24 and 5-25, which show damage category without averaging over zones. The agreement in the distribution and severity of damage was found to be good, and this confirmed the applicability of the general approach of modelling openings in such a way. It can also be concluded that in this case there was not a clear benefit in modelling individual openings, basically due to the relatively light damage the building suffered.

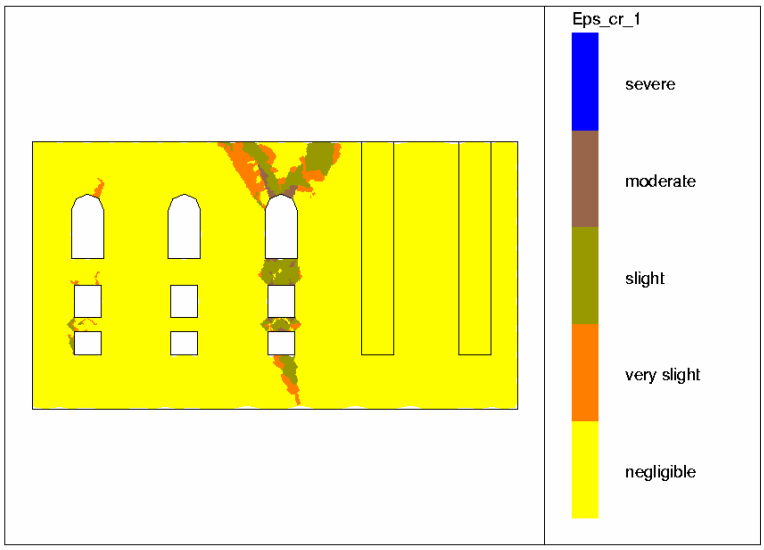

Figure 5-24: Damage to north façade predicted by Analysis 2

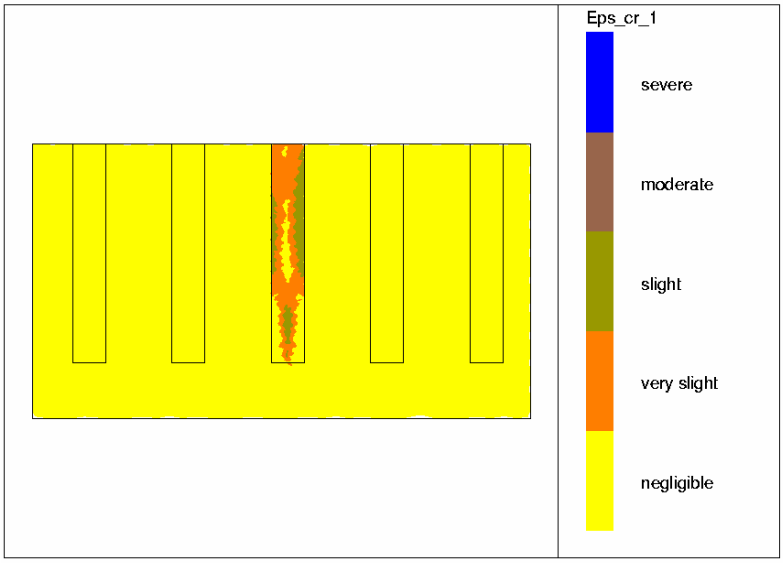

Figure 5-25: Damage to north façade predicted by analysis Maddox4b7

5.7.2 Variation of stiffness of regions of reduced stiffness

Analysis reference	Stiffness of regions of reduced stiffness (% of full masonry stiffness)	Maximum settlement on building footprint (mm)	Maximum N façade damage category
Maddox5w13	40	10.9	Moderate
Maddox5f20	20	11.3	Moderate
Maddox5f80	80	11.3	Moderate

For the base building model, the stiffness of the vertical regions of reduced stiffness in the north façade was set at 40% of the intact façade stiffness (Section 5.4.3). Although this was based on a reduction in stiffness corresponding to a physical reduction in cross-sectional area at the openings, it was still felt to be useful to examine the sensitivity of the solution to the variation of this percentage.

The table above summarises the set of analyses. In this case the base analysis was taken as Maddox5w13, which has building weight 130% of the original value. Figure 5-26 shows the settlement profiles obtained along the north façade footprint. The profiles for Maddox5w13 and Maddox5f80 are similar, as are the extent and severity of damage to the façade. However with the reduction to 20% stiffness in Maddox5f20, an even greater distortion occurs at the right end of the façade where it joins the west façade. In addition, a hogging region about 10m from the left end is expressed in the profile, and reflected in further damage to the façade in this area (Fig. 5-27). This hogging region was not, however, observed (Fig. 5-11), and therefore the implication is that 20% stiffness was too low and that the value of 40% obtained from simple physical considerations is sufficiently accurate. This is also confirmed by the results in Section 5.7.1 above.

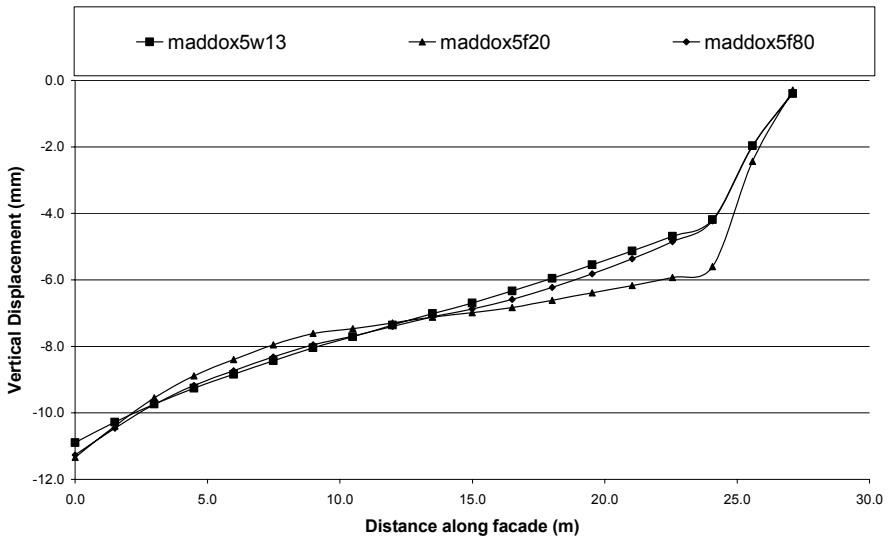

Figure 5-26: Settlement profiles along north façade; variation of stiffness of vertical regions of reduced stiffness

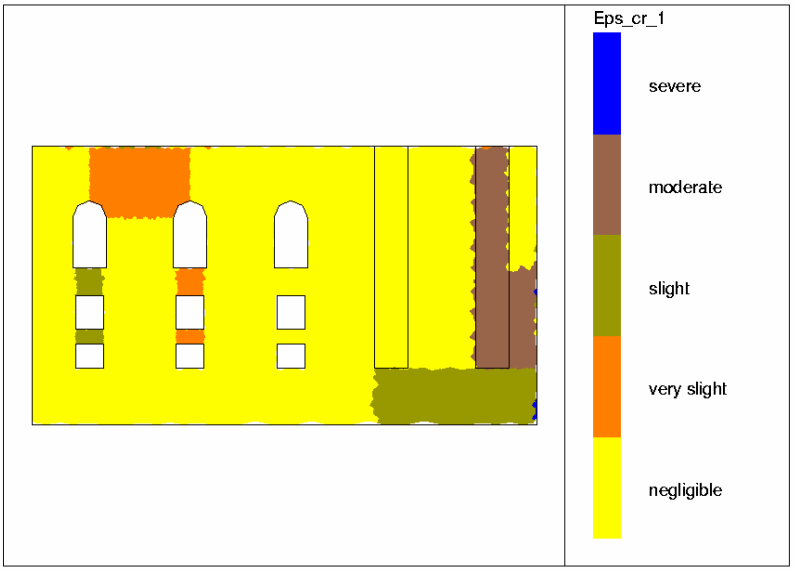

Figure 5-27: Damage category for north façade, building with 20% stiffness vertical regions (maddox5f20)

5.7.3 Representation of foundation stiffness

After the main analyses described in Section 5.5 were carried out, consideration was given to the possible influence of the stiffness of the building foundation on the response, because the observed response of the façade appeared at that stage to be a lot stiffer than that obtained in the combined model, as illustrated by Figure 5-11.

Relatively little detail was known about the foundation construction, but it was reasonable to assume that they were of mass masonry, set on the terrace gravels. This would not be expected to have a significant influence on the global stiffness of the façade.

The church had an additional feature of a vaulted masonry basement structure covering the entire plan area of the building. There was a possibility that this could act as a raft in itself, linking the response of the façades nearest the shaft to those furthest away, and causing the overall response to be more like a rigid body rotation, as observed. Attempts were made to include this basement structure in the model. It was assumed to be 2m thick with a Young's modulus of masonry of 10GPa.

A first attempt was made to model the raft using shell elements of the same type as used in the shaft lining. However, the analysis failed to converge, because of the low out-of-plane bending stiffness of the shells. Therefore, the model was re-meshed with

provision for a solid raft in the top of the soil within the building footprint. This model was then used for the sensitivity analyses discussed in Section 5.6, with the raft having been given the same properties as the surrounding soil.

When the raft was given elastic properties with a Young's modulus of 10GPa and an almost infinite strength, the settlement pattern in Figure 5-28 was obtained with the normal weight building. Essentially the same result was obtained with just the raft and no building façades in the model. The result showed that the raft prevented any significant settlement within the building footprint, and thus was too stiff. The same outcome was observed when the stiffness of the raft was reduced by a factor of ten. The elastic raft thus responded too stiffly, in a similar manner to elastic façades (Section 5.6.5). A less stiff response would have been obtained if the raft could be modelled as elastic, no-tension masonry, but a three-dimensional implementation of this model is not yet available. The improved results presented in Section 5.6 for a building without a raft when the soil was re-meshed with a finer mesh reduced the necessity for pursuing this line of research any further.

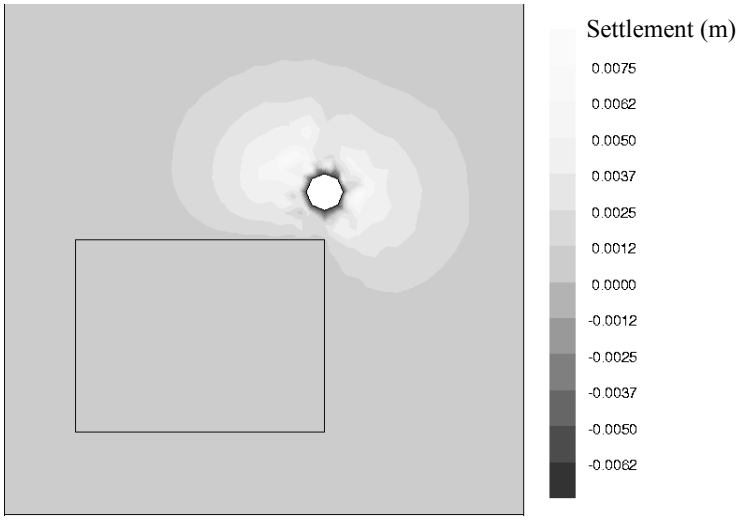

Figure 5-28: Surface settlements for combined model with elastic raft

5.8 Discussion

This case history was the first to be analysed for this project. Attempting to analyse it stimulated a number of improvements to the OXFEM program to make it more user-friendly, in particular at the pre-processing stage as described in Chapter 4. Most of the analyses were carried out using the Sun UltraSparc 2 workstation (Section 4.5) and run times were relatively long, limiting the depth of the study.

The case history was monitored and documented to the level of detail that is typically provided in commercial projects where the aim is to convince a building owner that no damage has occurred to their structures. Settlements of potentially vulnerable buildings were measured as the excavation proceeded. Building condition surveys were carried out before and after construction. The settlement monitoring appears to have been carefully executed, and the data to be accurate.

The case history has the disadvantage that, since the whole settlement field around the shaft was not recorded, it is not possible to obtain a firm figure for the volume loss. This is a problem because previous analyses have shown, and this study confirms, that the settlement of a building due to tunnelling depends on the volume loss and also on its own self-weight. Without a firm figure for the volume loss, it is not possible to separate these effects.

The church building was of a structural form that lent itself very well to analysis by the techniques developed at Oxford. The main structure of the building was easily identifiable: load-bearing masonry walls in a simple geometry of a rectangular box. Other features that would have been more difficult to model accurately, such as the tower and portico, could be neglected with justification. The site conditions were predominantly London clay, which is a well-documented material for which a good constitutive model was available. The properties of the soil could be confirmed with fair confidence from the site investigation results, although a more detailed study would have been desirable to improve the accuracy of the model.

The other main disadvantage of the case history was that there was no positively discernible damage recorded for the church due to construction of the shaft and the tunnel.

This will of course be typical of any case history of a well-engineered project. However, there is reasonable evidence from the settlement observations that the façades did not simply respond elastically to the excavation but distorted to a degree that implied nonlinear behaviour. The precise distribution of damage that resulted was not recorded, so there is nothing to compare directly with the model's outcome, except general confirmation of the result from the model that the damage should be no more than "Slight".

The 'greenfield' settlements predicted by the model looked plausible, and the philosophy of modelling the shaft as initially excavated and fully lined and with the volume loss modelled by shrinking the lining in the usual way is justified. The soil model performed satisfactorily.

In the combined model with the building, the distribution of settlements looks reasonable, with the building responding almost as a rigid body with relatively light damage. However, the magnitude of the building settlement is approximately twice what was observed. This could be either because the volume loss was too great, or because the effects of building self-weight have been exaggerated in the model. The former is the most likely explanation, because the best agreement between the model and observations was obtained when the volume loss was halved, to 1%. A possible mechanism for the latter explanation would be that the bearing pressure of the building weight on the soil was too great. Distributing the weight of the façades on the soil by means some kind of foundation could mitigate this. Given the uncertainty as to the cause of the larger than observed building settlement, the addition of a foundation is recommended for future research.

The initial analyses with 2% volume loss did not give particularly good agreement with observations in the detail of the building performance. Interaction of the façade with the ground was demonstrated, with higher damage correlated with a hogging region of the settlement profile, with a "hinge" forming in the façade. This is the kind of behaviour that would be often be expected in practice, and may well have occurred if the settlements of the church had been greater than observed in this case.

The usefulness of the technique of modelling openings by vertical regions of reduced stiffness has been proved for this case, where the building distortions and damage were

relatively low. A reasonable result is obtained by reducing the intact façade stiffness in proportion to the reduction in cross-section measured on a vertical section through the openings. If façades are highly stressed, stress concentrations around individual openings may become more important, in which case they should be modelled explicitly.

The overall amount of damage predicted by the model was in a reasonable range, and the elastic, no-tension material model performed satisfactorily, provided the loading was applied over a sufficiently large number of load steps. The usefulness of graphical averaging techniques originally used by Liu (1997) was confirmed.

The meshes for the building façades were relatively refined, due to the need to discretise around individual openings. However the importance of the mesh density in the soil beneath the building was highlighted, as a by-product of an attempt to model a raft foundation. With a finer mesh, the behaviour of the building changed significantly, with the location of damage moving along the north façade. This indicated that the change in the relative stiffness of the response of the soil and façade in the model due to the change in mesh density was significant. It was not possible to experiment further with mesh density for this case history, due to the limitation of computing resources. Further improvement in accuracy would have been possible, but probably would have been marginal, as the local element size in the soil under the building was down to 2m, which is nearly as small as the typical feature size in the building.

The final damage pattern in the refined model discussed in Section 5.6 is interesting. The damage in the east façade was located around the large opening, as expected. In the north façade, in which the effect of individual openings was shown to be small when they were replaced with regions of reduced stiffness, the main damage was concentrated at the far end of the façade from the shaft. At first sight, this seems an unlikely outcome that was not observed in the field, although it could be argued that no one would have thought to look for damage at that location. The settlement profile shows a sudden jump from zero settlement at the end to about 3mm within 3m (Fig. 5-19, model Maddox5b), where the damage is concentrated. Interestingly, 2mm of settlement was also observed within a short

distance of the end of the façade, although this one reading is not really enough evidence to prove the mechanism occurred.

Vertical displacements at the end of the façade are constrained to be equal to those of the connecting façade. Thus there is also a degree of restraint vertically because of the resistance of the connecting façade to settlement. This restraint appears to have been significant in determining the final distribution of damage. Whether this effect occurs in real buildings would be an interesting subject for future research.

The sensitivity analyses showed that building weight distribution and soil strength and stiffness are more important influences on the performance of the building than the absolute value of building stiffness. Variations in effective building stiffness within a façade due to the presence of openings are, however, important to the behaviour, as demonstrated in the east façade of this model.

An attempt to model the basement structure of the church as a raft foundation gave unrealistic results, with the raft itself performing far too stiffly. The fact that it could only be modelled elastically by OXFEM undoubtedly contributed to the problem. A masonry model of the raft may have given better results. It is difficult to assess the real influence of the basement structure on the church and whether it contributed to the global behaviour, which was nearly rigid body rotation.

ANALYSIS OF THE EFFECTS OF THE HARBOUR APPROACH TUNNEL ON HOUSES AT RAMSGATE, KENT

5.9 Introduction

Monitoring of this site was carried out in early 1999. A large diameter tunnel was bored by a novel tunnelling method at low cover beneath a row of two storey houses. Precise levelling and monitoring of existing cracks was conducted. The data showed that the row of houses responded relatively flexibly in the transverse direction to the passage of the tunnel. Movements were recorded of the existing cracks.

It proved possible in the numerical model to reproduce the 'greenfield' settlement trough observed on site, even though it differed from that of conventional bored tunnelling. The transverse behaviour of the terrace was also modelled successfully. The importance of modelling internal structural walls and the effects of openings in reducing structural stiffness was emphasised.

5.10 Background to the case history

5.10.1 Overview of the construction project

The 2.2km Ramsgate Harbour Approach Road was constructed in 18 months from April 1998. The purpose of the route is to provide an improved access to the Port of Ramsgate from the main road to the west.

The alignment of the single-carriageway route commences at a roundabout on the London road, descending towards the south in a cutting. It then passes through a single bore 800m long tunnel under the chalk cliffs, emerging on the foreshore close to the port (Figure 6-1).

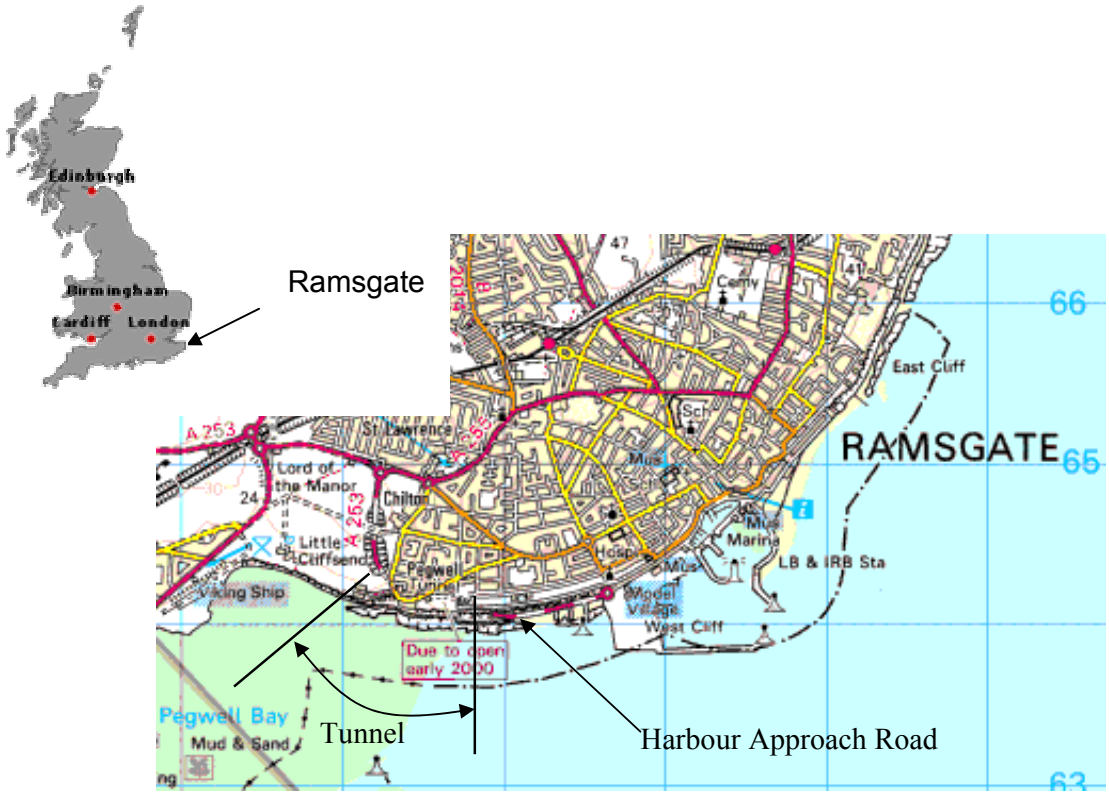

Figure 6-1: Location of Ramsgate Harbour Approach Road and tunnel

The original proposal for the tunnel was for 260m of cut-and-cover construction where the cover to the original ground surface was lowest, followed by 550m of bored tunnel, to be constructed with a sprayed concrete primary lining. However, the contractor submitted an alternative design, which was accepted, in which the entire tunnel was to be bored using the Perforex pre-vaulting method (Morgan, 1999). This was to be the first use of this French tunnelling system in the United Kingdom.

The change of construction method meant that a terrace of cottages on Pegwell Road at the western end of the tunnel section, originally due to be demolished for the cut-and-cover construction, could now be saved. The alignment of the tunnel was lowered to give a minimum of 6m of cover over the crown beneath the cottages, and to pass beneath a nearby major sewer. The cottages then became a focus of interest for monitoring of ground and structure movements. Data was collected as part of this project, forming the second case history for analysis.

5.10.2 Ground conditions

A detailed ground investigation was carried out prior to construction, employing a range of techniques including rotary coring and sampling for laboratory testing, falling head permeability tests, pressuremeter (high pressure dilatometer) testing and surface wave geophysics. The underlying formation for the entire tunnel drive was identified as competent Upper Chalk, with a typical CIRIA grade of A2 (CIRIA, 1994). Over the first 300m of the drive, the depth to the Upper Chalk ranges from 0.3m to 3.95m, with an average of 2.4m. The competent chalk is typically overlain with weathered chalk of grade B4 to Dm.

At the location of the cottages, the weathering profile of the chalk, together with the overlying surface layers, was found to be of critical importance to tunnelling operations. A cross-section at the cottages is shown in Figure 6-2, indicating the presence of a buried river valley in which the depth of weathering of the chalk increases significantly.

The tunnel invert at the cottages is within chalk that is structured and relatively unweathered, but still rather weak. The crown of the tunnel passes through weathered to highly weathered chalk, classified on site as low plasticity clay. The cover of chalk over the crown reduces to only 1 to 2m. Overlying this is a layer of 2 – 3m of red 'brickearth',

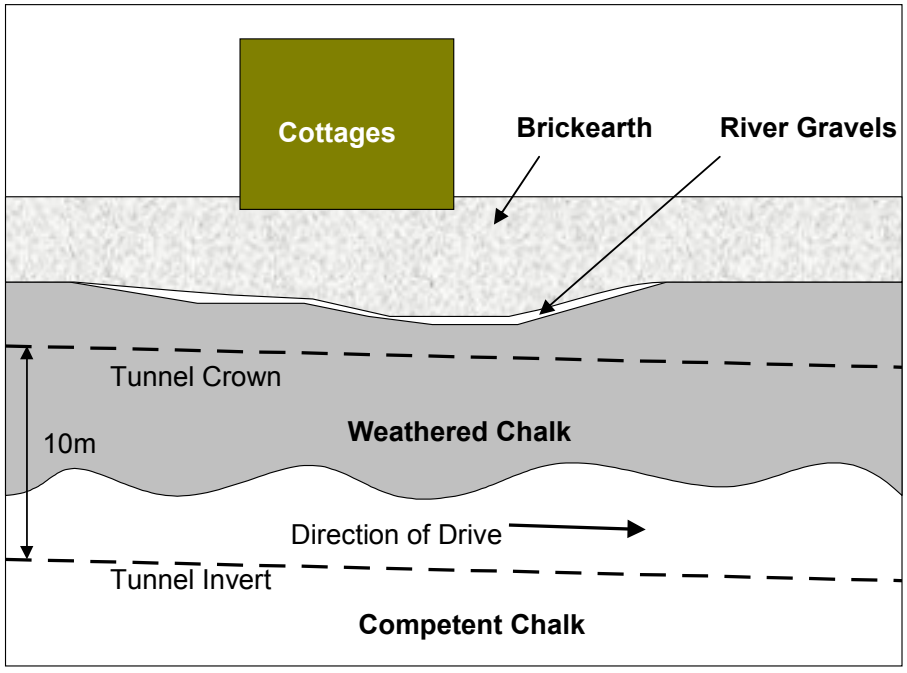

Figure 6-2: Cross-section showing ground conditions at Pegwell Road cottages

classified as a low to intermediate plasticity clay with a substantial silt fraction. This is in turn overlain by about 1m of made ground and road surfacing.

5.10.3 Tunnel construction

The tunnel is approximately 11m in diameter, with an arched profile and a flat invert. The principle of the Perforex method is that a supporting arch or 'pre-vault' is cast ahead of the tunnel face to provide advanced support (Crow and Newman, 1999). A 5m long chainsaw on the front of the machine (Figure 6-3) is used to cut a 200mm deep, arched slot around the sides and crown of the bore. A second head on the machine sprays concrete into the slot to form the pre-vault. In order to maintain good control of ground movements at Ramsgate, the slot was opened up in short sections, 2 – 3m in length on alternate sides on the face.

The pre-vaults served as the primary lining. Once the pre-vault concrete had cured to strength of 8MPa, the tunnel face was advanced using standard excavation equipment. At the end of each stage of advance, the face was usually sprayed with a 50mm layer of concrete to increase its factor of safety against localised failure. The invert was then excavated up to the face to a depth of 200mm and a reinforced concrete slab cast. The machine then advanced by use of feet on hydraulically activated rams. The face was further supported throughout the cycle by sacrificial fibreglass dowels, up to 18m long.

The designer determines the factor of safety of the tunnel primary lining, depending on

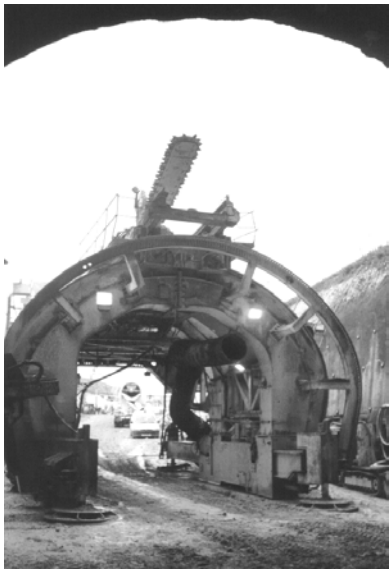

Figure 6-3: Perforex tunnelling machine entering partially completed tunnel

the ground conditions, by varying the overlap of the pre-vaults. The length of advance per cycle of operations varied between 2.5m and 4.5m throughout the drive. With one complete cycle taking typically 24 hours, the advance rate varied from 12m per week to over 20m. Slower advance rates were used in the vicinity of the cottages, with a higher factor of safety at this location.

5.10.4 Pegwell Road cottages

The tunnel passed beneath the row of eight terraced cottages, Nos. 83 to 97 Pegwell Road, with a cover beneath the foundations of only about 6m. The angle in plan between the tunnel axis and the line of the front of the cottages is 40^o (Figure 6-4). The cottages consist of a terrace of eight similar properties, dating from the early 1900's, with a ground and first floor and no basements. A two-storey extension wing at the back of each cottage is joined to one other property, and the cottages are staggered relative to each other by 2m.

The structural form is load bearing brick masonry on shallow strip foundations, with wooden suspended floors and ceilings. Alterations have taken place in many of the cottages, often involving removal of internal walls to create larger rooms. However the main load bearing walls – the front, rear and party walls – have been retained in each case. These are solid masonry, nine inches (220mm) thick. The openings to the front and rear

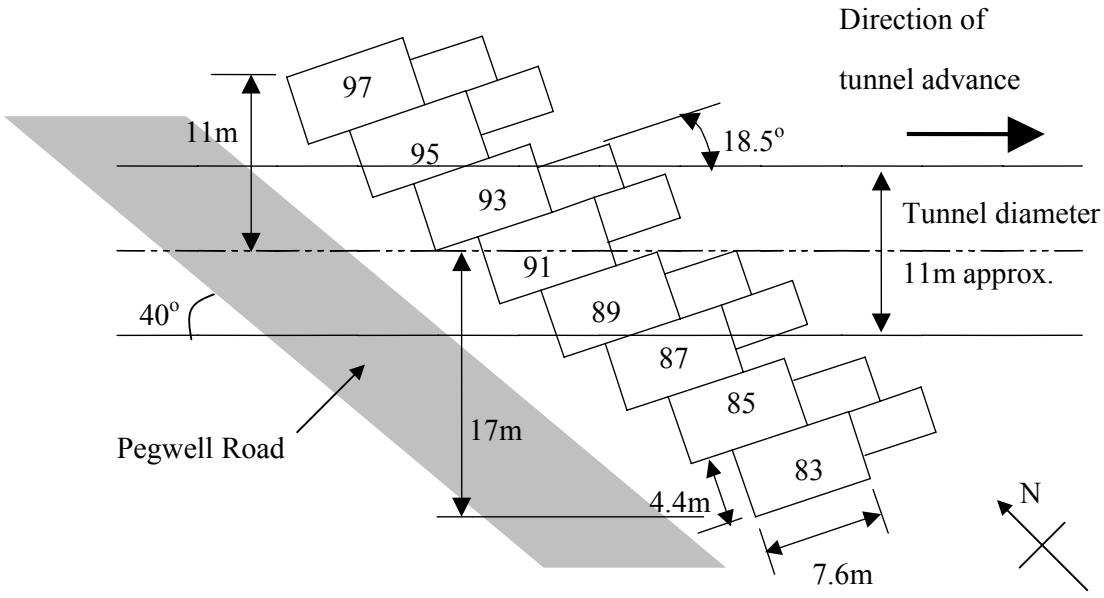

Figure 6-4: Plan on Pegwell Road cottages showing tunnel alignment

have also remained largely as originally constructed (Figure 6-5).

Structural surveys of the cottages were carried out prior to tunnel construction. The majority were found to be in reasonable condition for their age, with only occasional hairline cracking in interior and exterior walls. There was evidence of reconstruction of brickwork and re-pointing of No. 97, the only cottage to have been underpinned recently (due to subsidence). However No. 83, at the south end of the terrace, was found to be suffering from the effects of ground movement, with widespread cracking including a 50mm wide crack on the first floor on the rear elevation adjacent to the party wall with No. 85. The evidence suggested that the rear of No. 83 had tilted away from the remainder of the terrace and towards the nearby cliffs to the south.

It was not expected that No. 83 would be directly affected by the tunnelling settlements, as it lay outside the predicted settlement trough. However, there was concern that movement of No. 85 on the edge of the hogging part of the trough could cause the large crack between No. 85 and No. 83 to open. Thus No. 83 was monitored extensively during construction.

5.10.5 Monitoring regime

A monitoring programme in the area of Pegwell Road and the cottages was instigated

Figure 6-5: Views to the front and rear of terrace of Pegwell Road cottages

by the contractor to ensure the safety of its operatives, the works and the general public using Pegwell Road. Additional monitoring was specified for this project.

As the tunnel drive approached Pegwell Road from the west, it passed beneath an open field. Three transverse arrays of precise levelling points were monitored in this field, giving important information on the 'greenfield' settlement behaviour induced by the Perforex tunnelling method.

An array of precise levelling points was also set up along the footpath immediately in front of the cottages. The data from these was taken as representative of the 'greenfield' settlements at the actual location of the cottages. Further arrays were set up in the back gardens of the cottages and in the land behind them, although here the tunnel depth was greater and the ground conditions changed somewhat from those prevailing at the cottages.

In addition to the precise levelling, inclinometer tubes were also installed around the cottages. These were monitored manually during construction. Although they gave an indication of subsurface ground behaviour, the quality and repeatability of the results was not sufficient to provide useful additional information.

The contractor also carried out comprehensive in-tunnel monitoring, measuring rate of advance, convergence and crown settlement.

The monitoring programme for the cottage structures was specified for this project and agreed with the contractor. Three types of instrumentation were involved: precise levelling points, crack telltales and Demec stud arrays.

Precise levelling studs were drilled and resin-grouted into the masonry at each end of each of the load-bearing party walls at the locations shown in Figure 6-6, with the aim of measuring the transverse settlement trough at the front and rear of the cottages.

Crack telltales comprise a pair of plastic strips, with a scale and cross hairs, fastened either side of a pre-existing crack. They record horizontal and vertical translations and rotations, with a range of ±20mm perpendicular to the crack and ±10mm parallel to it. Experience showed that accuracies of ±0.2mm on individual readings were achievable. These were placed where there was a concern that large movements (of the order of

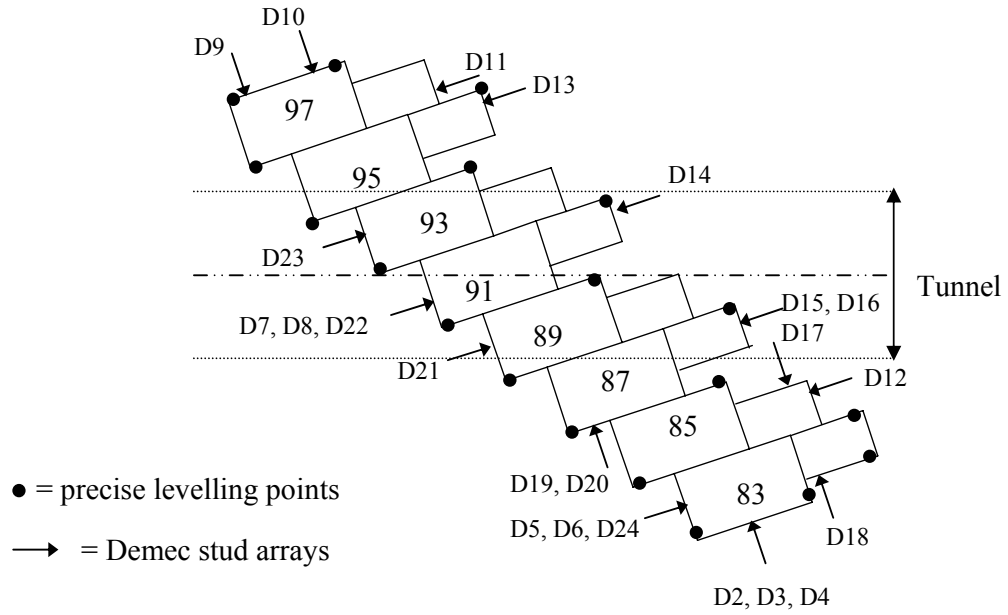

Figure 6-6: Plan of cottages showing locations of precise levelling points and Demec arrays

millimetres) might take place. In practice this meant 11 locations inside and outside No. 83 Pegwell Road, the cottage heavily damaged by subsidence.

Demec studs are metal studs approximately 3mm in diameter, glued on to each side of a pre-existing crack, in pairs for measuring unidirectional movement or in an array of three for detecting movement in two orthogonal directions. The distance between the studs is measured by a Demec gauge, a hand-held mechanical gauge capable of recording movements to accuracy of at least ±0.1mm over a range of ±3mm. 22 Demec arrays were located on smaller (typically 1 – 2mm wide) pre-existing cracks on the external faces of the cottages, often located close to windows and doors. Details of these locations are given in Table 6-1. For safety reasons, arrays could be located no more than 2.5m above ground level in positions that were accessible by ladder, but there were no significant pre-existing cracks above this level.

The instrumentation was installed in October and November 1998. A survey carried out on 14th December 1998 was used as the baseline set of readings. Daily monitoring was commenced on 21st January 1999, when the tunnel heading was 30m from the cottages. The face passed under the front of the cottages on 1st February, and daily monitoring

continued until 26th February, when the face had advanced to 15m beyond the southern end of the cottages. Monitoring continued at weekly intervals until the end of March.

Demec set number	Location		
	House no.	Front/rear/ side	Detailed description
D1	83	Side	R side of wall, 1m above ground
D2	83	Side	Centreline of wall, close to ground
D3	83	Side	Centreline of wall, 500mm above ground level
D4	83	Side	Centreline of wall, 1m above ground level
D5	83	Front	Beneath ground floor bay window, on R side
D6	83	Front	Beneath ground floor bay window, on L side
D7	91	Front	Beneath ground floor bay window, on centreline
D8	91	Front	Beneath ground floor bay window central pane, on R side
D9	97	Side	1m above ground, 1.5m from R end
D10	97	Side	1m above ground, 1.5m from L end
D11	97	Rear	500mm above ground on L side
D12	85	Rear	Above rear window
D13	95	Rear	Top R corner of larger rear window
D14	91	Rear	Below rear window, on R side
D15	87	Rear	Above rear window, on L side
D16	87	Rear	Above rear window, on R side
D17	85	Rear	On side wall of rear extension, above L window on centreline of window
D18	83	Rear	On side wall of rear extension, above L window
D19	85	Front	Side rendered wall of No. 87, lower L corner
D20	85	Front	Side rendered wall of No. 87, R side 2m above ground level
D21	89	Front	Beneath ground floor bay window, on centreline
D22	91	Front	Above ground floor bay window, on centreline
D23	93	Front	Above L pane of ground floor bay window
D24	83	Front	On concrete window sill of ground floor bay window, central pane

Table 6-1: Locations of Demec arrays on Pegwell Road cottages

5.11 Observed settlements and effects on structures

5.11.1 Settlement monitoring

The development with time of the settlement troughs along the front and rear façades of the cottages as the tunnel passed beneath is shown in Figures 6-7 and 6-8. The settlements reached limiting values approximately two weeks after the tunnel face passed, although the majority of settlement occurred in the first four days. The maximum settlement observed at the front was 13.4mm, and at the rear 18.4mm. The greater value at the rear was most probably due to lower chalk cover, greater depth of brickearth above the tunnel, and a greater proportion of highly weathered material present in the face. The maximum settlement on the footpath in front of the cottages was 12.8mm, similar to the value on the front of the cottages.

The final settlement troughs are shown in Figure 6-9. They can be approximated reasonably well by the empirical Gaussian model for surface settlements (Section 2.3.2). This can be demonstrated by plotting y^2 against $\ln(S_{max}/S)$ for each trough, as shown in Figure 6-10. If the Gaussian model were accurate, the points would plot on straight lines with gradient $2i^2$, where i is the trough width parameter. The agreement is reasonably good, with i calculated to be 4.5m and 5.2m at the front and rear respectively. These are

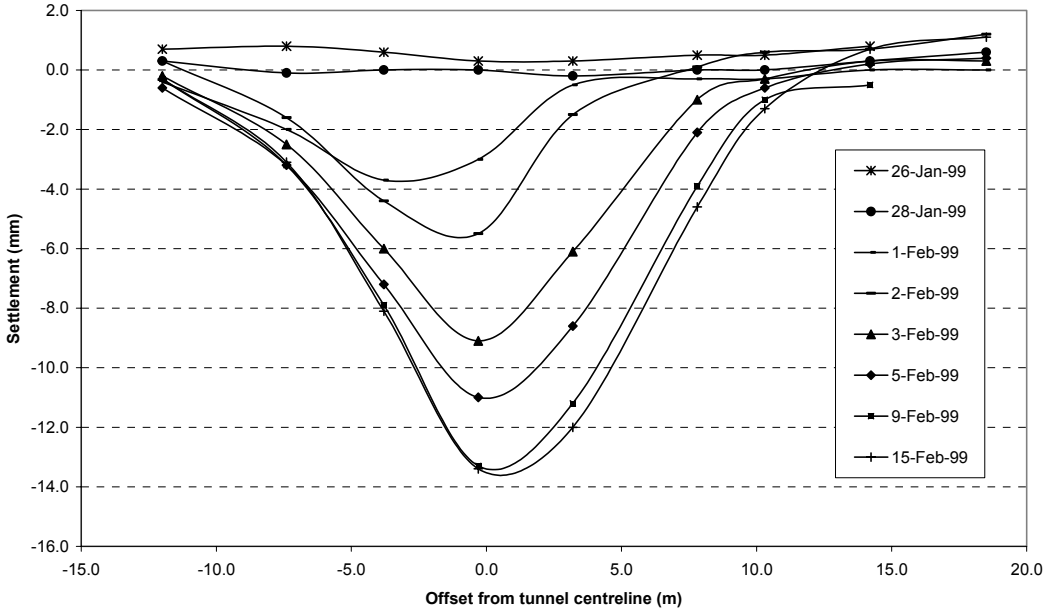

Figure 6-7: Development of settlement trough along front facades of cottages

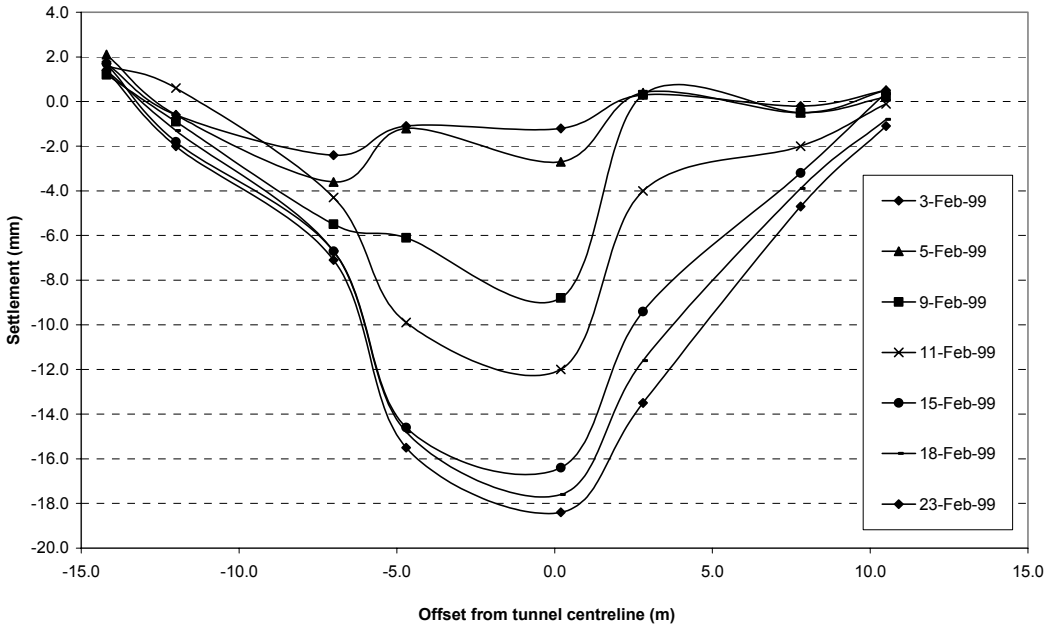

Figure 6-8: Development of settlement troughs along rear façades of cottages

similar to the values calculated for the settlement arrays in the field to the west of Pegwell Road, suggesting that the buildings responded in a relatively flexible manner, not modifying the 'greenfield' trough significantly. The value of *i* for the footpath is somewhat greater, at 6.6m, but the data shows more scatter than for the cottages and the trough shape looks asymmetric, so the conclusion is less clear.

Based on the observed troughs the volume loss is calculated to be 0.151m^3/m at the front of the cottages and 0.229m^3/m at the rear. With a tunnel face area of approximately

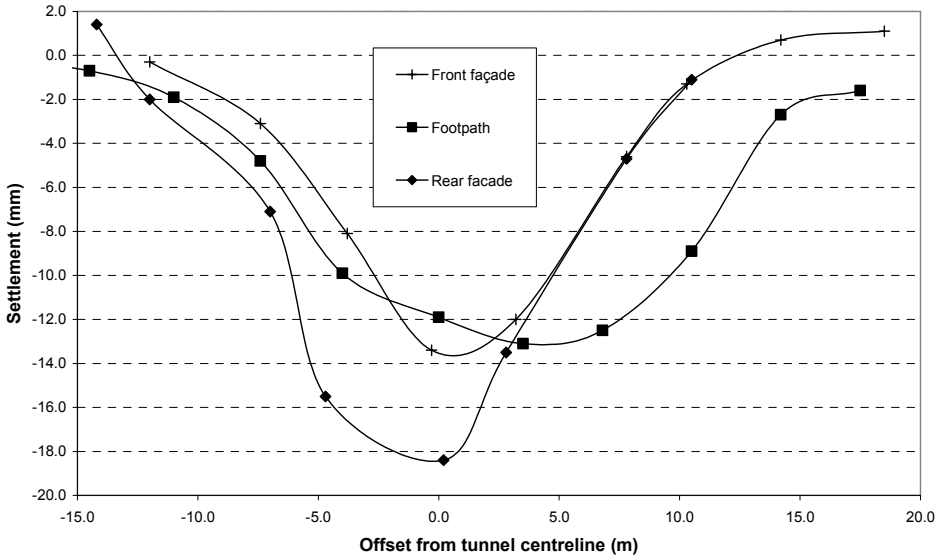

Figure 6-9: Final settlement troughs at Pegwell Road cottages

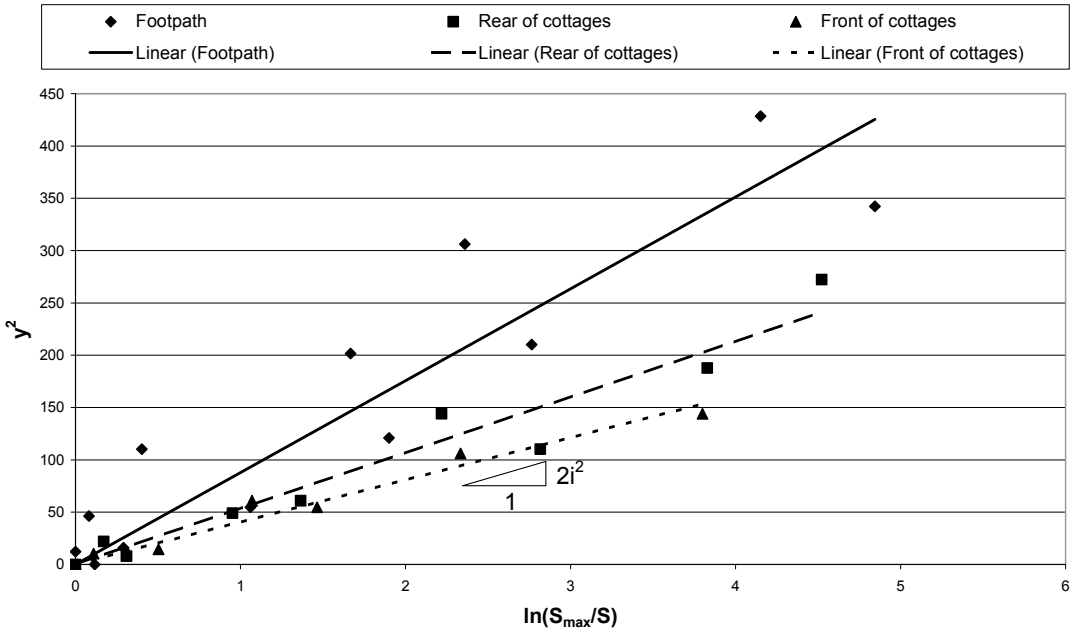

Figure 6-10: Calculation of trough width parameter *i* at Pegwell Road cottages

110m^2, this implies 0.14% and 0.21% "ground loss" respectively. These values are similar to those observed elsewhere in the tunnel drive. The probable reasons for these low values of volume loss are the relatively good ground (competent chalk up to springing level) and the pre-vaulting technique enabling support to be introduced ahead of the tunnel face.

The depth z_0 of the tunnel centreline at the cottages is about 11m, and hence the ratio i/z_0 is in the range 0.40 to 0.50. This is similar to the value of 0.43 calculated by O'Reilly and New (1982) for bored tunnelling through stiff clay, in their case London clay. Thus it might be concluded that the settlement behaviour is determined by the brickearth and weathered chalk behaving as a cohesive materials, in line with established prediction methods. However, later in the drive, as the tunnel advanced into competent chalk and z_0 increased to over 20m, the trough width remained almost unchanged, with i/z_0 therefore decreasing to 0.2.

A probable explanation for the settlement observations lies in the tunnelling method and the mechanisms by which the volume loss is occurring. The primary lining is actually cast against the ground ahead of the face, so there is no equivalent of the annular void around a shield, or tail void behind as in conventional bored tunnelling. Thus the remaining possible sources of apparent radial volume loss are (i) overbreak in cutting the pre-vault

slot that is not filled with sprayed concrete, and (ii) deflection of the primary lining after excavation.

Significant overbreak was known to have occurred, particularly in the structureless chalk at the start of the drive. However, compaction grouting was used to control movement of the ground. There is no evidence that, even when overbreak did occur, the whole slot was not completely filled with sprayed concrete.

Monitoring of in-tunnel deflections of the primary lining indicated crown settlements of about 12mm (Morgan, 1999), and convergence of up to 8mm. It would be expected that this movement be transmitted to the surface as a form of radial ground loss.

In addition to radial loss, face loss may occur. At Ramsgate, this might be expected to be less than in conventional open face bored tunnelling, because the mechanism of flow of the soil into the face was restricted by the pre-vault and face dowels.

The ground conditions at the face will also influence the volume loss mechanisms. Much of the drive was entirely within fairly competent structured chalk. This would give a stable bore with little overbreak, face loss or heave. Therefore, in the deeper sections, volume loss was likely to be caused exclusively by crown deflection, giving the relatively narrow troughs observed. At the start of the drive and at the cottages, where the cover was low and the ground conditions poorer, the other mechanisms discussed above may have contributed to the volume loss.

5.11.2 Effects on structures

The effects of the tunnelling settlements on the masonry cottages was recorded by the Demec arrays and crack telltales detailed in Section 6.2.5. The Demec arrays were located on existing cracks distributed around the cottages, whereas the crack telltales were concentrated on No. 83.

In the interpretation of the results from the Demec arrays, there is justification for considering those on No. 83, the heavily damaged cottage, separately from the remainder. The settlement results confirmed that No. 83 lay outside the zone of influence of the

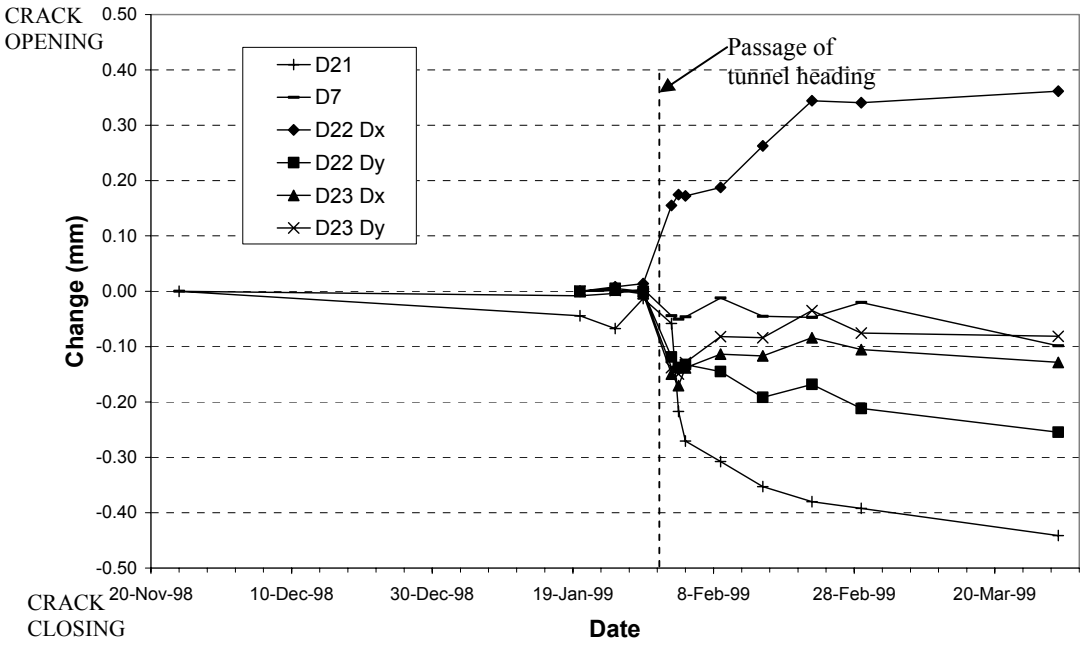

Figure 6-11: Records from Demec arrays showing significant movement on front of cottages Nos. 85 to 97 Pegwell Road

tunnel, so that if any movement of pre-existing cracks was recorded, the cause of it was unlikely to be the tunnelling. The remaining cottages, Nos. 85 to 97, will be discussed first.

Figure 6-11 shows the results from Demec arrays on the front of these cottages where the total movement at the end of the monitoring period in March was 0.05mm or greater, and Figure 6-12 shows the corresponding results from the rear. In the legend, "Dx" denotes horizontal movement (either opening or closing) and "Dy" denotes vertical movement, where an array of three studs measured movements in two directions. The timing of the movements is strongly correlated with the arrival of the tunnel face on 1st February, indicating the sensitivity and repeatability of this type of monitoring. The magnitudes of the typical movements, at 0.4mm – 0.5mm, correlate with a damage category of "Very slight" according to the Burland *et al.* (1977) classification.

Results for a majority of the arrays on the cottages other than No. 83, namely D8, D9, D12, D13, D15, D16, D17, D19 and D20 are not plotted because there was no detectable movement. The arrays that are plotted are concentrated on the cottages close to or over the tunnel, Nos. 89 to 95, as might be expected. Two conclusions can be drawn. The first is that hairline or small cracks up to 1 – 2mm in masonry buildings may remain stable over a

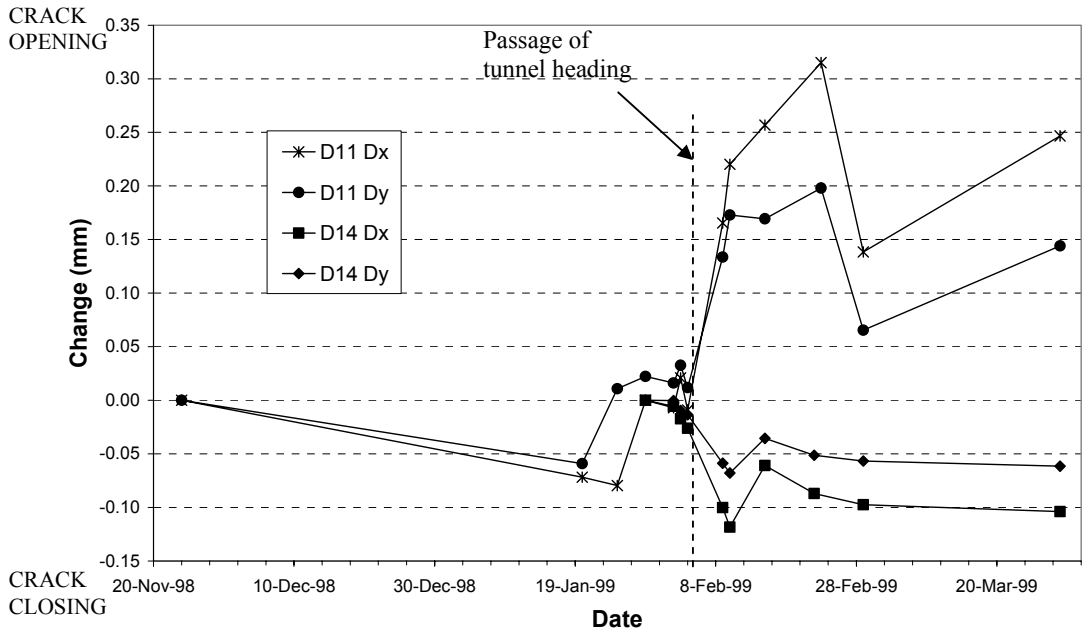

Figure 6-12: Records from Demec arrays showing significant movement on rear of cottages Nos. 85 to 97 Pegwell Road

typical four-month period if the buildings are not subjected to any significant ground movements. The second is that when ground movements, for example due to tunnelling, do occur, the response of the building includes movements on existing cracks. Therefore an understanding of the initially cracked state of a building is important.

It is interesting to note that more of the cracks were observed to close up due to the tunnelling than to open further. The location of the cracks on the façades, in particular whether they are high up or low down, and their relationship with the hogging and sagging regions of the settlement trough may be examined, but the conclusions are not always clear-cut. For example, D11 on the rear is close to ground level in the hogging region and opened by about 0.25mm, which is consistent with the façade acting as a deep beam with the neutral axis at foundation level (Section 2.4.2.1). D14, low down on the rear of No. 91 in the sagging region, closed, rather than opening as might be expected if the neutral axis was at mid-height of the façade. On the front, D22, which is just above a ground floor window in the sagging region, opened. D21, which is low down in the hogging region, and D23, higher up in the sagging region, both closed, as might be expected.

The Demec arrays located on No. 83 showed a scatter of movements, peaking at only 0.2mm and not strongly associated with the time of passage of the tunnel. The telltales

recorded larger movements, up to 2mm (Fig. 6-13). Most are again not strongly associated with the passage of the tunnel, and therefore are more likely to be due to diurnal and seasonal variations in temperature and water content of the masonry. The main 50mm crack, indicated by line reference "T6 R Dx" in Figure 6-13, opened by 2mm just after the passage of the tunnel, but then stabilised.

A visual inspection of the cottages, a month after the tunnel heading had passed, highlighted only two significant cracks that were not thought to have existed prior to construction:

1. Internal, visible on both sides of party wall between No. 93 and No. 91, on first floor towards rear. Running vertically floor to ceiling, typically 1.5mm wide.
2. Internal, in party wall No. 93/No. 91 but only visible from No. 91, running vertically for most of height of stair opening, typically 1.0mm wide, maximum 2.0mm at the top.

Both of these cracks are consistent with the cottages Nos. 93 and 91 being subjected to a greater settlement at the rear than at the front, as supported by the observed settlement troughs.

The effect of tunnelling beneath the cottages may be summarised as causing movements at existing cracks together with a small number of new cracks. Some, but not

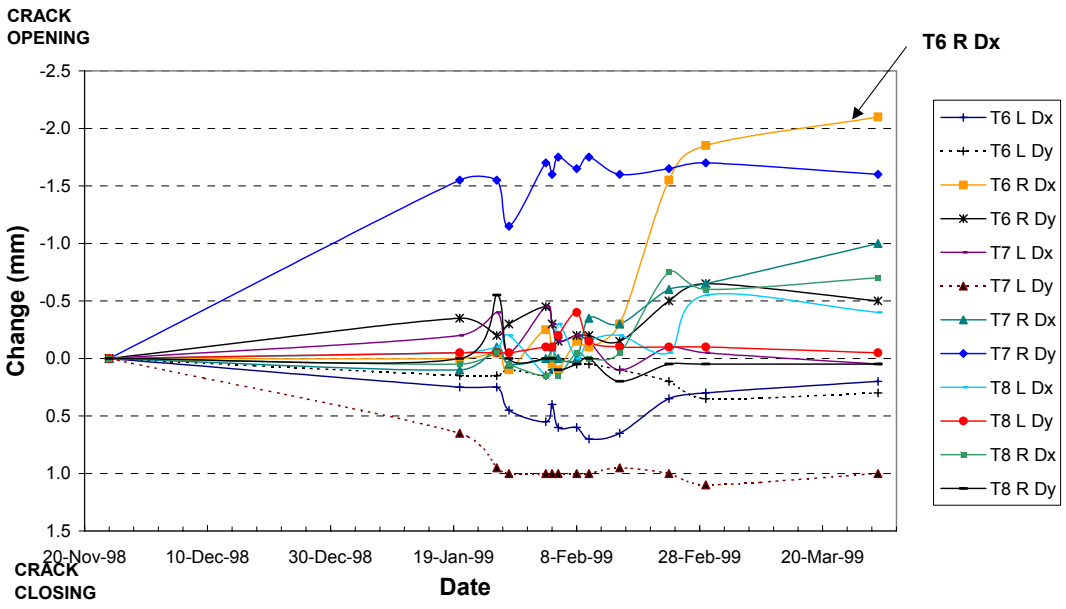

Figure 6-13: Records from crack telltales at No. 83 Pegwell Road

all, of the individual crack movements can be explained in terms of the current theory of building façades acting as deep beams. A damage prediction for the cottages using the method of Burland and Wroth (1975), based on the observed settlement trough, yields "Slight" as the expected damage category. The observations are more consistent with "Very slight" damage. In particular, significant cracking opening up from the top of the façades in the important hogging region, for which the theory takes the neutral axis for bending to be at foundation level, was not observed.

5.12 Modelling aims and assumptions

5.12.1 Overview

A good understanding of the 'greenfield' settlement response of the ground was obtained at Ramsgate. The first priority in the numerical modelling of the site was to reproduce this 'greenfield' behaviour. The buildings would then be added to form a combined model. Emphasis was placed on studying the transverse response to tunnelling of the terrace of cottages as a whole. It proved not possible within this project to investigate the longitudinal response to the advancing tunnel.

5.12.2 Ground

In order to model the site, simplifying assumptions are necessary concerning ground levels and strata thickness. The ground level and strata interfaces dip towards the south in the direction of Pegwell Road, following the buried river valley (Figs. 6.2 and 6.4), with a level difference of 2m between the north and south ends of the terrace. This difference was neglected, and the top surface of the model taken as a horizontal plane. Ground surface, tunnel level and strata boundaries were assumed to be as prevailing at the location where the tunnel axis intersects the centreline of the cottages in plan. Figure 6-2 shows how this implies a depth of brickearth that is an average between that in the lowest point of the buried valley and that in the far field away from the cottages.

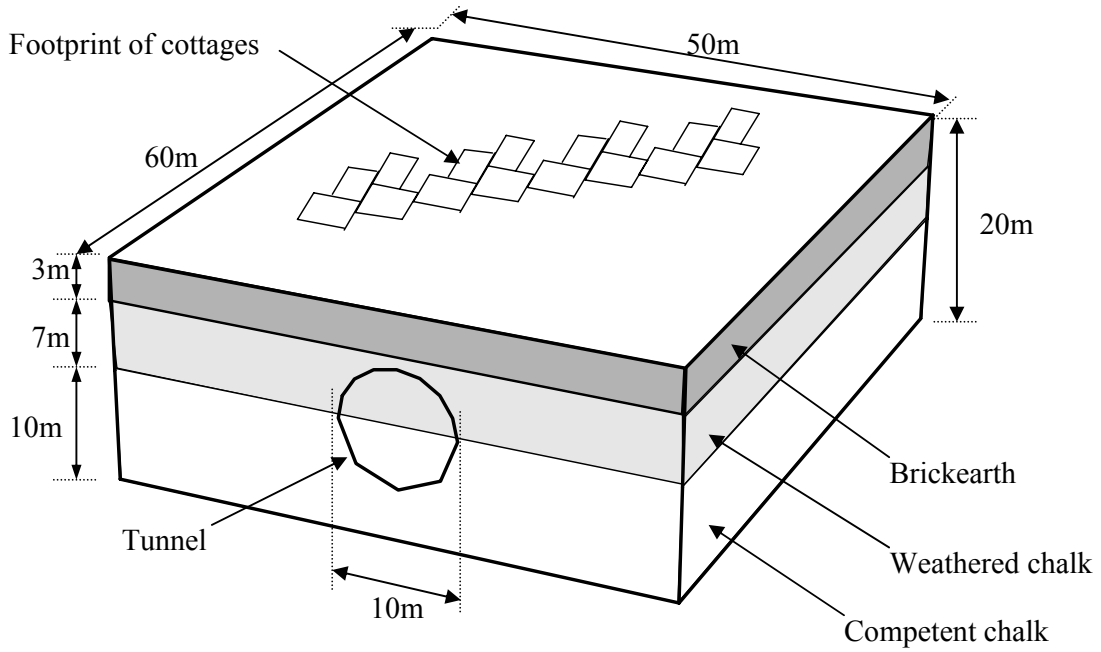

Figure 6-14: Model of ground at Ramsgate site

The top surface of the model was set at approximately foundation level of the cottages, 1m below ground level. The brickearth was taken as 3m thick and the weathered chalk as 7m thick, with competent chalk to depth. The tunnel axis was 10m below the top of the model, co-incident with the interface between weathered and competent chalk. The boundaries of the model were set outside the zones of influence of both the tunnel and the buildings, following a similar pattern to the Maddox Street model (Section 5.4.1). Figure 6-14 shows the model dimensions and strata depths assumed.

Properties for the main soil strata were obtained from the Geotechnical Interpretative Report for the construction project. The brickearth was classified as low to intermediate plasticity clay, with a coefficient of consolidation obtained from oedometer tests in the range 2 – 6m^2/yr. It can be shown that an assumption of undrained behaviour is reasonable for a 2m thick layer over a period of two weeks whilst short term tunnelling settlements take place. This was confirmed by observation on site of a number of trenches opened up for service diversions in the area, which remained stable for longer than this. The kinematic hardening model (Houlsby, 1999) was therefore suitable for modelling the brickearth. Hand vane tests gave an average undrained strength s_u of 60kPa. Data on shear

modulus was limited to surface wave geophysics carried out in the area of the cottages, which indicated *G* increasing at a rate of 60MPa/m.

The weathered chalk was also classified from the boreholes as stiff clay. There was unfortunately little testing carried out on this material for the ground investigation. For the purposes of the modelling, it was assumed to have properties intermediate between the brickearth and Upper Chalk (the latter having been extensively tested). The average rate of increase of *G* with depth from surface wave geophysics was 80MPa/m. Taking a constant rigidity index equal to the average value of 1500 in the brickearth led to an increase in s_u with depth of 40kPa/m, although there was no direct site data to support this.

The Upper Chalk was described as a jointed rock, with high undrained strengths in the range 1000 – 1500kPa. Because it lies below tunnel springing level, it was expected to have less influence on the ground movements than the other strata. To simplify the model, an elastic material model was applied. The shear modulus was assumed to increase with depth at 125MPa/m, to agree with data from pressuremeter testing that indicated a stiffness of around 1400MPa at 16m below ground.

Profiles of the shear modulus and undrained shear strength assumed for the different strata are shown in Figure 6-15. The Figure shows a further simplification made, in which the brickearth and weathered chalk were combined into one layer.

5.12.3 Tunnel

The tunnel lining was modelled using shell elements, following the principles established for this project. The tunnel section was approximated as a regular polygon (Fig. 6-16), in a similar way to the Maddox Street shaft. Because the tunnel passes at low cover beneath the building footprint where a high mesh density was required, eight segments were used for the top half of the tunnel.

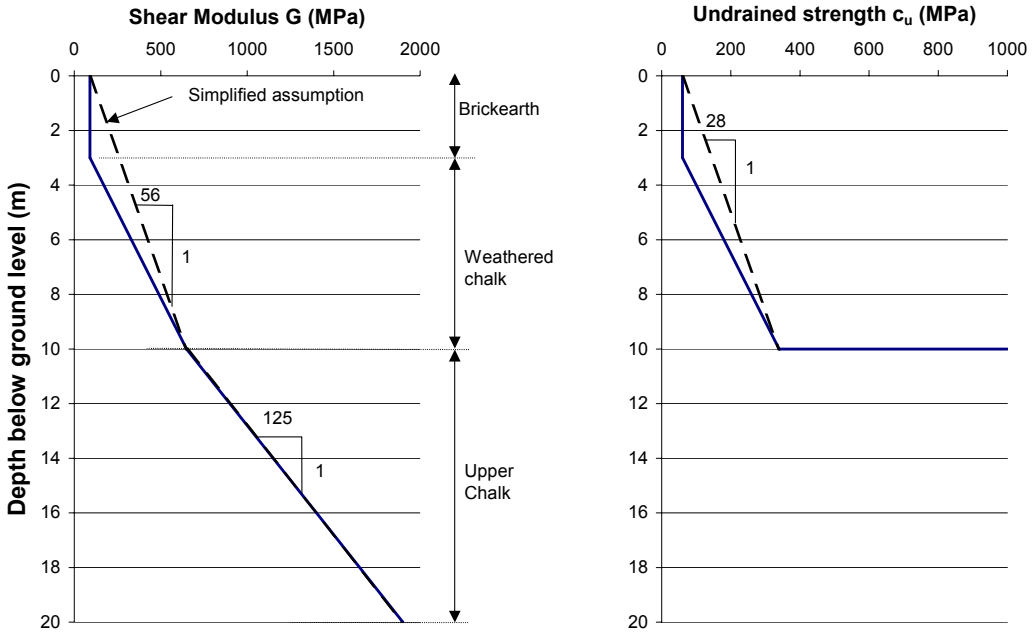

Figure 6-15: Modelling assumptions for geotechnical parameters

A high value of stiffness was chosen for the tunnel lining to prevent convergence problems, as for the Maddox Street model (Section 5.4.2). It proved necessary to increase the Young's modulus from the value of 100MPa used for Maddox Street to an artificially very high value of 190GPa. This was because 100MPa was not sufficiently large compared to the stiffness of the surrounding soil, in this case chalk. The OXFEM routine that shrinks the lining by a uniform strain calculates the nodal forces required to do so assuming that the lining is unrestrained. If the lining is restrained by a relatively stiff soil, the nodal forces are not large enough to cause the lining to shrink.

The tunnel was modelled as straight, level and parallel to the sides of the ground block.

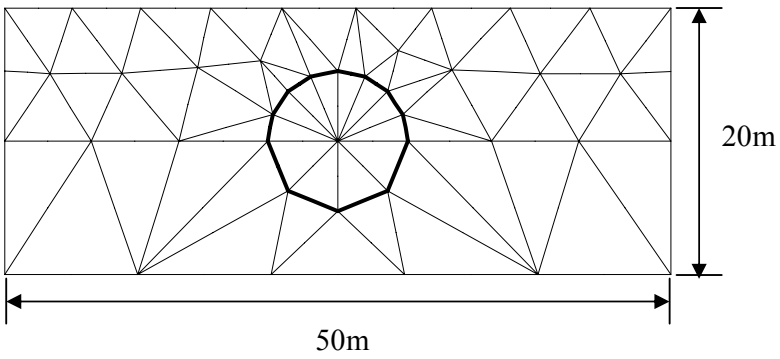

Figure 6-16: View on end of meshed ground block showing tunnel cross-section

5.12.4 Buildings

The cottages were initially modelled as a staggered terrace in plan. It was decided at an early stage to neglect the rear extensions of the cottages, because their effect on the transverse settlement behaviour of the terrace as a whole was thought to be small. It was found that neglecting them gave significant benefits in reducing the number of d.o.f. in the model, particularly in the critical region in the ground immediately beneath the building. The plan layout of the main load-bearing walls of the cottages shown in Figure 6-6 was simplified to that shown in Figure 6-17(a).

When this model was run, it did not converge to a solution in the first loading stage (application of building self-weight). The input file was checked for errors and masonry and soil stiffnesses varied, but the explanation of the problem was not obvious. Attention was focussed on the staggered arrangement of the cottages, which implied one wall tied to another at a position other than its end. This was a feature not present in the Maddox Street model, but the work of Liu (1997) implied that this arrangement should not cause problems.

By building up a cottage one wall at a time, it was confirmed that there is no problem in principle with the staggered arrangement. However it was discovered that the convergence problem was a function of the position of a single cottage in plan. If a cottage was placed over the tunnel as shown in Figure 6-17(b), stage 1 of the analysis was successful, but if the cottage was positioned remote from the tunnel (Fig. 6-17(c)), it was not. The only difference between the two locations was the degree of refinement of the soil mesh

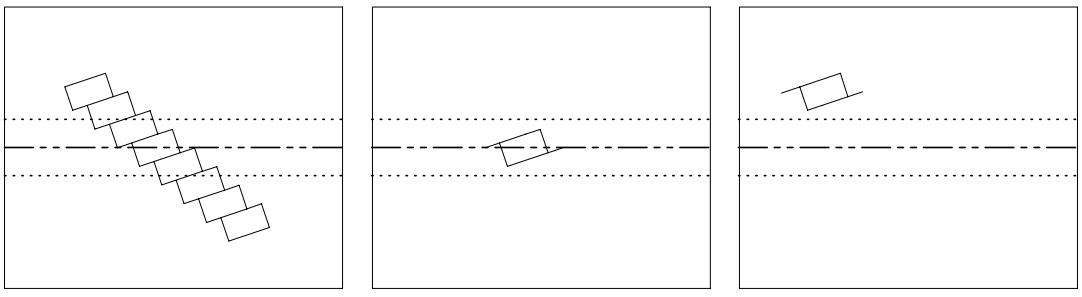

(a) Staggered arrangement **(b) Single cottage over centreline** **(c) Single cottage far from tunnel**

Figure 6-17: Representation of building footprint in plan

underlying the cottages, with the mesh somewhat coarser away from the tunnel. The staggered wall arrangement was more prone to instability when combined with a coarse soil mesh. Refining the mesh under the entire building footprint was not feasible, so the wall arrangement was further simplified to that shown in Figure 6-18, and this pattern was used for the remainder of the study.

The load-bearing masonry walls were modelled with a self-weight of 20kN/m^3 and with stiffness consistent with a thickness of 220mm and a Young's modulus of 2GPa. The elastic, no-tension masonry constitutive model was used, with the other parameters set as given in Table 3-1.

As in the Maddox Street model, it was considered important to take account of the presence of openings such as doors and windows. At Maddox Street, the openings were large and played an important role in initiating damage in a building that did not span across the whole settlement bowl but was positioned in the hogging region. However at Ramsgate the buildings span across the entire trough, and the openings are more uniformly distributed. Therefore the expectation was that they would have less impact on the global building behaviour than at Maddox Street. Therefore provision was initially made only to represent openings as vertical regions of reduced stiffness, as shown in Figure 6-19, in line with the philosophy followed at Maddox Street (Section 5.4.3).

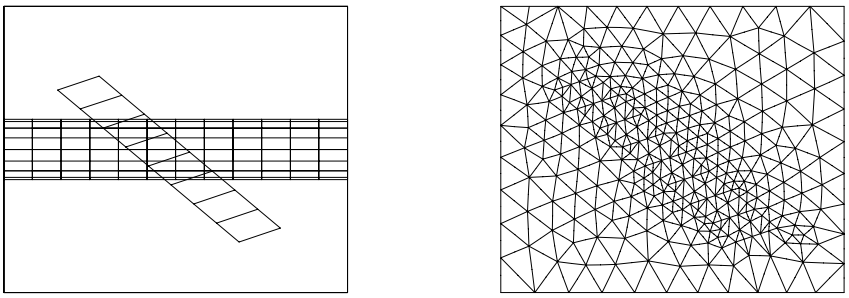

(a) Plan on building and tunnel **(b) Mesh on ground surface**

Figure 6-18: Final model arrangement

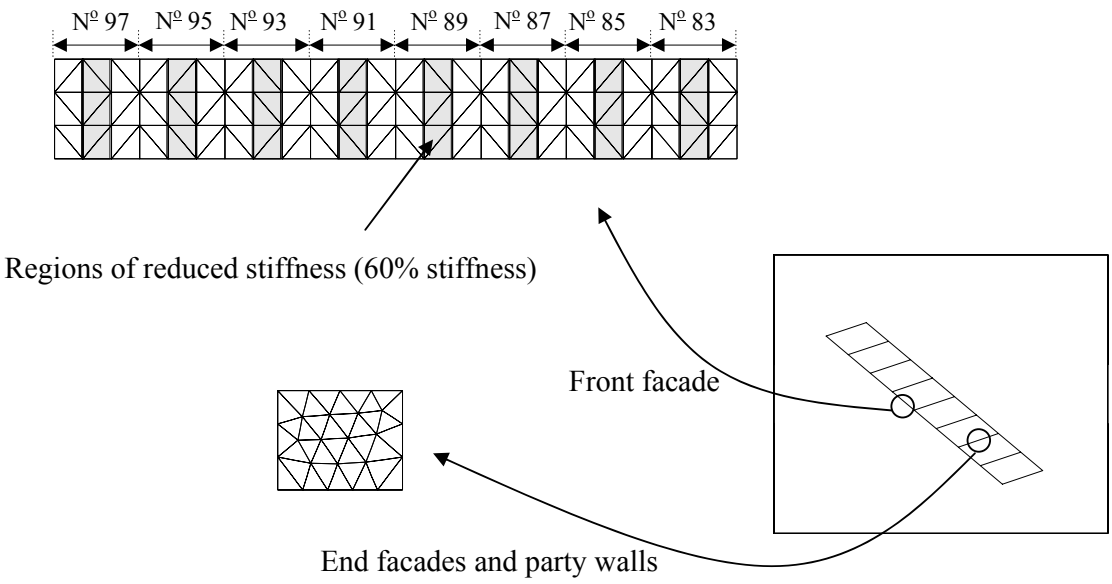

Figure 6-19: Modelling of building facades

5.12.5 Analysis sequence

The stage-by-stage analysis sequence used for the Maddox Street model and detailed in Section 5.4.4 was also used for the Ramsgate model. Provision was made in the meshing of the tunnel to enable it to be excavated in up to 12 increments (Fig. 6-18(a)). In the event, only modelling with single increment excavation was completed for this project, primarily due to the long run times of the model.

5.13 Description of analyses made

5.13.1 Overview

The first priority with the analysis programme was to test the 'greenfield' model, to confirm that the soil mesh and tunnel excavation were functioning properly and that the 'greenfield' settlement trough observed on site was adequately represented in the model. In the meshing of the ground block (Fig. 6-20), it had been necessary to increase the element size significantly away from the tunnel to minimise the total number of d.o.f. in the model,

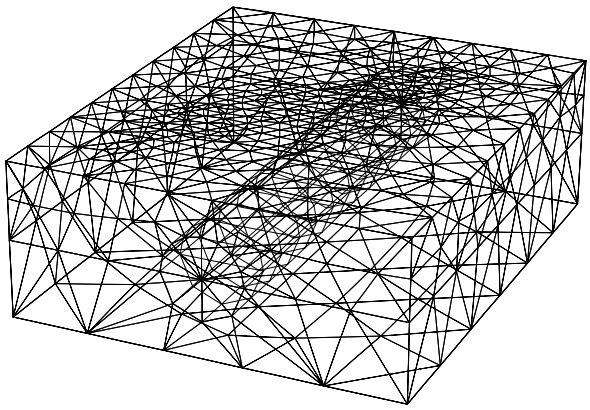

Figure 6-20: Finite element mesh for the ground
(7723 nodes, 4917 soil elements and 1152 shell lining elements)

and it was particularly important to ensure that this did not adversely affect the settlement behaviour of the ground in the model.

Following the 'greenfield' modelling, combined analyses including the building were carried out. The ability of the model to reproduce the global transverse behaviour and the amount and distribution of damage to the façades was examined. The benefit of using the elastic, no-tension model compared to a standard elastic model for the building was assessed.

5.13.2 'Greenfield' analyses

An initial series of 'greenfield' analyses were carried out, in which the lining was shrunk to model 1% volume loss. Figure 6-21 shows the resulting contours of surface settlement, once the mesh had been refined such that the settlement response at the building location was judged to be satisfactorily smooth. The maximum settlement under the building footprint is about 36mm, confirming that a volume loss applied was greater than that observed in the field. More crucially at this stage, the trough width parameter i is 11m, compared to values of 4.5m – 6.2m observed on site.

A series of analyses was then carried out in an attempt to improve this model by reducing the trough width. The trough width observed on site was very narrow, and an explanation of this in terms of most of the ground loss occurring due to crown deflection

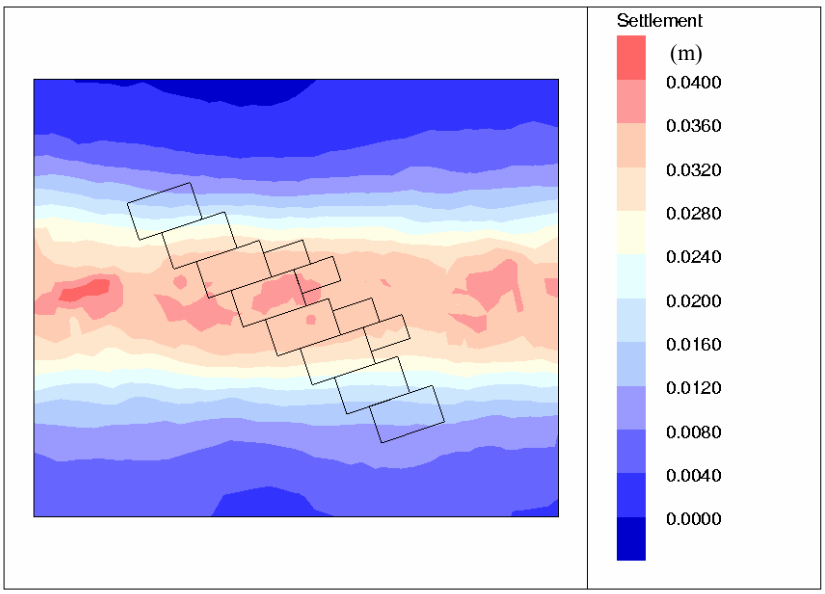

Figure 6-21: Surface settlements from initial 'greenfield' model, 1% volume loss
(building footprint shown but building not present)

was discussed in Section 6.3.1. In order to better reflect the site observations in the model, options for shrinking the lining in different ways, together with addition of external fixity to the lining, were explored, as tested in the two-dimensional analysis series discussed in Section 3.3.2. Based on the hypothesis that crown settlement was a major contributing factor to the surface settlement trough shape observed, an analysis was carried out shrinking the top half of the lining only, as shown in Figure 6-22. Without horizontal fixity at the springing level, *i* was reduced to 8.4m, but with fixity, *i* was further reduced to 5m. The shrinkage strain was adjusted to 2% to give a maximum settlement of 20mm at the location of the buildings (Fig. 6-23(a)). This was regarded as a satisfactory 'greenfield'

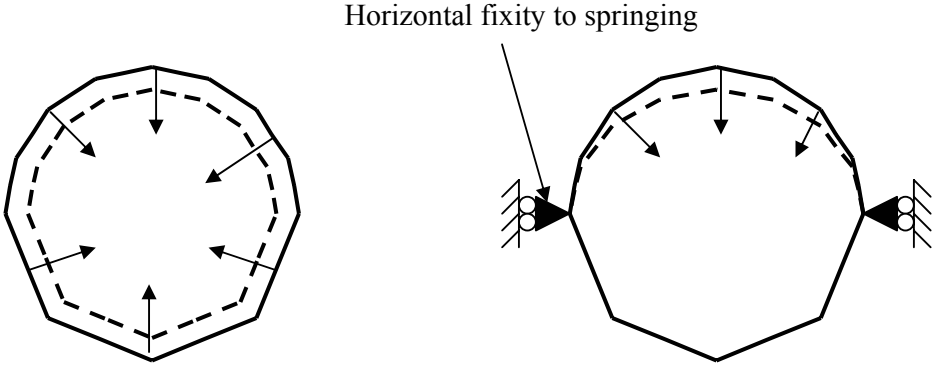

(a) Conventional **(b) Shrinking top half only**

Figure 6-22: Options for shrinking tunnel lining to model ground loss

model as a preliminary to the combined analysis stage. The trough shapes obtained from the model are compared with those observed in the field in Figure 6-24.

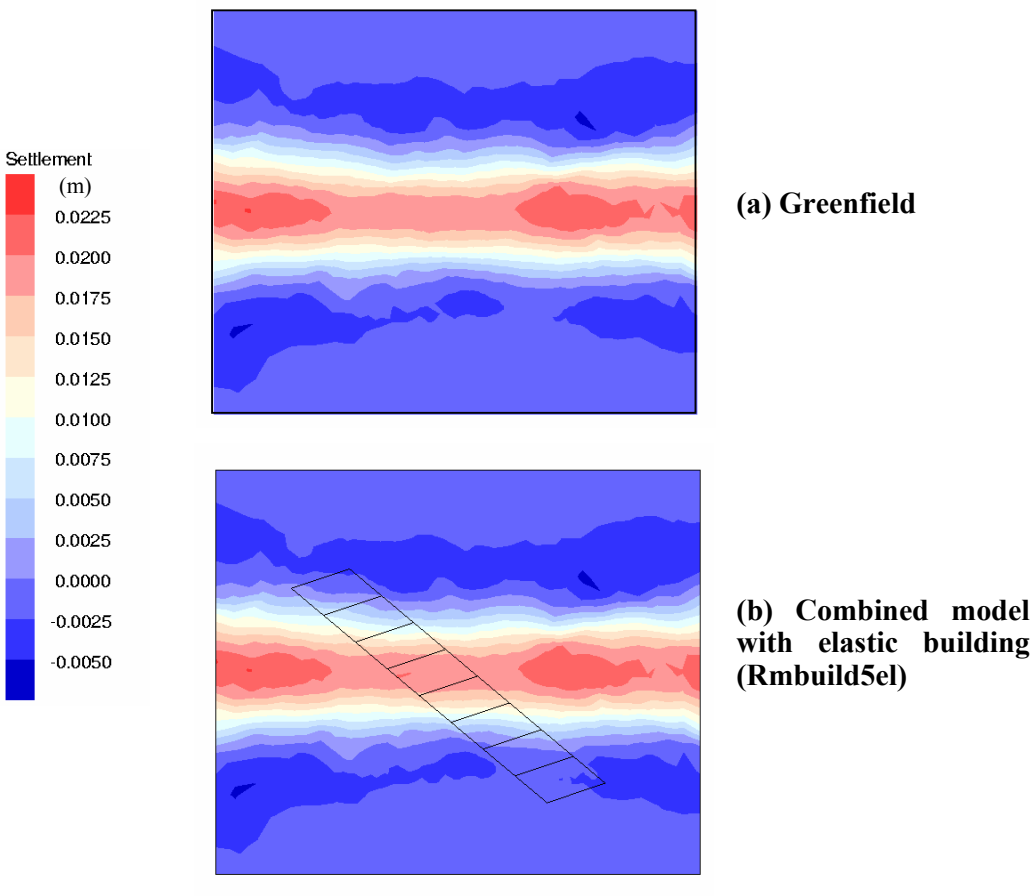

Figure 6-23: Comparison of surface settlements from 'greenfield' and combined models

5.13.3 Combined analyses including building

Analyses were carried out to compare the response of a building with or without internal party walls, with or without regions of reduced stiffness to model openings, and to compare masonry and elastic material models for the building. A summary of the main analyses carried out is given in Table 6-2.

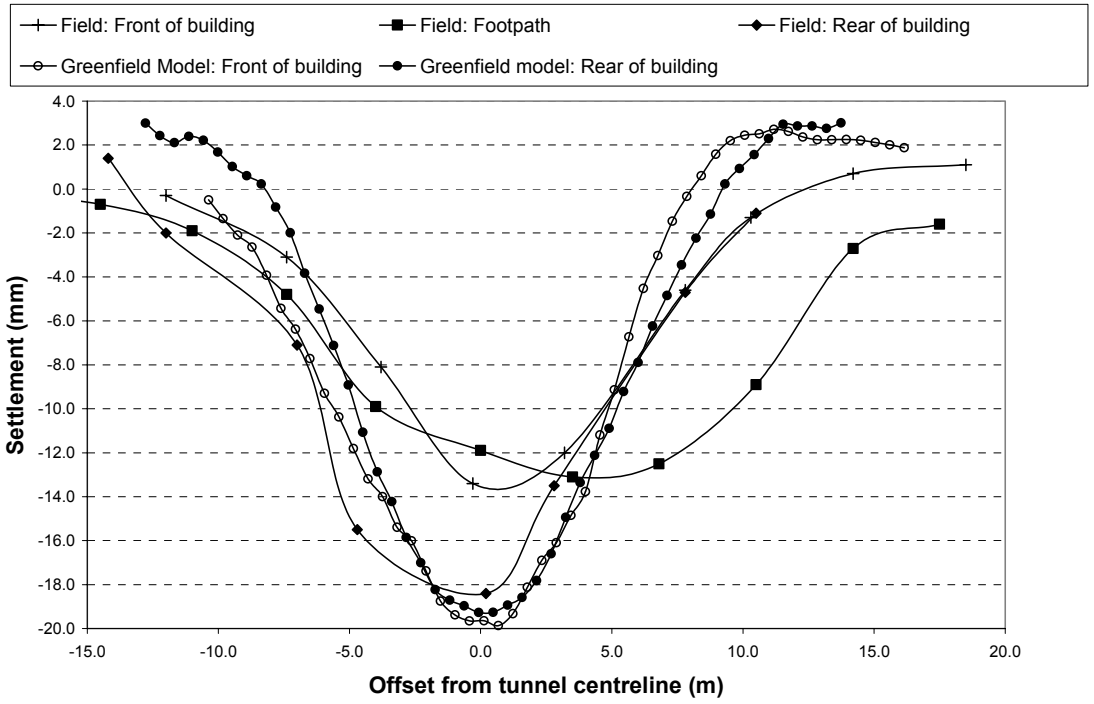

Figure 6-24: Comparison of settlement troughs observed in field with results of 'greenfield' model

Analysis reference	Shrinkage strain to tunnel lining	Façade layout	Regions of reduced stiffness for openings	Material model
Rmbuild4	2%	No party walls	No	Masonry
Rmbuild4a	2%	No party walls	Yes, 60% stiffness	Masonry
Rmbuild5	2%	Include party walls	Yes, 60% stiffness	Masonry
Rmbuild5el	2%	Include party walls	Yes, 60% stiffness	Elastic

Table 6-2: Details of combined analyses of Ramsgate site

The elastic analysis with the party walls, Rmbuild5el, would be expected to exhibit the stiffest building response overall. Even in this model, however, the ground settlements were not modified significantly compared to the 'greenfield' case (Fig. 6-23). This

indicates that the long and not very tall terrace is relatively flexible in longitudinal bending.

Comparison between analyses Rmbuild4 and Rmbuild4a shows the effect of introducing vertical regions of reduced stiffness to model openings in the building. Figure 6-25 shows the damage distributions on the front façade. Rmbuild4a, which includes the reduced stiffness regions, shows significantly less damage than Rmbuild4. The Figure shows contours averaged over length scales comparable to finite element mesh size. The results for the rear were similar. The distribution of the damage is seen to be mainly along the bottom edge of the façades in the sagging region. There is a small amount of damage initiation from the top in the hogging region on one side of the trough.

Figure 6-26 shows the results in terms of cracking damage and crack pattern for the front façades, when the party walls were added to the model. Figure 6-27 shows the corresponding results for the rear. The severity of the cracking damage has again reduced compared to the models without party walls, although the plots of crack patterns show that cracking is occurring in the model over a wide extent of the façades. The presence of the party walls appears to be having a stiffening effect on the overall response of the building, controlling the level of cracking to within the "Negligible" category over the majority of the area.

If the cracking strains shown in Figures 6-26 and 6-27 are averaged over regions

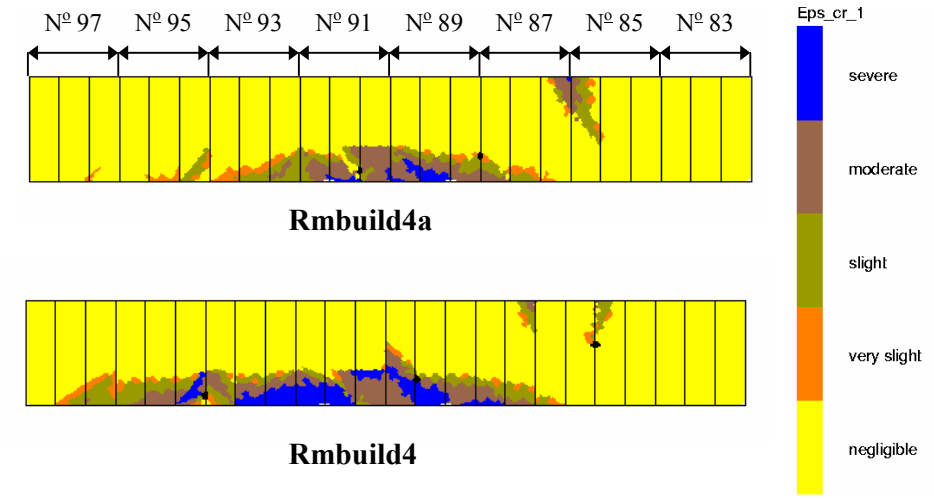

Figure 6-25: Damage categories for front façades, for analyses without party walls

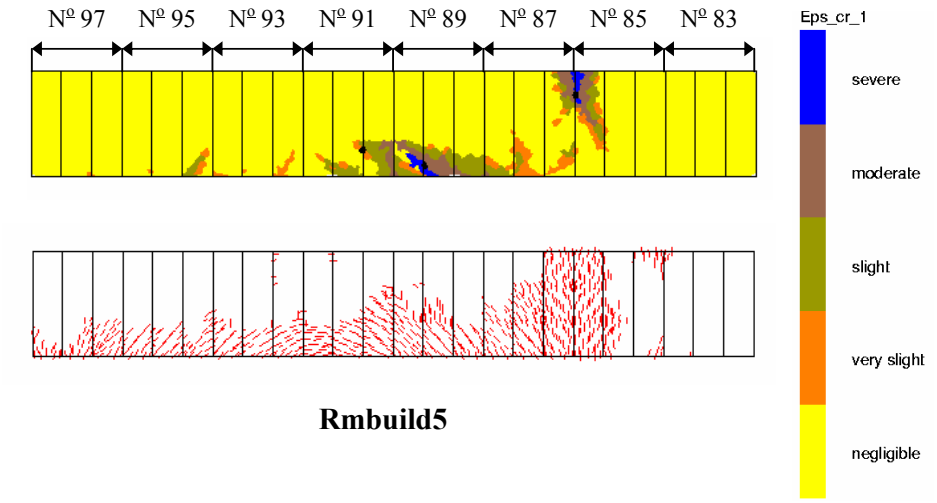

Figure 6-26: Damage categories and crack patterns for front façades, for analysis including party walls

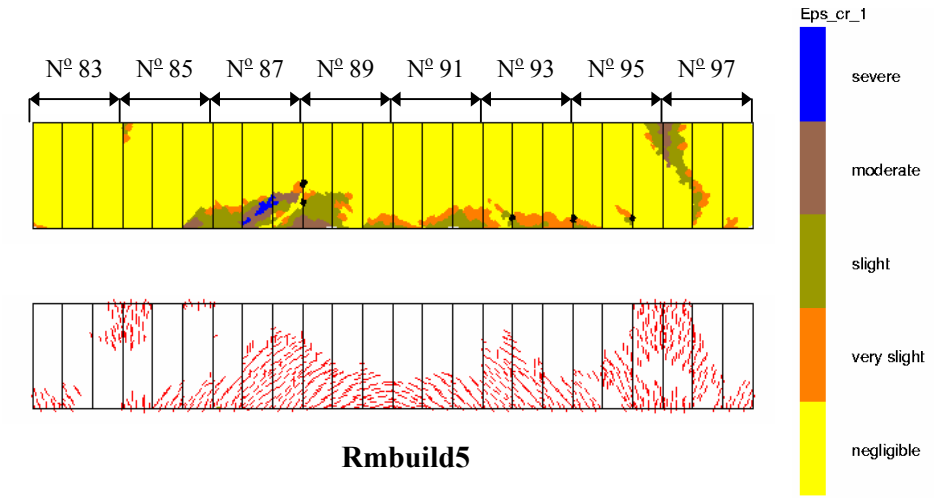

Figure 6-27: Damage categories and crack patterns for rear façades, for analysis including party walls

bounded horizontally by the zones of reduced stiffness and dividing the façades into two halves in the vertical direction, the result is shown in Figure 6-28. The maximum damage categories by this method are seen to be "Slight" on both front and rear façades.

Figure 6-29 shows the results for the front and rear for the *elastic* model with party walls, Rmbuild5el. In the elastic model, the damage category is correlated with the maximum principal strain in the façades. The damage is even more restricted in extent and severity and is much more concentrated in the regions of reduced stiffness in the centre of each façade than was the case with the masonry model. The dark spots on the vertical lines

between regions of different stiffness are highly localised areas of "Moderate" damage. Their length scales are comparable to the spacing between integration points in the mesh, and their origin is therefore likely to be numerical, rather than as a result of a real damage distribution.

The damage distributions obtained in the models may be compared with that observed

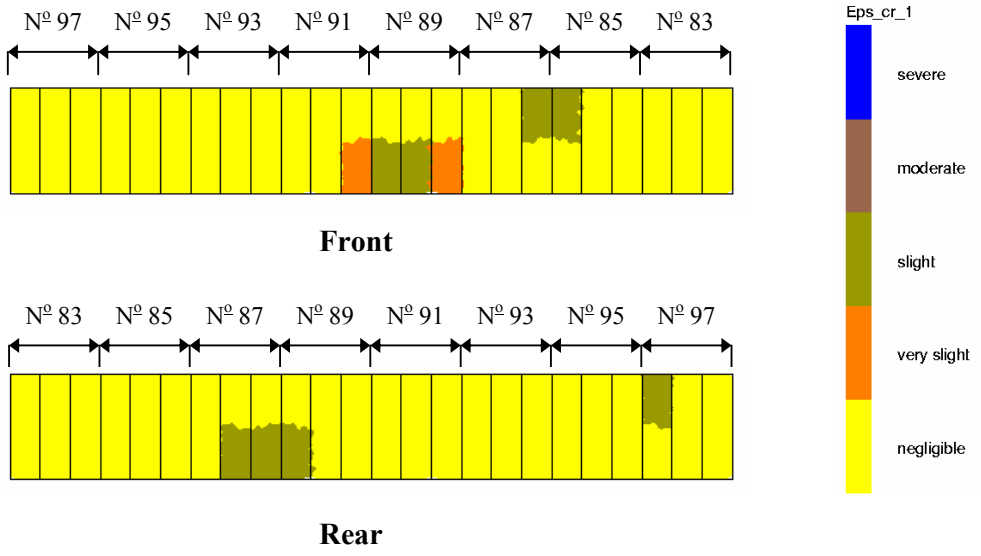

Figure 6-28: Averaged damage categories for analysis with party walls (Rmbuild5)

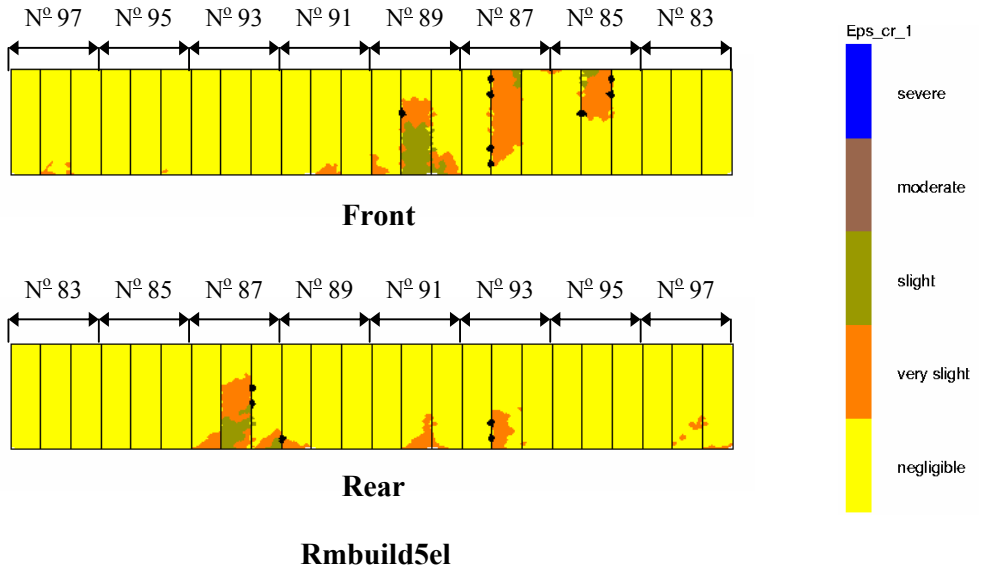

Figure 6-29: Damage categories derived from maximum tensile strain for elastic model with party walls

in the crack monitoring on site. The Demec arrays recording most response due to tunnelling were D21 and D22 situated on the front of cottages Nos. 89 and 91 respectively, immediately above the tunnel. Smaller movements were also picked up by D23 (front of No. 93), D7 (front of No. 91) and D14 (rear of No. 91). Movement was also detected at D11, which is farther from the tunnel, on the rear of No. 97. This point was, however, found to lie in the hogging region of the settlement trough, where damage was initiated from the top of the façade, as shown clearly in Figure 6-27 for the masonry material model and with somewhat less emphasis in Figure 6-29 for the elastic model. Therefore, the overall damage distributions shown in Figures 6-26 and 6-27 for the masonry model look more plausible than that shown in Figure 6-29 for the elastic model. This helps to confirm the value of the masonry modelling approach.

Table 6-3 shows the sequence of damage for the party walls, moving down the terrace from north to south, for the analysis Rmbuild5 (masonry material model for building). The analysis predicts very light damage for all the walls except the two (nos. 7 and 8) that are positioned close to the tunnel axis and entirely within the sagging region of the settlement trough.

The damage to party walls 7 and 8 is concentrated along the interface with the front and rear façades. This is a similar behaviour to that seen in the Maddox Street model, for example Figures 5-18 and 5-27. The vertical restraint provided by the adjoining façades again appears to be initiating damage. Figure 6-30(a) shows the mode of deformation of wall no. 7 located over the tunnel, which shows warping deformation at the ends of the façade as it is forced to follow the vertical settlement of the main façades together with the ground movements imposed on it due to the tunnelling (the deformations have been magnified by a factor of 100 in the Figure). Figure 6-30(b) shows the deformation of a typical party wall away from the tunnel, no. 9, which exhibits behaviour close to rigid body rotation, with consequently much lower damage.

Wall No.	Contours of damage category	Cracking pattern	Location in plan = tunnel centreline
5	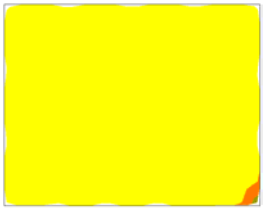	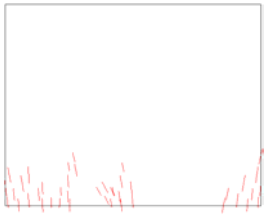	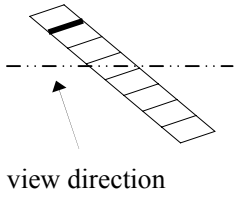
6	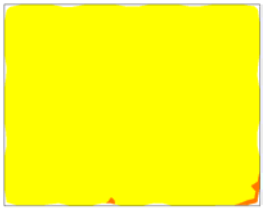	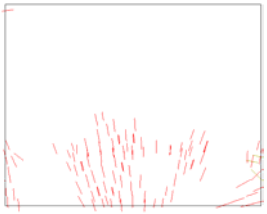	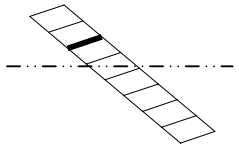
7	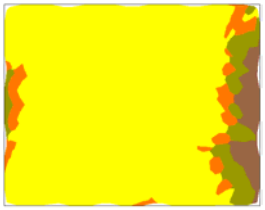	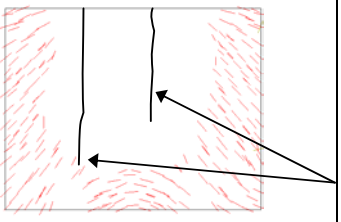	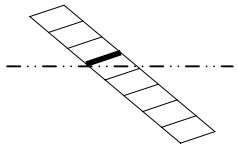
8	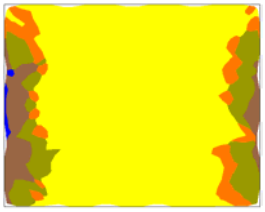	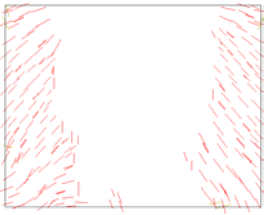	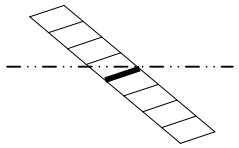
9		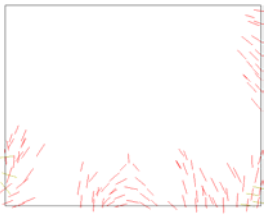	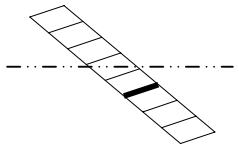
10		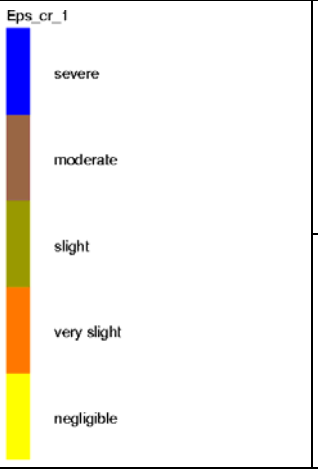	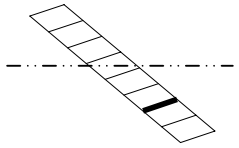
11			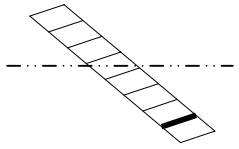

Table 6-3: Damage categories and crack patterns for party walls, analysis Rmbuild5

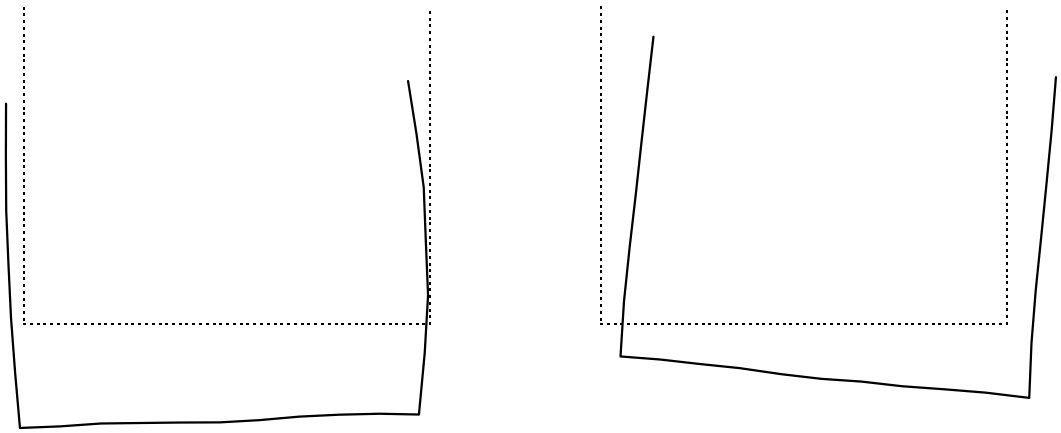

(a) Party wall no. 7 **(b) Party wall no. 9**

Figure 6-30: Deformation of party walls, analysis Rmbuild5

The new cracking observed on site in wall no. 7 (Section 6.3.2) is also indicated in Table 6-3. Both of these significant cracks appeared to propagate from the top of the party wall, and are consistent with the party wall undergoing hogging deformation in the field. A possible cause for this is the higher overall final settlement observed at the rear of the cottages due to the ground conditions (Section 6.3.1). The front end of party wall no. 7 is approximately over the tunnel centreline, and the rear end is about 2.5m north of the centreline. Examination of Figure 6-24 shows that the final differential settlement between the front and rear of wall no. 7 was about 3mm. This is similar to that obtained in the model (although with greater settlement at the front rather than the rear, due to the skew of the tunnel). The results from the model suggest that this degree of differential settlement, of the order of 1/2000 of the length of the party wall, should not have caused significant damage. The same conclusion would be reached from a stage one assessment according to existing techniques (Section 1.3).

A much more likely explanation for the observed damage to party wall no. 7 is that it is the result of the passage of the longitudinal settlement trough ahead of the advancing tunnel face. The data presented in Figures 6-7 and 6-8 show that on the 5th February, the front end of the party wall had settled by 11mm, whereas the rear had not yet responded significantly to the tunnel advance. At that time, the differential settlement along wall no. 7

was about 9mm, 1/850 of its length and much more consistent with the observed damage. It is likely that better agreement between model and field would have been obtained if the incremental advance of the tunnel had been modelled. This shows the necessity for three-dimensional modelling that includes incremental advance, which should be attempted in the future when sufficient computing resources are available.

5.14 Discussion

This case history was the second to be analysed for this project. The calculations were carried out on the Oxford Supercomputer, after the OXFEM program had been optimised for performance, and parallelised.

The site data has the advantage of having been recorded as an integral part of this project. This meant that it was possible to tailor the instrumentation and the monitoring programme to a certain extent towards the specific objective of verifying a combined numerical model of the Pegwell Road cottages and tunnel for this project. The data could also be verified and its repeatability assessed as the tunnel advanced. The most successful instrumentation was also the simplest – precise levelling points and monitoring of existing cracks. Building surveys were carried out before and soon after construction.

The site was the first application in the U.K. of the Perforex pre-vaulting tunnelling method. The tunnel passed with low cover beneath the cottages in a location where the ground conditions were somewhat variable and not ideal for tunnelling. It was also quite close to the start of the drive. These factors led to the contractor being particularly thorough with his own monitoring, and this also contributed to the good quality of the data available to this project, in particular of the ‘greenfield’ settlement profile above the tunnel ahead of the critical structures. This turned out to be especially important, as the trough was narrower than expected for a traditional bored tunnel in the ground conditions prevailing. This is believed to be due to a substantial proportion of the settlements being caused by deflection of the crown of the tunnel lining rather than face or radial loss mechanisms. It proved to be possible to reproduce this ‘greenfield’ behaviour in the model, using the facetted shell element lining for the tunnel and shrinking only the top half to

model the volume loss. However, this experience illustrates that it is necessary to have good knowledge of the expected 'greenfield' settlement behaviour to obtain useful predictions from a combined numerical model.

The site lent itself to analysis by the numerical techniques that are the subject of this project, for similar reasons to the Maddox Street site. The soil types were cohesive and could be expected to respond in an undrained manner in the short term to the passage of the tunnel. The soil properties were reasonably well documented in the ground investigation, apart from the weathered chalk for which some assumptions were required. Protective measures such as compensation grouting were not used. The cottages were of load-bearing masonry construction on shallow foundations. Because the cottages were staggered in plan, the arrangement of load-bearing walls was quite complicated in plan, and it was found to be impractical in this project to model this faithfully, as a considerably higher number of degrees of freedom would have been required in both the building and ground. Therefore the front and rear façades were simplified to be straight. However it is judged that the effect of this assumption on the transverse behaviour of the terrace of cottages as a whole was not significant.

An interesting aspect of this site was the cracked condition of the cottages prior to construction, and how it changed due to the tunnelling. Initially, most of the cottages had small numbers of hairline to fine cracks, up to about 1.5mm in size. Thus, prior to construction, the damaged state was "Negligible" to "Very slight". Many of these pre-existing cracks were monitored, and movements occurred, of the order of 0.5mm, that could be measured reliably and that were strongly correlated in time with the passage of the tunnel. Thus the effect of construction may be assessed as causing damage in the range "Negligible" to "Very slight". The exception was the end cottage, No. 83, which was already damaged to "Moderate" level. However, this was located outside the settlement trough and incurred no further settlement. If, however, it had experienced settlements, it would be hard to justify a numerical model that could not represent the initial cracked state, and this may be a useful area for further research, although the likelihood in practice

of tunnelling under a highly damaged building without strengthening or protective measures may not be great.

The volume loss was low, and therefore although the settlement trough was narrow, curvatures were low enough that current assessment methods predicted only “Slight” damage to the cottages. Thus the structure was expected to be relatively flexible transversely. This was confirmed on site and also reproduced in the model.

A series of three-dimensional combined models of the site was analysed, in which masonry and elastic material models for the structure were compared, and the effects assessed of including the party walls between cottages, and vertical regions of reduced stiffness to model the main openings in the façades. The best correspondence with the field observations, in terms of both severity and distribution of damage, was when both party walls and vertical regions of reduced stiffness were included. With these features, the masonry model predicted a maximum damage category of “Slight” on the main façades, with damage in both the sagging and hogging regions. An equivalent model but with elastic façades also predicted “Slight” damage, and therefore both models were in agreement with current assessment methods. However, the masonry model predicted damage more widely distributed along the façades, and this was in better agreement with the observed changes to existing cracks.

Although the numerical models consistently predicted propagation of damage downwards from the top of the façades in the hogging region of the settlement trough, this was not clearly evident on site. This, and the fact that the growth of cracking on site was consistent with “Negligible” to “Very slight” damage, indicates that the models are overestimating the damage, as was the case for Maddox Street. The most likely explanation of this is that real masonry has a small tensile strength of perhaps 1 – 2 N/mm^2, which has not been represented in the model. Enhancing the elastic, no-tension masonry material model to include a small but realistic tensile strength is therefore recommended as a subject for future research.

The inclusion of the party walls in the combined model had an important stiffening effect upon the global response of the terrace of cottages. Damage was induced in the

model in the party walls closest to the tunnel. In this situation, the advantages of the three-dimensional combined modelling approach over conventional 2-D idealisations may be seen. It is hard to see how the current assessment techniques could be applied to the party walls that have a low aspect ratio and a degree of restraint at the ends, and therefore cannot be assumed to act as simple beams, especially with the added complication of a skew relative to the settlement trough.

The numerical model predicted damage to the party walls that was concentrated at the ends where they were joined to the main façades. This effect was also observed in the Maddox Street model, and appears to be related to the vertical restraint provided by the adjoining façade. It is not clear whether this effect occurs in real buildings, and further research on the behaviour of such connections between façades is recommended. The data from Ramsgate does not prove either way whether such restraint existed. The actual cracking observed on site suggests that the party walls were subjected to significant hogging, with growth of cracking from the top on the centreline. This damage could not be accounted for by the final differential settlement between the front and rear of the cottages, and is likely to have been caused the occurrence of a much larger differential settlement during the passage of the tunnel. A numerical model that included incremental advance of the tunnel would be expected to give a significantly improved prediction of this phenomenon.

6 ANALYSIS OF MANSION HOUSE, LONDON, DUE TO TUNNEL CONSTRUCTION ASSOCIATED WITH THE DOCKLANDS LIGHT RAILWAY

6.1 Introduction

From the outset of this project, the Mansion House appeared to be a very promising site for analysis, as it included a tunnel, London clay soil and a masonry building which was extensively monitored during construction and from which good data was obtained, including that of cracking to the building.

The Mansion House is located in the heart of the City of London. Tunnelling works for the Docklands Light Railway were carried out in two phases from 1988 to 1991. The response of the building and the performance of the instrumentation were the subject of three papers published in the Proceedings of the Institution of Civil Engineers in 1994. The raw data from the monitoring was obtained for this project in April 1998 after negotiations, through Howard Humphreys, with the various member parties of the Committee for the Long-Term Monitoring of the Mansion House and with the original clients for the construction work.

The Mansion House is a large and complicated masonry building, and therefore was a considerable challenge for the modelling techniques developed in this project, in the pre-processing, analysis and post-processing stages. The computing resources available in 1999 were just sufficient for the task of carrying out a single stage analysis of the site.

6.2 Background to the case history

6.2.1 Overview

The background to the project is described in the three papers published in 1994: Frischmann *et al*., Forbes *et al*. and Price *et al*. Tunnels were constructed under or close to the Mansion House (Fig. 7-1) in connection with the extension of the Docklands Light Railway (DLR) from Tower Gateway to Bank, in the heart of the City. The first tunnel, constructed in 1988, was a 3.05m passenger foot tunnel that ran directly under the building, causing a maximum settlement of 8mm, which was greater than expected (Frischmann *et al*., 1994). Prior to the second phase of tunnel construction, which did not actually take place under the building but was within its zone of influence, a back analysis of the building was conducted using the data from the first tunnel. This indicated that protective measures would be required for the second tunnel, and tie bars were therefore installed at various locations in the building.

During construction of the second phase in 1990-91, the building was monitored extensively using precision levelling, electro-levels, a water-levelling system, crack monitoring and wall movement monitoring by invar wire extensometers (Price *et al.*, 1994). The technology of many of these monitoring systems was relatively novel at the time, although many have come into routine use since on, for example, the Jubilee Line Extension.

Summary data from the monitoring of the first tunnel is presented by Frischmann *et al*. (1994), and Price *et al*. (1994) and Forbes *et al*. (1994) give further data from the second phase. It was judged that the published information was insufficient for a back analysis to be carried out for this project, and therefore the raw data was sought.

Mott MacDonald acted as consultants to the DLR, and commissioned the monitoring programme at Mansion House in order to satisfy the owner of the building, the City of London Corporation, and their advisors, Pell Frischmann Consulting Engineers and Sir William Halcrow and Partners. Mott MacDonald in turn brought in the services of

Figure 7-1: The Mansion House, London (Frischmann *et al.*, 1994)

specialists to help with the monitoring programme – the Building Research Establishment (BRE) and Dr Richard Bassett, lecturer at University College London.

Mott MacDonald and the Committee for the Long-Term Monitoring of the Mansion House gave their consent for access to all the data in their possession. Formal approval for use of the data was required from a number of bodies, including Railtrack and the Corporation of London, and this was obtained. The data in Mott MacDonald's possession was viewed and the relevant documents selected for copying in April 1998.

6.2.2 The 1988 works

The first phase of construction in 1988 involved driving a 3.05m diameter tunnel to provide a pedestrian link from the DLR to the Waterloo and City Line. The tunnel was excavated west to east under the northern end of the Mansion House, on a slight skew, as shown in the plan in Figure 7-2. The tunnel axis is approximately 13.5m below the basement level of the building. Excavation was by hand, and great care was taken with the workmanship to minimise settlements, mainly by ensuring that once the lining was erected, the annulus behind it was grouted as soon as possible.

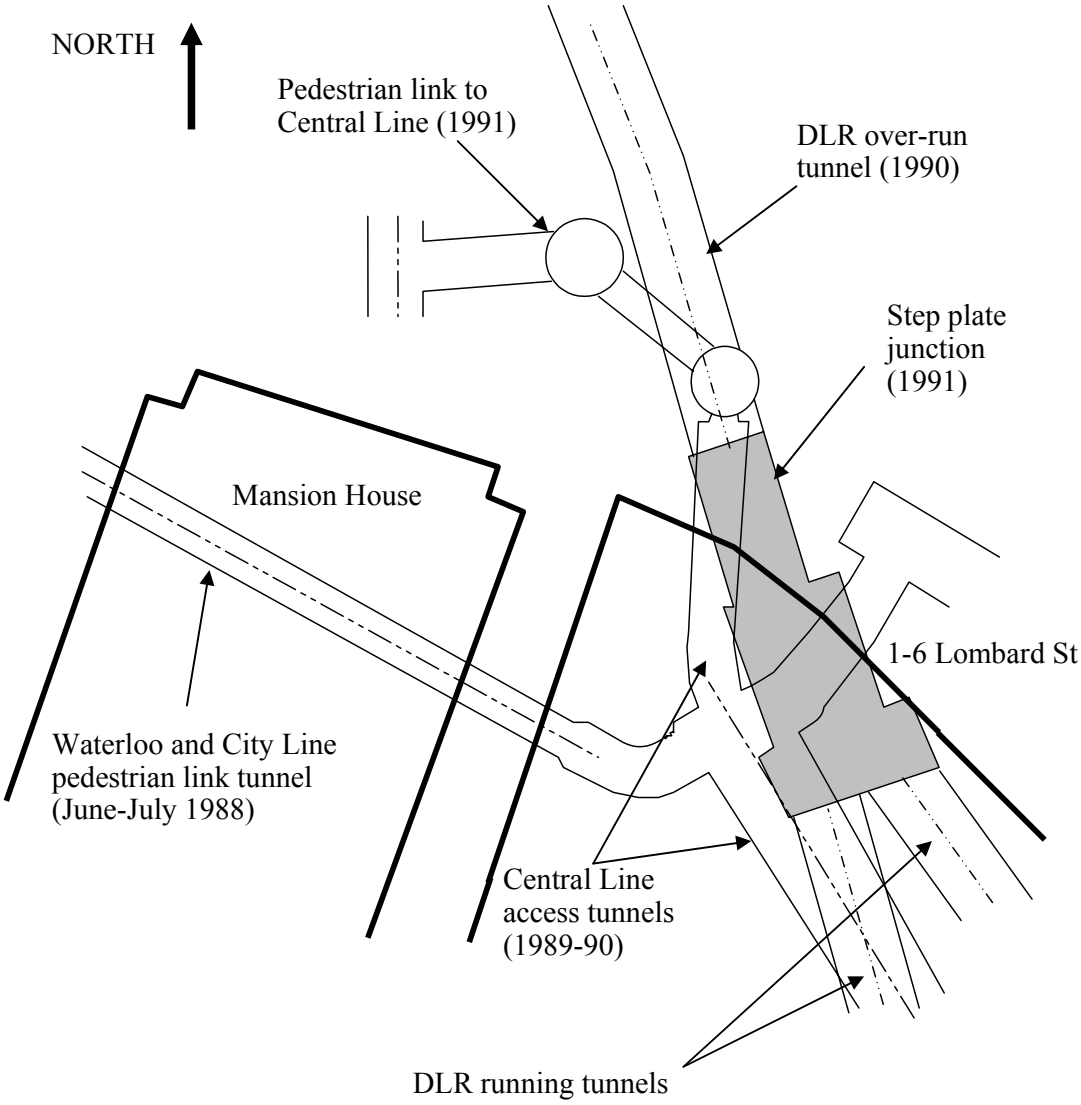

Figure 7-2: Key plan of the Mansion House site showing tunnelling operations

The tunnel diameter was originally designed to be 4.0m but this was reduced to 3.05m after a prediction of damage according to the method of Burland and Wroth (1975). Construction took place in June and July 1988. The settlement of the Mansion House was monitored by means of precise levelling points both inside and outside the building. The development of the settlements in 1988 and 1989 along the west façade is shown in Figure 7-3.

In the short term after construction in 1988, a settlement trough was observed to develop, with a maximum of about 5mm settlement over the tunnel. This was about half

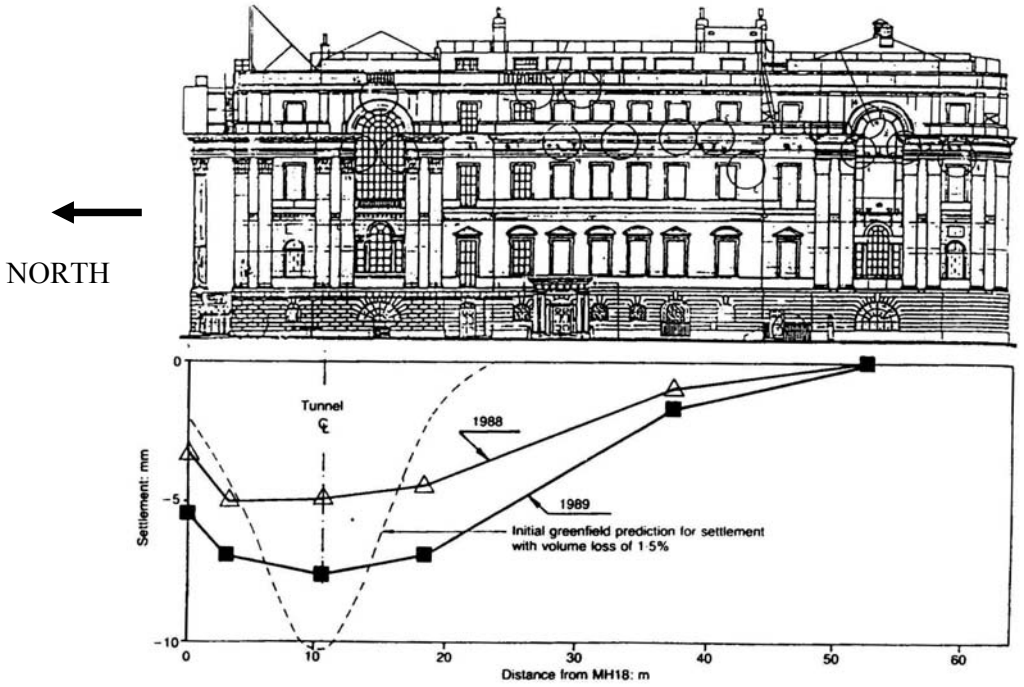

Figure 7-3: Development of settlement profile beneath west façade of building due to 1988 construction of Waterloo & City Line link tunnel (Powderham, 1994)

the predicted 'greenfield' settlement, and the trough was also significantly widened, suggesting interaction effects between the building and the ground. Monitoring continued into 1989, and after about a year settlements were found to have increased to 8mm maximum. In 1989, the building occupants started to report opening of cracks, mainly at high level in internal walls above the tunnel (Frischmann *et al.*, 1994).

This medium-term increase in settlements caused a lot of concern to the building owners. New predictions were made of the likely effects of other tunnelling operations planned in the vicinity, based on a back analysis of the 1988 tunnelling. Two-dimensional linear finite element analyses of the east and west façades, together with the ground and tunnel, were carried out to assess the contribution of structure stiffness to the combined structure and ground behaviour. In these, the structure stiffness was varied until agreement was obtained with the observed profiles shown in Figure 7-3. It was necessary to provide a spring to model the vertical restraint of the north façade on the east and west façades. The stiffness of this spring could only be obtained by trial. The need for such a spring is obviated by a three-dimensional analysis.

Further tunnelling works constructed from July 1988 to December 1989 are usually grouped with the 1988 passenger link tunnel and together described as the first phase of tunnelling under Mansion House (Mott MacDonald, 1991). These works consisted of some high level (*i.e.* shallow) station tunnels and shafts constructed under the neighbouring building 1-6 Lombard Street to connect with the 1988 passenger link tunnel and provide an access to the DLR from the Central Line (Fig. 7-2).

Most of these works under 1-6 Lombard Street lay outside the zone of influence of the Mansion House, or were predicted to cause only small settlements of it. 1-6 Lombard Street itself is a relatively modern concrete-framed building that responded in a stiff manner to the excavation beneath it by settling uniformly by 30mm. However, these works had the interesting effect of apparently triggering further settlement of the northeast corner of the Mansion House, where the settlement increased from 6mm in August 1989 to 12.5mm by August 1990. These further settlements may have been caused in part by continued long-term response to the original 1988 tunnel.

6.2.3 The 1990/91 works

A second phase of tunnelling took place commencing in August 1990, consisting of the following works (Fig. 7-2):

1. A 5.5m diameter over-run tunnel for the DLR, approximately 40m below ground level, constructed from August to November 1990.
2. A step-plate junction between the over-run tunnel and the two DLR running tunnels, in which the over-run tunnel is progressively enlarged by hand from 5.5m diameter to a maximum of 11.5m diameter (November 1990 – March 1991).
3. Completion of the pedestrian link to the Central Line by means of a 3.5m diameter tunnel 15m below ground. This was realigned to lie as far as possible outside the zone of influence to the Mansion House, to minimise the settlement effects on the building.

These proposals caused further concern to the building owners. It was apparent that, due to the location of the proposed tunnelling just outside the building footprint to the

north-east, much of the northern half of the building would lie within the hogging region of the settlement trough. It was feared that this might cause damage at the higher levels within the building.

A detailed analysis was therefore carried out on behalf of the building owners (Frischmann *et al*., 1994). The north façade and the north wall of the ballroom running parallel to it were modelled as two-dimensional Vierendeel frames, representing masonry walls with a large number of openings for doors and windows. The 'greenfield' settlements predicted from the 1990/91 works were imposed on the frame models and the maximum tensile bending strains in the frame members calculated. Where there was cracking present, the stiffness of the frame members was reduced by 50%. Sensitivity analyses were carried out in which the Young's modulus of the masonry was varied, and it was found that the maximum tensile strains were sensitive to this parameter, varying in the range 0.02 – 0.05%.

The conclusion from the analyses was that protective measures of some kind were required to reduce the likelihood of damage to the walls of the Mansion House in the hogging region of the settlement trough. The options initially considered were a piled cut-off wall around the northeast corner of the building, or isolation of the building from its foundations by supporting it on jacks that would be adjusted to negate the tunnelling-induced settlement. These options were considered to be expensive and excessively risky. However, by realigning the Central Line link tunnel away from the Mansion House, the maximum predicted settlement was reduced and an alternative protective method became feasible. This involved inserting tie bars at high levels parallel to a number of vulnerable walls within the building. The tie bars were tensioned to prestress the masonry in compression. During the construction in 1990 and 1991 a sophisticated monitoring system recorded ground and structure response (Price *et al.*, Forbes *et al.*, 1994). Further damage was avoided but additional settlements of up to 18mm were observed.

6.2.4 Choice of strategy for modelling of Mansion House

It is apparent from the foregoing discussion that the Mansion House site is a complex one, in which many tunnelling operations have taken place in close proximity, in both time and space. There is evidence of interaction between structures and the ground, and between structures, for example the response of the Mansion House due to the tunnelling under 1-6 Lombard Street. The long-term settlements due to one phase of tunnelling appear to be superimposed on the short-term response due to the following events, making interpretation difficult. It therefore became necessary, once the data had been obtained, to make a decision as to which phase of tunnelling should be analysed first.

There was a choice of three construction events, which had distinct identifiable effects on the Mansion House, and which therefore could be viewed as three separate case histories. The events were firstly the construction of the Waterloo & City Line to DLR passenger link tunnel directly under the building in June 1988; secondly the construction of a number of high level tunnels under 1-6 Lombard Street in 1988-89; finally the construction of the overrun tunnel and step-plate junction adjacent to the Mansion House from August 1990 to March 1991. Each event caused about 6mm maximum short-term settlement, although the distribution of the settlement and damage was different in each case.

The first case had the advantage that the observations were not affected by medium to long-term effects from previous events. The building was also reported undamaged prior to construction (Pell Frischmann, 1985). This was the only case where tunnel construction happened actually under the building, the tunnel being of very simple geometry. Monitoring of the building itself was limited to precise levelling and condition surveys documented cracking of the masonry. It was the only event that definitely caused damage to the building. Therefore, this case was suitable for a combined three-dimensional analysis of the building and the tunnel plus a relatively small region around.

In the second case, construction under the neighbouring 1-6 Lombard Street caused large settlements of that structure, which in turn appeared to have caused movements of the Mansion House by a mechanism of soil-structure interaction that is not fully understood.

There was no further damage to Mansion House. The data available was again the precise levelling of the perimeters of the two buildings and the surrounding area. This case lent itself to a model of a wide extent of the ground and the two buildings, to a lesser level of detail, with the intention of reproducing the soil-structure interaction observed. The buildings and some of the ground could be modelled elastically. However, this type of modelling was not the primary aim of the project, and so was not considered any further.

The third case was quite typical of a modern tunnelling situation close to a building in London, in which damage was largely avoided by protective measures, in this example the installation of tie bars in critical areas. The building was extensively monitored both internally and externally, and this case was the one given most coverage in the published papers in 1994.

However, the geometry of the step-plate junction tunnel is complex and represents a major challenge to the practical application of the modelling procedures. A procedure for modelling the effects of the tie bars would be required. A model was conceivable, perhaps with the aim of investigating the effect of making practical simplifications to the geometry. The investment in time and effort would be considerable, and the verification data obtained would have the limitation that no damage to the building occurred. It was therefore decided that the first case, the 1988 passenger link tunnel, would be the subject of a three-dimensional model. For the remainder of this chapter, the discussion will be limited to this case history.

6.2.5 Ground conditions

Information about the ground conditions at the Mansion House site was obtained from a number of sources: Pell Frischmann (1985), Frischmann *et al*. (1994) and Powderham (1994). The site is typical of central London in being underlain by a considerable depth of London clay, within which most of the tunnels, including the passenger link tunnel, were excavated. The London clay is overlain by a layer of 1 – 2m of dense flood-plain gravel. A particular feature of the Mansion House site is that the River Walbrook passes the building about 50m to the west. This has led to the deposition of surface deposits of alluvium.

Above this are approximately 6m of made ground and fill. A section showing the main strata, the tunnel and the building is shown in Figure 7-4.

6.2.6 The Mansion House building

The Mansion House was constructed in 1738-39 as a substantial town house. The load-bearing structure is solid masonry walls, consisting of red bricks with plaster coating on the inside and stone cladding on the outside. The floors are of timber suspended construction, and the roof is of slate supported on timber roof trusses.

The building measures approximately 60m by 30m in plan, and about 25m in height. A basement exists under the northern two-thirds of the building in plan. Above this is the ground floor and, in the original structure, three further floors. A fourth floor of lighter construction was added later over part of the plan area (Fig. 7-4).

Plans of each of the main floors are shown in Figure 7-5(a) – (e). The basement is of heavy construction, and the walls progressively decrease in thickness with height up the building. In the centre of the building, there was originally an open courtyard, which was later roofed over and incorporated within the habitable space. To achieve this, numerous new and sizeable openings were made, particularly at ground level, reducing the overall rigidity of the building.

There are two other large rooms within the building, which may have had an important effect on its overall behaviour. The first is the ballroom, which runs across the full width of the building close to the northern end and is two storeys in height on the second and third floors. The second is the even larger Egyptian Hall, which runs the full height and full width of the building at the southern end. Both of these halls have large windows at each side (see Figure 7-3).

The Mansion House was originally founded on timber piles into the alluvium, and became prone to foundation movement in the middle of the nineteenth century, presumably as the timber degraded. In 1868 the wooden piles were reinforced with concrete. Further settlements occurred around 1901, almost certainly due to the construction of the Central Line nearby. The structure was underpinned then, and again in 1931, when extensive

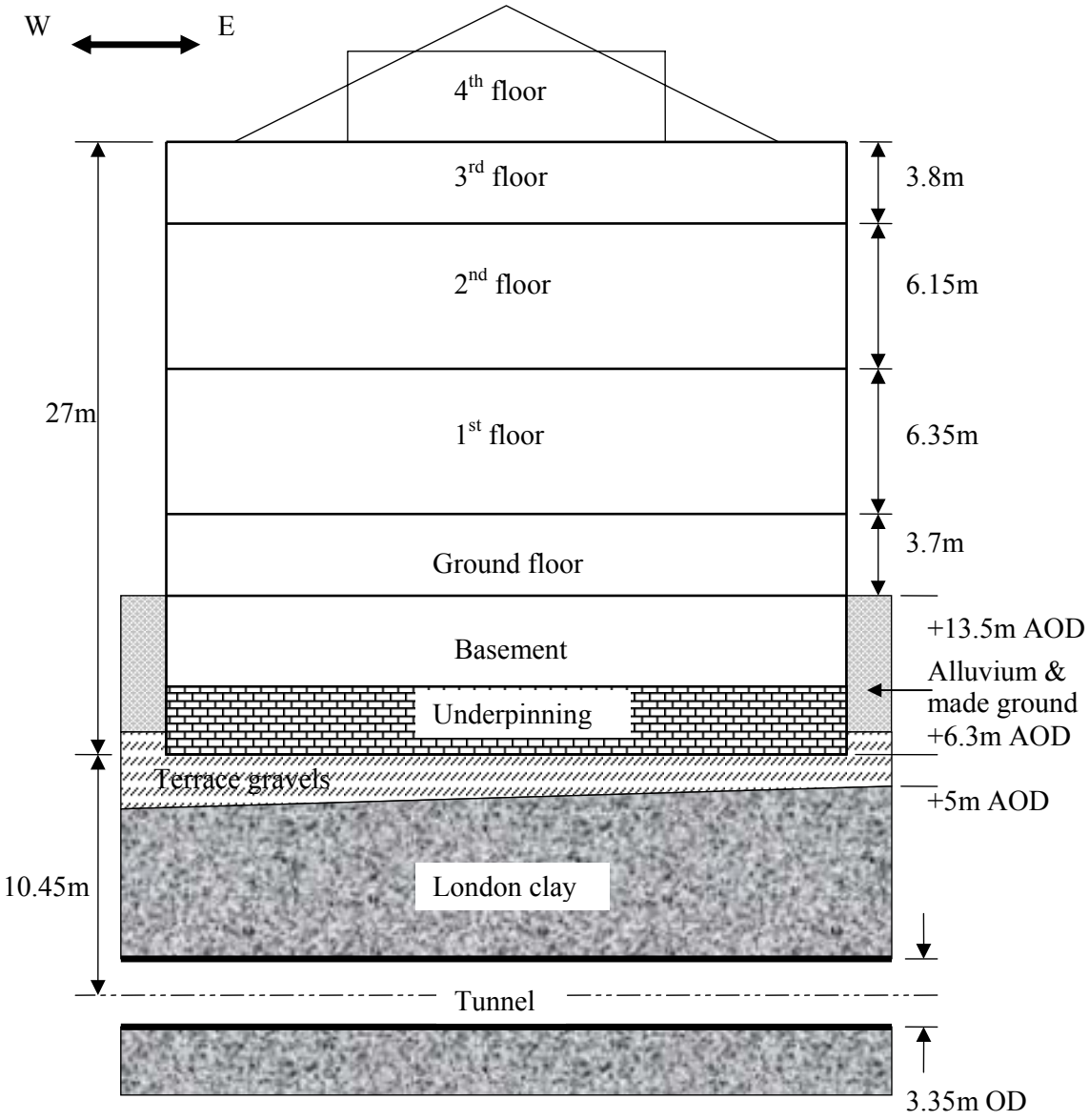

Figure 7-4: Section through Mansion House site showing building, tunnel and geological strata

restoration took place. The underpinning technique involved replacing the timber piles with yellow London Stocks brick masonry walls (Pell Frischmann, 1985). This appears to have been carried out throughout the building, taking the foundation level down to the flood plain gravels, at approximately +6.3m AOD (Fig. 7-4).

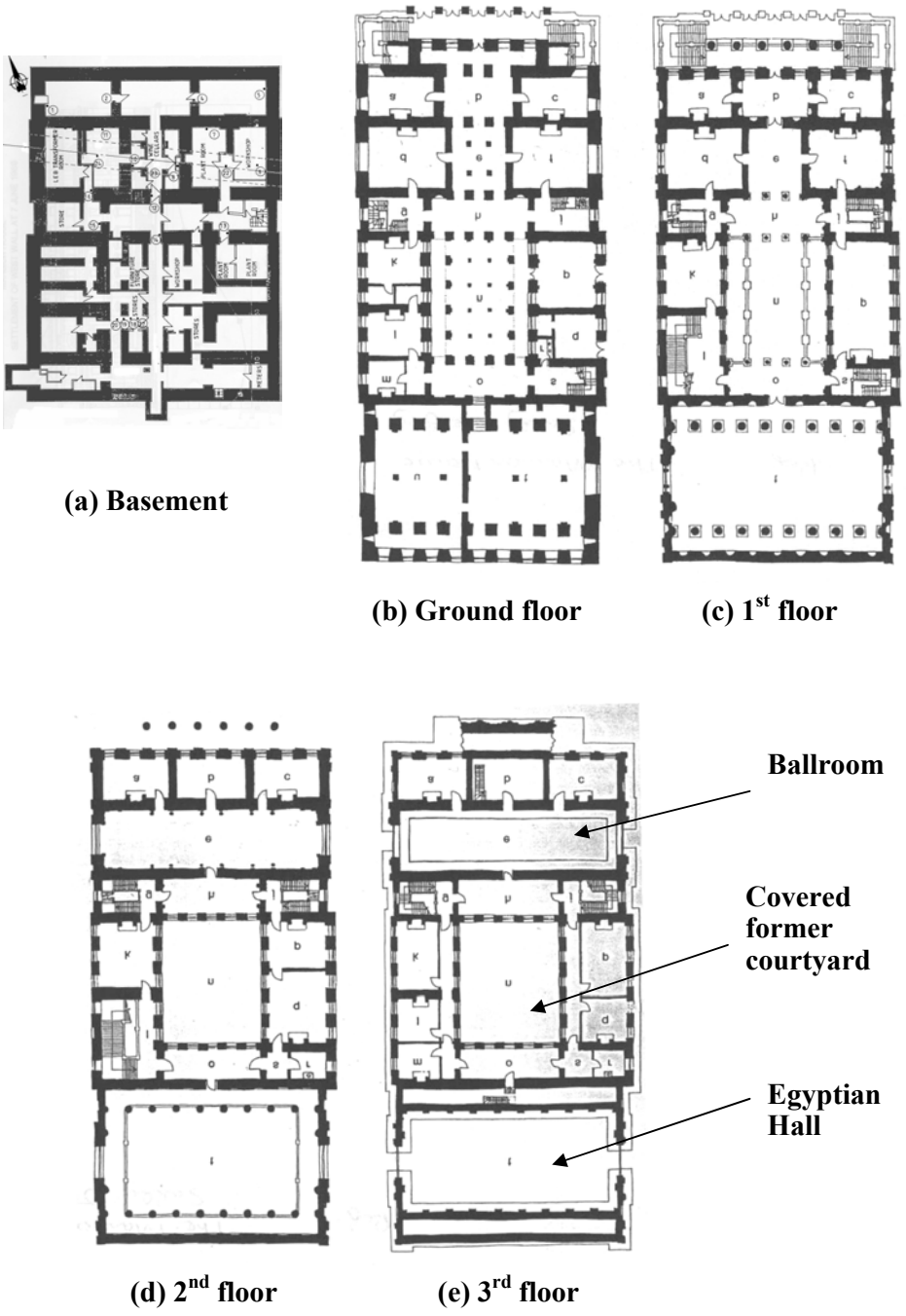

Figure 7-5: Floor plans of Mansion House (Jeffery, 1993)

Over the history of the Mansion House, substantial settlements are thought to have taken place in the area, as evidenced by levels recorded over a period of time on an Ordnance Datum on a nearby building. One masonry course on the building drops in level by 200mm from the southeast to northwest corner. These settlements are consistent with the effects of construction of the Central Line around 1900, which must have caused

considerable damage to the structure that has subsequently been repaired. Thus in a survey in 1985 (Pell Frischmann, 1985) the condition of the structure as a whole was described as good for its age, with just isolated cracking.

6.3 Observed settlements and effects on the structure due to the 1988 passenger link tunnel

6.3.1 Introduction

As discussed in Section 7.2, the case history of the excavation of the Waterloo and City Line passenger link tunnel in 1988 was chosen for analysis in this project.

6.3.2 Monitoring regime

Precise levelling points were installed, prior to the construction, on the exterior of the building around the entire perimeter close to ground level, and in the basement of the building, drilled into either the basement walls or floor. The distribution of the levelling points is shown in Figure 7-6. Data from the monitoring of these points during the period 1st June 1988 to 9th August 1989 are reported by Halcrow (1989). Readings were taken at intervals of two to three days during construction (June – July 1988), reducing to weekly thereafter until October 1988, and then at monthly intervals.

Condition surveys of the building were carried out before and after construction. In 1985, a routine inspection of the building was carried out (Pell Frischmann, 1985). In January 1988, prior to construction, Vigers surveyors carried out a more detailed inspection. A post-construction survey was carried out by Pell Frischmann between August and October 1989.

Locations of cracking were recorded in the 1988 and 1989 surveys. Some Demec arrays (Section 6.2.5) had been placed by English Heritage engineers on existing cracks, following the 1985 survey. In January 1989, when the building occupants became aware of new cracking, further Demec arrays were installed, and yet more Demec arrays were installed in June 1989. The content of the building condition surveys, including data from

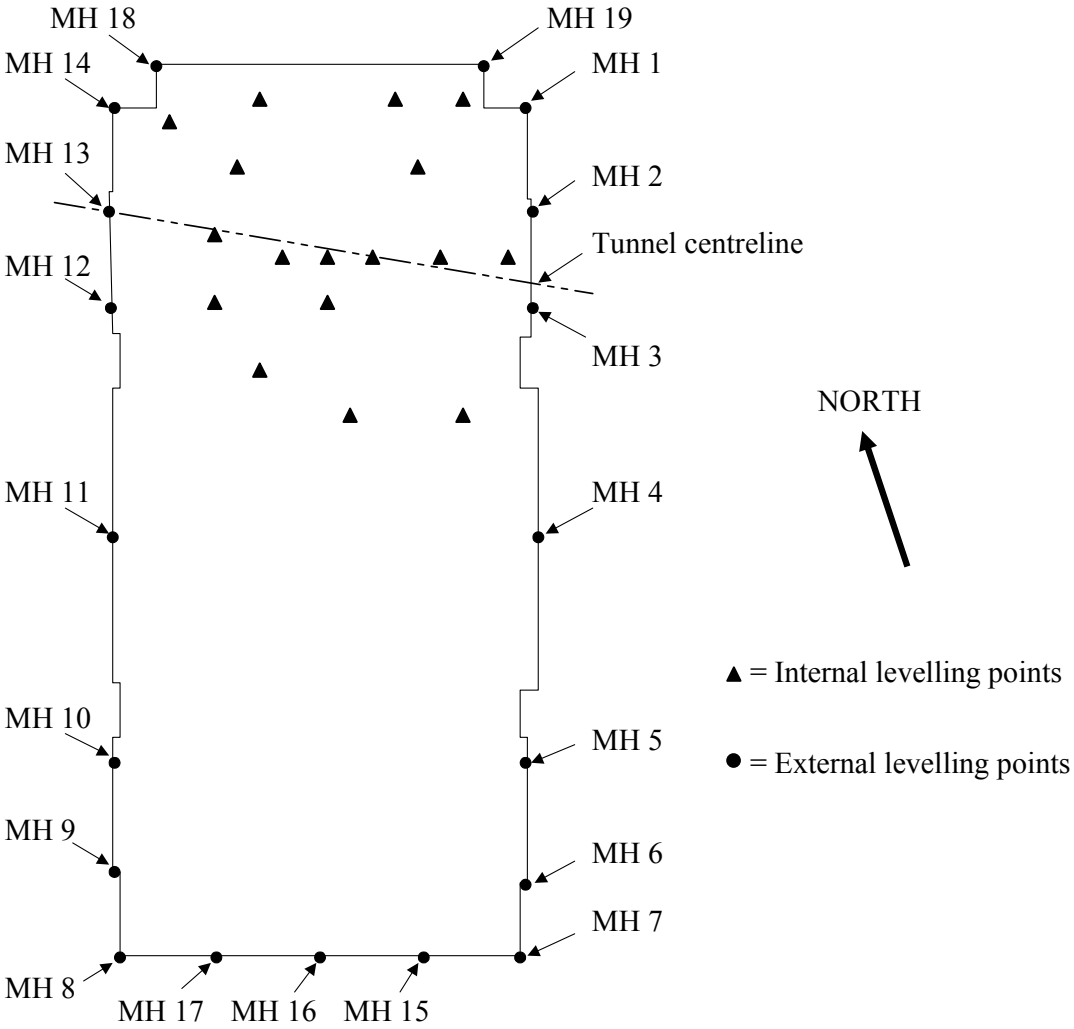

Figure 7-6: Locations of external and internal precise levelling points

many of the Demec arrays, was reported by Pell Frischmann (1989).

6.3.3 Settlement monitoring

Figure 7-7 shows the development with time, over a period of one year, of the settlements of a number of external monitoring points. Points MH 7 and MH 8 at the south end of the building show no discernible change over the period, indicating that the south façade was not affected by the tunnelling. The points MH 1 and MH 14 at the north corners of the building, and points MH 3 and MH 13 on the tunnel centreline show movements that are correlated with the construction operations but then show further increase over the

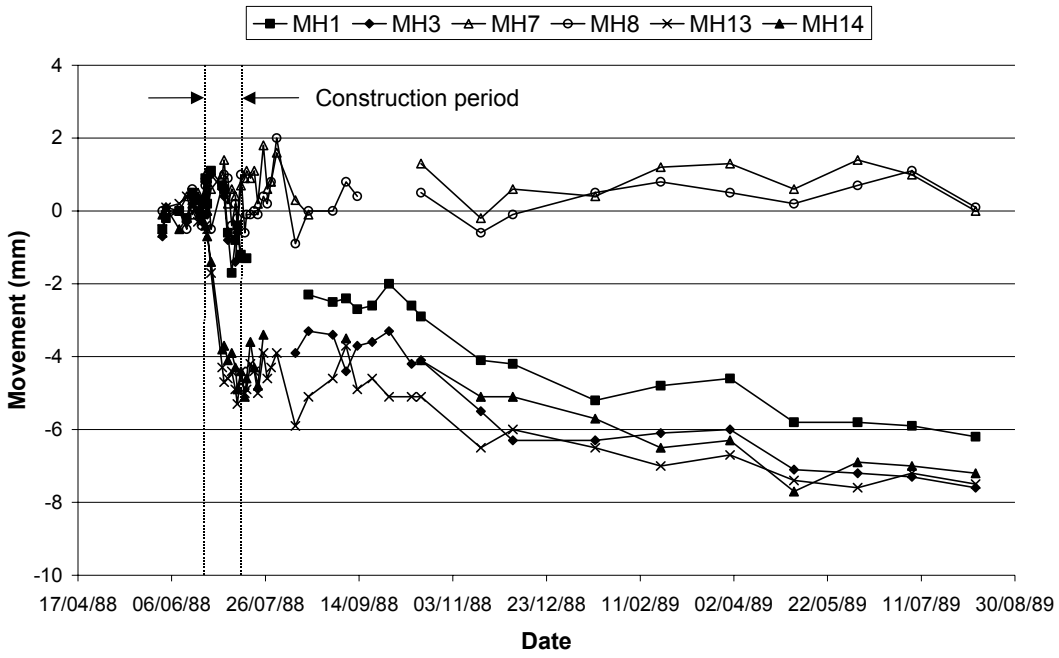

Figure 7-7: Development of settlements with time for selected external monitoring points

following months, with a tendency for a slight acceleration of movement between October and December 1988. This may be correlated with the time when the building occupants reported the occurrence of new cracking in January 1989.

Figures 7-8 and 7-9 show the development of settlements with time plotted along the longer east and west façades of the building. Distinct settlement troughs are evident. The west façade showed a more rapid response than the east façade by the end of construction on 13th July 1988, probably because excavation took place from west to east. The maximum settlement of both façades reached about 7.5mm one year after construction. The data from the monitoring points within the building basement are consistent with those from the exterior.

If the data from the west façade are taken as more representative of structure behaviour, then the volume loss calculated from the area under the settlement half-trough was 1.4% at the end of construction and 3.3% after one year, based on a 3.35m tunnel outside diameter. The trough width parameter *i* is approximately 14m throughout. The expected 'greenfield' value of *i* assuming ground level at underpinning level (+6.3m AOD), according to the empirical formula proposed by O'Reilly and New (1982) for cohesive soils (Section 2.3.2),

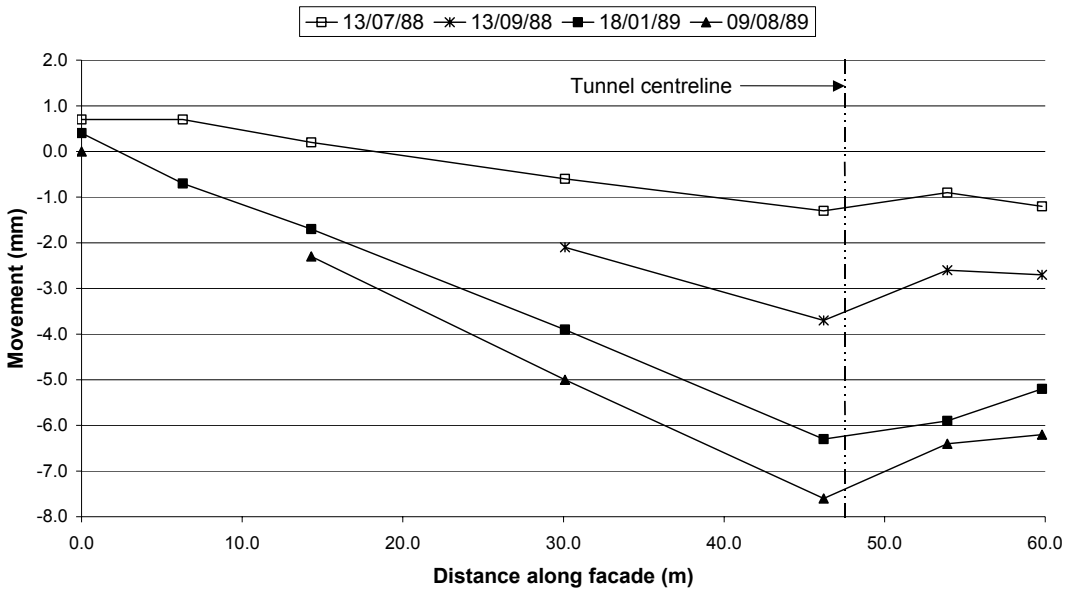

Figure 7-8: Development of settlement profiles along the east façade

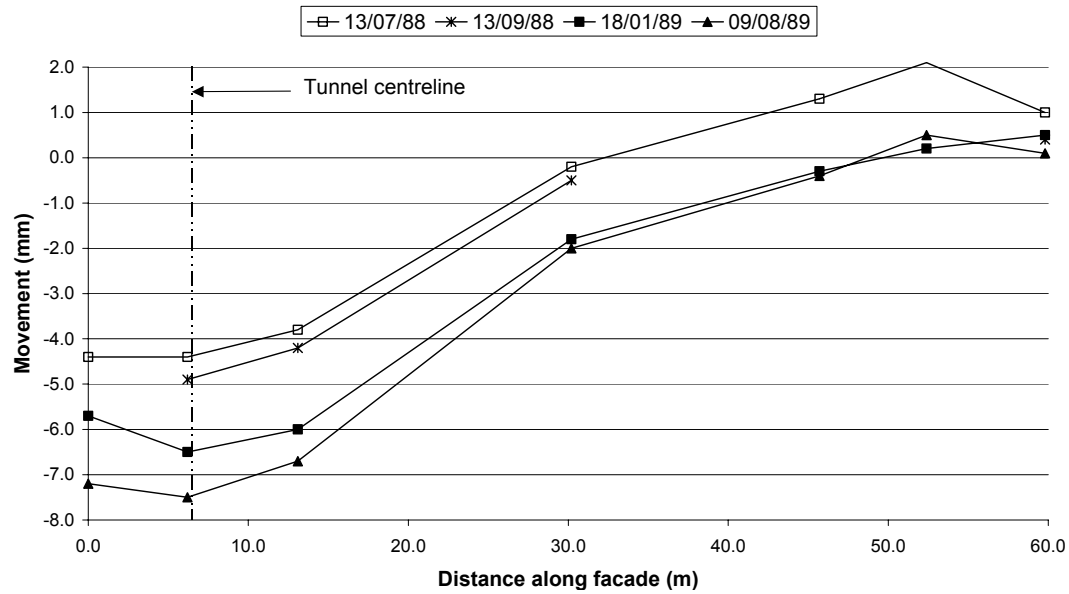

Figure 7-9: Development of settlement profiles along the west façade

is 5.2m. Therefore it is apparent that significant widening of the settlement trough has occurred, due to the presence of the structure.

Frischmann *et al*. (1994) report further increases in settlements of the east and west façades, maintaining a similar trough shape, up to July 1990 (at which time the maximum settlement was 12mm). However, as discussed in Section 7.2.4, it is difficult to ascertain

whether these were a continuance of the response to the 1988 passenger link tunnel or whether they were triggered in part by the works beneath 1-6 Lombard Street.

It should be noted that the north façade settled almost uniformly in response to the tunnelling.

6.3.4 Effects on structure

The cracking occurring in the Mansion House in the period 1988-89 is reported in detail by Pell Frischmann (1989) and summarised by Frischmann *et al*. (1994). The damage was concentrated at the northern end of the building above or close to the tunnel alignment. The worst affected area was the ballroom, where cracks of up to 4mm opened up in the north and south walls and on the balcony that runs around the perimeter of the hall at third floor level. Cracking was also reported in the north façade and in some of the walls perpendicular to it. The damage in these areas may be classified as "Moderate" according to Burland *et al*. (1977) (Table 2-1).

Figure 7-10 shows the crack pattern reported in the critical north and south ballroom walls. Frischmann *et al*. explain the pattern in terms of three causes:

1. Cracking initiating from the top of both walls at a number of locations along their length as the hogging region of the longitudinal settlement trough advanced, as the tunnel passed from west to east beneath the ballroom.
2. Vertical cracking of the north ballroom wall consistent with horizontal tensile strains due to the tunnelling.
3. Inclined cracking of both walls consistent with a settlement of the southeast corner of the ballroom, which is directly over the tunnel.

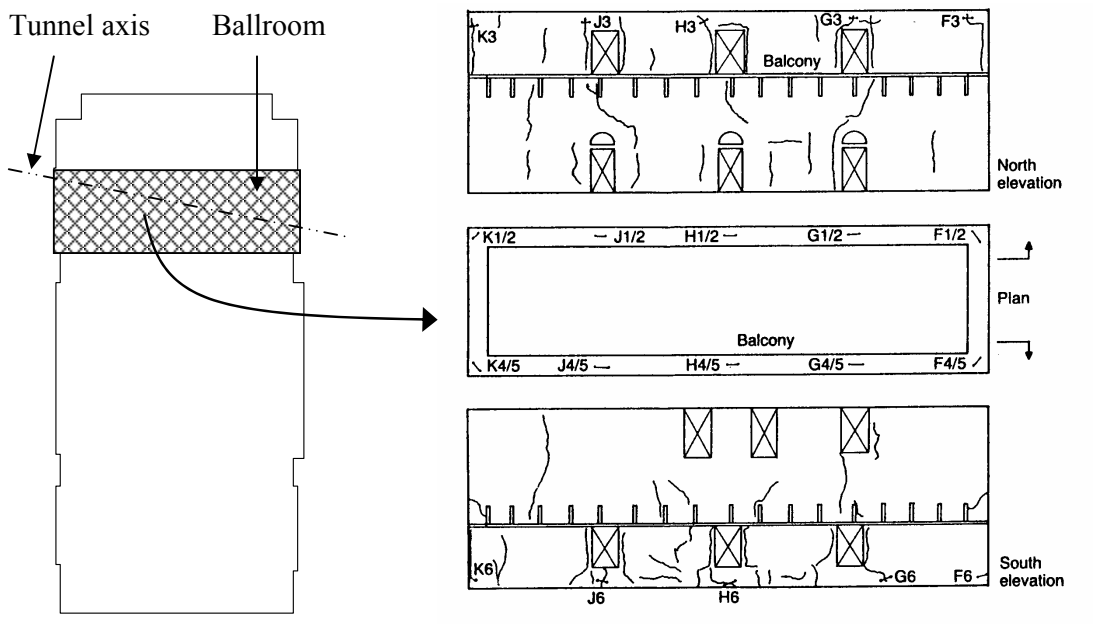

Figure 7-10: Observed cracking in ballroom (Frischmann *et al*., 1994)

6.4 Modelling aims and assumptions

6.4.1 Overview

The first stage of modelling was to represent the tunnel and ground without the building, *i.e*. the 'greenfield' situation, as for the Ramsgate site. In this case, there was no 'greenfield' field data available from the passenger link tunnel, as it passed for almost all its length under the Mansion House or other structures. Therefore the only alternative for the verification of the 'greenfield' model was comparison with predictions using the Gaussian model.

Once the 'greenfield' model had been verified, the building was added. A model was sought that adequately represented the key features of the building including major openings, internal walls and the stiff basement. It was found that, for a number of reasons, it was not possible within this project to achieve the level of detail originally desired. In particular, it was not possible to include the internal walls.

6.4.2 Ground and tunnel

Simplifying assumptions were necessary in the modelling of the ground and tunnel, along similar lines to those already made for the Maddox Street and Ramsgate sites.

The top surface of the model was set at underpinning level of the building (+6.3m AOD). The effect of the 7.2m depth of soil above this level that was not modelled directly was represented by means of a uniform surcharge of 144kN/m^2 over the model surface.

The underpinning to the building is founded in the flood plain gravels, but they are only 1 – 2m thick at this location. Therefore the entire ground block was approximated as consisting of London clay.

The boundaries of the ground block were set parallel and perpendicular to the axis of the tunnel, as for the Ramsgate model. The footprint of the building was therefore skewed at an angle of approximately 12^o from the longest dimension of the ground block (Fig. 7-11). The tunnel was partitioned within the ground block in five sections to enable the modelling of an incremental advance in five stages. This was later increased to six sections and the ground block enlarged following 'greenfield' analyses, as discussed in Section 7.5.1.

From the experience gained with the Maddox Street model, and in the knowledge that the Mansion House building was somewhat larger, heavier and more complex than St. George's Church, provision was made at the start for a foundation within the soil beneath the building. Partitions were made within the soil volume to enable the option of either having a 2m thick 'raft' foundation under the entire building, or 2m x 2m section strip footings under the four exterior façades. The intention was that the material properties of these foundation volumes could be chosen to model soil, concrete or masonry as required. The geometry of the model with the building included is shown in Figure 4-1 in Chapter 4.

It became apparent, however, that the mesh generator in the I-DEAS pre-processing suite (Section 4.2.2) was unable to generate a mesh including features with such fine detail relative to the model size. Therefore it was necessary to increase the raft thickness to 3m and the footing widths to 6m. To achieve this, it was regarded as necessary to incorporate

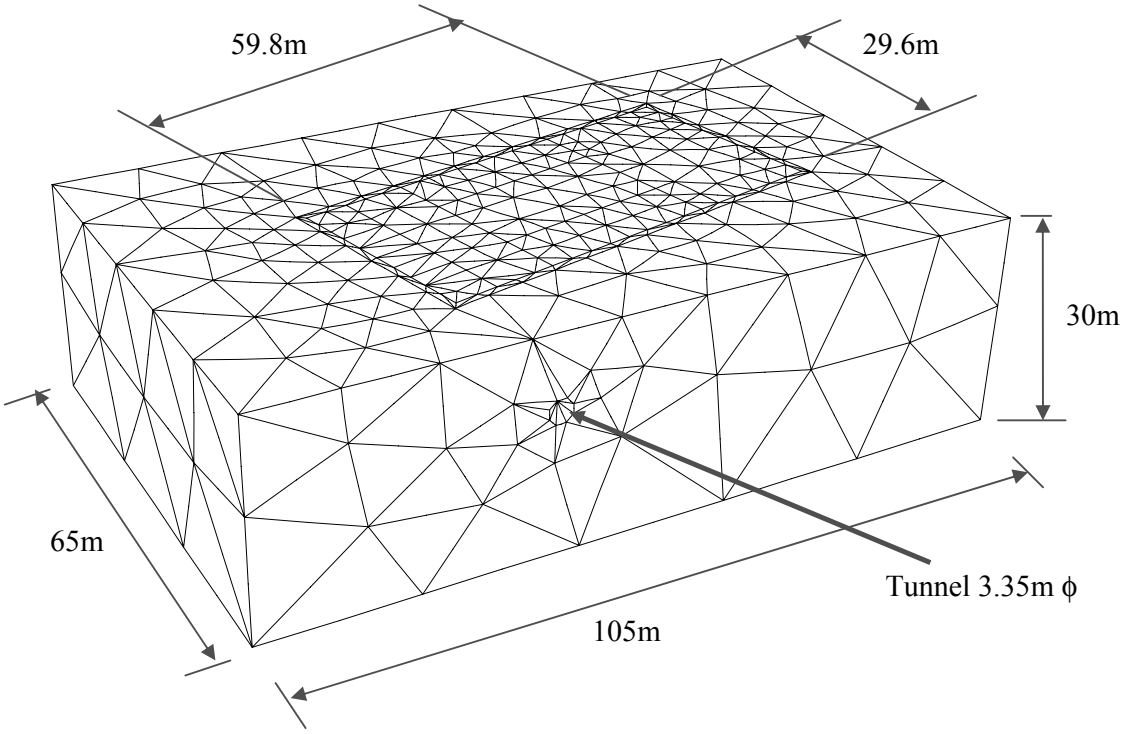

Figure 7-11: Mansion House ground block dimensions and mesh

the underpinning within the ground block rather than as part of the building façades. The model surface was raised by 3m, to represent the basement level of the building. These problems with the meshing of the raft foundation only became apparent when analyses were carried out with the building included to the model.

The geometry of the final model with a building consisting of four external façades only is shown in Figure 7-12. The tunnel was modelled as octagonal with the same cross-sectional area as the actual tunnel, following the philosophy of previous models.

There was no specific information available on geotechnical properties for the site. Therefore, for the London clay, the variations of properties with depth below ground level used were the same as used at Maddox Street (Section 5.4.1). This meant that the undrained shear strength was 85kPa at the top surface of the model and increased with depth at 6kPa/m, and the rigidity index was 500.

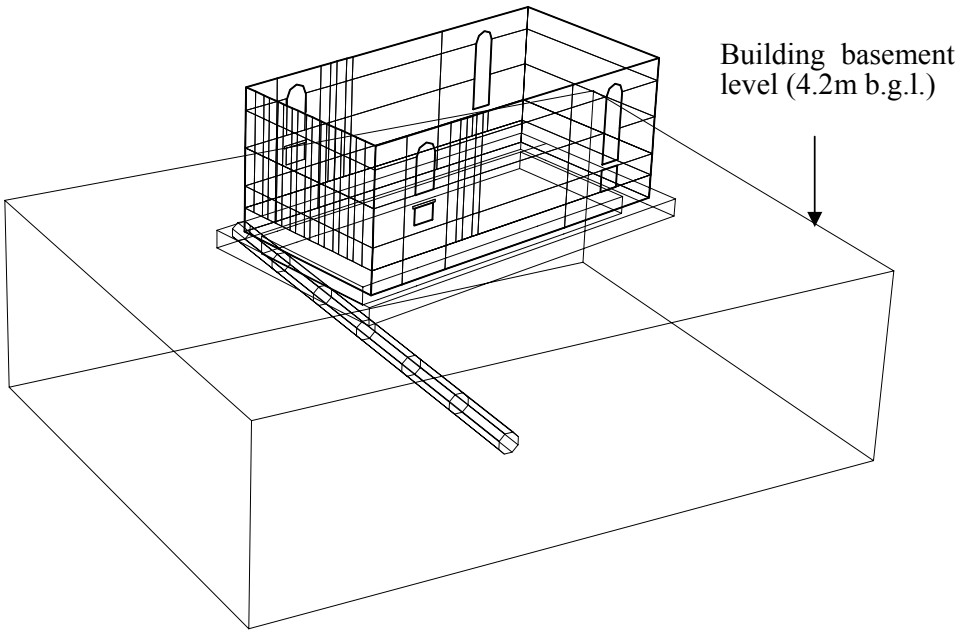

Figure 7-12: Wireframe geometry of final Mansion House model with 3m thick foundation and six tunnel excavation stages

6.4.3 Building

A number of assumptions were made in order to represent the Mansion House in a finite element model. These concerned the issues of wall layout, wall thicknesses, storey heights and provision for openings.

Experience with the Ramsgate model showed that internal walls could have an important influence on the settlement response of structures. Indeed, at Mansion House some of the most serious damage occurred to the internal walls of the ballroom (Fig. 7-10). At the outset, it was appreciated that it was not possible to include every internal wall in the Mansion House model, and therefore, as for Ramsgate, choices were required as to which walls were necessary.

By examination of the floor plans of each storey given by Jeffery (1993) (Fig. 7-5) and with knowledge of the history of the building, it was apparent that the most important internal walls, which ran through the entire height of the building, were those bounding the ballroom, former central courtyard and the Egyptian Hall. Therefore, only these walls were modelled. The choice is shown in Figure 7-13. A model was assembled including these

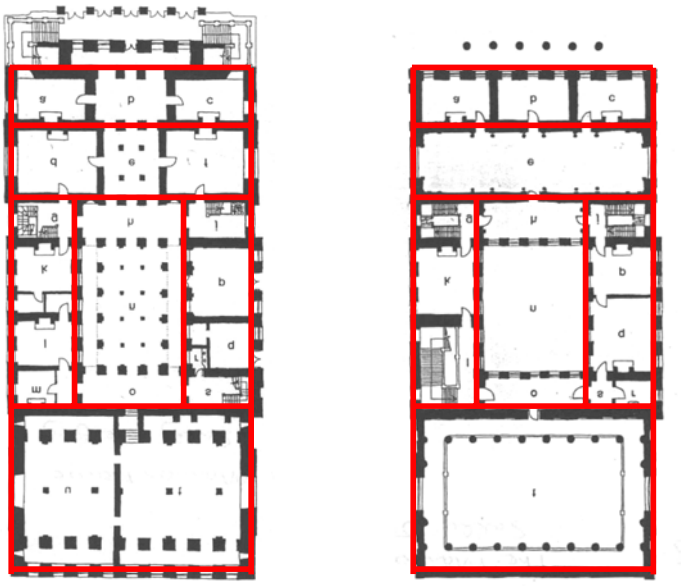

(a) Ground floor **(b) 2nd floor**

Figure 7-13: Choice of main load-bearing walls for modelling

internal walls, as illustrated in Figure 4-1. However it was found that the execution time for the analysis was long, and therefore the model was simplified to one consisting of just the external walls of the building, as shown in Figures 7-12 and 7-14.

Copies of floor plans and sections originating from the records of the City of London Corporation were obtained from Mott MacDonald with the monitoring data. From these, storey heights and wall thicknesses could be scaled. The storey heights varied slightly around the building but could be approximated as 4m, 3.7m, 6.35m, 6.15m and 3.8m for the basement, ground and 1st to 3rd floors respectively.

Wall thicknesses varied over the range 500mm – 2m. The wall thickness determines the value of Young's modulus to assign to the 2-D façade elements in the model, and so each wall thickness requires a separate material model number in the OXFEM input file. Eight different wall thicknesses were enabled: 500mm, 800mm, 1000mm, 1.2m, 1.3m, 1.5m, 1.7m and 1.9m. With hindsight, it would have been preferable to reduce this number to simplify the input file and reduce the possibility for errors.

Openings in the masonry walls were modelled as a combination of vertical regions of reduced stiffness and discrete openings in the mesh. The major openings in the external façades were associated with the ballroom and Egyptian Hall. There were also some large

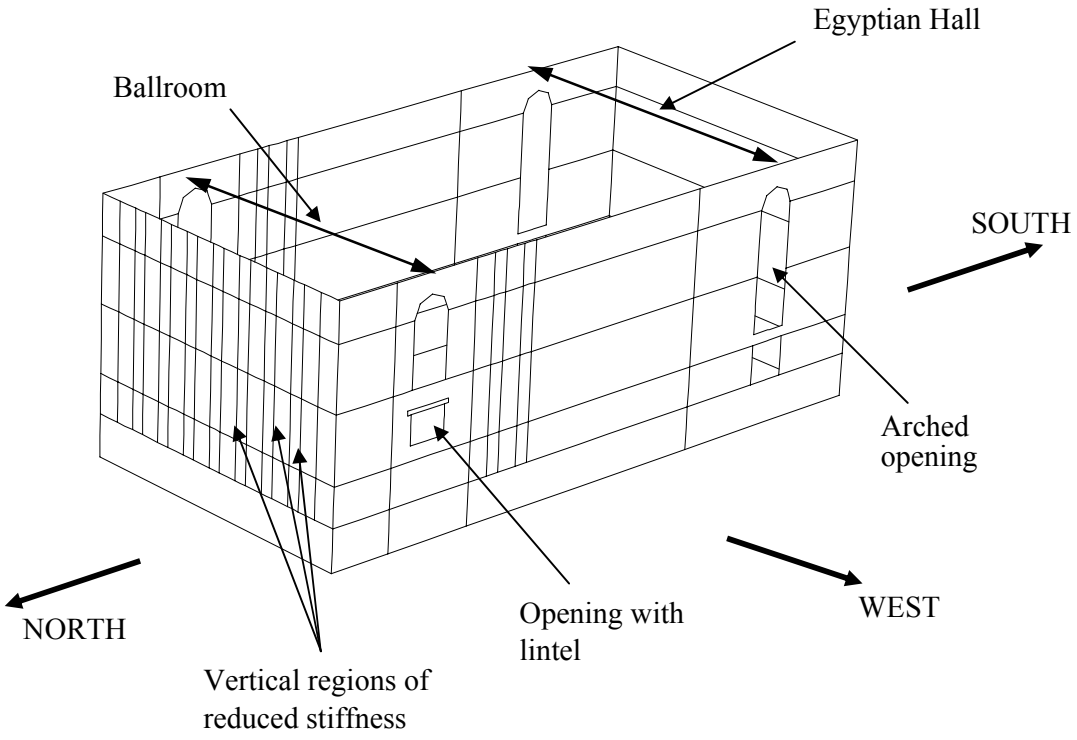

Figure 7-14: Geometry of building façades showing treatment of openings

openings in internal walls, particularly from the ballroom and Egyptian Hall into the former central courtyard. These were modelled as discrete openings. Where the opening was arched, it could be modelled as such, but where it was rectangular, an elastic lintel was required above the opening to prevent its premature collapse.

The north, east and west façades also had a large number of standard-sized windows, which were represented by vertical regions of reduced stiffness, with 60% of the intact façade stiffness. The wireframe geometry of the building is shown in Figure 7-14.

In the meshing of the façades, the discrete openings were initially made void of elements. However it became apparent that premature collapse was occurring in the large openings for the Egyptian Hall. Therefore all the openings were meshed with elements, and a low stiffness (10% of the stiffness of the 500mm thick wall) allocated. This was sufficient to stabilise the opening in the analysis. The mesh for the building model (before the discrete openings were meshed) is shown in Figure 7-15.

For the calculation of stiffness for the masonry elements, the Young's modulus of the masonry material was assumed to be 1GPa throughout. This was the same figure as used in the analyses reported by Frischmann *et al*. (1994) (Section 7.2.3). This is lower than the range of values of 3.8 – 10.4GPa reported by Frischmann *et al*. (1994) from laboratory testing of cores taken from the Mansion House. Lime mortar is used in the structure and a mass stiffness in the range 1 – 5GPa would normally be expected. Thus the assumption of 1GPa is on the low side of this range, which provides allowance for the structure having pre-existing cracks.

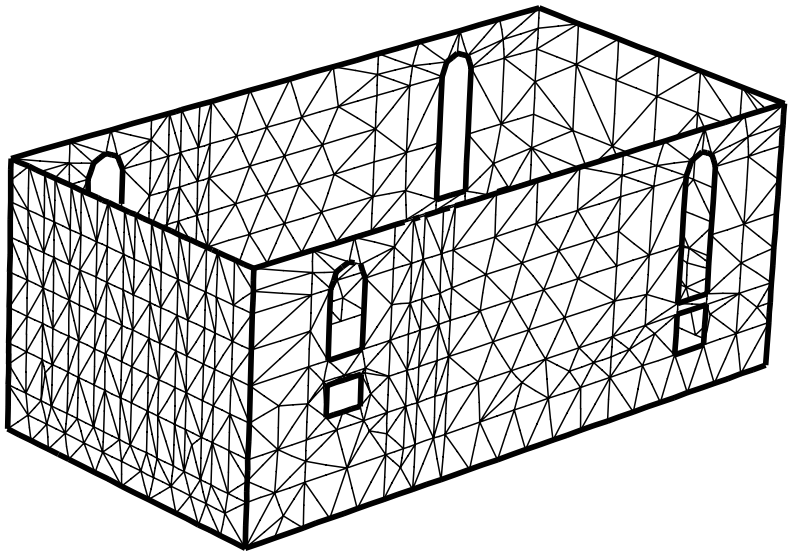

Figure 7-15: Finite element mesh for building consisting of four external façades

6.4.4 Analysis sequence

For a typical model, the analysis sequence used was similar to that for the Maddox Street (Section 5.4.4) and Ramsgate (Section 6.4.5) models. Due to the size and weight of the building and the overall complexity of the model, it was found necessary to increase the number of steps over which application of self-weight, excavation and volume loss were applied. Therefore, a typical sequence was as follows:

1. Apply initial stresses to the soil and self-weight to the building over 50 steps.

2. Allow 10 steps with no further loading, then zero all displacements and strains and "heal" all cracking in masonry.

3. Remove elements from the tunnel and switch on corresponding lining elements over 80 steps.

4. Allow 10 steps with no further loading.

5. Apply radial shrinkage to lining to model volume loss, over 80 steps

6. Allow 10 steps with no further loading and then output nodal and Gauss point results.

7. Repeat stages 3 to 6 for further stages of excavation.

6.5 Description of analyses made

6.5.1 'Greenfield' analyses

'Greenfield' analyses were carried out with the tunnel excavated in one stage and with the tunnel excavated incrementally in five stages. In both cases a volume loss of 2% was assumed initially. Figure 7-16 shows contour plots of surface settlement generated in the incremental analysis. The settlement profile is reasonably smooth but the settlements at the end of the analysis are larger at the left side, from which the tunnel heading advanced. This problem stimulated a reassessment of the model, and an increase in the ground block size and mesh density in the soil.

The surface settlements on a cross-section through the initial 'greenfield' model and the revised model at the building footprint are shown in Figure 7-17. Also shown are predictions of settlements at underpinning level of the building, applying the Gaussian model and using the method developed by Mair *et al*. (1993) for prediction of subsurface settlements, because underpinning level is 7.2m below actual ground level. The maximum settlements over the tunnel from the finite element analyses are less than predicted, but away from the tunnel the finite element analysis predicts larger settlements. However, the positions of the points of inflexion and therefore the value of the trough width parameter i are similar in the finite element model and the Gaussian prediction. The settlements close

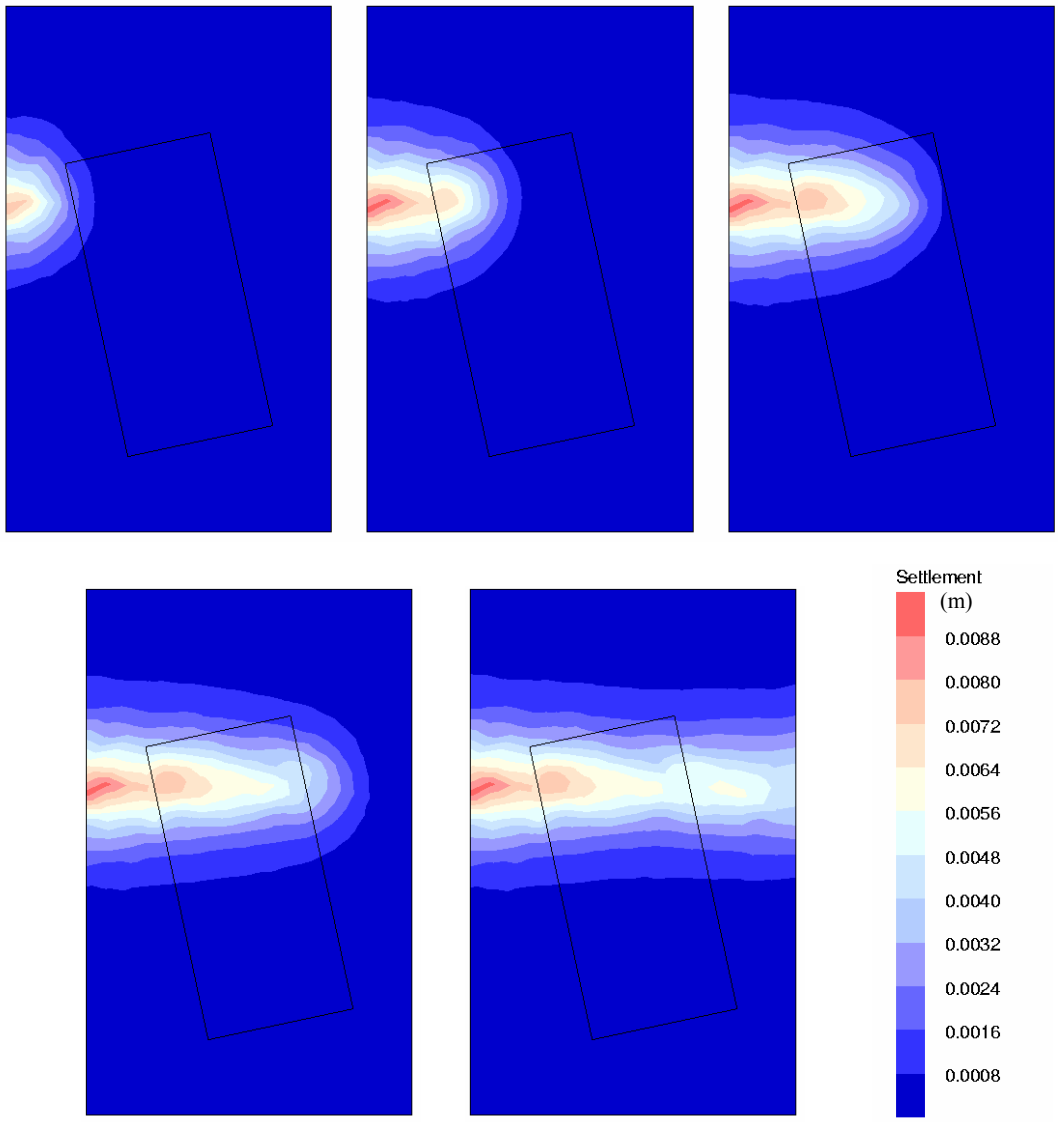

Figure 7-16: Contour plots of surface settlements from 'greenfield' analysis with incremental advance of the tunnel and 2% volume loss

to the tunnel axis from the improved 'greenfield' model approximate well to the Gaussian assumption with 1.4% volume loss, which is believed to be the value of volume loss at the end of construction (Section 7.3.3). Therefore this 'greenfield' model with 2% volume loss was taken as the base 'greenfield' model to which the building was then added.

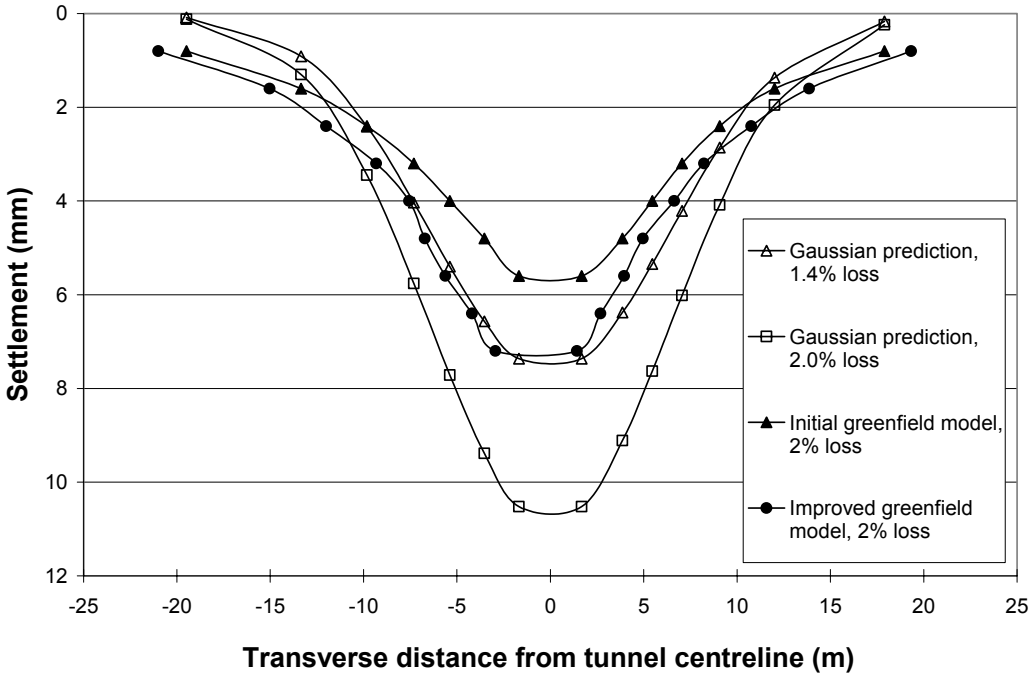

Figure 7-17: 'Greenfield' settlements from analysis and comparison with Gaussian predictions of subsurface settlements

6.5.2 Combined analysis including building

When the building was initially added to the model, convergence problems occurred, which led to a careful examination of the model. By testing the performance of parts of the model in turn, using elastic façades and varying the self-weight and stiffness, it became apparent that there were problems to be overcome with both the foundation to the building and with the façades themselves.

Concerning the foundation, it was discovered that the meshing of the 2m thick raft foundation was defective, with elements missing, even though the I-DEAS program itself reported no error. This served to highlight the importance of carrying out manual checks on the mesh, the most simple of which is to calculate the overall volume of the elements in the model. It also illustrates that commercial software cannot be relied upon as being totally reliable. Attempts were made to re-mesh the model with the 2m thick raft but it became evident that it was not possible. Therefore the foundation thickness was increased to 3m and the width of the strip footings increased to 6m. The footings were taken to represent the underpinning to the building as discussed in Section 7.4.2.

The choice of material properties for the raft foundation or strip footings became an important issue. The original intention had been to assign elastic parameters to model the stiffness of masonry or concrete. However, with the dimensions having been increased, the stiffness contribution of the foundation would have become too large. There was no real evidence to suggest that the underpinning to the building itself formed a stiff continuous structure. Therefore, to be conservative, and to avoid the foundation contributing too much stiffness, its modulus was set to be equal to that of the surrounding soil, but its strength was set to be high (1000kPa). This gave a foundation that performed satisfactorily in preventing failure of the soil during the first loading stage when self-weight was applied.

Once the foundation problems had been overcome, and the problem of premature failure at major openings in the façades had been solved, as discussed in Section 7.4.3, results were obtained from a model in which the tunnel was excavated in one increment, with 2% volume loss, under a building with external façades on strip footings but no internal walls (*i.e.* as shown in Figure 7-12). The surface settlement contours at the end of the analysis are shown in Figure 7-18, and the cracking damage categories and crack patterns for the north, west and east façades are shown in Figures 7-19 to 7-21. The south

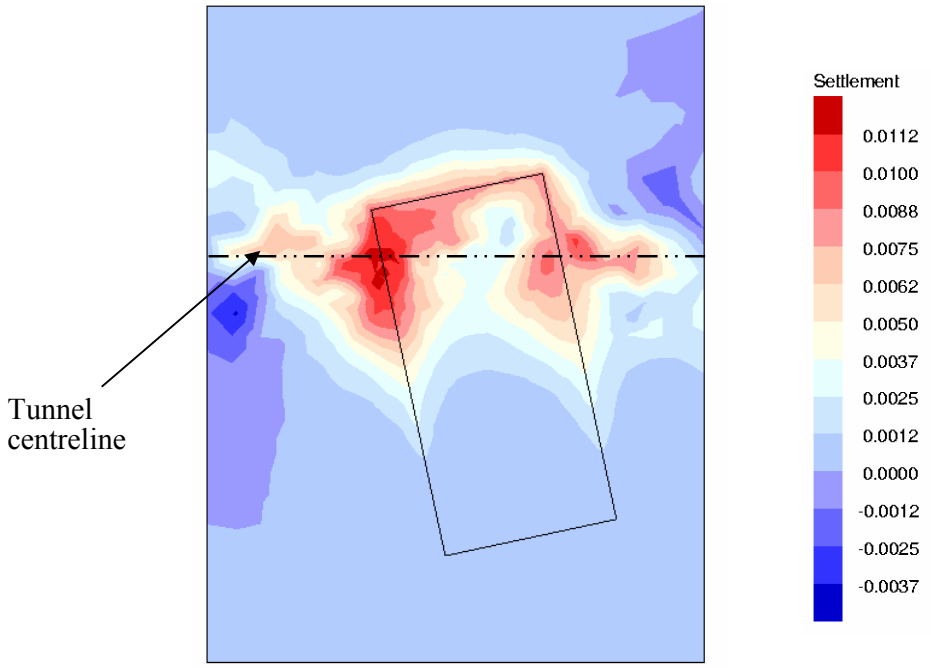

Figure 7-18: Surface settlements from combined model

façade, remote from the tunnel, did not settle significantly and was almost undamaged.

The contours show the tendency for settlements to have increased under the north end of the building, compared to the 'greenfield', to a maximum of about 12mm. The settlement effects have propagated further away from the tunnel along the east and west façades than in the 'greenfield' case. The response is similar to that at Maddox Street (Fig. 5-9), which was also a heavy and stiff building, and contrast with that of Ramsgate (Fig. 6-23(b)), which was a light, flexible building. The settlement response is not as smooth as in the models of the other sites, and it is likely that the model would have benefited from a more refined mesh in the soil.

The maximum settlements are concentrated over the tunnel centreline at the northwest corner of the building. This is reflected in the damage plots for the façades, which show a concentration of damage at this corner (Figs. 7-19 and 7-20). The crack pattern, which shows vertical or near vertical cracks at the western end of the north façade and to a lesser extent at the northern end of the west façade, shows the predominant mode of response to be downwards shear of the corner of the building. On the north façade, the damage is concentrated in the stiff "pillar" of masonry near the corner, having propagated upwards rather than sideways into the adjacent vertical region of reduced stiffness that models a column of windows. The stiffness of the load path up the "pillar" is increased because it is connected to the adjacent façade. In general, the north façade shows widespread cracking,

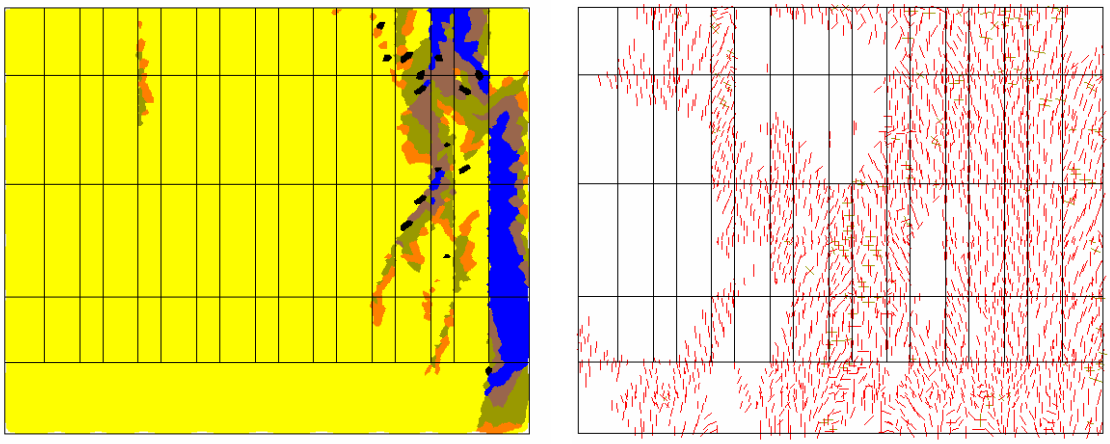

Figure 7-19: Damage category and crack pattern for north façade

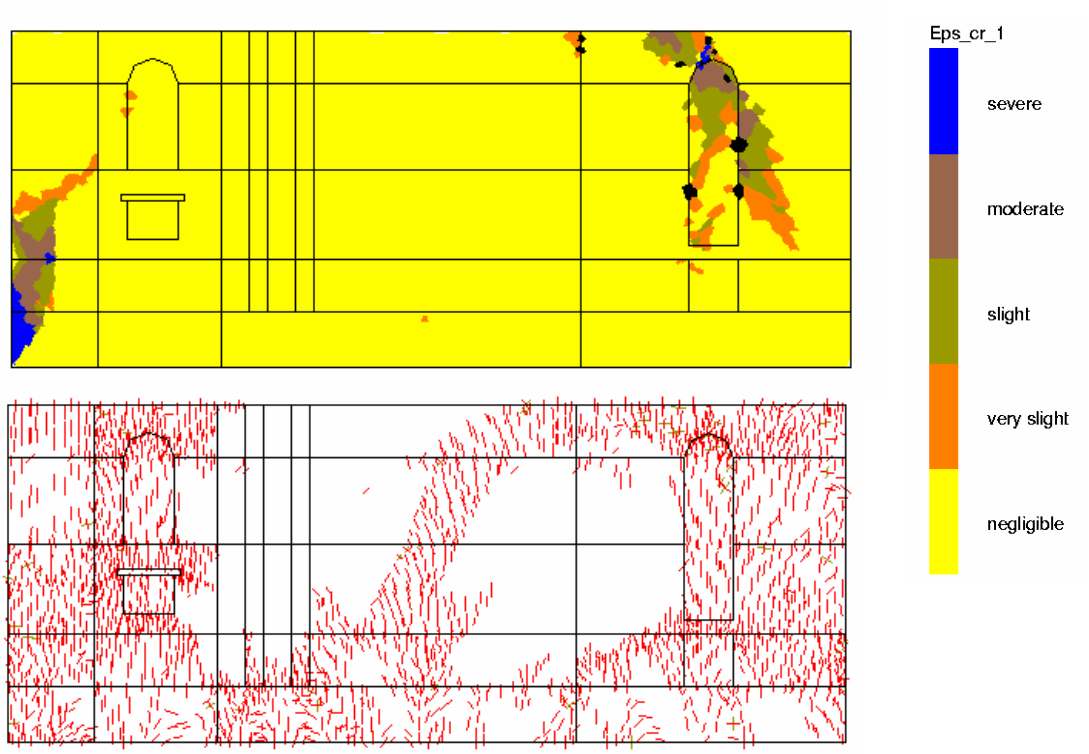

Figure 7-20: Damage category and crack pattern for west façade

but it is distributed over almost the whole area and the damage category is mostly no more than "Negligible". This may be a typical feature of a façade that is relatively uniform and with no major openings. In the field, the only cracks registered in the north façade were at third floor level around the centreline, behind the portico, which was the only area high above ground level that could be easily accessed. The model prediction that fairly distributed damage occurred to the north façade is not unreasonable, but the model may have over-estimated the degree of concentration of damage at the corner, due to the restraint in the connection with the other façade, as also observed in the Maddox Street model.

The west façade (Fig. 7-20) shows a concentration of damage at the north end, correlating to that on the north façade. Although there is cracking around the ballroom openings, it is does not register more than "Negligible". The concentration of damage is further away from the tunnel, in the hogging region of the settlement trough and in particular associated with the large Egyptian Hall window. The extent to which the

cracking has been concentrated at the Egyptian Hall has probably been over-estimated by the model, because little detail has been provided in the middle portion of the façade in between the major openings, where there are in fact many standard-sized windows (Figs. 7-1 and 7-3) which would have increased the flexibility of the façade in this area. Nevertheless, the phenomenon of hogging damage initiating from the top of masonry façades is a known one, and was also seen in the Maddox Street and Ramsgate models.

There is evidence from the cracking pattern of localised arching at low level on the west façade, just to the south of the tunnel axis. Arching could not form closer to the corner of the building because it requires horizontal restraint to provide a horizontal reaction to the arch thrust, and there is no horizontal restraint at the ends of façades.

The response of the east façade (Fig. 7-21) is similar to the west façade but the effects are less pronounced. The damage in the hogging region is still evident, but over the tunnel the façade appears to have arched, with no significant damage.

Overall, it appears that the response of the building may be summarised as consisting of localised shear deformation at the corner over the tunnel, localised arching of the façades

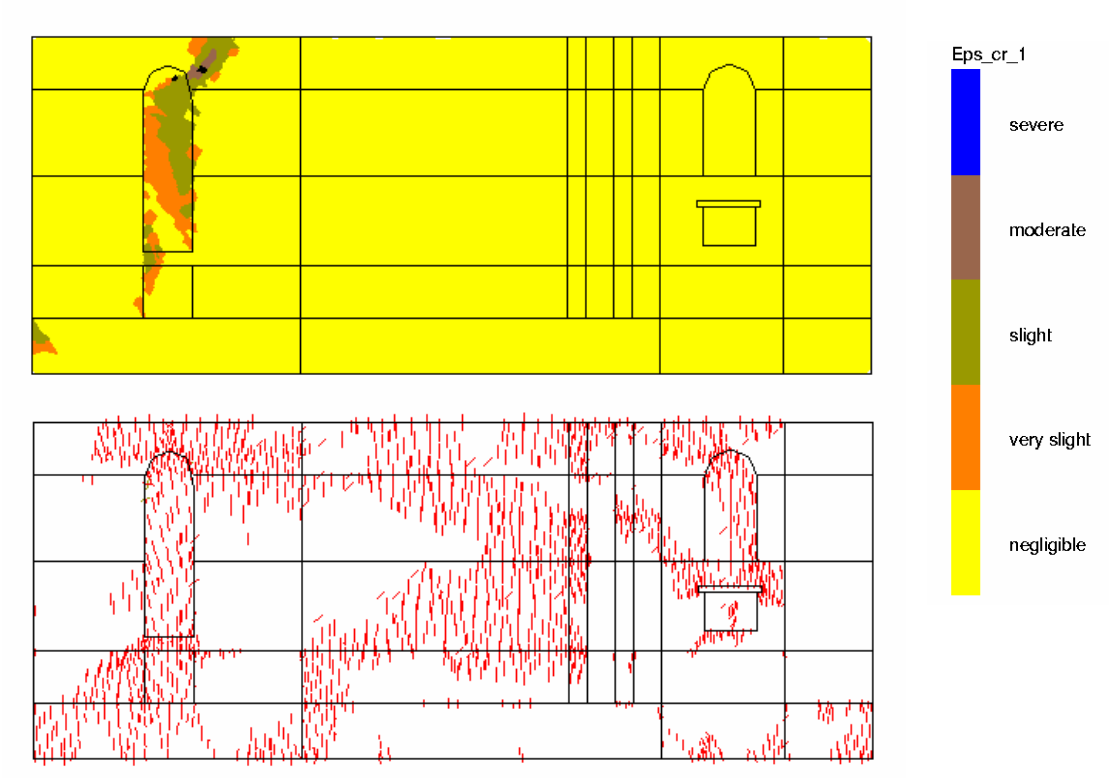

Figure 7-21: Damage category and crack pattern for east façade

adjacent to the tunnel, and damage in the hogging region far from the tunnel. These behaviours are illustrated in Figure 7-22.

The settlement profiles along the north, west and east façades from the field and model are compared in Figures 7-23 to 7-25. In each case, the settlements recorded immediately after construction on 13th July 1988 are given, together with the development of later settlements on 18th January 1989 and 9th August 1989, as shown in Figures 7-8 and 7-9.

It can be seen that along all three façades the settlements predicted by the model agree much better with the final settlements in the field (albeit with a slight over-estimate) than with the short-term settlements. The apparent volume loss in the model is approaching 4% as indicated by settlements along the east and west façades, although only 2% loss was applied to the tunnel lining. The large settlements of the building are of course balanced by smaller settlements than 'greenfield' elsewhere in the model, in the other half of the settlement trough north of the building and, interestingly, to the east and west of the

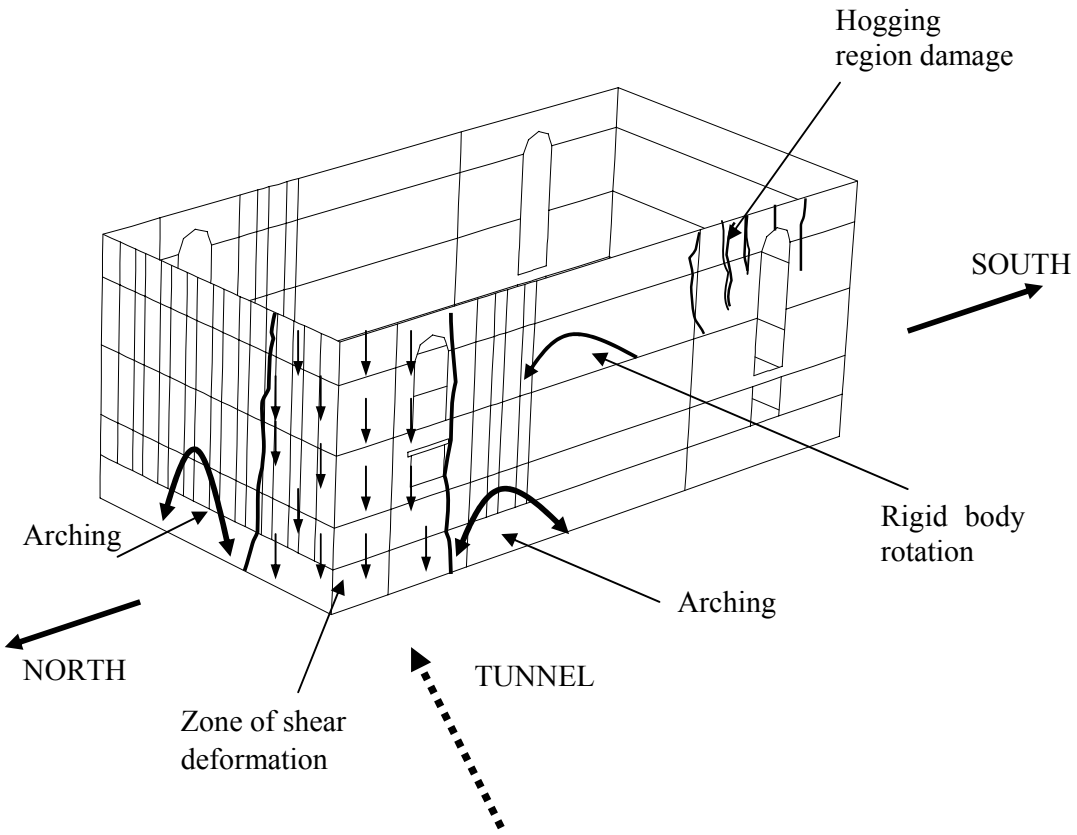

Figure 7-22: Model response to tunnelling beneath northwest corner of Mansion House

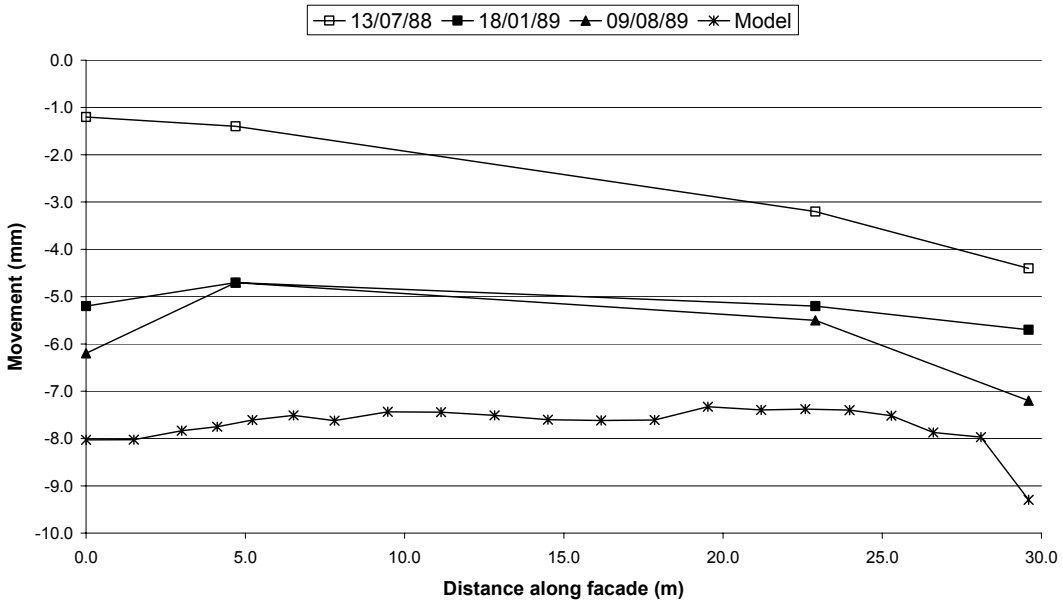

Figure 7-23: Comparison of settlements along north façade from field and model

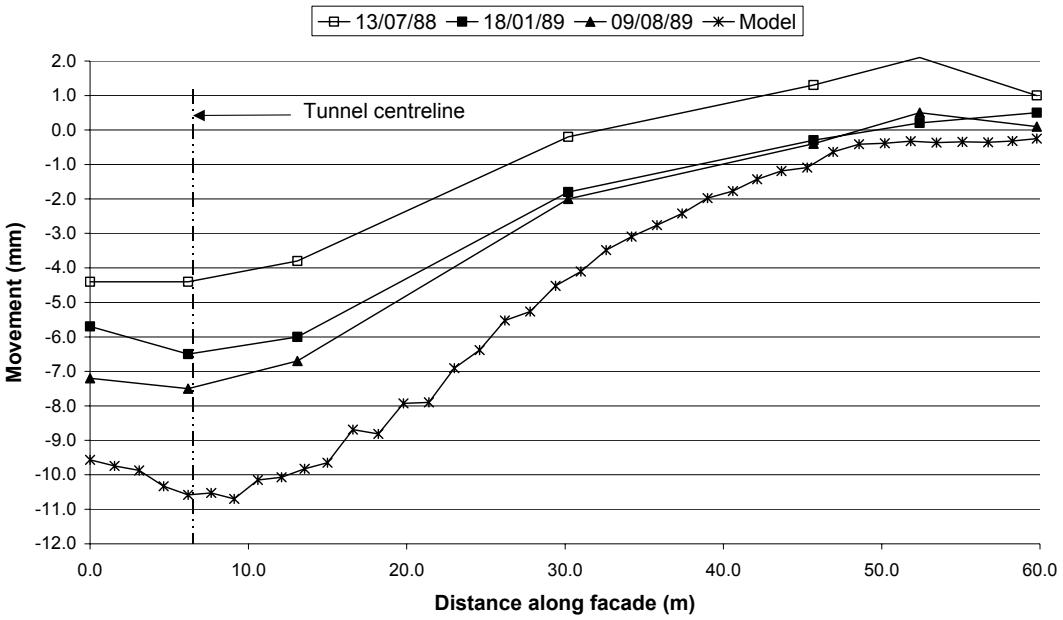

Figure 7-24: Comparison of settlements along west façade from field and model

building, as can be seen in Figure 7-18.

This effect, of building weight driving further settlements beneath it due to disturbance to the ground from tunnelling was also observed in the work of Liu (1997), discussed in Section 3.2, and there was also evidence of its occurrence in the Maddox Street model. At Mansion House, for the first time, there is field evidence of this effect. The 1988 passenger

link tunnel was excavated with great care beneath the Mansion House, and the settlements at the end of construction were consistent with a low volume loss of around 1.5% having been achieved, as hoped. With time, the settlements increased substantially. The fact that the behaviour in the field was time-dependent is interesting, and it is not obvious whether it was the time-dependent behaviour of the soil or the masonry that caused the phenomenon. This should be a subject for future research.

The detailed settlement response of the façades is worthy of consideration. Figure 7-23 shows how the model predicted approximately uniform settlement of the north façade, a pattern that was also observed on site. The localised shear deformation at the west end of the façade can be seen on the right. The site data also suggest such deformation occurring, but in a less localised way than in the model.

Figure 7-24 shows that, for the west façade, which is the one most affected by the tunnelling, the distribution of settlements in the model agrees well with that in the field, although there has been a general over-prediction by about 30%. This could be either due to the volume loss being too great, or the effect of building weight being exaggerated in the model. It is not possible to separate these effects and be sure of the cause, for the same reason as at Maddox Street (the lack of independent verification of volume loss). However, for the reasons discussed above, there is good evidence to suggest that a volume loss of 2% used in the model was reasonable. Therefore, as at Maddox Street, the effects of building weight have probably been over-estimated. At Maddox Street the reason was that a foundation was not modelled. At Mansion House, the foundation was given high strength but only the stiffness of soil, and therefore the prediction could perhaps be improved by increasing the foundation stiffness. In addition the critical internal walls to the ballroom were not included in the model. These would be expected to stiffen the response of the structure, as seen in the Ramsgate model, and reduce the resulting settlements of the east and west façades.

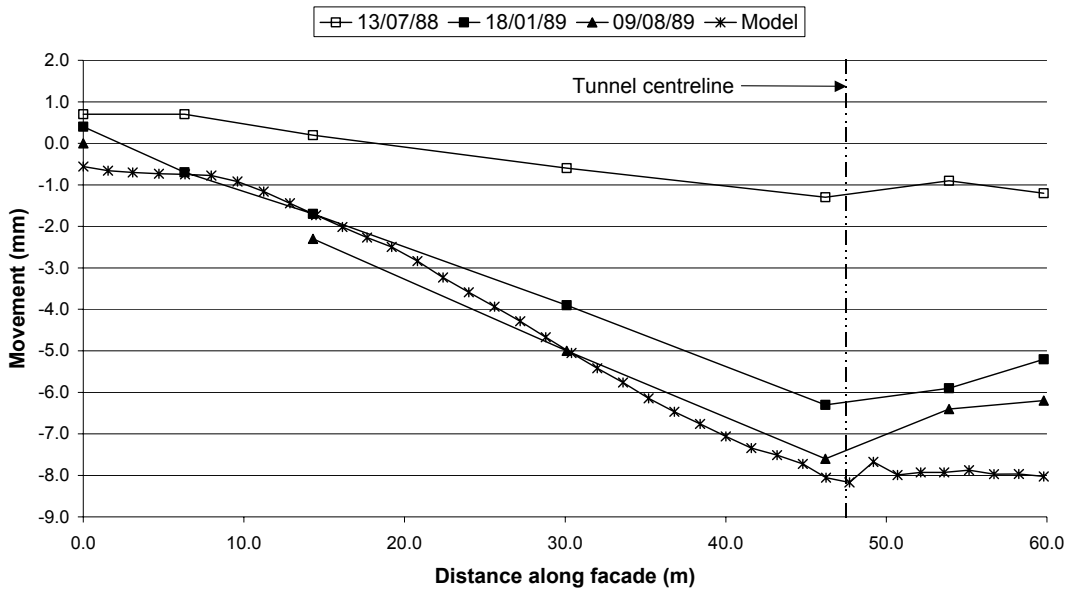

Figure 7-25: Comparison of settlements along east façade from field and model

The profile of settlements along the west façade shows a number of small steps between the tunnel centreline and about 30m along the façade. This was also observed by Liu (1997) in 2-D analyses and is a sign of the mechanism of arching occurring, as shown in Figure 3-3. This supports the evidence for arching from the crack patterns and damage distribution (Figs. 7-20 and 7-22). This ability of a real façade to arch is not taken into account in the current design methods that are based on modelling the building as an elastic beam following the 'greenfield' profile (Section 2.4.2.1). It could explain why the 'hogging' damage, when it occurs, is located further from the tunnel than the point of maximum hogging curvature in the 'greenfield' settlement trough. This effect has occurred in the Mansion House model and was also seen in the Ramsgate and Maddox Street models.

The prediction of settlements along the east façade agrees better with the field measurements (Fig. 7-25). The structure is able to span more effectively across the tunnel than on the west side because the tunnel is not as close to the end of the building. Therefore the soil is less highly stressed beneath the building and deformations are less in the model.

6.6 Discussion

The Mansion House case history was the final example for which a combined three-dimensional model was analysed in this project. Comprehensive raw data from the monitoring of the original construction was obtained. The tunnelling at Mansion House could be regarded as three distinct case histories, of which the first, the construction of a 3.05m diameter tunnel directly under the building, was chosen for analysis. The site, consisting of a bored tunnel in London clay together with a masonry building, was ideal as a case history for this project, and had indeed been influential on the direction of the research programme as a whole from a fairly early stage.

Detailed drawings of the building were available, together with descriptive data on soil strata. Data on soil properties was unfortunately not provided, and therefore assumptions were necessary that may have reduced the accuracy of the results such that final damage predictions for the building may be inaccurate by up to one category, as shown by the two-dimensional parametric studies presented in Chapter 3.

The model required to represent the Mansion House was considerably more complex than previous models. Practical difficulties were encountered with the mesh generation and the run times of the completed models were significantly longer than previous models, up to 3 days on the Oxford Supercomputer for a model with the tunnel wholly excavated in one increment. Therefore it was not possible, within the constraints of the available computing resources, to achieve a level of detail that was desirable to represent numerically all the physical phenomena that occurred on the site. In particular, the site data suggested that the advance of the longitudinal settlement trough from west to east beneath the building caused hogging damage high up in the internal walls of the ballroom at the north end of the building. It was not possible to examine this in this project as the run times for a model with sufficient incremental stages of advance would have been close to 20 days. The observed damage to the internal walls of the ballroom due to the tunnelling suggested that they contributed significantly to the overall structural behaviour, but it was also not possible to include them in the model in this project. There was also an indication from the results of the model that was analysed that it would have benefited from a more

refined mesh in the ground. If this had been possible, the response of the building might have been altered, in particular the location and to a lesser extent the severity of damage, as was experienced in the Maddox Street and Ramsgate models. Thus there would be benefit, when significantly increased computing resources become available, in re-assessing the combined three-dimensional model of the Mansion House.

The analysis that was achieved in this project nevertheless highlighted some important aspects of the performance of the modelling techniques when applied to Mansion House. The model showed that the response of a fairly tall masonry building to tunnelling, at a relatively shallow depth beneath, contains components of shear deformation, arching and bending behaviour (leading to hogging region damage). It is hard to see how all these phenomena can be understood without a realistic model of the building façades, using a plausible constitutive model for the masonry such as the elastic, no-tension model.

The relative magnitude of shear deformation, arching and bending effects is important because a masonry structure is able to accommodate arching well, but is vulnerable to tensile damage due to bending, and to a lesser extent to shear deformation. In the model analysed in this project, arching had an important influence on the building behaviour, limiting the damage to the façades. Support for this mechanism exists in the field data, in that no significant damage to the external façades was reported. The actual field response of the building was dominated by the damage to the ballroom walls believed to be due to the advance of the tunnel, as discussed above, and due to shear deformation, also mainly in the ballroom walls.

Shear deformation leading to high levels of damage at the northwest corner of the building was noted in the model. Such high, localised damage was not reported on site. This is evidence that the constitutive model for the masonry is somewhat too abrupt in its characteristics, causing premature and intense localised cracking, and that a softening of the stress-strain response would be beneficial, as would the introduction of a realistic tensile strength for masonry. This was also a conclusion from the Maddox Street and Ramsgate modelling.

Damage due to bending, particularly in the hogging region of the settlement trough, was seen in the model. The damage was limited and concentrated at the windows of the Egyptian Hall, somewhat remote from the tunnelling. A similar phenomenon of hogging damage at a remote location was seen in the Maddox Street model. The ability of the façade to arch may be pushing the region of critical hogging damage further away from the tunnel than would otherwise be the case, and probably also reducing its intensity.

Therefore, adequate representation of arching effects within masonry façades is emerging as important if a realistic model of such a structure is to be created. Current design approaches, such as those developed by Potts and Addenbrooke (1997), do not take advantage of this beneficial effect. In the two-dimensional work of Liu (1997), the effect of openings in restricting the development of arches was noted. It may be that the only way to obtain a realistic model of a masonry façade is to include every discrete opening. Increased computing resources are likely to enable this in the near future, and its necessity is recommended as a subject for further research.

The presence of a foundation to the building was represented in the modelling of the Mansion House. This foundation was required to prevent the premature failure of the building, as is indeed the case in the real building. The model of the foundation was very simplified: the soil strength in strips beneath the walls of the building was merely increased to a high value. No attempt was made to model the stiffness of the foundation realistically. Foundation stiffness is, however, very difficult to assess in practice. Attempts to assign real masonry or concrete properties are likely to give a response that is far too stiff, as was observed in the Maddox Street model.

The interaction of the weight of the building with the ground that had been disturbed by the excavation of the tunnel, and the resulting increase in settlements under the building, was a fascinating aspect of the Mansion House modelling. It is again difficult to envisage how this behaviour could be represented without a three-dimensional model. A reasonable approximation to the Gaussian prediction of ‘greenfield’ settlements had been obtained in a model without the building. When the building was added, the effect of its weight was to drive further settlements under the building when the tunnel was excavated, increasing the

volume of the settlement trough across the building footprint, and thus increasing the *apparent* volume loss. The key point is that there is evidence that this behaviour also occurred in the field, such that the agreement of the field settlements with the final settlements from the model was good. The increase in settlements under the building occurred over a period of about six months. The exact cause of the response seen in the field is an important subject for further research as it may have implications for tunnelling under other large, heavy and prestigious buildings in the future. If it can be shown that the response seen in the model would have occurred over a period of time in the field due to time-dependent response of the soil beneath the building, and of the masonry, then an important feature of the combined three-dimensional modelling procedure would have been verified.

7 CONCLUDING REMARKS

7.1 Summary and main findings of this project

7.1.1 Research context of the project

This project forms part of a programme of research on prediction of settlement damage to surface structures due to tunnelling in soft ground. The research programme was initiated in response to the increasing amount of tunnelling in urban areas as cities develop and congestion at street level grows. This part of the programme was concerned with the verification of numerical modelling procedures by application to real sites.

It is well understood that tunnelling in soft ground causes settlements, due to the volume loss that occurs when the sides of the bore move in as the tunnel advances. These settlements may in turn cause damage to surface structures, in particular to vulnerable types, such as old masonry structures. Although it is unlikely that the damage will cause structural failure, repairs could entail significant cost.

Case history data has been, and will continue to be, important in gaining an understanding of this problem. However, it is not possible to develop design methods for prediction of settlement damage effects from field data alone. Laboratory and centrifuge modelling have been tried, but numerical techniques, as used in this project, appear to show the most promise. Other researchers have also used numerical modelling, but have tended to simplify the problem too much, for example by idealising it as two-dimensional, reducing the building to a simple beam, or expressing the building response as a function of the ‘greenfield’ settlement behaviour.

7.1.2 Overview and key features of the project

In this programme of research, it was appreciated from the start that the problem of tunnelling beneath a building is essentially three-dimensional. Modelling procedures were developed in phase one of the programme that are tailored towards the particular problem of tunnelling in stiff, overconsolidated clay beneath a load-bearing masonry building. The tunnelling process is modelled in such a way that the volume loss at the tunnel can be accurately controlled. The building is modelled as planar façades, tied together and to the ground, with the vertical displacements at connections between façades constrained to be equal. The building may be placed at any orientation with respect to the tunnel, and the tunnel may be advanced in stages beneath the building. The key aspect of the work at Oxford is that the building is modelled together with the ground and tunnel, in a combined or "fully coupled" three-dimensional analysis.

Preliminary analysis of the problem in two dimensions carried out for this project and by previous researchers has shown the importance of a sufficiently accurate representation of both the weight and stiffness of a building, if realistic settlement behaviour is to be captured. The overall settlements are driven by the building weight, whereas the stiffness of the building, and in particular the stiffness distribution and the effect of openings, governs the response within the building and the development of such phenomena as arching and shear deformation. This project has shown that all of these factors interact, and has confirmed that the only way adequately to model the building weight and stiffness is in three dimensions.

The assessment of settlement effects on surface structures, during the design of a tunnelling scheme, is often made by means of a three-stage approach, as discussed in Chapter 1. The site data presented in this project, and the analyses carried out, have provided evidence that stage two, in which the 'greenfield' settlements are applied to a model of the building, is a conservative approach. This result was expected. The modelling procedures verified in this project have the potential to provide a tool for assessment at stage three, the detailed assessment stage, although some further enhancements are required, as discussed below.

The original objective of this project was to obtain case history data from three to four sites involving tunnelling beneath a masonry building, and carry out verification analyses. It is difficult to obtain good data of this type, because protective measures are often applied in the field, to avoid building damage. In the event, good quality data was obtained from three sites. Further data was obtained from other sites that did not exactly fit the project criteria, but which perhaps could be used in future research. In addition, it was found that the Mansion House site could be considered as containing three tunnelling events, only one of which was analysed for this project, leaving scope for further research.

Data from two of the three sites reported in this thesis had not been published prior to this project. The sites chosen all met the project criteria and had the advantage that between them they captured a wide range of configurations of the tunnelling excavation and building. The excavations consisted of a shaft, a shallow tunnel and a relatively deep tunnel, positioned off the corner of the building, under the middle of the building and under one end of the building respectively. Two of the buildings were large, prestigious buildings, which both responded in a stiff manner to the tunnelling settlements. The third was a long building that was relatively flexible transverse to the tunnel. Thus the capability of the three-dimensional modelling in representing a wide range of situations has been demonstrated.

7.1.3 Maddox Street shaft site

The case history of the construction of a shaft in Maddox Street, adjacent to a church, was the first to be modelled for this project. The geometry of the building could be simplified, with justification, to a rectangular box of four façades. The shaft was modelled as already excavated and a volume loss applied. A plausible distribution of ‘greenfield’ settlements was obtained. Because the entire settlement field around the shaft was not recorded, it was not possible to obtain a firm figure for the volume loss, making it difficult to separate the effects upon overall settlements of volume loss and building weight. The best agreement between model and field data was when the volume loss was set to 1%. In this case, the response of the building in the model was almost a rigid-body tilting towards

the excavation, with a small amount of non-linear response. This was similar to the behaviour implied by the field data. The effect of the building weight was to drive the settlements to significantly larger values than in the 'greenfield'. The model predicted a maximum damage category of "Slight", probably a small over-prediction of the actual damage.

A technique of modelling series of openings in the masonry façades by vertical regions of reduced stiffness was first used in this case, and proved successful. The approach used was to reduce the stiffness of the intact façade in proportion to the reduction in cross-section measured on a vertical section through the openings. The technique was also used in models of other sites. From the experience gained over the whole project, it is recommended that the technique is used for openings that do not fall in zones of the façade where significant arching might occur, or for single larger openings that may act as stress concentrators, particularly in the hogging region of the settlement response. Examples of the latter situation were the large opening on the east façade of the Maddox Street church, and the windows in the Egyptian Hall in the Mansion House.

The damage in the north façade of the Maddox Street church model was concentrated in shear deformation at the end remote from the actual shaft. Similar damage at the ends of façades was observed in the models of the other sites. The most likely reason for this damage is the restraint provided, in the vertical direction, by the façade joining perpendicularly. This aspect of the real behaviour of masonry buildings is not well understood, and is notoriously difficult to model in two dimensions. The conclusion from this project is that the effect of the restraint has probably been over-estimated. Smoothing the stress-strain response of the masonry constitutive model, and introducing a finite tensile strength for the masonry might improve predictions.

The location of damage in the Maddox Street model was changed when the mesh density in the ground immediately beneath the building was increased. The importance of the mesh density in the soil was also confirmed in the models of the other sites. It is likely that further improvements in model results would have been made if the mesh density had been further increased, especially in the Ramsgate and Mansion House models. The

maximum model size was limited in this project by the available computing resources to be around 30,000 degrees of freedom. It is believed that at least 60,000, and perhaps up to 100,000, degrees of freedom are required accurately to model a building, combined with the ground and tunnel, by these techniques. This implies an increase in resources by a factor of at least eight above that available to this project, because the processing time is mainly determined by the number of arithmetic operations conducted on the frontal matrix, which increases in proportion to the cube of the size of the matrix (Section 4.5). It may be noted that the computing resources available for this sort of calculation have continued to grow, and this trend may be expected to continue.

A programme of sensitivity analyses was carried out on the three-dimensional Maddox Street model, varying building weight and stiffness and soil properties. The analyses broadly confirmed what had already been established in two-dimensional analysis, *i.e*. that the building weight and distribution of stiffness within façades (for example due to the presence of large openings) are more important influences on the performance of the building than the absolute value of building stiffness. The importance of carrying out a careful site investigation was highlighted by results that showed that the damage category predicted for the building varied by up to one category as the soil properties were varied over the range of accuracy normally available. An accuracy of ±30% is required in the values of the initial shear modulus G_0 and the undrained strength s_u in order to gain benefit from the numerical modelling.

7.1.4 Ramsgate Harbour tunnel site

Good quality data was obtained, as part of this project, from the second site to be analysed, the Ramsgate Harbour Approach Tunnel. This tunnel was constructed by a novel method that generated a narrower settlement trough than would be expected for a traditional bored tunnel. It proved possible to reproduce the ‘greenfield’ behaviour in the model by applying fixity to the tunnel lining and only applying the volume loss to the top of the tunnel, demonstrating the capability of the modelling procedures for the tunnel process.

The row of cottages beneath which the tunnel passed exhibited a number of cracks, up to about 1.5mm in size, prior to construction. A number of these cracks were monitored, and it was particularly interesting to observe how movement occurred across some of the cracks that had been stable, in direct response to the tunnelling. The effect of construction was assessed as causing damage in the range “Negligible” to “Very slight”.

A series of three-dimensional combined models of the site was analysed. In every case, the structure responded flexibly, with no significant modification to the ‘greenfield’ settlement trough. This was in agreement with the site observations. It was found to be desirable to include the party walls between the cottages in the model, which showed the advantage of adopting a three-dimensional approach. The party walls had the effect of stiffening the global transverse response of the terrace as a whole, confining the damage to a region more consistent with that observed in the field. The model again over-predicted the maximum damage category as “Slight”, as at Maddox Street.

The model predicted damage in both the hogging and sagging regions of the settlement trough. In most cases, there was no direct relationship between the behaviour of specific cracks in the field and the damage distribution across the façades in the model. This was not, however, only an issue for the model. The behaviour of the cracks also did not support the assumptions underpinning the current design methods, namely that the building behaves as a beam with the neutral axis at ground level in the hogging region and at mid-height in the sagging region. This illustrates the difficulties that there are in formulating theories for the behaviour of masonry buildings subjected to settlements. More research is needed in this area at a fundamental level.

The results of the Ramsgate model, in particular the damage to the party walls, would have been altered if an analysis had been carried out with an incremental advance of the tunnel heading. Unfortunately the run times with the computing resources available were too long to enable this to be included in this project.

7.1.5 Mansion House site

The final case history analysed, the Mansion House site, required the most complex finite element model. It was not possible to model the building in sufficient detail to represent the main internal walls, or incremental advance of the tunnel heading. These features would have been necessary to reproduce the main damage observed on site, which was to the internal walls of the ballroom. Nevertheless, lessons were learned from the modelling of this complex masonry building.

The response of the model of this tall masonry building to a shallow, skewed tunnel beneath one end contained components of shear deformation, arching and bending (leading to hogging region damage). The relative magnitude of these components is important, because a masonry structure is able to accommodate arching well, but is vulnerable to tensile damage due to bending, and a lesser extent to shear deformation. It is hard to envisage how they could be adequately represented without a three-dimensional model of the building. It appeared in the model that localised arching close to the tunnel protected a large area of the critical west façade from damage. Support for such arching mechanisms exists in the field data, in that no significant damage to the external façades was reported. Current design approaches, such as those developed by Potts and Addenbrooke (1997), do not take advantage of the beneficial effect of arching.

In the two-dimensional work of Liu (1997), the effect of openings in restricting the development of arches was noted. It may be that the only way to obtain a realistic model of a masonry façade is to include every discrete opening. Increased computing resources are likely to enable this in the near future, and its necessity is recommended as a subject for further research.

A foundation was provided in the modelling of the Mansion House, to prevent collapse of the building under its own self-weight. This was achieved by increasing the soil strength to a high value locally beneath the building. The stiffness of the foundation, which is very difficult to assess in practice, was not modelled, although it is likely that if real masonry or concrete stiffness was assigned, the effect would have been to stiffen the overall response of the building significantly. This was demonstrated in a trial analysis with the Maddox

Street model. The field settlement data do not suggest the existence of a stiff foundation, but instead agree quite well with the settlement distribution predicted by the model as implemented. It is unlikely that a typical shallow foundation to a building is able to act as a stiff, continuous structure unless it is specifically designed, and reinforced, to do so.

The effect of the weight of the building in increasing the settlements beneath it was a particular feature of the Mansion House. Such a phenomenon was also noted in the Maddox Street model, and it is again difficult to envisage how this behaviour could be represented without a three-dimensional model. A reasonable approximation to the Gaussian prediction of 'greenfield' settlements had been obtained in a model without the building. With the building included in the model, significantly higher settlements occurred when the tunnel was excavated. The final settlements in the model agreed quite well with those observed in the field about six months after construction. Thus there is evidence that the effect of building weight in driving settlements in response to tunnelling is a real one, although further investigation into why the field response did not occur immediately is needed. This finding has implications for tunnelling under large and heavy buildings.

7.1.6 Improvements to software and hardware and resulting performance

Undertaking this research stimulated a number of enhancements to the analysis software. The necessity for this was anticipated at the outset of the project. Many of the enhancements were made to reflect improvements in the performance of the hardware, in particular the introduction of the Oxford Supercomputer, OSCAR. There were two main areas of improvement – streamlining of the whole analysis process (from pre-processing through the analysis stage to post-processing) and increasing computational power at the analysis stage.

Enhancements to the whole analysis process included improving the efficiency of the input information by implementing sets of nodes and elements, moving to allocatable arrays and more flexible data structures within OXFEM to facilitate easier expandability of the program, reducing the number of utility programs, producing documentation and

introducing test problems to improve the reliability of the OXFEM program as it is continually developed. The importance was realised of maintaining a methodical approach to the development of individual models and of the modelling process as a whole. The use of a commercial mesh generator was of great value, but independent checking of the output from such a program is strongly recommended, as errors do occur.

Computational power was improved by the move to parallel processing, and by associated changes to the array handling within the frontal solver to reflect the processes occurring at the system architecture level. Making these enhancements gave an appreciation of the important practical implications of attempting to carry out large-scale non-linear finite element analyses. As discussed above, even larger models will be required in future, to improve the predictions of settlements and building damage. Assuming continued use of the frontal solver, an increase in computing resources by a factor of at least eight is required. There may therefore be advantage in moving to alternative solution techniques that are more efficient for solving sparse sets of equations.

As a result of the enhancements to the software and hardware, and the experience gained in modelling a number of real sites for this project, an overall assessment could be made of the performance of the process as a whole for the purposes of carrying out a stage three assessment of an actual site. It was found that, once information about a site had been obtained, and fundamental decisions about the idealisation of the structure, ground and tunnel made, the pre-processing stage of generating the finite element mesh, and going on to produce the OXFEM input data file, took one to two weeks to carry out.

Run times were still significant for the larger models such as Mansion House, such that a typical model with one tunnelling increment would take two to three days to run. Assuming that around ten analyses might be required, to allow for sensitivity analyses varying the main parameters in the model, the analysis phase would take about a month. Much of the post-processing would be done concurrently with the analyses, but at least two further weeks would be required for detailed examination of the results and for reporting. Therefore a stage three assessment using these techniques would probably take two to three months to complete. The computing resources are the main constraint on the

timescale; so only one person would be required for this time. Assuming a qualified engineer was involved, and including an allowance for computing resources, a total cost of around £25,000 at 2002 prices is estimated.

7.2 Conclusions

The main conclusions from this project are as follows:

1. In any numerical modelling procedure for prediction of tunnelling effects on structures, it is always important to adequately reproduce the 'greenfield' settlement trough without the building present. Some previous numerical work has had difficulty in this area, but this study achieved satisfactory results that agreed with the Gaussian prediction provided the tunnel was relatively deep, *i.e*. with a cover to diameter (*C*/*D*) ratio greater than 3. Evidence was obtained that indicated that for shallow tunnels (C/D < 3), the Gaussian model predicts a trough width that is too narrow, and hence over-predicts curvatures and therefore building damage.

2. In the case of large, heavy buildings, the effect of building weight in driving further settlements was observed in the 3-D modelling as in the earlier 2-D work of Liu (1997). There is evidence in the data from Mansion House that this may also be a real effect in the field.

3. The importance of arching in the behaviour of larger masonry buildings is confirmed. It can only occur when the settlement trough is spanned, as noted by Augarde (1997). The modelling of Mansion House indicates that this is likely to be the mechanism by which the east and west façades of the building escaped significant damage in the field. Because the arching occurred around the corner of the building, it could only be demonstrated in a 3-D analysis with a realistic representation of the building façades.

4. The models generally over-predicted the damage by one category compared to that observed in the field, for example predicting “Slight” instead of “Very slight” damage. The distribution of damage also tended to be more localised in area than observed in the field. It is thought that softening the tensile stress-strain response of the elastic, no-tension masonry constitutive model, and introducing a small but realistic tensile strength for the masonry may mitigate these two effects.

5. It was demonstrated, in the modelling of more than one of the sites, that the presence of internal walls and large openings could have important effects on the response of the building as a whole. A three-dimensional analysis including incremental advance of the tunnel would be necessary to reproduce some types of damage observed in the field, particularly in internal walls in buildings.

6. The representation of columns of smaller windows in façades by vertical regions of reduced stiffness in the model was found to be a successful approach, provided the openings are not in a region of significant shear deformation or where arching is important to building behaviour. In these cases, the representation of discrete openings is recommended.

7. Most of the models analysed on this project did not represent the building foundations by extra stiffness in the model. Only increased soil strength was applied, in the case of the Mansion House model. From the experience gained in this project in the comparison of the model results with field data, it is believed that this approach is satisfactory. It is recommended that foundation stiffness is only included if the foundations are of a reinforced concrete raft, or similar, and that any such modelling should be subject to further, careful verification.

8. For reliable results from these modelling procedures, the mesh density in the soil immediately beneath the building should be comparable with that in the building itself. To

achieve this in practice, the typical overall model size should be increased to around 60,000 to 100,000 degrees of freedom. This will require an approximately eight times increase in computing resources beyond that available in 1999, assuming the continued use of the frontal solver technique.

9. Overall, the modelling procedures examined in this project have been shown to have excellent potential as a tool for stage three assessments of tunnelling effects on surface masonry structures. There are no reasons in principle why the techniques could not be extended to tunnelling in other ground conditions, for example granular materials, other structural forms such as steel- and concrete-framed buildings, buildings with piled foundations and bridges.

Comparisons may be drawn between the above conclusions and the lessons reported from concurrent research that involved monitoring of a large number of buildings on the Jubilee Line Extension (Burland *et al*., 2001). One conclusion of the JLE researchers is that "building stiffness can substantially reduce the greenfield site relative deflections". This was also observed in the Maddox Street and Mansion House models. The JLE project stimulated the research of Potts and Addenbrooke (1997) on the numerical modelling of the ground coupled to a simplified building in two dimensions (Section 2.4.3.2). Burland *et al*. (2001) recognise that this type of analysis needs to be extended to three dimensions.

Little damage occurred to buildings due to the excavation of the JLE. Burland *et al*. (2001) imply that less damage occurred than expected, and that much of the expensive compensation grouting carried out may have been unnecessary. Where damage did occur, it tended to be concentrated at connections between structures. There may be a relationship between this general observation and the tendency, in the numerical models in this project, for damage to occur at junctions between façades and at openings. Burland *et al*. (2001) also highlighted the need to appreciate the history of the site and the building construction. In comparison, this project has shown the particular importance of building weight, due to

its effect on the initial stress distribution in the ground, the volume loss and the ground response beneath the building, as seen in the Maddox Street and Mansion House models.

The total cost of the JLE project was around £800k including contributions in kind from industrial collaborators (Burland *et al*., 1996). This illustrates the relatively high monetary cost of obtaining sufficient field observations to draw meaningful conclusions, as compared with this project in which numerical modelling was utilised together with field monitoring.

7.3 Recommendations for future research

1. To improve the correlation between model results and field observations of damage, the masonry constitutive model should be enhanced with a softened stress-strain response and a realistic tensile strength for masonry.

2. Larger model sizes are required to improve accuracy of predictions. To enable this, examination of the use of techniques other than the frontal solver method for solution of the stiffness equations of the model is recommended.

3. With significantly increased computing resources, there would be benefit in re-assessing the combined three-dimensional model of the Mansion House. Only one of the three main tunnelling events at this site was modelled in this project, and the other two show potential for further verification of the modelling procedures.

4. Increased computing resources would also enable more analyses with incremental advance of the tunnel heading in the model. This feature is necessary to adequately represent some of the building behaviour observed in the field.

5. In the modelling approach, vertical displacements at the end of façade are constrained to be equal to those of the connecting façade. This restraint appears to have been significant

in determining the final distribution of damage. Whether this effect occurs in real buildings would be an interesting subject for future research.

6. Comparison of field data and modelling results on this project has shown that it is not possible to predict the development of a particular crack in a building façade by means of a numerical model. The field data at Ramsgate showed that individual cracks do not behave in a way that is consistent with the boundary conditions applied to the building as a whole. Further research is recommended into the reasons for this phenomenon.

8 REFERENCES

Anagnostou, G., Kostikas, Ch., Iakovides, G. and Vasilakopoulou, G. (1997). Athens Metro – design and construction of shallow tunnels to control settlements of surface structures. *In: Proc. Int. Symposium Tunnelling '97*, London, 2-4 September. London: Institution of Mining and Metallurgy, 709-720.

Attewell, P.B. and Selby, A.R. (1989). Tunnelling in compressible soils: Large ground movements and structural implications. *Tunnelling and Underground Space Technology*, 4 (4).

Attewell, P.B. and Woodman, J.P. (1982). Predicting the dynamics of ground settlement and its derivatives caused by tunnelling in soil. *Ground Engineering*, 15 (8), 13-22.

Augarde, C.E. (1997). *Numerical modelling of tunnelling processes for the assessment of damage to buildings*. Thesis (DPhil). University of Oxford.

Augarde, C.E., Burd, H.J., and Houlsby, G.T. (1995). A three-dimensional finite element model of tunnelling. In: *Proc. 5th Int. Sympos. on Numerical Models in Geomechanics (NUMOG V)*, Davos, Switzerland, 6-8 September. Rotterdam: Balkema, 457-462.

Augarde, C.E., Burd, H.J., and Houlsby, G.T. (1998). Some experiences of modelling tunnelling in soft ground using three-dimensional finite elements. *In: Proc. 4th European Conf. on Numerical Methods in Geotechnical Engineering (NUMGE98)*, Udine, 14-16 October. Wien: Springer Verlag, 603-612.

Barratt, D.A. and Tyler, R.G. (1976). *Measurements of ground movement and lining behaviour on the London Underground at Regent's Park*. TRRL Laboratory Report 684.

Bloodworth, A.G. and Macklin, S.R. (2000) Ground and structure response to a hand driven decline in London clay. *In: Proc. Int. Sympos. on Geotechnical Aspects of Underground Construction in Soft Ground*, Tokyo, 21-23 July 1999. Rotterdam: Balkema, 75-80.

Bloodworth, A.G., Augarde, C.E. and Houlsby, G.T. (1999). Transferring a non-linear finite element code to the Oxford Supercomputer, Oscar. *In: Proc. 7th Int. Conf. on Civil and Structural Engineering Computing*, Oxford, 13-15 September. Edinburgh: Civil-Comp Press, 85-94.

Boscardin, M.D., and Cording, E.J. (1989). Building response to excavation-induced settlement. *Journal of Geotechnical Engineering*, *ASCE*, 115 (1), 1-21.

Bowers, K.H., Hiller, D.M. and New, B.M. (1996). Ground movement over three years at the Heathrow Express trial tunnel. *In: Proc. Int. Sympos. on Geotechnical Aspects of Underground Construction in Soft Ground*, London, April. Rotterdam: Balkema, 647-652.

Breth, H. and Chambosse, G. (1975). Settlement behaviour of buildings above subway tunnels in Frankfurt clay. *In: Proc. Conf. Settlement of Structures*, Cambridge, April 1974. London: Pentech Press, 329-336.

Broms, B.B. and Bennermark, H. (1967). Stability of clay in vertical openings. *Journal of Soil Mechanics and Foundations*, *ASCE*, 193, 71-94.

Burd, H.J. (1986). *A large displacement finite element analysis of a reinforced unpaved road*. Thesis (DPhil). University of Oxford.

Burd, H.J., Houlsby, G.T., Augarde, C.E. and Liu, G. (2000). Modelling the effects on masonry buildings of tunnelling-induced settlement. *Proceedings ICE Geotechnical Engineering*, 143 (1), 17-29.

Burland, J.B., Broms, B.B. and de Mello, V.F.B. (1977). Behaviour of foundations and structures. *In: Proc. 9th ICSMFE State-of-the-Art Report, Vol. 3*, Tokyo, July. Japan: Japanese Society of Soil Mechanics and Foundation Engineering, 495-546.

Burland, J.B., Mair, R.J., Linney, L., Jardine, F.M. and Standing, J.R. (1996). A collaborative research programme on subsidence damage to buildings: Prediction, protection and repair. *In: Proc. Int. Sympos. on Geotechnical Aspects of Underground Construction in Soft Ground*, London, April. Rotterdam: Balkema, 773-778.

Burland, J.B., Simpson, B. and St. John, H.D. (1979). Movements around excavations in London clay. *In: Proc. 7th ECSMFE, Vol. 1*, Brighton. Rotterdam: Balkema.

Burland, J.B., Standing, J.R. and Jardine, F.M. (eds.) (2001). *Building response to tunnelling. Case studies from the Jubilee Line Extension, London. Volume 1 Projects and Methods*. London: Thomas Telford.

Burland, J.B. and Wroth, C.P. (1975). Settlement of buildings and associated damage. *In: Proc. Conference on Settlement of Structures*, Cambridge, April 1974. London: Pentech Press, 611-654.

Calvello. M. and Taylor, R.N. (2000). Centrifuge modelling of a spile-reinforced tunnel heading. *In: Proc. Int. Sympos. on Geotechnical Aspects of Underground Construction in Soft Ground*, Tokyo, 21-23 July 1999. Rotterdam: Balkema, 345-350.

Chow, L. (1994). *Prediction of surface settlement due to tunnelling in soft ground*. Thesis (MSc). University of Oxford.

CIRIA (1994). *Foundations in chalk*. Project Report No. 11.

Clark, G.T. (1993). Modelling and analysis of shafts and tunnels for the SSC. *In: Proc. 5th Int. Conf. On Computing in Civil and Building Engineering*, Anaheim, USA, June. New York: ASCE, 622-629.

Collins, I.F. and Houlsby, G.T. (1997). Application of thermomechanical principles to the modelling of geotechnical materials. *Proc. Royal Society, Series A*, 453, 1975-2001.

Cooper, M.L. and Chapman, D.N. (2000). Settlement, rotation and distortion of Piccadily Line tunnels at Heathrow. *In: Proc. Int. Sympos. on Geotechnical Aspects of Underground Construction in Soft Ground*, Tokyo, 21-23 July 1999. Rotterdam: Balkema, 213-218.

Crow, M.R. and Newman, T.G. (1999). Tunnelling using the pre-vaulting system in chalk for the Ramsgate Harbour Approach Tunnel, United Kingdom. *In: Proc. Int. Symposium Tunnel Construction and Piling '99*, London, September. London: Brintex Ltd.

Davis, E.H., Gunn, M.J., Mair, R.J. and Seneviratne, H.N. (1980). The stability of shallow tunnels and underground openings in cohesive material. *Géotechnique*, 30 (4), 397-416.

De Moor, E.K. and Taylor, R.N. (1989). Model studies of the behaviour of deep tunnels in clay. *In: Proc. 12th ICSMFE, Vol. 2*, Rio de Janeiro, 13-18 August. Rotterdam: Balkema, 909-912.

De Schrijver, P. and Hemerijckx, E. (1991). Results of geotechnical instrumentation monitoring the pre-metro tunnelling works under the River Scheldt at Antwerp, Belgium. *In: Proc. 10th ECSMFE, Vol. 2*. Rotterdam: Balkema. 797-800.

Dias, D., Maghazi, M. and Kastner, R. (2000). Three-dimensional simulation of slurry shield tunnelling. *In: Proc. Int. Sympos. on Geotechnical Aspects of Underground Construction in Soft Ground*, Tokyo, 21-23 July 1999. Rotterdam: Balkema, 351-356.

Eisenstein, Z., Heinz, H. and Negro, A. (1994). On three-dimensional ground response to tunnelling. *In: Tunnelling in Soil and Rock, Proc. GEOTECH '84*, Atlanta, May. New York: ASCE, 107-127.

El Nahhas, F., El Kadi, F. and Ahmed, A. (1992). Interaction of tunnel linings and soft ground. *Tunnelling and Underground Space Technology*, 7 (1).

Finno, R.J. and Clough, G.W. (1985). Evaluation of soil response to EPB shield tunnelling. *Journal of Geotechical Engineering, ASCE*, 111 (2), 155-173.

Forbes, J., Bassett, R.H. and Latham, M.S. (1994). Monitoring and interpretation of movement of the Mansion House due to tunnelling. *Proceedings ICE Geotechnical Engineering*, 107 (2), 89-98.

Forth, R.A. and Thorley, C.B.B. (1995). Ground and building settlement due to tunnelling in Hong Kong. *In: Proc. 5th Int. Symposium on Land Subsidence*, The Hague, October. Wallingford: IAHS, 149-160.

Frischmann, W.W., Hellings, J.E. and Snowden, C. (1994). Protection of the Mansion House against damage caused by ground movements due to the Docklands Light Railway Extension. *Proceedings ICE Geotechnical Engineering*, 107 (2), 65-76.

Garrod, B. and Finch, A. (1997). Toronto Transit Commission, Sheppard Subway, design of twin tunnels. *In: Proc. Int. Symposium Tunnelling '97*, London, 2-4 September. London: Institution of Mining and Metallurgy, 451-461.

Grant, R.J. and Taylor, R.N. (1996). Centrifuge modelling of ground movements due to tunnelling in layered ground. *In: Proc. Int. Sympos. on Geotechnical Aspects of Underground Construction in Soft Ground*, London, April. Rotterdam: Balkema, 507-512.

Grant, R.J. and Taylor, R.N. (2000). Evaluating plasticity solutions for the response of clay around tunnels. *In: Proc. Int. Sympos. on Geotechnical Aspects of Underground Construction in Soft Ground*, Tokyo, 21-23 July 1999. Rotterdam: Balkema, 373-378.

Gunn, M. (1993). The prediction of surface settlement profiles due to tunnelling. *In: Predictive Soil Mechanics: Proc. Wroth Memorial Symposium*, Oxford, 27-29 July 1992. London: Thomas Telford, 304-316.

Halcrow (1989). *Settlement of the Mansion House updated to 9 August 1989*. Report to the City of London Corporation.

Hanafy, E.A. and Emery, J.J. (1981) Advancing face simulation of tunnel excavations and lining placement. *In: Proc. Int. Conf. On Ground Movements and Structures*, Cardiff, April 1980. London: Pentech Press, 377-394.

Houlsby, G.T. (1999) A model for the variable stiffness of undrained clay. *In: Proc. Int. Symposium on Pre-failure Deformation Characteristics of Geomaterials*, Torino, September. Rotterdam: Balkema.

Houlsby, G.T., Burd, H.J. and Augarde, C.E. (1999). Analysis of tunnel-induced settlement damage to surface structures. *In: Proc. 12th ECSMGE*, Amsterdam, 7-10 June. Rotterdam: Balkema, 147-152.

Houlsby, G.T., Liu, G. and Augarde, C.E. (2000). A tying scheme for imposing displacement constraints in finite element analysis. *Communications in Numerical Methods in Engineering*, 16 (10), 721-732.

Jardine, R.J., Potts, D.M., Fourie, A.B. and Burland, J.B. (1986). Studies of the influence of non-linear stress-strain characteristics in soil-structure interaction. *Géotechnique*, 36 (3), 377-396.

Jeffery, S. (1993). *The Mansion House*. London: Phillimore & Co. Ltd.

Kim, S.H., Burd, H.J. and Milligan, G.W.E. (1996). Interaction between closely spaced tunnels in clay. *In: Proc. Int. Sympos. on Geotechnical Aspects of Underground Construction in Soft Ground*, London, April. Rotterdam: Balkema, 543-548.

Kimura, T. and Mair, R.J. (1981). Centrifugal testing of model tunnels in soft clay. *In: Proc. 10th ICSMFE, Vol. 1,* Stockholm, 15-19 June. Rotterdam: Balkema, 319-322.

Kuwano, J., Takahashi, A., Honda, T. and Miki, K. (2000). Centrifuge investigation on deformations around tunnels in nailed clay. *In: Proc. Int. Sympos. on Geotechnical Aspects of Underground Construction in Soft Ground*, Tokyo, 21-23 July 1999. Rotterdam: Balkema, 245-250.

Lake, L.M., Rankin, W.J. and Hawley, J. (1996). *Prediction and effects of ground movements caused by tunnelling in soft ground beneath urban areas*. CIRIA Project Report No. 30.

Lee, K.M. and Rowe, R.K. (1991). An analysis of three-dimensional ground movements: The Thunder Bay Tunnel. *Canadian Geotechnical Journal*, 28 (1), 25-41.

Lee, K.M. and Rowe, R.K. (1990a). Finite element modelling of the three-dimensional ground deformations due to tunnelling in soft cohesive soils: Part 1 – methods of analysis. *Computers and Geotechnics*, 10 (2), 87-109.

Lee, K.M. and Rowe, R.K. (1990b). Finite element modelling of the three-dimensional ground deformations due to tunnelling in soft cohesive soils: Part 2 – results. *Computers and Geotechnics*, 10 (2), 110-138.

Linney, L.F. (1999). Geotechnical aspects of the Jubilee Line Extension, London. *In: Proc. 12th ECSMGE, Vol. 3*, Amsterdam, June. Rotterdam: Balkema, 1653-1664.

Liu, G. (1997). *Numerical modelling of damage to masonry buildings due to tunnelling*. Thesis (DPhil). University of Oxford.

Lu, Y.C., Samuel, H.R. and Chudleigh, I. (1999). Response of a masonry arch tunnel to underground tunnelling. *In: Proc. 5th Int. Symposium on Field Measurements in Geomechanics*, Singapore, December. Rotterdam: Balkema.

Macklin, S.R. (1999). The prediction of volume loss due to tunnelling in overconsolidated clay based on heading geometry and stability number. *Ground Engineering*, 32 (4), 30-33.

Macklin, S.R. and Field, G.R. (1999). The response of London clay to full-face TBM tunnelling at West Ham, London. *In: Proc. Int. Conf. On Urban Ground Engineering*, Hong Kong, 11-12 November 1998. London: Thomas Telford.

Mair, R.J. (1979). *Centrifugal modelling of tunnel construction in soft clay*. Thesis (PhD). University of Cambridge.

Mair, R.J. (1993). Developments in geotechnical engineering research: Application to tunnels and deep excavations. *Proceedings ICE Civil Engineering*, 93 (1), 27-41.

Mair, R.J., Gunn, M.J. and O'Reilly, M.P. (1981). Ground movements around shallow tunnels in soft clay. *Proc. 10th ICSMFE, Vol. 1*, Stockholm, 15-19 June. Rotterdam: Balkema, 323-328.

Mair, R.J. and Taylor, R.N. (1993). Prediction of clay behaviour around tunnels using plasticity solutions. *In: Predictive Soil Mechanics: Proc. Wroth Memorial Symposium*, Oxford, 27-29 July 1992. London: Thomas Telford, 449-463.

Mair, R.J., Taylor, R.N. and Bracegirdle, A. (1993). Subsurface settlement profiles above tunnels in clays. *Géotechnique*, 43 (2), 315-320.

Mair, R.J., Taylor, R.N. and Burland, J.B. (1996). Prediction of ground movements and assessment of risk of building damage due to bored tunnelling. *In: Proc. Int. Sympos. on Geotechnical Aspects of Underground Construction in Soft Ground*, London, April. Rotterdam: Balkema, 713-718.

Mathworks, Inc. (1997). *The Student Edition of MATLAB: Version 5 User's Guide*. New Jersey: Prentice Hall.

McCaul, C., O'Reilly, M.P. and Crabb, G.I. (1986). Settlements over a small diameter tunnel driven by hand and machine in London clay. *Municipal Engineer (ICE)*, 3 (6), 311-322.

Mihalis, I and Kavvados, M. (2000). Ground movements caused by TBM tunnelling in the Athens Metro project. *In: Proc. Int. Sympos. on Geotechnical Aspects of Underground Construction in Soft Ground*, Tokyo, 21-23 July 1999. Rotterdam: Balkema, 269-274.

Mitchell, J.K., Baxter, C.D.P. and Soga, K. (1997). Time effects on the stress-deformation behaviour of soils. *In: Proc. Sakuro Murayama Memorial Symposium*, Kyoto, April.

Morgan, S.R. (1999). Prevaulting success at Ramsgate Harbour. *Tunnels and Tunnelling International*, 31 (7), 31-34.

Morton, K. and Au, E. (1975). Settlement observations on eight structures in London. *In: Proc. Conf. Settlement of Structures*, Cambridge, April 1974. London: Pentech Press, 183-203.

Mott MacDonald Civil Ltd. (1991). *The Mansion House. Final Report*. Report to the London Docklands Light Railway, April.

Nakai, T. Farias, M.M., Matsubara, H. and Kusunoki, S. (2000). Effects of excavation sequence on the 3D settlement of shallow tunnels. *In: Proc. Int. Sympos. on Geotechnical Aspects of Underground Construction in Soft Ground*, Tokyo, 21-23 July 1999. Rotterdam: Balkema, 403-408.

Netzel, H. and Kaalberg, F.J. (1999). Numerical damage risk assessment studies on masonry structures due to TBM-tunnelling in Amsterdam. *In: Geotechnical Aspects of Underground Construction in Soft Ground, An International Symposium*, Tokyo, 21-23 July, Pre-print Volume of Proceedings. Tokyo: Japanese Geotechnical Society, 235-244.

O'Reilly, M.P. (1988). Evaluating and predicting ground settlements caused by tunnelling in London clay. *In: Proc. Int. Symposium Tunnelling '88*, London 18-21 April. London: Institution of Mining and Metallurgy, 231-241.

O'Reilly, M.P and New, B. (1982). Settlement above tunnels in the United Kingdom- their magnitude and prediction. *In: Proc. Int. Symposium Tunnelling '82*, London, 7-11 June. London: Institution of Mining and Metallurgy, 173-181.

Peck, R.B. (1969). Deep excavations and tunnelling in soft ground. *In: Proc. 7th ICSMFE, State-of-the-art Volume*, Mexico City. Mexico: Sociedad Mexicana de Mecánica de Suelos, 225-290.

Pell Frischmann & Partners, Consulting Engineers (1985). *Mansion House evaluation study, Volume 1*. Report to City of London Corporation, October.

Pell Frischmann & Partners, Consulting Engineers (1989). *Effects on the Mansion House of future tunnelling works for the Docklands Light Railway*. Report to City of London Corporation, October.

Polshin, D.E. and Tokar, R.A. (1957). Maximum allowable non-uniform settlement of structures. *In: Proc. 4th ICSMFE, Vol. 1*, London, 12-24 August. London: Butterworth, 402-405.

Potts, D.M. (1976). *Behaviour of lined and unlined tunnels in sand*. Thesis (PhD). University of Cambridge.

Potts, D.M. and Addenbrooke, T.I. (1997). A structure's influence on tunnelling-induced ground movements. *Proceedings ICE Geotechnical Engineering*, 125 (2), 109-125.

Powderham, A.J. (1994). An overview of the observational method: Development in cut and cover and bored tunnelling projects. *Géotechnique*, 44 (4), 619-636.

Price, G., Longworth, T.I. and Sullivan, P.J.E. (1994). Installation and performance of monitoring systems at the Mansion House. *Proceedings ICE Geotechnical Engineering*, 107 (2), 77-87.

Quqing, G. (1990). Construction of underground works in Shanghai, P.R.C. *Tunnelling and Underground Space Technology*, 5 (4).

Rowe, R.K. and Lee, K.M. (1989). Parameters for predicting deformations due to tunnelling. In: *Proc. 12th ICSMFE, Vol. 2,* Rio de Janeiro, 13-18 August. Rotterdam: Balkema, 793-796.

Rowe, R.K., Lo, K.J. and Kack, G.J. (1983). A method of estimating surface settlement above tunnels constructed in soft clay. *Canadian Geotechnical Journal*, 20 (1), 11-22.

Samuel, H.R., Mair, R.J., Lu, Y.C., Chudleigh, I., Addenbrooke, T.I. and Readings, P. (2000). The effects of boring a new tunnel under an existing masonry tunnel. *In: Proc.*

Int. Sympos. on Geotechnical Aspects of Underground Construction in Soft Ground, Tokyo, 21-23 July 1999. Rotterdam: Balkema, 293-298.

Schmidt, B. (1969). *Settlements and ground movements associated with tunnelling in soil*. Thesis (PhD). University of Illinois.

Shirlaw, J.N. and Doran, S. (1988). Ground movements and settlements caused by tunnelling for the Singapore Mass Rapid Transit System. *In: Proc. Int. Symposium Tunnelling '88*, London, April. London: Institution of Mining and Metallurgy, 295-314.

Simic, D. and Craig, R.N. (1997). Lisbon Metro- Settlement behaviour of large-diameter shield-driven and NATM tunnels. *In: Proc. Int. Symposium Tunnelling '97*, London, 2-4 September. London: Institution of Mining and Metallurgy, 421-438.

Simons, N.E. and Som, N.N. (1970). *Settlement of structures on clay with particular emphasis on London clay*. CIRIA Report 22.

Simpson, B. (1994). A model of interaction between tunnelling and a masonry structure. *In: Proc. 3rd European Conf. on Numerical Methods in Geotechnical Engineering*, *ECONMIG '94*, Manchester, September. Rotterdam: Balkema, 221-228.

Skempton, A.W. and MacDonald, D.H. (1956). Allowable settlement of buildings. *Proceedings ICE Part III*, 5, 727-768.

Sloan, S.W. and Randolph, M. (1983). Automatic element reordering for finite element analysis with frontal solution schemes. *Int. J. of Numerical Methods in Engineering*, 19, 1153-1181.

Soga, K., Bolton, M.D., Au, S.K.A., Komiya, K., Hamelin, J.P., Van Cotthem, A., Buchet, G. and Michel, J.P. (2000). Development of compensation grouting modelling and control system. *In: Proc. Int. Sympos. on Geotechnical Aspects of Underground Construction in Soft Ground*, Tokyo, 21-23 July 1999. Rotterdam: Balkema, 677-680.

Stallebrass, S.E. and Taylor, R.N. (1997). The development and evaluation of a constitutive model for the prediction of ground movements in overconsolidated clay. *Géotechnique*, 47 (2), 235-253.

Sugiyama, T., Nomoto, T., Nomoto, M., Ano, Y., Hagiwara, T., Mair, R.J., Bolton, M.D. and Soga, K. (2000). Application of compensation grouting to the Docklands Light Railway Extension project in London. *In: Proc. Int. Sympos. on Geotechnical Aspects of Underground Construction in Soft Ground*, Tokyo, 21-23 July 1999. Rotterdam: Balkema, 319-324.

Swoboda, G. and Hafez, N.M. (1995). Structural analysis of shotcrete in tunnelling. *In: Proc. 7th Engineering Foundation Conf. Shotcrete for Underground Support*, Telfs, Austria, June. New York: ASCE, 170-179.

Verruijt, A. and Booker, J.R. (1996). Surface settlements due to deformation of a tunnel in an elastic half plane. *Géotechnique*, 46 (4), 753-756.